CASE FILE COPY

OCT 10 73
RECEIVED
NASA STI FACIL
INPUT BRA

NUMERICAL ANALYSIS OF STIFFENED SHELLS OF REVOLUTION

Volume I of VII

by V. Svalbonas

1. REPORT NO. NASA CR-2273	2. GOVERNMENT ACCESSION NO.	3. RECIPIENT'S CATALOG NO.	
4. TITLE AND SUBTITLE Numerical Analysis of Stiffened Shells of Revolution Volume I of VII *		5. REPORT DATE September 1973	
		6. PERFORMING ORGANIZATION CODE	
7. AUTHOR(S) V. Svalbonas		8. PERFORMING ORGANIZATION REPORT # M381	
9. PERFORMING ORGANIZATION NAME AND ADDRESS Grumman Aerospace Corporation Bethpage, New York 11714		10. WORK UNIT NO.	
		11. CONTRACT OR GRANT NO. NAS 8-27468	
12. SPONSORING AGENCY NAME AND ADDRESS National Aeronautics and Space Administration Washington, D.C. 20546		13. TYPE OF REPORT & PERIOD COVERED Contractor Report	
		14. SPONSORING AGENCY CODE	

15. SUPPLEMENTARY NOTES

*A list of all seven volumes, by sub-title, is on the back side of this page

16. ABSTRACT

This report contains the theoretical analysis background for the STARS-2 system of programs. The present theory does not attempt to rediscover the importance of such practical configurations in shells of revolution as those containing branching. This is due to the fact that since the STARS program was created for practical shell designers and analysists initially, rather than being an analytical research tool, such options have continually been available in all versions since its inception in 1963. The present report contains the theory involved in the axisymmetric nonlinear and unsymmetric linear static analyses, and the stability and vibrations (also critical rotation speed) analyses involving axisymmetric prestress, which are programmed and available in the STARS-2S, -2B, and -2V programs respectively. It also contains the theory for nonlinear static, stability, and vibrations analyses, involving shells with unsymmetric loadings, which is not presently available in the above computer programs.

The user's manuals for the statics program and the stability and vibrations programs are available as Volumes II and III of this series, respectively.

17. KEY WORDS		18. DISTRIBUTION STATEMENT	
19. SECURITY CLASSIF. (of this report) Unclassified	20. SECURITY CLASSIF. (of this page) Unclassified	21. NO. OF PAGES 209	22. PRICE 3.00

VOLUME   I. Theory Manual for STARS-2S, 2B, 2V Digital Computer Programs

VOLUME II. Users' Manual for STARS-2S - Shell Theory Automated for
            Rotational Structures - 2 (Statics), Digital Computer Program

VOLUME III. Users' Manual for STARS-2B, 2V - Shell Theory Automated
            for Rotational Structures - 2 (Buckling, Vibrations), Digital
            Computer Programs

VOLUME IV. Engineer's Program Manual for STARS-2S - Shell Theory
           Automated for Rotational Structures - 2 (Statics), Digital
           Computer Program

VOLUME V. Engineer's Program Manual for STARS-2B - Shell Theory
           Automated for Rotational Structures -2 (Buckling), Digital
           Computer Program

VOLUME VI. Engineer's Program Manual for STARS-2.V - Shell Theory
           Automated for Rotational Structures -2 (Vibration), Digital
           Computer Program

VOLUME VII. Satellite Programs for the STARS System

TABLE OF CONTENTS

SUMMARY

The contents of this report can be divided into five basic parts. The first part presents the state of the art in shell of revolution analysis, and briefly presents the theoretical advantages and disadvantages of the main numerical methods. The second part (Chapters 1 - 3) describes the static analysis pertinent to the STARS-2S program, and, in addition, presents the necessary equations for extension into nonlinear analysis of unsymmetric loading. The third part (Chapter 4) deals with the analysis of the classical buckling loads of shells of revolution under axisymmetric loadings (STARS-2B program), and unsymmetric loadings (not programmed). The fourth part (Chapter 5) deals with vibrations. The vibration and critical speed analyses involving axisymmetric prestress are programmed in the STARS-2V program while the analyses involving unsymmetric prestress remain unprogrammed. The final part (Chapter 6) presents several analytical studies performed with the STARS programs, where certain formulation advantages, or discrepancies with other analyses were uncovered.

It will be noted that the present eigenvalue formulation for the axisymmetric problem has several advantages over previous formulations. Possible similar advantages for the unsymmetric problem are discussed in Chapter 4, however there are many unanswered questions in this more complex area. Several comparative studies need to be carried out before a more accurate picture of even potential advantages can be drawn.

TABLE OF FIGURES

LIST OF SYMBOLS

Lower Case Latin:

e_{ij}	Linear strain
$\{f\}$	Local force matrix
h	Shell thickness
k	Shell curvature
$[k]$	Stiffness matrix
m	Distributed moment load
n	Fourier harmonic number
o	Subscript meaning reference surface
r_1	Meridional radius of curvature
r_2	Circumferential radius of curvature
r_c	Ring centroidal radius
r_o	Radius of revolution
s	Arc length
u	Circumferential shell displacement
v	Meridional shell displacement
w	Normal shell displacement (positive inward)

Upper Case Latin:

A   Area

B   Subscript meaning buckling increment

C   Eccentricity of reinforcement

D   Bending stiffness

E   Young's modulus

E_i Direct strain components in large strain theory

F   Distributed loads on the shell

G   Shear modulus

H   Lame′ coefficients; total thickness of sandwich shell

I   Subscript meaning inside surface of ring; moment of inertia

J   Effective transverse shear stress resultant; torsional constant

K   Extensional stiffness

[L]   Load matrix

M   Bending stress resultant

N   Membrane stress resultant

O   Subscript meaning outside surface of ring

P   Pressure; number of load cases

Q   Transverse shear stress resultant

R   Subscript denoting reinforcement

S   Stiffener spacing

T   Temperature

U, V, W   Harmonic amplitudes of the circumferential, meridional, and radial components of displacement respectively

Z, R, θ   Global coordinate system

Greek

α, β, γ	General curvilinear coordinates
α	Coefficient of thermal expansion
ω	Rotation of the normal to the middle surface of the shell; natural frequency ; rotation speed
ϵ_{ij}	Strain of the large displacement theory
Γ_i	Shear components of the large strain theory
ζ	Shell coordinate normal to the middle surface of the shell (positive inward)
θ, φ	Circumferential and meridional shell coordinates
σ_{ij}	Normal components of stress
ν	Poisson's ratio
τ_{ij}	Shearing components of stress
ζ_i	Distance to the surface of the shell from the neutral plane
Ω	Harmonic amplitude of shell rotation
Δ	Deformation
$\{\delta\}$	Local displacement matrix

INTRODUCTION TO NUMERICAL ANALYSIS OF SHELLS

Recent innovations in digital computer technology have enabled designers to analyze shell structures of complex configurations without unduly restrictive approximations. A number of versatile computer programs, based on various methods of analysis are presently available for the analysis of shells of revolution. With the exception of closed form solutions, the most commonly employed numerical methods of analysis will be briefly discussed and compared in the sequel.

Finite Difference Method: This method was first employed by Radkowski, et al. [1, 2]* in analyzing layered shells of revolution subjected to axisymmetric loading. In these references, the two second-order differential equations of the theory presented by Reissner [3] were solved by using central differences with a constant mesh. The resulting simultaneous algebraic equations were solved by Potter's method [4]. Reference 1 is one of the few references wherein the finite difference method is employed in analyzing branched shells. Only "Y branches" are considered. Sepetoski, et al. [5] employed a similar approach to study problems which do not involve shell branching. However, the simultaneous equations resulting from the application of finite differences were solved by a non-matrix Gaussian elimination technique. Moreover, in this reference, the effects of the grid sizes and of the error accumulation in the Gaussian elimination technique on the convergence of the solution were studied. Budiansky and Radkowski [6] extended the technique presented in Reference 1 to the analysis of shells of revolution (including shells with " Y branches ") subjected to unsymmetric loading, using a shell theory presented by Sanders [7].

---

* Numbers in brackets refer to the bibliography at the end of the report.

The load was expanded in Fourier series and a variable finite difference grid pattern was used. Greenbaum [8] presented a refinement for the analysis of shells closed at the apex. Capelli, et al. [9] included the effect of shear deformation and extended the technique of Reference 6 to shells of variable thickness in the circumferential direction. The variable thickness was expanded in a Fourier series, and the thickness harmonic amplitudes were coupled with the load harmonic amplitudes, necessitating a modification of the procedure of Reference 6 to provide coupled harmonic solutions.

Techniques similar to Reference 6 were applied in References 10, 11, 12 to nonlinear problems. Hubka [10] presented an analysis of orthotropic, axisymmetrically loaded, shells of revolution, wherein non-linear terms were included in the equilibrium equations. Problems involving shells with two boundaries, subjected to distributed and concentrated line loads, were considered using Reissner's theory. The two second-order differential equations were solved using finite difference approximations with a variable grid. Options for forward, central, and backward differences were included. The resulting simultaneous equations were solved by a Gaussian elimination method specialized to banded matrices [13]. Nonlinear problems were solved by first solving the linear problem, and employing the computed in-plane stress resultants as input for the solution of the nonlinear equations. A similar method was utilized by Wilson and Spier [14, 15] to solve axisymmetric nonlinear shell problems using the equations of Reissner [16]. Moreover, they modified Potter's technique by adding an iteration procedure for solving the simultaneous nonlinear equations. In this iteration process the matrices generated by the solution of the linear equations were used as the first approximation in the solution of the non-linear problem. The procedure was repeated using the output of the previous iteration. This method converges very slowly for problems with significant nonlinear

effects and it is necessary to use small load increments for higher values of the load. It was recognized by the authors that a Newtonian-type iteration technique [17, 18] would be more suitable inasmuch as its convergence could be proven. Bushnell [19] utilized the Newton-Raphson method to solve nonlinear problems of orthotropic, eccentrically stiffened shells of revolution. The effect of the stiffeners was treated by "smearing"* the properties of the closely spaced rings and stringers over their spacing. Critical loads at buckling for a shell subjected to axisymmetric loads (for cases in which the buckling mode is also axisymmetric) are established with this technique. The buckling load in established as the last load for which the Newton iteration method converges.

The same technique, with a more approximate iteration procedure was first applied to shells of revolution subjected to unsymmetric loading by Ball [20, 21]. Inasmuch as the loading is expanded in a Fourier series, the nonlinear terms included in the Sanders shell theory [7], used in Reference 20, couple the Fourier harmonics. The equations are uncoupled by first solving the linear problem, and using the results to obtain and introduce into the equations a numerical value for every nonlinear term. The resulting uncoupled equations are solved by the methods of Reference 6, each solution providing the numerical values for the subsequent iteration. The buckling load is defined as the last load for which the solution converges. Stability cases where the buckled shape is out-of-phase with the applied load cannot be considered. With this technique, it should be noted that the number of

---

* See Appendix A for a further discussion of this technique.

3

sets of uncoupled equations which must be solved is not constant, but increases as convergence progresses, inasmuch as coupling terms involving more harmonics are evaluated numerically as the analysis progresses. Greenbaum and Conroy [22] found that for certain problems the technique of Reference 20 did not converge, and hence utilized a Newton iteration procedure. Moreover, it was determined that the formulation of the problem in terms of sets of four second-order differential equation results in numerical inaccuracies in the finite difference solution. For this reason the formulation of the problem in terms of sets of eight first-order equations was employed. Complexities of this nature in the use of finite differences are discussed in Reference 23. The technique presented in Reference 22 has certain inconsistencies. In using the Newton iteration procedure, the cross-coupling terms of the various harmonic amplitudes are dropped in order to work with uncoupled sets of equations. In addition, some terms from the Sanders' shell theory are also dropped. Finally, the analysis of Reference 22 cannot be used for post-buckling analysis or for establishing the critical load at buckling where the buckling mode is out-of-phase with the load.

Eigenvalue problems of vibrations and stability of shells have also been solved using the finite difference method. Cooper [24] has investigated the stability and natural vibrations of shells of revolution with two end boundaries, under axisymmetric prestress, using the methods of Reference 6. The nonlinear theory presented by Sanders [7] is used to establish the equations of both the prestress state, and the incrementally disturbed state. In the vibration problem the perturbation displacements are assumed proportional to $e^{i\omega t}$, and the frequency determinant is evaluated for a sequence of assumed values of the frequency, until the correct frequency is obtained as the one for which the determinant vanishes. Central differences

4

with a constant mesh are employed to reduce the four second-order

differential equations to algebraic equations. The latter are solved by

Potters' method. This method is modified [25] in order to avoid spurious

changes of sign of the determinant. The numerical procedure for establishing

the buckling load is identical to that for establishing the frequency in the

vibration problem. In the stability analysis, the prebuckling stress-resultants

and deformations are considered. In the vibration analysis, the rotational

inertia is omitted. Rossettos and Tene [26, 27] applied a very similar

technique to the analysis of layered and orthotropic shells. The sole difference

was that they utilized second-order finite difference approximations in order

to consider boundary conditions at the two ends with an accuracy consistent with

that used for the analysis of the remainder of the shell. Heard and Fulton [28]

also used an almost identical technique with a variable finite difference mesh.

In References 29-37, a program for solving shell stability problems is presented.

This program includes the effects of eccentric reinforcement on shells

(smearing technique is used). Both the prebuckled and stability equations

are treated by applying central differences to two fourth-order differential

equations, and solving the resulting set of algebraic equations by use of

the method presented in Reference 38. If the prebuckling state is established

on the basis of a linear analysis, the stability equations may be conveniently

approximated by the form $([A] + \lambda [B])\{x\} = 0$. Thus, the power method

[39] may be employed to establish the critical load at buckling, avoiding

the uncertainties inherent in the determinant evaluation method. In solving stability

problems with the aforementioned program (BOSOR) the prebuckled state

may be established by the nonlinear analysis of Reference 19. In such

an eventuality, the determinant evaluation method is utilized.

Two-dimensional finite difference solution techniques have been used in solving vibration and stability problems in References 40 and 41. These two-dimensional techniques result in very large matrices, and therefore should be employed only in the absence of an alternative method (e.g. to investigate a shell cutout problem).

Finite Element Method: In applying the finite element method which is actually an application of the Rayleigh-Ritz numerical technique, to the analysis of shells of revolution, two distinct types of elements have been employed: the discrete triangle or quadrilateral; and the revolved conical or curved elements. Each of the foregoing elements have special advantages and specific areas of application. Generally, in the application of finite elements to shell analysis, the following two basic questions remain to be resolved:

1. What is the effect of the geometric approximations between the elements and the actual shell surface, on the solution of the problem.

2. Is it necessary to explicitly include rigid-body motion terms in the displacement function employed in the solution.

The first conical frustum element was introduced by Meyer and Harmon [42] The deformation of this element included membrane and bending components, and continuity of slopes and displacements was enforced on the inter-element nodal circles. The deformation of the element was established on the basis of an analytical solution for a cone loaded solely along the edge, and shell problems involving edge loading only were solved using the force method. Grafton and Strome [43] derived the matrices for a conical element using the displacement method. Simple polynomial forms were utilized to represent the deformation state. Friedrich [44] used a thick conical element whose deformation included shear deflections established by simple beam theory. Another conical element using an analytical edge-loaded cone solution for the deformation of the element was formulated by

6

Lu, et al. [45], using the displacement method. Percy, et al. [46], and

Wilson [47], were the first to apply conical elements to solve problems

of shells subjected to unsymmetric loads. The non-symmetry was

analyzed by use of Fourier series. In Reference 46 the effects of

utilizing various order polynomials to represent the displacement functions,

were investigated.

A thorough study of the conical frustum element was performed by

Percy, et al. , [46] and by Jones and Strome [48]. They encountered

considerable disadvantages in the use of this element for the analysis of

doubly-curved shells. For predominantly membrane problems, due to the

change of angle between adjacent elements, the kinks at the nodes produce

calculated meridional bending moments where none exist. For problems

wherein the rotations at the boundary are unconstrained, erroneous

displacements of the boundary are calculated. Moreover, it is essential

to use extremely short cone elements a considerable distance in from the

end boundaries. As indicated in Reference 48, optimization of shells by

careful variation of the thickness or geometry is not possible when conical

frustum elements are used. In static problems using conical elements ,

some of the errors cancel each other. However, this cannot be anticipated

in the case of dynamic analyses where rapid meridional membrane stress

variation may occur. To overcome the foregoing difficulties, Jones and

Strome [49] introduced a doubly-curved revolved element where the coordinates,

slope, and hoop principal radius of curvative, were continuous

functions throughout, and, at the nodal circles, were identical to those of

the actual shell. However, the meridional radius of curvature was a

discontinuous function at the nodal circles. A similar element with special

refinements for application at the apex of a shell was developed by Stricklin,

et. al. [50]. Khojasteh-Bakht [51] developed the matrices for a doubly-curved

revolved element matching the tangents and curvatures of adjacent elements at the nodal circles. A geometrically still more refined revolved element was produced by Brombolich and Gould [52].

Stricklin, et.al., used the elements of Reference 50 to solve nonlinear problems of axisymmetrically loaded shells whose thickness and material properties were both axisymmetric [53] and non-axisymmetric [54]. The non-axisymmetric, nonlinear problems resulted in a set of simultaneous equations involving coupled harmonic amplitudes similar to that solved in Reference 9 (on the basis of finite difference techniques): It has been shown that it was not necessary to include explicit rigid body displacement terms [50, 54, 55, 56] in the deformation functions of these revolved curved elements.

Dynamic and stability problems were also solved by the use of these revolved elements. Klein and Sylvester [57] and Bacon and Bert [58] solved shell vibration problems by using conical frustum elements. The latter authors included transverse shear deformation and rotatory inertia, and analyzed sandwich shells. Mode shapes and frequencies of orthotropic shells of revolution were found by Leimbach, et.al. [59], and subsequently by Adelman, et.al. [60, 61] using elements better fitting the geometry of the shell. The mode shapes of sandwich shells were calculated by Abel and Popov [62], and nonlinear vibration problems were considered by Stricklin et.al. [63]. Navaratna, et.al. [64] applied both the conical frustum and the curved revolved elements to the solution of linear buckling problems, for shells of revolution subjected to axisymmetric loads. Each possible Fourier harmonic mode of buckling must be checked to find the lowest eigenvalue.

It should be noted that the principal advantage of utilizing revolved finite elements instead of finite differences is that arbitrarily branched shells of revolution may be analyzed in a routine manner by using revolved finite elements.

8

Shells were also analyzed using discrete triangular or quadrilateral elements. Flat triangular elements were developed for this purpose by Melosh [65]. These elements accounted for membrane and bending flexibility, and may be used to analyze shells with material properties ranging from isotropic to aelotropic. Zienkiewicz, et. al. [66] applied triangular plate elements to the analysis of thin arch dams. Notwithstanding the continuous interest in these applications [67], flat elements may be more inadequate than the conical frustra [48] in the representation of curved surfaces, particularly in predominantly membrane stress areas. Solutions obtained using a number of flat elements were tested for convergence [68, 69], and it was concluded that solutions of bending problems of curved structures employing these elements do not always converge. In addition, since the use of flat elements for the solution of problems involving curved structures requires very large matrices, flat elements should be limited to problems involving arbitrary shells or shell cutouts, for which large matrices are obtained no matter what element is used.

The inadequacies of flat elements led to the development of curved quadrilateral and triangular elements. The more general curved triangular elements can readily describe arbitrary cutout boundaries. The earliest constant curvature quadrilateral element was developed by Gallagher [70] by applying the shell theory (non-shallow) presented by Novozhilov [71]. Although the displacement function chosen does not include rigid body terms nor does it lead to displacement continuity at the element boundaries, the results obtained converge satisfactorily. Geometrically more flexible quadrilateral elements were developed using shallow shell theory [72] and finite differences by Szilard and West [73], and subsequently by Tsui, et. al. [74], who also included the effects of shear deformation.

9

Bogner, et. al. [75] developed a cylindrical element wherein the displacement function includes both rigid body motion and satisfies the compatibility requirements. This element was later used to study nonlinear shell behavior [76]. More recently, a large variety of curved quadrilaterals have been developed: Conner and Brebbia [77, 78] (the Marquerre [79] shallow shell theory with nonlinear effects was employed in Reference 78), Cantin and Clough [80] (cylindrical element with a thorough discussion of the requirements for inclusion of rigid body motion terms in the displacement function), Wempner, et. al. [81] (transverse shear deformation is included), Ahmad, et. al. [82] (transverse shear deformation is included), and Key and Beisinger [83] (the displacement function is represented by Hermitian polynomials, and shear deformation is included).

In Reference 73, vibration problems were first solved using curved quadrilaterals. More recently, Olson and Lindberg [84] established mode shapes and frequencies of curved fan blades employing curved quadrilateral elements. Greene, et. al. [85] also used a quadrilateral to study shell vibration problems. The shell theory utilized is the non-shallow shell theory of Novozhilov. The element of Reference 70 was used by Gallagher and Yang [86] in problems of stability of shells.

Early work in the development of curved triangular elements was performed by Utku [87, 88], Prince [89], and Svalbonas [90]. Utku utilized the Marguerre shallow shell theory, and included shear deformation effects. Prince employed the three sub-element technique [91] to develop a constant curvature trianglar shell element, based on the non-shallow shell theory of Novozhilov. The three sub-element method was also utilized in Reference 90 in conjunction with the non-shallow shell theory of Novozhilov, to develop a family of orthotropic, arbitrarily curved, triangular

10

shell elements. Curved triangular elements were recently developed by:
Argyris and Scharf [92] (63 degree of freedom element in a "natural"
coordinate system), Dhatt [93] (shallow shell theory with shear deformation),
Strickland and Loden [94] (Novozhilov shallow shell theory), and Bonnes,
et. al. [95] (three sub-domain method with Reissner [96] shallow shell
theory).

It should be noted, that the accuracy of solutions obtained by using discrete
doubly-curved finite elements has mainly been verified only for simple classical
problems. Thus, before definite conclusions can be drawn as to the
suitability of some of these elements for solving problems involving shells with
complex cutouts, additional, broader, comparisons must be made.

Numerical Integration Method: This method was utilized in a general form
in References 97, 98, and 99. Cohen [97] analyzed orthotropic shells of
revolution, using the non-shallow shell theory of Novozhilov and the Runge-
Kutta method of forward integration. The resulting system of equations is
solved by Gaussian elimination. Both thermal and mechanical loads are
considered, however, shell branching is not included. The unsymmetric
loadings are expanded in Fourier series, and each harmonic is analyzed
separately. Kalnins [98] solved similar isotropic shell problems using
the Reissner shell theory, the Adams integration method, and the Gaussian
elimination technique. Again the analysis is limited to problems involving
two end boundaries. Mason et. al. [99] analyzed isotropic shells with
completely arbitrary branching characteristics, subjected to axisymmetric
load, using the nonlinear Love-Reissner-Kempner [100] shell theory and
the Runge-Kutta method of forward integration. The arbitrary branching
was accomplished with a finite element type (direct stiffness method) solution
of the matrix equations. The nonlinear solution was identical to that of

Reference 10, discussed previously. Rung, et. al. [101, 102] extended
this method to the analysis of shells of revolution subjected to unsymmetric
loading, using a linear shell theory. The direct stiffness matrix solution
technique was adapted by Svalbonas [103] to orthotropic, second-order shell
theory, including the effects of shear deformation and thickness stretch.
In this reference, the nonlinear analysis of shells of revolution under
unsymmetric loading is discussed, using a similar technique to that later
utilized by Ball [20] (see finite difference discussion). The aforementioned
method was applied to the analysis of shells of revolution comprised of
orthotropic layers [104], and of sandwich construction with shear deformable
cores [105]. Another nonlinear analysis of shells of revolution, with two
end boundaries, under an axisymmetric load, was presented by Kalnins and
Lestingi [106]. In this reference, a form of Newton's method was employed
to solve the nonlinear problem. The numerical integration technique, in
connection with Guyan [152] reduction, was applied to the analysis of orthotropic
stiffened shells subjected to static loads in the STARS-II program developed for
NASA by Svalbonas, et al. [107-110]. This program may be employed in the solution
of problems of shells of revolution with arbitrary geometry as shown in Fig. 1.
Moreover, this program may be used in conjunction with discrete finite element
analysis [111].

Calculations of natural frequencies and modes of vibration of shells of
revolution using numerical integration was first accomplished by Kalnins
[112], who included the effect of rotatory inertia. The problems solved
entail isotropic shells with two end boundaries. The frequencies are
established by evaluating the frequency determinant. Orthotropic, ring-stiffened
shells were analyzed by Cohen [113], who used numerical integration and a Stodola
type [114] iteration technique. This iteration technique commences by assuming a
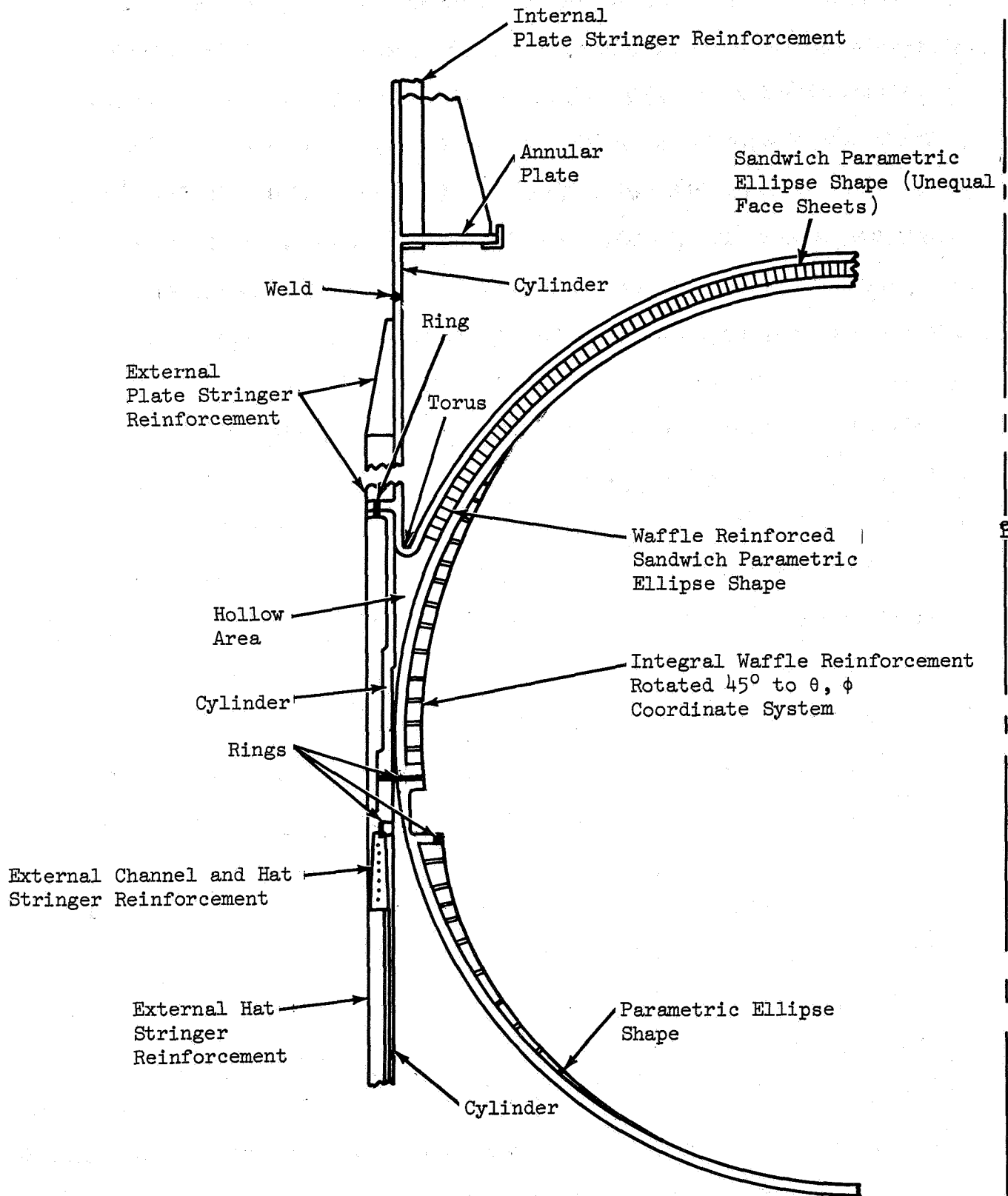value for the displacement components, setting the frequency to unity, and evaluating

Figure 1   Saturn S-II Stage Common Bulkhead (thermal, pressure,and concentrated
line loadings applied)

numerically the inertia terms. These values of the inertia terms are substituted in the equations of motion resulting in a set of nonhomogeneous equations, the solution of which yields a first estimate of the mode shapes. An estimate of the frequency is then obtained by evaluating the Rayleigh quotient. This value of the frequency, together with the estimated values of the mode shapes are used to obtain a new set of numerical values for the inertia terms. The process then continues until the mode shapes obtained from two successive iterations vary by an acceptable error. It can be proven that this method, also known as the inverse power method [115], converges to the smallest frequency.

The frequency determinant evaluation method as well as the Stodola method have certain advantages and disadvantages [116]. In the Stodola method, the lowest eigenvalue cannot be skipped, as is possible with the determinant evaluation method; however, if higher values of frequency are needed, the Stodola method requires modifications for "sweeping-out" the lower frequencies, and eigenvalue shifts to avoid slow convergence [114].

A generalization of the Stodola method was used by Cohen [117] to analyze the stability of orthotropic, ring-stiffened shells of revolution with two end boundaries, subjected to axisymmetric loading, employing the non-shallow shell theory of Novozhilov. Numerical integration by the Runge-Kutta method, and Gaussian elimination are used in the solution. The prebuckled state is obtained on the basis of a nonlinear solution and thus, the critical load and mode at buckling are established by solving a sequence of modified eigenvalue problems. The lowest buckling load corresponding to each Fourier harmonic buckling mode is established. The critical load at buckling is the smallest of these loads. A similar analysis including the capability of analyzing shells with "Y" branches, using the determinant evaluation method, was presented by Kalnins [118]. In this reference an attempt

is made at establishing the critical load at buckling for shells of revolution
of certain geometries subjected to single-harmonic unsymmetric loading.

Comparison of Methods: The three methods discussed herein are approximate
methods and, consequently, must be checked for accuracy or convergence
of their results. The finite element and finite difference methods require
at least two analyses with different grids to establish whether of the size
of the grid used yields satisfactory solutions. The results obtained from a
single solution by the numerical integration method, however, may be checked
automatically for each shell segment. Moreover, the representation of a
shell by finite elements involves geometric approximations which are not
required in the numerical integration method. A disadvantage of the
numerical integration method is that accuracy is lost when the shell is long.
This however, is overcome by segmenting the shell into shorter pieces.

A serious difficulty with the finite difference method is the instability
of the solution at fine mesh sizes, and the slow convergence of the results
obtained from single precision computer programs. For a stiffened cylinder,
an example of the instability of the solution is shown in Figure 2. Introduction
of double precision requires a reduction of the number of mesh points which
appreciably limits the scope of a program [31]. It should be noted that the solution
may not always converge asymptotically as the number of finite difference
stations increases [40]. In References 26, 27, and 119 it was indicated
that the error associated with finite difference approximations of a given
order is larger close to the boundary. Thus, the overall accuracy of the
results may be increased if finite difference approximations of higher order
are used at the end boundaries. Generally, in order to accurately establish
the stress distribution near the shell boundary or at regions of high
stress variation, or to properly locate shell discontinuities in curvature,
thickness, etc., a mesh of variable spacing is required. However, the regions
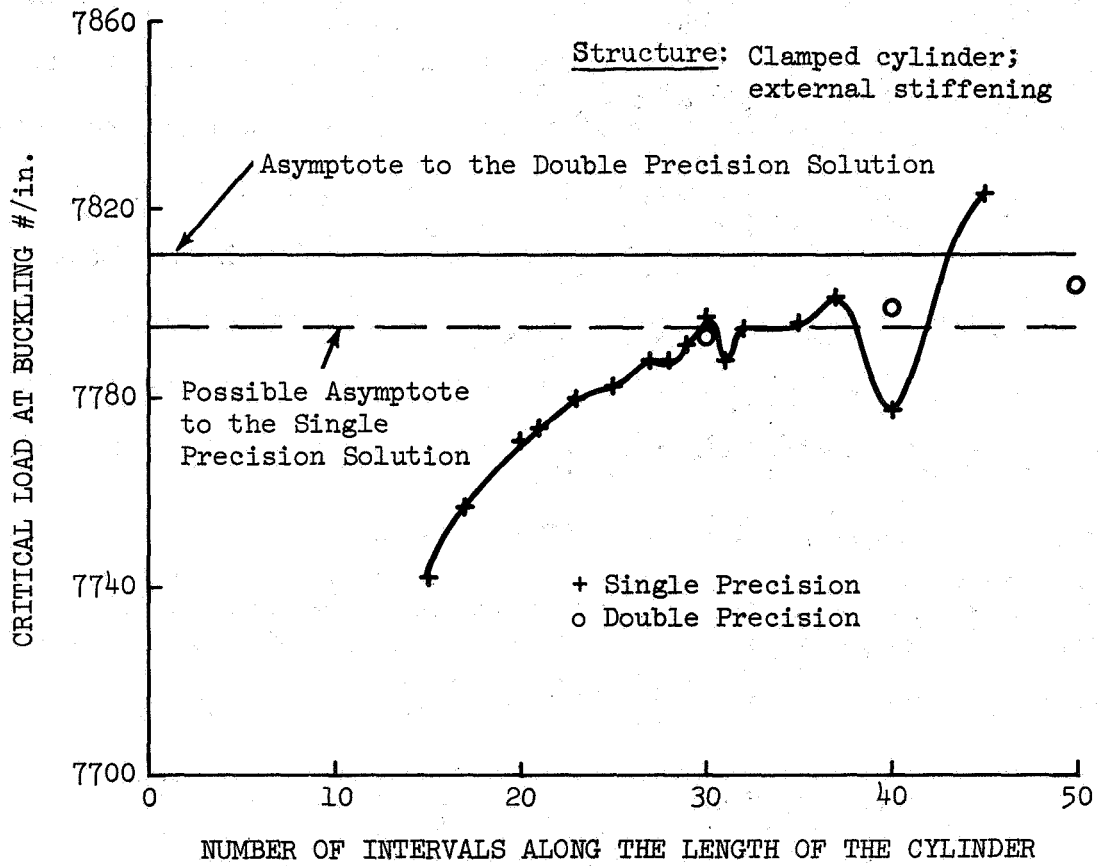
Figure 2   Critical Axial Load as Function of Mesh Size for Cylinder Subjected
to Axial Compression [From Reference 31]

of high stress variation cannot be predicted apriori and, consequently,

the mesh of the first trial may be extremely fine in some regions

of the shell and very coarse in others. In the use of variable mesh, the

variation of the order of the error in the formulas, must also be considered.

In the numerical integration method, however, the aforementioned difficulties

are eliminated by automatically controlling the integration interval so as to

obtain a solution of uniform accuracy. Finally, the errors in the Runge-

Kutta integration formulas are of the order of h^5, whereas, in the finite

differences employed in the aforementioned references, the error is of

the order of h^2. In Figure 3 a comparison is presented of the results obtained

by finite differences and by the numerical integration method for spherical

caps subjected to uniform pressure.

Finite element analysis of shells involves both mathematical

approximations (those associated with a Rayleigh-Ritz analysis) and geometric

approximations. The geometric approximations associated with revolved

finite elements are discussed in detail in Reference 48. As previously

noted, an advantage of the finite element method is that it may be

employed to analyze arbitrarily branched shells in a routine manner.

Numerical integration methods can also be employed to analyze arbitrarily

branched shells [107], moreover, to obtain the same accuracy in the solution,

much coarser idealizations can be used with the numerical integration method than

with the finite element method. Finally, the components of stress and dis-

placement obtained by the numerical integration method are of the same

accuracy, whereas, the order of accuracy of the components of stress

obtained by the finite element method is less than the order of accuracy of

the components of displacements.

$$\mu^2 = 2\sqrt{12(1-\nu^2)}\ (H/h)$$

$$\gamma = \frac{(12[1-\nu^2])^{3/2}\ a^4 p\alpha^4}{4Eh^4}$$

N=Number of finite difference stations

——— Numerical Integration

— — — Finite Difference

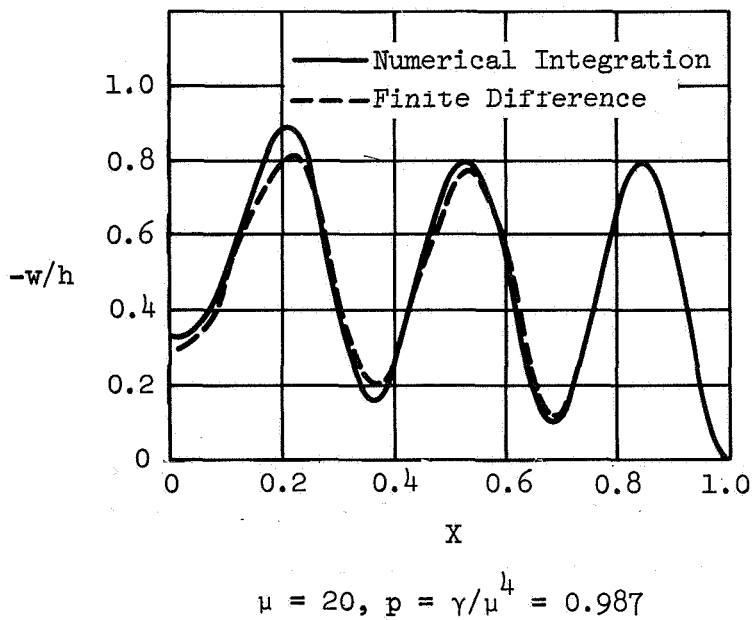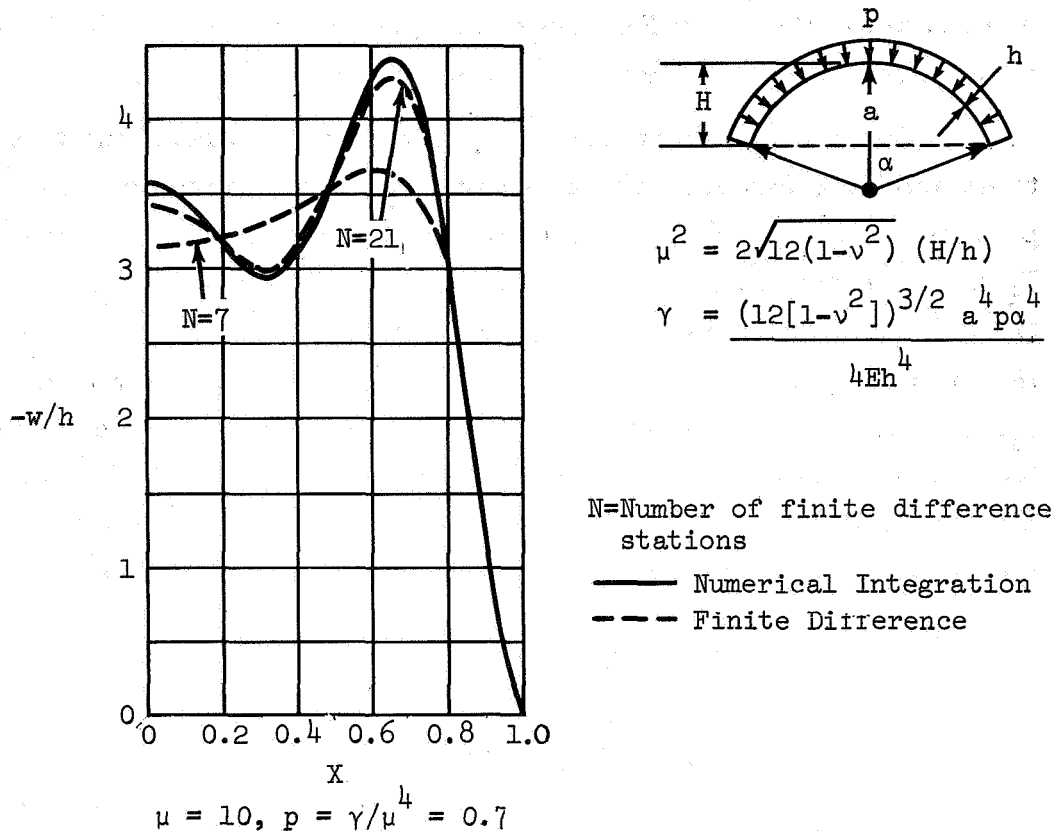$\mu = 10,\ p = \gamma/\mu^4 = 0.7$

$\mu = 20,\ p = \gamma/\mu^4 = 0.987$

Figure 3 Normal Deflection of Spherical Caps Under Uniform Pressure (Finite Differences Versus Numerical Integration) [From Reference 106]

CHAPTER 1

FORMULATION OF THE GENERAL NONLINEAR SHELL EQUATIONS

<u>Strain-Displacement Relations</u>:   The nonlinear strain-displacement equations for the Love-Reissner-Kempner shell theory are developed in Reference 100. A synopsis of this development ensues.

Consider a deformable body in a state of stress due to surface tractions and body forces. The deformation in the neighborhood of a material point is defined by the unit elongations E_α, E_β, E_γ, and the unit shears $\Gamma_{\alpha\beta}$, $\Gamma_{\beta\gamma}$, $\Gamma_{\alpha\gamma}$ referred to a system of orthogonal curvilinear coordinates α, β, γ. E_i ($i = \alpha, \beta, \gamma$) represent the change of length per unit length, due to the deformation of a line element which was in the ith direction prior to deformation. Γ_{ij} ($i, j = \alpha, \beta, \gamma$) represent the change in angle, due to the deformation between two line elements which prior to deformation were in the ith and in the jth directions ($i \neq j$). The unit elongations and shears are related to the strain components e_{ij} ($i, j = \alpha, \beta, \gamma$) by the following relations [121]

$$E_\alpha(1 + \frac{1}{2}E_\alpha) = e_{\alpha\alpha}$$

$$E_\beta(1 + \frac{1}{2}E_\beta) = e_{\beta\beta}$$

$$E_\gamma(1 + \frac{1}{2}E_\gamma) = e_{\gamma\gamma}$$

$$\sin\Gamma_{\alpha\beta} = \frac{e_{\alpha\beta}}{(1 + E_\alpha)(1 + E_\beta)}$$

$$\sin\Gamma_{\beta\gamma} = \frac{e_{\beta\gamma}}{(1 + E_\beta)(1 + E_\gamma)}$$

$$\sin\Gamma_{\gamma\alpha} = \frac{e_{\gamma\alpha}}{(1 + E_\gamma)(1 + E_\alpha)}$$

(1-1)

The strain components, e_{ij}, are sufficient and convenient measures of the deformation in the neighborhood of a material point, defined in terms of the displacement components by the following relations [121]

$$e_{\alpha\alpha} = e_{\alpha\alpha} + \frac{1}{2}[e_{\alpha\alpha}^2 + (\frac{1}{2}e_{\alpha\beta} + \omega_\gamma)^2 + (\frac{1}{2}e_{\alpha\gamma} - \omega_\beta)^2]$$

$$e_{\beta\beta} = e_{\beta\beta} + \frac{1}{2}[e_{\beta\beta}^2 + (\frac{1}{2}e_{\beta\gamma} + \omega_\alpha)^2 + (\frac{1}{2}e_{\beta\alpha} - \omega_\gamma)^2]$$

$$\epsilon_{\gamma\gamma} = e_{v\gamma} + \frac{1}{2}[e_{\gamma\gamma}^2 + (\frac{1}{2}e_{\gamma\alpha} + \omega_\beta)^2 + (\frac{1}{2}e_{\gamma\beta} - \omega_\alpha)^2$$

$$(1-2)$$

$$\epsilon_{\alpha\beta} = \epsilon_{\beta\alpha} = e_{\alpha\beta} + e_{\alpha\alpha}(\frac{1}{2}e_{\alpha\beta} - \omega_\gamma) + e_{\beta\beta}(\frac{1}{2}e_{\alpha\beta} + \omega_\gamma) + (\frac{1}{2}e_{\alpha\gamma} - \omega_\beta)(\frac{1}{2}e_{\beta\gamma} + \omega_\alpha)$$

$$\epsilon_{\beta\gamma} = \epsilon_{\gamma\beta} = e_{\beta\gamma} + e_{\beta\beta}(\frac{1}{2}e_{\beta\gamma} - \omega_\alpha) + e_{\gamma\gamma}(\frac{1}{2}e_{\beta\gamma} + \omega_\alpha) + (\frac{1}{2}e_{\beta\alpha} - \omega_\gamma)(\frac{1}{2}e_{\gamma\alpha} + \omega_\beta)$$

$$\epsilon_{\gamma\alpha} = \epsilon_{\alpha\gamma} = e_{v\alpha} + e_{\gamma\gamma}(\frac{1}{2}e_{\gamma\alpha} - \omega_\beta) + e_{\alpha\alpha}(\frac{1}{2}e_{\gamma\alpha} + \omega_\beta) + (\frac{1}{2}e_{\gamma\beta} - \omega_\alpha)(\frac{1}{2}e_{\alpha\beta} + \omega_\gamma)$$

The quantities e_{ij} and ω_i $(i, j = \alpha, \beta, \gamma)$ are defined by [121]

$$e_{\alpha\alpha} = (1/H_\alpha) u,_\alpha + (H_{\alpha,\beta}/H_\alpha H_\beta) v + (H_{\alpha,\gamma}/H_\alpha H_\gamma) w$$

$$e_{\beta\beta} = (1/H_\beta) v,_\beta + (H_{\beta,\gamma}/H_\beta H_\gamma) w + (H_{\beta,\alpha}/H_\beta H_\alpha) u$$

$$e_{\gamma\gamma} = (1/H_\gamma) w,_\gamma + (H_{\gamma,\alpha}/H_\gamma H_\alpha) u + (H_{\gamma,\beta}/H_\gamma H_\beta) v$$

$$e_{\alpha\beta} = e_{\beta\alpha} = (H_\beta/H_\alpha)(v/H_\beta),_\alpha + (H_\alpha/H_\beta)(u/H_\alpha),_\beta$$

$$e_{\beta\gamma} = e_{\gamma\beta} = (H_\gamma/H_\beta)(w/H_\gamma),_\beta + (H_\beta/H_\gamma)(v/H_\beta),_\gamma$$

$$e_{\gamma\alpha} = e_{\alpha\gamma} = (H_\alpha/H_\gamma)(u/H_\alpha),_\gamma + (H_\gamma/H_\alpha)(w/H_\gamma),_\alpha$$

$$(1-3)$$

$$2\omega_\alpha = (1/H_\beta H_\gamma)[(H_\gamma w),_\beta - (H_\beta v),_\gamma]$$

$$2\omega_\beta = (1/H_\gamma H_\alpha)[(H_\alpha u),_\gamma - (H_\gamma w),_\alpha]$$

$$2\omega_\gamma = (1/H_\alpha H_\beta)[(H_\beta v),_\alpha - (H_\alpha u),_\beta]$$

$u(\alpha, \beta, \gamma)$, $v(\alpha, \beta, \gamma)$ and $w(\alpha, \beta, \gamma)$ are the components of displacement along the coordinates α, β, γ, respectively; $\omega_i(\alpha, \beta, \gamma)$ are referred to as the

components of rotation; H_α, H_β, H_γ, are the Lame coefficients of the α, β, γ coordinate system. We shall make the assumption that the unit elongations, the unit shears and the rotations are small as compared to unity. On this basis, it can be shown [121] that

$$E_i = \epsilon_{ij} \qquad i = j$$
$$\Gamma_{ij} = \epsilon_{ij} \qquad i \neq j \tag{1-4}$$

Taking into account that ω_i^2 may be of the order of magnitude of ϵ_{ij}, Equations (1-2) reduce to

$$\epsilon_{\alpha\alpha} = e_{\alpha\alpha} + \frac{1}{2}(\omega_\beta^2 + \omega_\gamma^2)$$

$$\epsilon_{\beta\beta} = e_{\beta\beta} + \frac{1}{2}(\omega_\alpha^2 + \omega_\gamma^2)$$

$$\epsilon_{\gamma\gamma} = e_{\gamma\gamma} + \frac{1}{2}(\omega_\alpha^2 + \omega_\beta^2)$$

$$\epsilon_{\alpha\beta} = e_{\alpha\beta} - \omega_\alpha \omega_\beta$$

$$\epsilon_{\beta\gamma} = e_{\beta\gamma} - \omega_\gamma \omega_\beta$$

$$\epsilon_{\gamma\alpha} = e_{\gamma\alpha} - \omega_\alpha \omega_\gamma \tag{1-5}$$

If the assumption is made that ω_i are of the same order of magnitude as ϵ_{ij}, the above relations reduce to

$$\epsilon_{ij} = e_{ij} \qquad i, j = \alpha, \beta, \gamma \tag{1-6}$$

Consider a thin shell. The position of points on the reference surface of the shell will be determined by the curvilinear coordinates α and β which are lines of principal curvature of the reference surface. The

21

position of a general point P of the shell will be specified by the coordinates α and β of the base of the perpendicular from point P to the reference surface, and the distance ζ measured along this perpendicular. Referring to Figure 4, for a shell of revolution, these coordinates are designated by θ, φ, and ζ. The Lame coefficients for a general shell of revolution may be written as

$$H_\alpha = r_o (1 - \zeta/r_2)$$

$$H_\beta = r_1 (1 - \zeta/r_1) \qquad (1-7)$$

$$H_\gamma = H_\zeta = 1$$

Referring to Figure 4, the Lame coefficients for the reference surface, when $\zeta/r \ll 1$, are the radii of curvature (r_o, r_1) of this surface, and must satisfy the Gauss-Codazzi compatibility relations [121] given by

$$r_{o,\varphi} = r_1 \cos \varphi \qquad (1-8)$$

In obtaining the above equations the following geometrical relation has been employed.

$$r_o = r_2 \sin \varphi \qquad (1-9)$$

In general, the displacement components in a shell may be expanded in a power series expansion of the ζ coordinate

$$u(\alpha, \beta, \zeta) = u(\alpha, \beta, 0) + \left(\frac{\partial u}{\partial \zeta}\right)_0 \zeta + \frac{1}{2}\left(\frac{\partial^2 u}{\partial \zeta^2}\right)_0 \zeta^2 + \ldots$$

$$v(\alpha, \beta, \zeta) = v(\alpha, \beta, 0) + \left(\frac{\partial v}{\partial \zeta}\right)_0 \zeta + \frac{1}{2}\left(\frac{\partial^2 v}{\partial \zeta^2}\right)_0 \zeta^2 + \ldots \qquad (1-10)$$

$$w(\alpha, \beta, \zeta) = w(\alpha, \beta, 0) + \left(\frac{\partial w}{\partial \zeta}\right)_0 \zeta + \frac{1}{2}\left(\frac{\partial^2 w}{\partial \zeta^2}\right)_0 \zeta^2 + \ldots$$

Δ_Z, Δ_R, $w \equiv \Delta_\zeta$, and $v \equiv \Delta_\phi$ lie
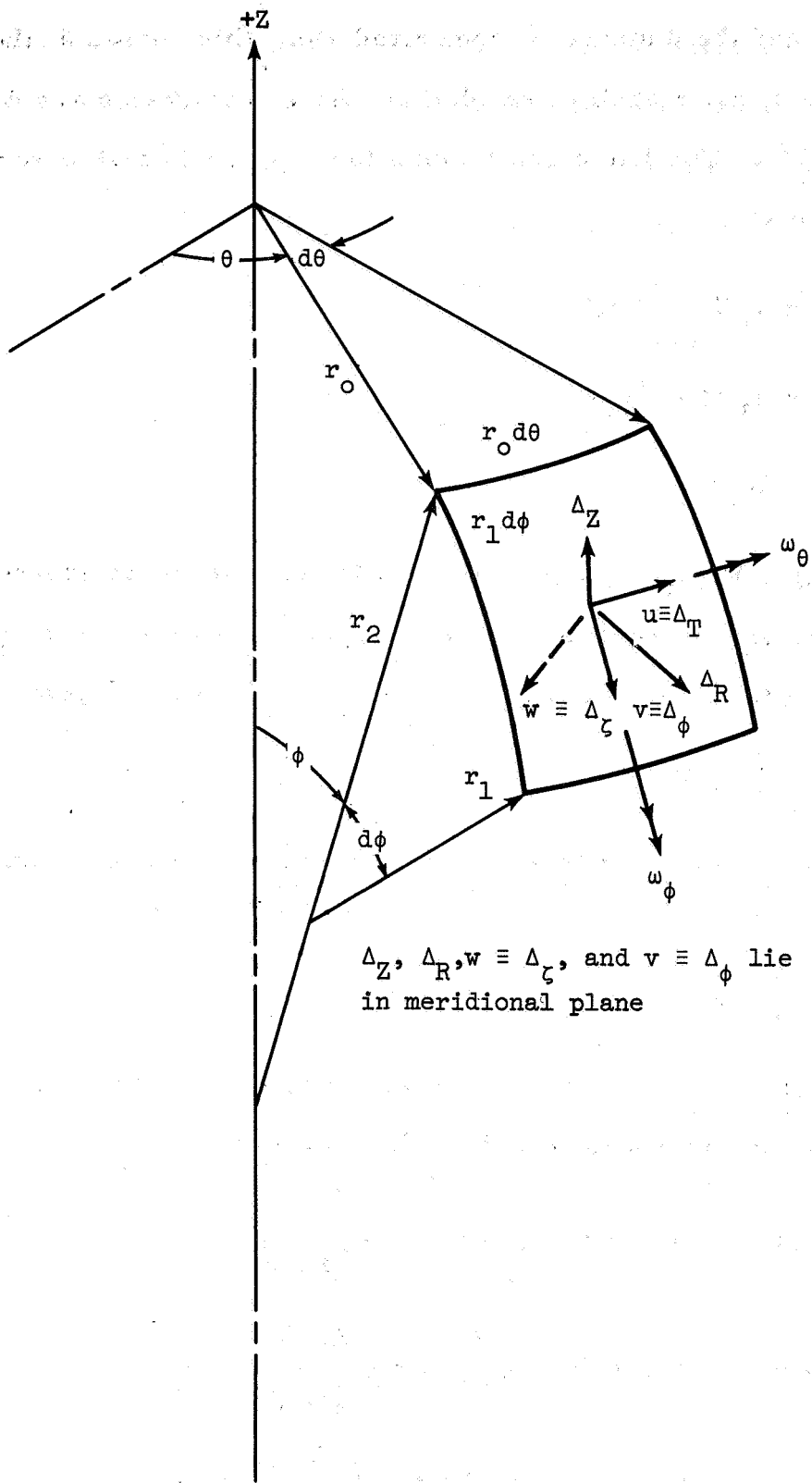in meridional plane

Figure 4   Shell Geometry and Displacements

We shall assume that it is sufficient to retain only the first two terms in the above series. This is equivalent to the Kirchoff assumption that a line normal to the reference surface remains straight subsequent to deformation. Moreover, we shall make the second Kirchoff assumption that a line normal to the reference surface remains normal to the deformed reference surface. This implies that $\epsilon_{\beta\zeta} = \epsilon_{\alpha\zeta} = 0$ at $\zeta = 0$. In addition, we shall assume that the second term in the expansion for $w(\alpha, \beta, \zeta)$ is small as compared to the first term and it can be disregarded. On this basis, Equations (1-10) reduce for a shell of revolution to

$$u(\theta, \varphi, \zeta) = u(\theta, \varphi) + \zeta\omega_\varphi$$

$$v(\theta, \varphi, \zeta) = v(\theta, \varphi) - \zeta\omega_\theta \qquad (1-11)$$

$$w(\theta, \varphi, \zeta) = w(\theta, \varphi)$$

Substituting Equations (1-11) into Equations (1-3), and using Equations (1-8) and (1-9) it can be shown that

$$e_{\theta\theta} = [1 - \zeta/r_2]^{-1}\left\{\frac{1}{r_o}(u+\zeta\omega_\varphi)_{,\theta} + \frac{\cos\varphi}{r_o}(v-\zeta\omega_\theta) - \frac{w}{r_2}\right\}$$

$$e_{\varphi\varphi} = [1 - \zeta/r_1]^{-1}\left\{\frac{1}{r_1}(v-\zeta\omega_\theta)_{,\varphi} - \frac{w}{r_1}\right\}$$

$$e_{\theta\varphi} = [1 - \zeta/r_2]^{-1}\left\{\frac{1}{r_o}(v-\zeta\omega_\theta)_{,\theta} - \frac{\cos\varphi}{r_o}(u+\zeta\omega_\varphi)\right\} + [1 - \zeta/r_1]^{-1}\left\{\frac{1}{r_1}(u+\zeta\omega_\varphi)_{,\varphi}\right\}$$

$$e_{\zeta\zeta} = e_{\varphi\zeta} = e_{\zeta\theta} = 0 \qquad (1-12)$$

$$\omega_\theta = \frac{1}{r_1}(w_{,\varphi} + v)$$

$$\omega_\varphi = -\frac{1}{r_o}(w_{,\theta} + u\sin\varphi)$$

24

$$2\omega_\zeta = [1-\zeta/r_2]^{-1}\left\{\frac{1}{r_o}(v-\zeta\omega_\theta),_\theta - \frac{\cos\varphi}{r_o}(u+\zeta\omega_\varphi)\right\} - [1-\zeta/r_1]^{-1}\left\{\frac{1}{r_1}(u+\zeta\omega_\varphi),_\varphi\right\}$$

The above relations correspond to the Flugge-Byrne shell theory [122, 123].

They may be further simplified by disregarding $\frac{\zeta}{r_i}$ (i = 1, 2) as compared to

unity. Thus, Equations (1-12) reduce to the following relations of

Love-Reissner-Kempner accuracy

$$e_{\theta\theta} = e_{\theta\theta_o} - \zeta k_\theta$$

$$e_{\varphi\varphi} = e_{\varphi\varphi_o} - \zeta k_\varphi \qquad\qquad (1\text{-}13)$$

$$e_{\theta\varphi} = e_{\theta\varphi_o} - 2\zeta k_{\theta\varphi}$$

where:

$$e_{\theta\theta_o} = \frac{1}{r_o}\left\{u,_\theta + v\cos\varphi - w\sin\varphi\right\}$$

$$e_{\varphi\varphi_o} = \frac{1}{r_1}\left\{v,_\varphi - w\right\}$$

$$e_{\theta\varphi_o} = \frac{1}{r_o}\left\{v,_\theta - u\cos\varphi\right\} + \frac{u,_\varphi}{r_1}$$

$$k_\theta = -\frac{1}{r_o}\left\{\omega_\varphi,_\theta - \omega_\theta\cos\varphi\right\} \qquad\qquad (1\text{-}14)$$

$$k_\varphi = \frac{1}{r_1}\omega_\theta,_\varphi$$

$$k_{\theta\varphi} = \frac{1}{2r_o}\left\{\omega_\theta,_\theta - \frac{r_o}{r_1}\omega_\varphi,_\varphi + \omega_\varphi\cos\varphi\right\}$$

and ω_θ, ω_φ have been defined in Equations (1-12).

For thin-walled shells, generally the rotation component ω_ζ is
considerably smaller than the rotation components ω_θ, ω_φ, and may be
disregarded. Thus, for thin shells, the non-linear strain Equations (1-5)
can be further simplified to give

$$\epsilon_{\theta\theta} = e_{\theta\theta} + \frac{1}{2} \omega_\varphi^2$$

$$\epsilon_{\varphi\varphi} = e_{\varphi\varphi} + \frac{1}{2} \omega_\theta^2$$

$$\epsilon_{\zeta\zeta} = \frac{1}{2} (\omega_\theta^2 + \omega_\varphi^2) \tag{1-15}$$

$$\epsilon_{\theta\varphi} = e_{\theta\varphi} - \omega_\theta \omega_\varphi$$

$\epsilon_{\beta\gamma} = \epsilon_{\varphi\zeta}$ and $\epsilon_{\alpha\gamma} = \epsilon_{\theta\zeta}$ are assumed negligible compared to $\epsilon_{\theta\varphi}$.

<u>Stress Resultant-Strain Relations</u>: The stress resultants may be defined as

$$N_\theta = \int \sigma_\theta d\zeta \qquad\qquad M_\theta = \int \sigma_\theta \zeta \, d\zeta$$

$$N_\varphi = \int \sigma_\varphi d\zeta \qquad\qquad M_\varphi = \int \sigma_\varphi \zeta d\zeta \tag{1-16}$$

$$N_{\varphi\theta} = +N_{\theta\varphi} = \int \tau_{\theta\varphi} d\zeta \qquad\qquad M_{\varphi\theta} = -M_{\theta\varphi} = + \int \tau_{\theta\varphi} \zeta \, d\zeta$$

$$N_{T\theta} = \int \frac{E_\theta (\alpha_\theta + \nu_{\theta\varphi}\alpha_\varphi) T}{1 - \nu_{\varphi\theta}\nu_{\theta\varphi}} d\zeta \qquad\qquad M_{T\theta} = \int \frac{E_\theta (\alpha_\theta + \nu_{\theta\varphi}\alpha_\varphi) T}{1 - \nu_{\varphi\theta}\nu_{\theta\varphi}} \zeta \, d\zeta$$

$$\tag{1-17}$$

$$N_{T\varphi} = \int \frac{E_\varphi (\alpha_\varphi + \nu_{\varphi\theta}\alpha_\theta) T}{1 - \nu_{\varphi\theta}\nu_{\theta\varphi}} d\zeta \qquad\qquad M_{T\varphi} = \int \frac{E_\varphi (\alpha_\varphi + \nu_{\varphi\theta}\alpha_\theta) T}{1 - \nu_{\varphi\theta}\nu_{\theta\varphi}} \zeta d\zeta$$

where T is the temperature distribution in the ζ direction, and the integrals are taken over the thickness of the shell (see Figures 5 and 6). In these definitions, the coordinate "ζ" is assumed negligible compared to "r". To this order of approximation, the difference between the inside and outside dimensions of an element of the shell becomes negligible [124]. If these assumptions were not made, then $N_{\theta\varphi} \neq N_{\varphi\theta}$ and $M_{\theta\varphi} \neq -M_{\varphi\theta}$, since the radii associated with the φ and θ directions are generally, unequal ($r_1 \neq r_2$).

Introducing the stress-strain relations for an orthotropic body in a state of plane stress into Equations (1-16), (1-17), using Equations (1-13), and

26
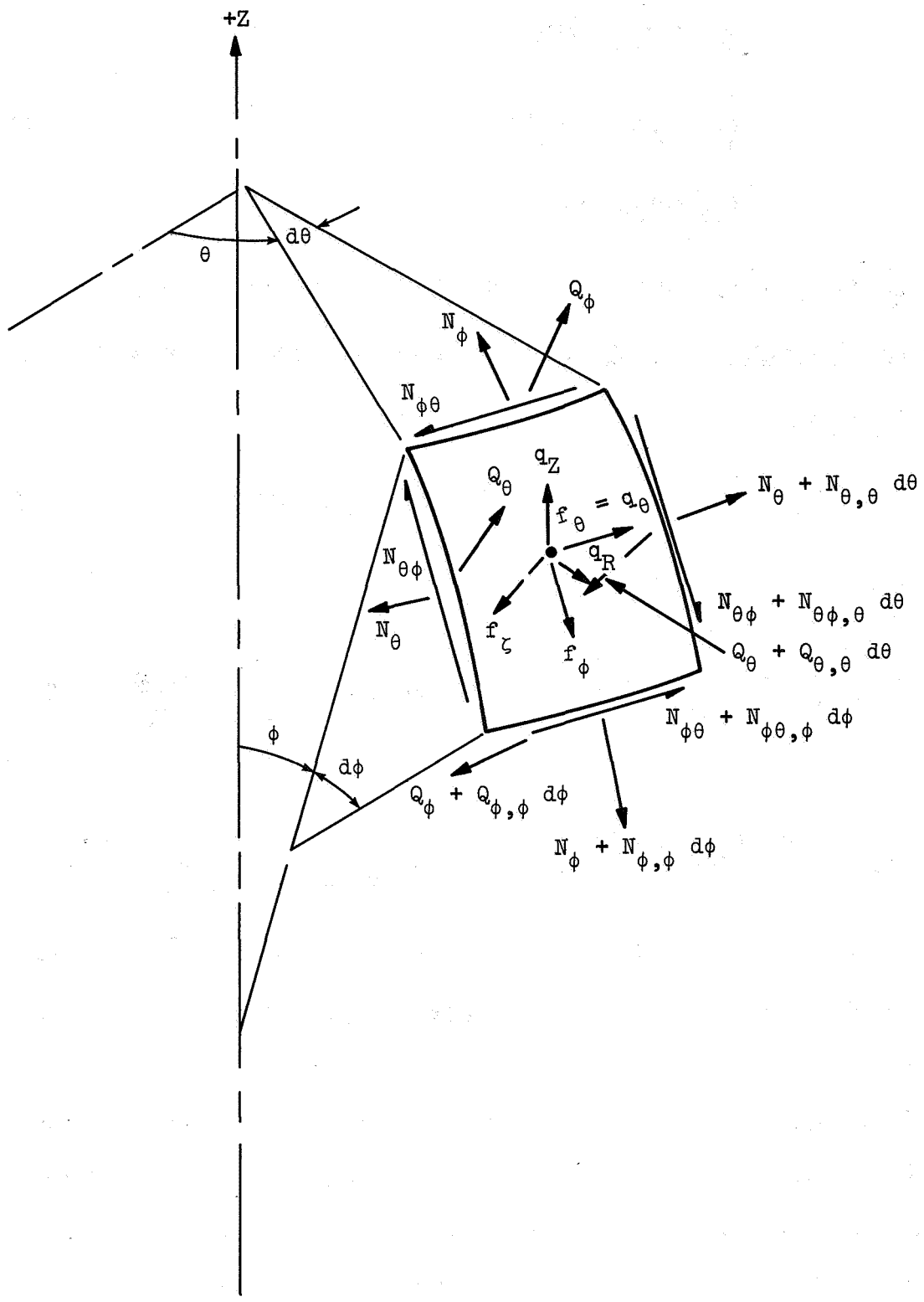
Figure 5 Forces on Shell Element

27
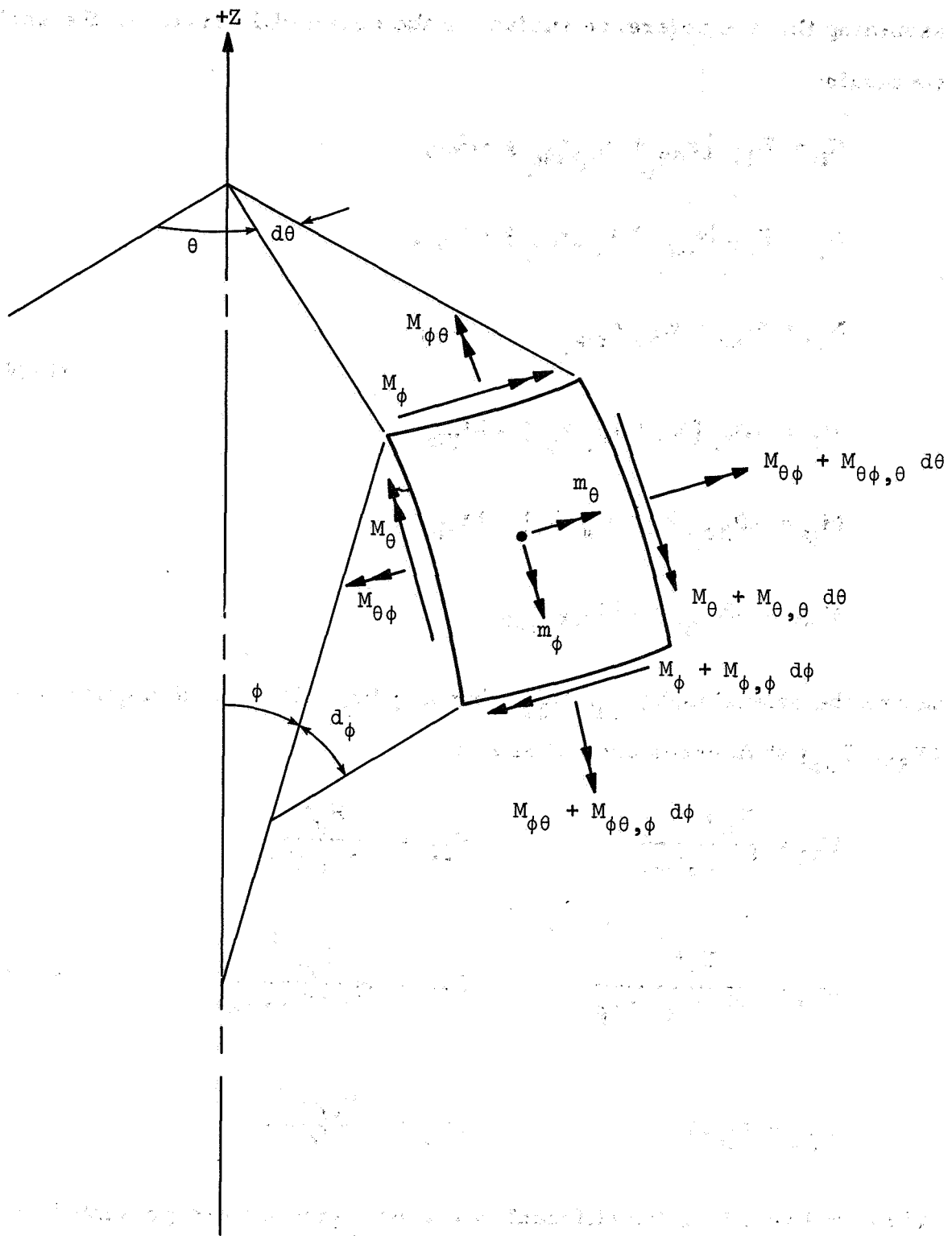
Figure 6 Moments On Shell Element

28

assuming that the reference surface is the centroidal surface of the shell, we obtain:

$$N_\theta = K_{11} \left[\epsilon_{\theta\theta_o} + \nu_{\theta\varphi} \epsilon_{\varphi\varphi_o} \right] - N_{T\theta}$$

$$N_\varphi = K_{22} \left[\epsilon_{\varphi\varphi_o} + \nu_{\varphi\theta} \epsilon_{\theta\theta_o} \right] - N_{T\varphi}$$

$$N_{\varphi\theta} = N_{\theta\varphi} = K_{33} \epsilon_{\varphi\theta_o}$$

$$M_\theta = -D_{11} \left[k_\theta + \nu_{\theta\varphi} k_\varphi \right] - M_{T\theta}$$

(1-18)

$$M_\varphi = -D_{22} \left[k_\varphi + \nu_{\varphi\theta} k_\theta \right] - M_{T\varphi}$$

$$M_{\varphi\theta} = -M_{\theta\varphi} = -2 D_{33} k_{\varphi\theta}$$

where the extensional (K_{11}, K_{22}), bending (D_{11}, D_{22}), and in-plane shear (K_{33}, D_{33}) stiffnesses are defined as

$$K_{11} = \frac{E_\theta h}{1 - \nu_{\varphi\theta} \nu_{\theta\varphi}} \qquad K_{22} = \frac{E_\varphi h}{1 - \nu_{\varphi\theta} \nu_{\theta\varphi}}$$

$$D_{11} = \frac{E_\theta h^3}{12(1 - \nu_{\varphi\theta} \nu_{\theta\varphi})} \qquad D_{22} = \frac{E_\varphi h^3}{12(1 - \nu_{\varphi\theta} \nu_{\theta\varphi})} \qquad (1\text{-}19)$$

$$K_{33} = G_{\varphi\theta} h \qquad D_{33} = \frac{G_{\varphi\theta} h^3}{12}$$

Additional relations for different wall cross-sections are presented in Figure 7.

Equilibrium Equations: In Reference 100 the following nonlinear stress equilibrium equations are obtained
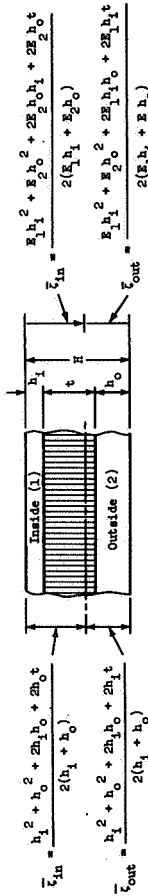
Figure 7. Shell Section Properties

Diagram (cross-section): Inside (1), Outside (2); dimensions h_i, t, h_o, H.

E, ν, Constant through thickness:

$$\bar{\zeta}_{in} = \frac{h_i^2 + h_o^2 + 2h_i h_o + 2h_o t}{2(h_i + h_o)}$$

$$\bar{\zeta}_{out} = \frac{h_i^2 + h_o^2 + 2h_i h_o + 2h_i t}{2(h_i + h_o)}$$

Unequal material properties for the face sheets.
Restriction: <u>properties are such that a neutral plane exists.</u>

$$\bar{\zeta}_{in} = \frac{E_i h_i^2 + E_o h_o^2 + 2E_o h_o t + 2E_o h_o t}{2(E_i h_i + E_o h_o)}$$

$$\bar{\zeta}_{out} = \frac{E_i h_i^2 + E_o h_o^2 + 2E_o h_o t + 2E_i h_o t}{2(E_i h_i + E_o h_o)}$$

Configuration	Extensional Stiffness	Flexural Stiffness	Shear Stiffness
Ortho-tropic	$K_{11} = \dfrac{E_\theta h_i}{1 - \nu_{\phi\theta}\nu_{\theta\phi}}$ $K_{22} = \dfrac{E_\phi h_i}{1 - \nu_{\phi\theta}\nu_{\theta\phi}}$	$D_{11} = \dfrac{E_\theta h_i^3}{12(1 - \nu_{\phi\theta}\nu_{\theta\phi})}$ $D_{22} = \dfrac{E_\phi h_i^3}{12(1 - \nu_{\phi\theta}\nu_{\theta\phi})}$	$K_{33} = G_{\phi\theta} h_i$ $D_{33} = \dfrac{G_{\phi\theta} h_i^3}{12}$
Equal Face Sheets	$K_{11} = \dfrac{E_{\theta_1} h_i}{1-\nu_{\phi\theta_1}\nu_{\theta\phi_1}} + \dfrac{E_{\theta_2} h_i}{1-\nu_{\phi\theta_2}\nu_{\theta\phi_2}}$ $K_{22} = \dfrac{E_{\phi_1} h_i}{1-\nu_{\phi\theta_1}\nu_{\theta\phi_1}} + \dfrac{E_{\phi_2} h_i}{1-\nu_{\phi\theta_2}\nu_{\theta\phi_2}}$	$D_{11} = \dfrac{E_{\theta_1} h_i^3}{12(1-\nu_{\phi\theta_1}\nu_{\theta\phi_1})} + \dfrac{E_{\theta_2} h_i^3}{12(1-\nu_{\phi\theta_2}\nu_{\theta\phi_2})} + h_i\left\{ \dfrac{E_{\theta_1}(\bar\zeta_{in}-\frac{h_i}{2})^2}{1-\nu_{\phi\theta_1}\nu_{\theta\phi_1}} + \dfrac{E_{\theta_2}(\bar\zeta_{out}-\frac{h_i}{2})^2}{1-\nu_{\phi\theta_2}\nu_{\theta\phi_2}} \right\}$ $D_{22} = \dfrac{E_{\phi_1} h_i^3}{12(1-\nu_{\phi\theta_1}\nu_{\theta\phi_1})} + \dfrac{E_{\phi_2} h_i^3}{12(1-\nu_{\phi\theta_2}\nu_{\theta\phi_2})} + h_i\left\{ \dfrac{E_{\phi_1}(\bar\zeta_{in}-\frac{h_i}{2})^2}{1-\nu_{\phi\theta_1}\nu_{\theta\phi_1}} + \dfrac{E_{\phi_2}(\bar\zeta_{out}-\frac{h_i}{2})^2}{1-\nu_{\phi\theta_2}\nu_{\theta\phi_2}} \right\}$	$K_{33} = h_i(G_{\phi\theta_1} + G_{\phi\theta_2})$ $D_{33} = \dfrac{h_i^3}{12}(G_{\phi\theta_1} + G_{\phi\theta_2}) + h_i\left[G_{\phi\theta_1}\left(\bar\zeta_{in} - \frac{h_i}{2}\right)^2 + G_{\phi\theta_2}\left(\bar\zeta_{out} - \frac{h_i}{2}\right)^2\right]$
Unequal Face Sheets	$K_{11} = \dfrac{E_{\theta_1} h_i}{1-\nu_{\phi\theta_1}\nu_{\theta\phi_1}} + \dfrac{E_{\theta_2} h_o}{1-\nu_{\phi\theta_2}\nu_{\theta\phi_2}}$ $K_{22} = \dfrac{E_{\phi_1} h_i}{1-\nu_{\phi\theta_1}\nu_{\theta\phi_1}} + \dfrac{E_{\phi_2} h_o}{1-\nu_{\phi\theta_2}\nu_{\theta\phi_2}}$	$D_{11} = \dfrac{E_{\theta_1} h_i^3}{12(1-\nu_{\phi\theta_1}\nu_{\theta\phi_1})} + \dfrac{E_{\theta_2} h_o^3}{12(1-\nu_{\phi\theta_2}\nu_{\theta\phi_2})} + \dfrac{E_{\theta_1} h_i(\bar\zeta_{in}-\frac{h_i}{2})^2}{1-\nu_{\phi\theta_1}\nu_{\theta\phi_1}} + \dfrac{E_{\theta_2} h_o(\bar\zeta_{out}-\frac{h_o}{2})^2}{1-\nu_{\phi\theta_2}\nu_{\theta\phi_2}}$ $D_{22} = \dfrac{E_{\phi_1} h_i^3}{12(1-\nu_{\phi\theta_1}\nu_{\theta\phi_1})} + \dfrac{E_{\phi_2} h_o^3}{12(1-\nu_{\phi\theta_2}\nu_{\theta\phi_2})} + \dfrac{E_{\phi_1} h_i(\bar\zeta_{in}-\frac{h_i}{2})^2}{1-\nu_{\phi\theta_1}\nu_{\theta\phi_1}} + \dfrac{E_{\phi_2} h_o(\bar\zeta_{out}-\frac{h_o}{2})^2}{1-\nu_{\phi\theta_2}\nu_{\theta\phi_2}}$	$K_{33} = G_{\phi\theta_1} h_i + G_{\phi\theta_2} h_o$ $D_{33} = \dfrac{G_{\phi\theta_1} h_i^3}{12} + \dfrac{G_{\phi\theta_2} h_o^3}{12} + G_{\phi\theta_1} h_i\left(\bar\zeta_{in}-\frac{h_i}{2}\right)^2 + G_{\phi\theta_2} h_o\left(\bar\zeta_{out}-\frac{h_o}{2}\right)^2$

$$r_1 N_{\theta,\theta} + \frac{1}{r_o}(N_{\varphi\theta}r_o^2)_{,\varphi} - Q_\theta r_1 \sin\varphi = -r_1 r_o(f_\theta^* + f_\theta)$$

$$(N_\varphi r_o)_{,\varphi} + r_1 N_{\varphi\theta,\theta} - N_\theta r_1 \cos\varphi - r_o Q_\varphi = -r_1 r_o(f_\varphi^* + f_\varphi)$$

$$(Q_\varphi r_o)_{,\varphi} + r_1 Q_{\theta,\theta} + r_o N_\varphi + N_\theta r_1 \sin\varphi = -r_1 r_o(f_\zeta^* + f_\zeta) \qquad (1\text{-}20)$$

$$-r_1 M_{\varphi\theta,\theta} - (M_\varphi r_o)_{,\varphi} + M_\theta r_1 \cos\varphi + r_1 r_o Q_\varphi = -r_1 r_o m_\theta$$

$$-(M_{\varphi\theta}r_o)_{,\varphi} - r_1 M_{\theta,\theta} - M_{\varphi\theta} r_1 \cos\varphi + r_1 r_o Q_\theta = -r_1 r_o m_\varphi$$

$$N_{\theta\varphi} - N_{\varphi\theta} + \frac{M_{\theta\varphi}}{r_2} + \frac{M_{\varphi\theta}}{r_1} = 0$$

where

$$f_\theta^* = \frac{1}{r_2}[N_\theta \omega_\varphi - N_{\varphi\theta}\omega_\theta]$$

$$f_\varphi^* = \frac{1}{r_1}[N_{\varphi\theta}\omega_\varphi - N_\varphi \omega_\theta]$$

$$f_\zeta^* = \frac{1}{r_o r_1}(\{r_1[N_{\varphi\theta}\omega_\theta - N_\theta \omega_\varphi]\}_{,\theta} + \{r_o[N_\varphi \omega_\theta - N_{\varphi\theta}\omega_\varphi]\}_{,\varphi}) \qquad (1\text{-}21)$$

$$f_\theta = F_\theta(1 + \epsilon_{\theta\theta_o} + \epsilon_{\varphi\varphi_o}) + F_\varphi \frac{u_{,\varphi}}{r_1} + F_\zeta \omega_\varphi$$

$$f_\varphi = F_\varphi(1 + \epsilon_{\theta\theta_o} + \epsilon_{\varphi\varphi_o}) + F_\theta \frac{v_{,\theta}}{r_o} - F_\zeta \omega_\theta$$

$$f_\zeta = F_\zeta(1 + \epsilon_{\theta\theta_o} + \epsilon_{\varphi\varphi_o}) - F_\theta \omega_\varphi + F_\varphi \omega_\theta \qquad (1\text{-}22)$$

where $F_i(i = \theta, \varphi, \zeta)$ are the applied forces tangential and normal to the deformed shell surface, whereas $f_i(i = \theta, \varphi, \zeta)$ are the forces along the undeformed coordinate system (see Ref. 137). The first three of Equations (1-20) are obtained by setting to zero the sum of the θ, φ and ζ components of all the forces acting on a shell element. The last three of Equations (1-20) are obtained by setting to zero the sum of the moments about the i_θ, i_φ, and

31

$\underline{i}_\zeta$ axis. As a result of the assumption that $\zeta \ll r$, the sixth equilibrium equation cannot be satisfied except for the special case of a sphere. However, within the framework of the present theory, this equation will not be employed in the solution of shell problems.

Boundary Conditions: As shown in Reference 100, for a unique solution either displacements or corresponding stress resultants may be specified on the boundary $\varphi = $ constant.

$$
\begin{array}{lll}
u & \text{or} & T_{\varphi\theta} \\[2mm]
v & \text{or} & N_\varphi \\[2mm]
w & \text{or} & J_\varphi^* = J_\varphi - r_1 f_\varphi^* \\[2mm]
\omega_\theta & \text{or} & M_\varphi
\end{array} \tag{1-23}
$$

The quantities $T_{\varphi\theta}$, J_φ^*, J_φ are referred to as the effective stress resultants and are defined by:

$$
T_{\varphi\theta} = N_{\varphi\theta} - \frac{M_{\varphi\theta}}{r_o} \sin \varphi
$$

$$
J_\varphi = Q_\varphi + \frac{M_{\varphi\theta,\theta}}{r_o} \tag{1-24}
$$

$$
J_\varphi^* = J_\varphi - N_{\varphi\theta}\omega_\varphi + N_\varphi \omega_\theta
$$

Convenient Form of the Shell Equations: In this section, the stress-resultant, strain relations and the stress-resultant equilibrium equations will be combined to obtain differential equations suitable for the Runge-Kutta integration procedure to be used in their solution [125-128]. Be eliminating the strains and curvatures in Equations (1-18), using Equations (1-13) through (1-15) and the relation between the elastic constants $\nu_{\theta\varphi} E_\theta = \nu_{\varphi\theta} E_\varphi$, the following relations between the stress resultants and the displacements may be obtained,

$$N_\theta = \nu_{\varphi\theta}N_\varphi + (K_{11} - \nu_{\varphi\theta}^2 K_{22})\left[\frac{u,_\theta + v\cos\varphi - w\sin\varphi}{r_o} + \frac{1}{2}\omega_\varphi^2\right] - N_{T\theta} + \nu_{\varphi\theta}N_{T\varphi}$$

$$N_\varphi = \nu_{\theta\varphi}N_\theta + (K_{22} - \nu_{\theta\varphi}^2 K_{11})\left[\frac{v,_\varphi - w}{r_1} + \frac{1}{2}\omega_\theta^2\right] - N_{T\varphi} + \nu_{\theta\varphi}N_{T\theta}$$

$$N_{\varphi\theta} = N_{\theta\varphi} = K_{33}\left[\frac{v,_\theta - u\cos\varphi}{r_o} + \frac{u,_\varphi}{r_1} - \omega_\theta\omega_\varphi\right] \qquad\qquad (1\text{-}25)$$

$$M_\theta = \nu_{\varphi\theta}M_\varphi - \frac{(D_{11} - \nu_{\varphi\theta}^2 D_{22})}{r_o}\left[\frac{w,_{\theta\theta} + u,_\theta \sin\varphi}{r_o} + \omega_\theta\cos\varphi\right] - M_{T\theta} + \nu_{\varphi\theta}M_{T\varphi}$$

$$M_\varphi = \nu_{\theta\varphi}M_\theta - (D_{22} - \nu_{\theta\varphi}^2 D_{11})\left[\frac{\omega_{\theta,\varphi}}{r_1}\right] - M_{T\varphi} + \nu_{\theta\varphi}M_{T\theta}$$

$$M_{\varphi\theta} = -\frac{D_{33}}{r_o}\left[\omega_{\theta,\theta} - \frac{r_o}{r_1}\omega_{\varphi,\varphi} + \omega_\varphi\cos\varphi\right]$$

Using Equations (1-12f), (1-24a), and (1-25c)

$$M_{\varphi\theta} = \left[\frac{-1}{\dfrac{r_o}{D_{33}} + \dfrac{\sin^2\varphi}{r_o K_{33}}}\right]\left\{2\omega_{\theta,\theta} + u\left(\frac{\cos\varphi}{r_1} - \frac{\cos\varphi\sin\varphi}{r_o}\right) - v,_\theta\left(\frac{\sin\varphi}{r_o} + \frac{1}{r_1}\right)\right.$$

$$\left. -2w,_\theta\ \frac{\cos\varphi}{r_o} + \omega_\theta\omega_\varphi\sin\varphi + \frac{T_{\varphi\theta}}{K_{33}}\sin\varphi\right\} \qquad\qquad (1\text{-}26)$$

The final form of the differential equations necessary for the Runge-Kutta integration procedure [128] may be divided into two groups. The first group of four differential equations is obtained by eliminating Q_θ from the

equilibrium equations, and by introducing the effective stress resultants defined by Equations (1-24) and their derivatives with respect to φ,

$$\frac{T_{\varphi\theta,\varphi}}{r_1} = -2T_{\varphi\theta}\frac{\cos\varphi}{r_o} - \frac{N_{\theta,\theta}}{r_o} + M_{\theta,\theta}\frac{\sin\varphi}{r_o^2} - M_{\varphi\theta}\frac{\cos\varphi}{r_o}\left[\frac{1}{r_1} - \frac{\sin\varphi}{r_o}\right]$$

$$- f_\theta - m_\varphi\frac{\sin\varphi}{r_o} - \frac{\sin\varphi}{r_o}\left[N_\theta\omega_\varphi - N_{\varphi\theta}\omega_\theta\right]$$

$$\frac{N_{\varphi,\varphi}}{r_1} = -N_\varphi\frac{\cos\varphi}{r_o} + N_\theta\frac{\cos\varphi}{r_o} - \frac{T_{\varphi\theta,\theta}}{r_o} - M_{\varphi\theta,\theta}\left[\frac{\sin\varphi}{r_o^2} + \frac{1}{r_o r_1}\right] + \frac{J_\varphi^*}{r_1}$$

$$- f_\varphi \tag{1-27}$$

$$\frac{J_{\varphi,\varphi}^*}{r_1} = -J_\varphi^*\frac{\cos\varphi}{r_o} - N_\theta\frac{\sin\varphi}{r_o} - \frac{N_\varphi}{r_1} - \frac{M_{\theta,\theta\theta}}{r_o^2} - 2M_{\varphi\theta,\theta}\frac{\cos\varphi}{r_o^2} - f_\zeta + \frac{m_{\varphi,\theta}}{r_o}$$

$$- \frac{1}{r_o}\left[N_{\varphi\theta}\omega_\theta - N_\theta\omega_\varphi\right]_{,\theta}$$

$$\frac{M_{\varphi,\varphi}}{r_1} = M_\theta\frac{\cos\varphi}{r_o} - M_\varphi\frac{\cos\varphi}{r_o} - 2\frac{M_{\varphi\theta,\theta}}{r_o} + J_\varphi + m_\theta$$

The second group of four differential equations is obtained by combining Equations (1-12e), (1-24a) and (1-25b, c, e).

$$\frac{u_{,\varphi}}{r_1} = u\frac{\cos\varphi}{r_o} - \frac{v_{,\theta}}{r_o} + \frac{T_{\varphi\theta}}{K_{33}} + \frac{M_{\varphi\theta}\sin\varphi}{r_o}\frac{1}{K_{33}} + \omega_\theta\omega_\varphi \tag{1-28}$$

$$\frac{v,_\varphi}{r_1} = \frac{w}{r_1} + (K_{22} - \nu_{\theta\varphi}^2 K_{11})^{-1} \{ N_\varphi - \nu_{\theta\varphi} N_\theta + N_{T\varphi} - \nu_{\theta\varphi} N_{T\theta} \} - \frac{1}{2} \omega_\theta^2$$

$$\frac{w,_\varphi}{r_1} = \omega_\theta - \frac{v}{r_1}$$

$$\frac{\omega_{\theta,\varphi}}{r_1} = (D_{22} - \nu_{\theta\varphi}^2 D_{11})^{-1} \{ -M_\varphi + \nu_{\theta\varphi} M_\theta - M_{T\varphi} + \nu_{\theta\varphi} M_{T\theta} \} \qquad (1-28)$$

In Equations (1-27) and (1-28) the stress resultants N_θ, $N_{\varphi\theta}$, the resultant moments M_θ, $M_{\varphi\theta}$, the rotation, ω_φ, and the effective stress resultant, J_φ, may be eliminated by using Equations (1-25a, d), (1-26), (1-24a, c) and (1-12f). The equations for these variables may be rewritten as,

$$N_\theta = \nu_{\varphi\theta} N_\varphi + (K_{11} - \nu_{\varphi\theta}^2 K_{22}) \left[\frac{u,_\theta + v\cos\varphi - w\sin\varphi}{r_o} + \frac{1}{2}\omega_\varphi^2 \right] - N_{T\theta} + \nu_{\varphi\theta} N_{T\varphi}$$

$$M_\theta = \nu_{\varphi\theta} M_\varphi - \frac{(D_{11} - \nu_{\varphi\theta}^2 D_{22})}{r_o} \left[\frac{w,_{\theta\theta} + u,_\theta \sin\varphi}{r_o} + \omega_\theta \cos\varphi \right] - M_{T\theta} + \nu_{\varphi\theta} M_{T\varphi}$$

$$M_{\varphi\theta} = \left[\frac{-1}{\frac{r_o}{D_{33}} + \frac{\sin^2\varphi}{r_o K_{33}}} \right] \left\{ 2\omega_{\theta,\theta} + u \left(\frac{\cos\varphi}{r_1} - \frac{\cos\varphi\sin\varphi}{r_o} \right) - v,_\theta \left(\frac{\sin\varphi}{r_o} + \frac{1}{r_1} \right) \right.$$

$$\left. -2w,_\theta \frac{\cos\varphi}{r_o} + \omega_\theta \omega_\varphi \sin\varphi + \frac{T_{\varphi\theta}}{K_{33}} \sin\varphi \right\} \qquad (1-29)$$

$$N_{\varphi\theta} = T_{\varphi\theta} + \frac{M_{\varphi\theta}}{r_o} \sin\varphi$$

$$\omega_\varphi = -\frac{w,_\theta}{r_o} - \frac{u \sin\varphi}{r_o}$$

$$J_\varphi = J_\varphi^* + N_{\varphi\theta}\omega_\varphi - N_\varphi\omega_\theta \qquad\qquad (1\text{-}29)$$

Equations (1-27) through (1-29) represent a complete formulation of the nonlinear problem for a thin orthotropic shell, on the basis of the Love-Reissner-Kempner theory. Analogous formulations may be obtained by employing other shell theories. The basic differences between the various formulations will be in the coefficients of the equations, and in the number of differential equations. For example, in theories involving shear deformation ten basic differential equations may be obtained [105].

For general doubly-curved shells, the above equations may be written with the angle φ as the independent variable, whereas, for cones and cylinders they may be written more conveniently with the arc length s (s = $r_1 d\varphi$) as the independent variable. The stress resultants and displacements involved in these equations may be expanded in Fourier series in the θ direction. Thus, Equations (1-27) and (1-28) will constitute a basic system of 8 first-order ordinary differential equations in the variable φ, and Equations (1-29) will constitute 6 algebraic equations. Notice, that derivatives of the shell geometric parameters do not appear in the coefficients of these equations. Moreover, notice that the 8 unknown variables are the quantities which enter into the appropriate boundary conditions on the edge φ = constant of a shell of revolution.

Equations (1-27) through (1-29) will be solved by a forward numerical integration procedure in conjunction with the direct stiffness matrix method (see Chapter 3). The stress resultants Q_φ and Q_θ, not involved in the above formulation, may be obtained from Equations (1-24b) and (1-20e),

36

which may be rewritten as

$$Q_\varphi = J_\varphi - \frac{M_{\varphi\theta,\theta}}{r_o}$$

$$Q_\theta = \left\{ \frac{3\cos\varphi}{r_o} - \frac{2\cos\varphi(r_o K_{33}+D_{33}\frac{\sin\varphi}{r_1})}{r_o^2 K_{33}+D_{33}\sin^2\varphi} \right\} M_{\varphi\theta} + \left[\frac{\frac{-1}{r_1}}{\frac{r_o}{D_{33}}+\frac{\sin^2\varphi}{r_o K_{33}}} \right] \left\{ 2\omega_{\theta,\theta\varphi} + u_{,\varphi}(\frac{\cos\varphi}{r_1} \right. $$

$$- \frac{\cos\varphi\sin\varphi}{r_o}) + u\left(\frac{\sin^2\varphi}{r_o} - \frac{\cos^2\varphi}{r_o} - \frac{\sin\varphi}{r_1} - \frac{r_{1,\varphi}\cos\varphi}{r_1^2} + \frac{r_1\cos^2\varphi\sin\varphi}{r_o^2}\right)$$

$$-v_{,\theta\varphi}\left(\frac{\sin\varphi}{r_o}+\frac{1}{r_1}\right) - v_{,\theta}\left(\frac{\cos\varphi}{r_o} - \frac{r_1\sin\varphi\cos\varphi}{r_o^2} - \frac{r_{1,\varphi}}{r_1^2}\right) - 2w_{,\theta\varphi}\frac{\cos\varphi}{r_o}$$

$$+2w_{,\theta}\left(\frac{\sin\varphi}{r_o} + \frac{r_1\cos^2\varphi}{r_o^2}\right) + T_{\varphi\theta,\varphi}\frac{\sin\varphi}{K_{33}} + T_{\varphi\theta}\frac{\cos\varphi}{K_{33}} + \omega_{\theta,\varphi}\omega_\varphi\sin\varphi$$

$$\left. +\omega_\theta\left(\omega_\varphi\cos\varphi + \frac{r_1\cos\varphi\sin\varphi}{r_o^2}[w_{,\theta}+u\sin\varphi] - \frac{\sin\varphi}{r_o}[w_{,\theta\varphi}+u_{,\varphi}\sin\varphi+u\cos\varphi]\right) \right\}$$

$$+\frac{M_{\theta,\theta}}{r_o} - m_\varphi \tag{1-30}$$

The simplicity of the aforegoing formulation of the basic shell equations results in greater accuracy in the numerical solution. Notice that Equation (1-30b) involves derivatives of shell geometric parameters. However, the computation of Q_θ is a secondary operation in the solution of the problem. In solutions of nonlinear unsymmetric loading problems with finite differences, this formulation has been found to yield more satisfactory results than one involving a basic system of four second-order differential equations [22].

37

As previously mentioned, Equations (1-27) through (1-29) constitute a complete formulation of the problem for a homogeneous orthotropic shell. For eccentrically reinforced shells, this formulation must be revised. If we consider the reinforcement as being smeared over its spacing length, a revision would be necessary in the Equations (1-18) to take into account the geometrical orthotropy and reinforcement eccentricity. This revision would affect only four of the Equations ((1-28b, d) and (1-29a, b)) if an appropriate shell reference surface is chosen.

The revised integrated Hooke's Laws (Equations (1-18))are derived for several cases of stiffening in Appendix A. Using these revisions, the following equations analogous to Equations (1-28b, d) and (1-29a, b) are obtained for shells with ring-stringer reinforcement:

$$
\frac{v,_\varphi}{r_1} = \frac{w}{r_1} - \frac{1}{2}\omega_\theta^2 + \left(K_{22} + \frac{C_{22}^2}{D_{22}} \right)^{-1} \left\{ N_\varphi + N_{T\varphi} + \frac{C_{22}}{D_{22}} (M_\varphi + M_{T\varphi}) - \frac{K_{12}}{r_o}(u,_\theta + v\cos\varphi \right.
$$

$$
\left. -w\sin\varphi) - \frac{K_{12}}{2}\omega_\varphi^2 - \frac{C_{22}D_{12}}{D_{22}} \left[\frac{w,_{\theta\theta} + u,_\theta \sin\varphi}{r_o^2} + \frac{\omega_\theta \cos\varphi}{r_o} \right] \right\}
$$

$$
\frac{\omega_{\theta,\varphi}}{r_1} = -\frac{C_{22}}{C_{22}^2 + K_{22}D_{22}} \left\{ N_\varphi + N_{T\varphi} - \frac{K_{12}}{r_o} (u,_\theta + v\cos\varphi - w\sin\varphi) - \frac{K_{12}}{2}\omega_\varphi^2 \right\}
$$

$$
+ \frac{K_{22}}{C_{22}^2 + K_{22}D_{22}} \left\{ M_\varphi + M_{T\varphi} - D_{12} \left[\frac{w,_{\theta\theta} + u,_\theta \sin\varphi}{r_o^2} + \frac{\omega_\theta}{r_o} \cos\varphi \right] \right\} \quad (1-31)
$$

$$N_\theta = K_{12} \left(K_{22} + \frac{C_{22}^2}{D_{22}} \right)^{-1} \left\{ N_\varphi + N_{T\varphi} + \frac{C_{22}}{D_{22}} (M_\varphi + M_{T\varphi}) \right\} - N_{T\theta} + \left(\frac{K_{11}}{r_o} - \frac{K_{12}^2}{r_o} \left[K_{22} \right. \right.$$

$$\left. + \frac{C_{22}^2}{D_{22}} \right]^{-1})(u_{,\theta} + v\cos\varphi - w\sin\varphi + \frac{r_o}{2} \omega_\varphi^2) - (C_{11} + \frac{K_{12} C_{22} D_{12}}{D_{22}} \left[K_{22} \right.$$

$$\left. + \frac{C_{22}^2}{D_{22}} \right]^{-1})(\frac{w_{,\theta\theta} + u_{,\theta}\sin\varphi}{r_o^2} + \frac{\omega_\theta}{r_o} \cos\varphi)$$

$$M_\theta = \frac{-D_{12} C_{22}}{C_{22}^2 + K_{22} D_{22}} \{ N_\varphi + N_{T\varphi} \} - M_{T\theta} + \frac{D_{12} K_{22}}{C_{22}^2 + K_{22} D_{22}} \{ M_\varphi + M_{T\varphi} \}$$

$$+ (\frac{C_{11}}{r_o} + \frac{D_{12} K_{12}}{r_o} [\frac{C_{22}}{C_{22}^2 + K_{22} D_{22}}])(u_{,\theta} + v\cos\varphi - w\sin\varphi + \frac{r_o \omega_\varphi^2}{2})$$

$$+ (D_{11} - \frac{D_{12}^2 K_{22}}{C_{22}^2 + K_{22} D_{22}})(\frac{w_{,\theta\theta} + u_{,\theta}\sin\varphi}{r_o^2} + \frac{\omega_\theta}{r_o} \cos\varphi) \qquad (1\text{-}31)$$

where the K_{ij}, C_{ij} and D_{ij} stiffnesses are defined by Equations (A-8) in Appendix A. Equations (1-31) have been derived on the basis of the stress resultant - strain relations (A-7) in Appendix A. The following more general form of Equations (1-31), valid for multilayered shells with general ring and stringer reinforcement, may be obtained by employing the stress resultant-strain relations (A-9) in Appendix A.

$$\frac{v,_\varphi}{r_1} = \frac{w}{r_1} - \frac{1}{2}\omega_\theta^2 + \left(K_{22} + \frac{C_{25}^2}{D_{22}}\right)^{-1}\left\{N_\varphi + N_{T\varphi} + \frac{C_{25}}{D_{22}}(M_\varphi + M_{T\varphi}) - (K_{12} + \frac{C_{15}C_{25}}{D_{22}})\left[\frac{1}{r_o}(u,_\theta\right.\right.$$

$$\left.\left. + v\cos\varphi - w\sin\varphi) + \frac{1}{2}\omega_\varphi^2\right] - (\frac{C_{25}D_{12}}{D_{22}} - C_{15})\left[\frac{w,_{\theta\theta} + u,_\theta \sin\varphi}{r_o^2} + \frac{\omega_\theta}{r_o}\cos\varphi\right]\right\}$$

$$\frac{\omega_{\theta,\varphi}}{r_1} = \left(C_{25} + \frac{K_{22}D_{22}}{C_{25}}\right)^{-1}\left\{\frac{K_{22}}{C_{25}}(M_\varphi + M_{T\varphi}) - N_\varphi - N_{T\varphi} + (K_{12} - \frac{K_{22}C_{15}}{C_{25}})\left[\frac{1}{r_o}(u,_\theta + v\cos\varphi\right.\right.$$

$$\left.\left. - w\sin\varphi) + \frac{1}{2}\omega_\varphi^2\right] - (C_{15} + \frac{K_{22}D_{12}}{C_{25}})\left[\frac{w,_{\theta\theta} + u,_\theta\sin\varphi}{r_o^2} + \frac{\omega_\theta}{r_o}\cos\varphi\right]\right\}$$

$$N_\theta = (N_\varphi + N_{T\varphi})(\frac{K_{12}}{K_{22}} - \left[\frac{K_{12}C_{25}}{K_{22}} - C_{15}\right]\left[C_{25} - \frac{K_{22}D_{22}}{C_{25}}\right]^{-1}) - N_{T\theta} + (\frac{K_{12}C_{25}}{K_{22}} - C_{15})\left(C_{25}\right.$$

$$\left. + \frac{K_{22}D_{22}}{C_{25}}\right)^{-1}\frac{K_{22}}{C_{25}}(M_\varphi + M_{T\varphi}) + \left\{(K_{11} - \frac{K_{12}^2}{K_{22}}) + (\frac{K_{12}C_{25}}{K_{22}} - C_{15})(C_{25} + \frac{K_{22}D_{22}}{C_{22}})^{-1}(K_{12}\right.$$

$$\left. - \frac{K_{22}C_{15}}{C_{25}})\right\}\left[\frac{1}{r_o}(u_\theta + v\cos\varphi - w\sin\varphi) + \frac{1}{2}\omega_\varphi^2\right] + \left\{(\frac{K_{12}C_{15}}{K_{22}} - C_{14}) - (\frac{K_{12}C_{25}}{K_{22}}\right.\quad(1\text{-}32)$$

$$\left. - C_{15})\left(C_{25} + \frac{K_{22}D_{22}}{C_{25}}\right)^{-1}(C_{15} + \frac{K_{22}D_{12}}{C_{25}})\right\}\left[\frac{w,_{\theta\theta}}{r_o^2} + \frac{u,_\theta\sin\varphi}{r_o^2} + \frac{\omega_\theta}{r_o}\cos\varphi\right]$$

$$M_\theta = (M_\varphi + M_{T\varphi})\left[\frac{D_{12}}{D_{22}} + (C_{15} - \frac{D_{12}C_{25}}{D_{22}})\left(K_{22} + \frac{C_{25}^2}{D_{22}}\right)^{-1}\frac{C_{25}}{D_{22}}\right] + (N_\varphi + N_{T\varphi})(C_{15}$$

$$- \frac{D_{12}C_{25}}{D_{22}}) \left(K_{22} + \frac{C_{25}^2}{D_{22}} \right)^{-1} - M_{T\theta} + \left\{ (D_{11} - \frac{D_{12}^2}{D_{22}}) - (C_{15} - \frac{D_{12}C_{25}}{D_{22}}) \left(K_{22} \right. \right.$$

$$\left. + \frac{C_{25}^2}{D_{22}} \right)^{-1} (\frac{C_{25}D_{12}}{D_{22}} - C_{15}) \right\} \left[\frac{w_{,\theta\theta} + u_{,\theta} \sin\varphi}{r_o^2} + \frac{\omega_\theta}{r_o} \cos\varphi \right]$$

$$+ \left\{ (C_{14} - \frac{D_{12}C_{15}}{D_{22}}) - (C_{15} - \frac{D_{12}C_{25}}{D_{22}}) \left(K_{22} + \frac{C_{25}^2}{D_{22}} \right)^{-1} (K_{12} \right.$$

$$\left. + \frac{C_{15}C_{25}}{D_{22}}) \right\} \left[\frac{1}{r_o} (u_{,\theta} + v\cos\varphi - w\sin\varphi) + \frac{1}{2} \omega_\varphi^2 \right] \qquad (1\text{-}32)$$

The above equations may replace the corresponding relations in Equations (1-28) and (1-29) which may then be combined with Equations (1-27) to form the complete set of equations for the analysis of problems involving a broad range of reinforced shells of revolution. In this formulation, the structure is symmetric about the axis of revolution, and thus, smearing for stringer reinforcement is unavoidable unless the formulation is further complicated by expanding the circumferential stiffness in a Fourier series, as shown in Reference 9. Ring reinforcement properties, however, need not nec- essarily be smeared in such an analysis (see Appendix B). Indeed, in buckling problems, smearing of the ring or stringer reinforcing yields un- satisfactory results in cases where the half wavelength of the axial or the circumferential buckle pattern is smaller than the spacing of the reinforce- ment. The error resulting from smearing of the ring or stringer reinforcing for the case wherein the reinforcement of cylinders is spaced at exactly one-half wavelength of the buckle pattern, is approximated in Reference [120]. In order to eliminate this difficulty for ring reinforcement, discrete ring equations are obtained in Appendix B, and cast into a form suitable for

inclusion in the numerical procedure to be employed. These equations may then be utilized in cases in which the smearing technique is not suitable.

It should be noted that Equations (1-27) through (1-29) do not apply at a closed apex of a shell. At the apex, the radius of revolution, r_o, vanishes, resulting in a singularity in these equations, as discussed in Reference 6 . This problem, however, may be circumvented as suggested in References 8 and 20 . The necessary differential equations and apex boundary conditions are derived in Appendix C.

CHAPTER 2

FOURIER SERIES EXPANSIONS

Efficient techniques are not readily available for the numerical solution of partial differential equations of the complexity of those formulated in Chapter 1. However, by expanding the applied loading and the shell functions in Fourier series expansions in the cylindrical coordinate , θ, it is possible to reduce the set of partial differential Equations (1-27, 28, 29) to sets of ordinary differential equations. The actual number of sets of ordinary differential equations will depend upon the type of load distribution considered, and the degree of accuracy required. These sets of ordinary differential equations may be solved by employing a standard numerical integration procedure such as the Runge-Kutta [125-128].

It is assumed that the applied surface loads can be satisfactorily represented by the terms for n = 0, 1, ... N of their Fourier series expansion

$$F_\theta = \sum_{n=0}^{N} (F_\theta^{'(n)} \sin \theta + F_\theta^{''(n)} \cos n\theta)$$

$$F_\varphi = \sum_{n=0}^{N} (F_\varphi^{'(n)} \cos n\theta + F_\varphi^{''(n)} \sin n\theta)$$

$$F_\zeta = \sum_{n=0}^{N} (F_\zeta^{'(n)} \cos n\theta + F_\zeta^{''(n)} \sin n\theta) \qquad (2-1)$$

$$m_\theta = \sum_{n=0}^{N} (m_\theta^{'(n)} \cos n\theta + m_\theta^{''(n)} \sin n\theta)$$

$$m_\varphi = \sum_{n=0}^{N} (m_\varphi^{'(n)} \sin n\theta + m_\varphi^{''(n)} \cos n\theta)$$

$$T = \sum_{n=0}^{N} (T^{'(n)} \cos n\theta + T^{''(n)} \sin n\theta)$$

Moreover, it is assumed that the displacement components, the rotations, and the stress resultants can also be represented satisfactorily with the terms for n = 0, 1, ...N of their Fourier series expansion.

$$u = \sum_{n=0}^{N} (U'^{(n)} \sin n\theta + U''^{(n)} \cos n\theta)$$

$$v = \sum_{n=0}^{N} (V'^{(n)} \cos n\theta + V''^{(n)} \sin n\theta)$$

$$w = \sum_{n=0}^{N} (W'^{(n)} \cos n\theta + W''^{(n)} \sin n\theta)$$

$$\omega_\theta = \sum_{n=0}^{N} (\Omega_\theta'^{(n)} \cos n\theta + \Omega_\theta''^{(n)} \sin n\theta)$$

$$\omega_\varphi = \sum_{n=0}^{N} (\Omega_\varphi'^{(n)} \sin n\theta + \Omega_\varphi''^{(n)} \cos n\theta)$$

$$N_\theta = \sum_{n=0}^{N} (N_\theta'^{(n)} \cos n\theta + N_\theta''^{(n)} \sin n\theta)$$

$$N_\varphi = \sum_{n=0}^{N} (N_\varphi'^{(n)} \cos n\theta + N_\varphi''^{(n)} \sin n\theta)$$

$$N_{\varphi\theta} = \sum_{n=0}^{N} (N_{\varphi\theta}'^{(n)} \sin n\theta + N_{\varphi\theta}''^{(n)} \cos n\theta)$$

$$M_\theta = \sum_{n=0}^{N} (M_\theta'^{(n)} \cos n\theta + M_\theta''^{(n)} \sin n\theta)$$

$$M_\varphi = \sum_{n=0}^{N} (M_\varphi'^{(n)} \cos n\theta + M_\varphi''^{(n)} \sin n\theta)$$

$$M_{\varphi\theta} = \sum_{n=0}^{N} (M_{\varphi\theta}'^{(n)} \sin \theta + M_{\varphi\theta}''^{(n)} \cos n\theta)$$

$$Q_\theta = \sum_{n=0}^{N} (Q_\theta'^{(n)} \sin n\theta + Q_\theta''^{(n)} \cos n\theta)$$

$$Q_\varphi = \sum_{n=0}^{N} (Q_\varphi'^{(n)} \cos n\theta + Q_\varphi''^{(n)} \sin n\theta)$$

(2-2)

44

$$N_{T\theta} = \sum_{n=0}^{N} (N_{T\theta}^{'(n)} \cos n\theta + N_{T\theta}^{''(n)} \sin n\theta)$$

$$N_{T\varphi} = \sum_{n=0}^{N} (N_{T\varphi}^{'(n)} \cos n\theta + N_{T\varphi}^{'(n)} \sin n\theta)$$

$$M_{T\theta} = \sum_{n=0}^{N} (M_{T\theta}^{'(n)} \cos n\theta + M_{T\theta}^{''(n)} \sin n\theta)$$

$$\text{(2-2)}$$

$$M_{T\varphi} = \sum_{n=0}^{N} (M_{T\varphi}^{'(n)} \cos n\theta + M_{T\varphi}^{''(n)} \sin n\theta)$$

$$T_{\varphi\theta} = \sum_{n=0}^{N} (T_{\varphi\theta}^{'(n)} \sin n\theta + T_{\varphi\theta}^{''(n)} \cos n\theta)$$

$$J_{\varphi} = \sum_{n=0}^{N} (J_{\varphi}^{'(n)} \cos n\theta + J_{\varphi}^{''(n)} \sin n\theta)$$

Linear Stress Analysis: In problems involving linear stress analysis,
or stability or vibrations of shells subjected to axisymmetric prestress loads,
the substitution of the Fourier series expansions (2-1, 2) into the sets of
partial differential equations (1-27, 28, 29) results in uncoupled sets of
ordinary differential equations. These sets may be solved separately in
establishing the amplitudes of the Fourier series expansions, which may
then be employed in Equations (2-2) to yield the stress resultants and
displacements. For instance, in problems of linear stress analysis of
homogeneous orthotropic shells, in which the applied surface loads can
be satisfactorily represented solely by the terms of the Fourier series
expansion (2-1) having primed amplitudes, Equations (1-27) through (1-29),
yield (N+1) sets, of the following relations -- one set for each value of $n(n=0, 1 .. N)$:

$$\frac{T_{\varphi\theta,\varphi}^{(n)}}{r_1} = -2T_{\varphi\theta}^{(n)} \frac{\cos\varphi}{r_o} + n\frac{N_{\theta}^{(n)}}{r_o} - nM_{\theta}^{(n)} \frac{\sin\varphi}{r_o^2} - M_{\varphi\theta}^{(n)} \frac{\cos\varphi}{r_o}\left[\frac{1}{r_1} - \frac{\sin\varphi}{r_o}\right] - F_{\theta}^{(n)}$$

$$-m_{\varphi}^{(n)} \frac{\sin\varphi}{r_o}$$

$$\frac{N_{\varphi,\varphi}^{(n)}}{r_1} = -N_\varphi^{(n)}\frac{\cos\varphi}{r_o} + N_\theta^{(n)}\frac{\cos\varphi}{r_o} - n\frac{T_{\varphi\theta}^{(n)}}{r_o} - nM_{\varphi\theta}^{(n)}\left[\frac{\sin\varphi}{r_o^2} + \frac{1}{r_o r_1}\right] + \frac{J_\varphi^{(n)}}{r_1} - F_\varphi^{(n}$$

$$\frac{J_{\varphi,\varphi}^{(n)}}{r_1} = -J_\varphi^{(n)}\frac{\cos\varphi}{r_o} - N_\theta^{(n)}\frac{\sin\varphi}{r_o} - \frac{N_\varphi^{(n)}}{r_1} + n^2\frac{M_\theta^{(n)}}{r_o^2} - 2nM_{\varphi\theta}^{(n)}\frac{\cos\varphi}{r_o^2} - F_\zeta^{(n)} + \frac{nm_\varphi^{(n}}{r_o}$$

$$\frac{M_{\varphi,\varphi}^{(n)}}{r_1} = M_\theta^{(n)}\frac{\cos\varphi}{r_o} - M_\varphi^{(n)}\frac{\cos\varphi}{r_o} - 2n\frac{M_{\varphi\theta}^{(n)}}{r_o} + J_\varphi^{(n)} + m_\theta^{(n)}$$

$$\frac{U_{,\varphi}^{(n)}}{r_1} = U^{(n)}\frac{\cos\varphi}{r_o} + n\frac{V^{(n)}}{r_o} + \frac{T_{\varphi\theta}^{(n)}}{K_{33}} + \frac{M_{\varphi\theta}^{(n)}\sin\varphi}{r_o K_{33}}$$

$$\frac{V_{,\varphi}^{(n)}}{r_1} = \frac{W^{(n)}}{r_1} + (K_{22} - \nu_{\theta\varphi}^2 K_{11})^{-1}\{N_\varphi^{(n)} - \nu_{\theta\varphi}N_\theta^{(n)} + N_{T\varphi}^{(n)} - \nu_{\theta\varphi}N_{T\theta}^{(n)}\}$$

$$\frac{W_{,\varphi}^{(n)}}{r_1} = \Omega_\theta^{(n)} - \frac{V^{(n)}}{r_1} \tag{2-3}$$

$$\frac{\Omega_{\theta,\varphi}^{(n)}}{r_1} = (D_{22} - \nu_{\theta\varphi}^2 D_{11})^{-1}\{-M_\varphi^{(n)} + \nu_{\theta\varphi}M_\theta^{(n)} - M_{T\varphi}^{(n)} + \nu_{\theta\varphi}M_{T\theta}^{(n)}\}$$

$$N_\theta^{(n)} = \nu_{\varphi\theta}N_\varphi^{(n)} + (K_{11} - \nu_{\varphi\theta}^2 K_{22})\left[\frac{nU^{(n)} + V^{(n)}\cos\varphi - W^{(n)}\sin\varphi}{r_o}\right] - N_{T\theta}^{(n)} + \nu_{\varphi\theta}N_T^{(}$$

$$M_\theta^{(n)} = \nu_{\varphi\theta} M_\varphi^{(n)} - \frac{(D_{11} - \nu_{\varphi\theta}^2 D_{22})}{r_o} \left[\frac{nU^{(n)} \sin\varphi - n^2 W^{(n)}}{r_o} + \Omega_\theta^{(n)} \cos\varphi \right]$$

$$-M_{T\theta}^{(n)} + \nu_{\varphi\theta} M_{T\varphi}^{(n)}$$

$$M_{\varphi\theta}^{(n)} = \left[\frac{-1}{\dfrac{r_o}{D_{33}} + \dfrac{\sin^2\varphi}{r_o K_{33}}} \right] \left\{ -2n\Omega_\theta^{(n)} + U^{(n)} \left(\frac{\cos\varphi}{r_1} - \frac{\cos\varphi \sin\varphi}{r_o} \right) + nV^{(n)} \left(\frac{\sin\varphi}{r_o} + \frac{1}{r_1} \right) \right.$$

$$\left. + 2nW^{(n)} \frac{\cos\varphi}{r_o} + T_{\varphi\theta}^{(n)} \frac{\sin\varphi}{K_{33}} \right\} \tag{2-3}$$

N is determined by the accuracy requirements of the load representation (2-1) and of the solution. A similar set of equations may be obtained for surface loads described satisfactorily by the terms of their Fourier series expansion (2-1) having double primed amplitudes, by substituting the second portion of Equations (2-2), into (1-27) through (1-29), or by substituting -n for n in Equations (2-3).

If a reinforced or a laminated shell is to be analyzed, the Fourier series expansions (2-1, 2) must be substituted into Equations (1-31) or (1-32) instead of into the corresponding Equations (1-28) through (1-29).

It should be noted, that in all the above mentioned cases, the axisymmetric torsional case (n= 0) is uncoupled from the axisymmetric non-torsional case.

47

Nonlinear Stress Analysis: Nonlinear stress analysis problems for shells may be classified in two major categories, characterized by axisymmetric and by unsymmetric loadings. The problem of stress analys of an orthotropic homogeneous shell of revolution subjected to axisymmetri loading is described by the following equations obtained by substituting the Fourier series expansions (2-1, 2) with n= 0 into the set of partial differenti equations (1-27) through (1-29).

$$
\frac{T_{\varphi\theta,\,\varphi}^{(0)}}{r_1} = -2T_{\varphi\theta}^{(0)}\frac{\cos\varphi}{r_o} - M_{\varphi\theta}^{(0)}\frac{\cos\varphi}{r_o}\left[\frac{1}{r_1} - \frac{\sin\varphi}{r_o}\right] - f_\theta^{(0)} - m_\varphi^{(0)}\frac{\sin\varphi}{r_o}
$$

$$
- \frac{\sin\varphi}{r_o}\left[N_\theta^{(0)}\,\Omega_\varphi^{(0)} - N_{\varphi\theta}^{(0)}\,\Omega_\theta^{(0)}\right]
$$

$$
\frac{N_{\varphi,\,\varphi}^{(0)}}{r_1} = -N_\varphi^{(0)}\frac{\cos\varphi}{r_o} + N_\theta^{(0)}\frac{\cos\varphi}{r_o} + \frac{J_\varphi^{*\,(0)}}{r_1} - f_\varphi^{(0)}
$$

$$
\frac{J_{\varphi,\,\varphi}^{*\,(0)}}{r_1} = -J_\varphi^{*(0)}\frac{\cos\varphi}{r_o} - N_\theta^{(0)}\frac{\sin\varphi}{r_o} - \frac{N_\varphi^{(0)}}{r_1} - f_\zeta^{(0)}
$$

$$
\frac{M_{\varphi,\,\varphi}^{(0)}}{r_1} = M_\theta^{(0)}\frac{\cos\varphi}{r_o} - M_\varphi^{(0)}\frac{\cos\varphi}{r_o} + J_\varphi^{(0)} + m_\theta^{(0)}
$$

$$
\frac{U_{,\,\varphi}^{(0)}}{r_1} = U^{(0)}\frac{\cos\varphi}{r_o} + \frac{T_{\varphi\theta}^{(0)}}{K_{33}} + \frac{M_{\varphi\theta}^{(0)}\sin\varphi}{r_o K_{33}} + \Omega_\theta^{(0)}\Omega_\varphi^{(0)}
$$

$$
\frac{V_{,\,\varphi}^{(0)}}{r_1} = \frac{W^{(0)}}{r_1} + (K_{22} - \nu_{\theta\varphi}^2 K_{11})^{-1}\{N_\varphi^{(0)} - \nu_{\theta\varphi}N_\theta^{(0)} + N_{T\varphi}^{(0)} - \nu_{\theta\varphi}N_{T\theta}^{(0)}\}
$$

$$
- \frac{1}{2}\Omega_\theta^{(0)}\Omega_\theta^{(0)} \tag{2-4}
$$

$$\frac{W, _\varphi}{r_1} = \Omega_\theta^{(0)} - \frac{V^{(0)}}{r_1}$$

$$\frac{\Omega_{\theta,\varphi}^{(0)}}{r_1} = (D_{22} - \nu_{\theta\varphi}^2 D_{11})^{-1} \{ -M_\varphi^{(0)} + \nu_{\theta\varphi} M_\theta^{(0)} - M_{T\varphi}^{(0)} + \nu_{\theta\varphi} M_{T\theta}^{(0)} \}$$

$$N_\theta^{(0)} = \nu_{\varphi\theta} N_\varphi^{(0)} + (K_{11} - \nu_{\varphi\theta}^2 K_{22}) \left[\frac{V^{(0)}\cos\varphi - W^{(0)}\sin\varphi}{r_o} + \frac{1}{2}\Omega_\varphi^{(0)}\Omega_\varphi^{(0)} \right]$$

$$-N_{T\theta}^{(0)} + \nu_{\varphi\theta} N_{T\varphi}^{(0)}$$

$$M_\theta^{(0)} = \nu_{\varphi\theta} M_\varphi^{(0)} - \frac{(D_{11} - \nu_{\varphi\theta}^2 D_{22})}{r_o} (\Omega_\theta^{(0)}\cos\varphi) - M_{T\theta}^{(0)} + \nu_{\varphi\theta} M_{T\varphi}^{(0)}$$

$$M_{\varphi\theta}^{(0)} = \left[\frac{-1}{\dfrac{r_o}{D_{33}} + \dfrac{\sin^2\varphi}{r_o K_{33}}} \right] \left\{ U^{(0)} \left(\frac{\cos\varphi}{r_1} - \frac{\cos\varphi\sin\varphi}{r_o} \right) + \Omega_\theta^{(0)}\Omega_\varphi^{(0)}\sin\varphi \right.$$

$$\left. + \frac{T_{\varphi\theta}^{(0)}}{K_{33}} \sin\varphi \right\}$$

$$J_\varphi^{(0)} = J_\varphi^{*(0)} + N_{\varphi\theta}^{(0)} \Omega_\varphi^{(0)} - N_\varphi^{(0)} \Omega_\theta^{(0)}$$

$$\Omega_\varphi^{(0)} = - \frac{U^{(0)}\sin\varphi}{r_o}$$

$$N_{\varphi\theta}^{(0)} = T_{\varphi\theta}^{(0)} + \frac{M_{\varphi\theta}^{(0)}}{r_o} \sin\varphi \qquad\qquad (2\text{-}4)$$

where

$$f_\theta^{(0)} = F_\theta^{(0)} \left(1 + \frac{V^{(0)}\cos\varphi - W^{(0)}\sin\varphi}{r_o} + \frac{1}{2}\Omega_\varphi^{(0)}\Omega_\varphi^{(0)} + \frac{V,_\varphi^{(0)}}{r_1} - \frac{W^{(0)}}{r_1}\right.$$

$$\left. + \frac{1}{2}\Omega_\theta^{(0)}\Omega_\theta^{(0)}\right) + F_\varphi^{(0)}\frac{U,_\varphi^{(0)}}{r_1} + F_\zeta^{(0)}\Omega_\varphi^{(0)}$$

$$f_\varphi^{(0)} = F_\varphi^{(0)} \left(1 + \frac{V^{(0)}\cos\varphi - W^{(0)}\sin\varphi}{r_o} + \frac{V,_\varphi^{(0)}}{r_1} - \frac{W^{(0)}}{r_1} + \frac{1}{2}\Omega_\varphi^{(0)}\Omega_\varphi^{(0)}\right.$$

$$\left. + \frac{1}{2}\Omega_\theta^{(0)}\Omega_\theta^{(0)}\right) - F_\zeta^{(0)}\Omega_\theta^{(0)}$$

$$f_\zeta^{(0)} = F_\zeta^{(0)} \left(1 + \frac{V^{(0)}\cos\varphi - W^{(0)}\sin\varphi}{r_o} + \frac{V,_\varphi^{(0)}}{r_1} - \frac{W^{(0)}}{r_1} + \frac{1}{2}\Omega_\varphi^{(0)}\Omega_\varphi^{(0)}\right.$$

$$\left. + \frac{1}{2}\Omega_\theta^{(0)}\Omega_\theta^{(0)}\right) - F_\theta^{(0)}\Omega_\varphi^{(0)} + F_\varphi^{(0)}\Omega_\theta^{(0)} \tag{2-5}$$

The nature of the nonlinear problem is evident from Equations (2-4) and

(2-5). For example in a linear analysis, if solutions were obtained for a

load described by $F_\theta^{(0)}$, and for a load described by $F_\zeta^{(0)}$, the sum of

these solutions would represent the solution under a load described by

$(F_\theta^{(0)} + F_\zeta^{(0)})$. In a nonlinear analysis, the sum of the two solutions will

not represent the solution for a load described by $(F_\theta^{(0)} + F_\zeta^{(0)})$.

The presence of the φ derivatives in the right-hand side of Equations

(2-5) does not result in additional complications. These derivatives could

be eliminated by using Equations (2-4e, f).

If reinforced or laminated shells are to be analyzed, the Fourier

series expansion (2-1, 2), with n= 0, must be substituted into Equations (1-31)

or (1-32) instead of into the corresponding Equations (1-28) through (1-29).

The formulation and solution of the nonlinear problem under unsymmetric

loading is more complex. In all prior formulations of this problem [20, 22,

50

103, 104] , the applied loading could be described by a Fourier half-series. Thus, a line of symmetry was assumed in the loading distribution. If this assumption is not made, the full series must be employed. In this case, substitution of Equations (2-1) and (2-2) into Equations (1-27) through (1-29) will yield linear terms of the following form

$$\left(\sum_{n=0}^{\infty} A^{'(n)} \cos n\theta + \sum_{n=1}^{\infty} A^{''(n)} \sin n\theta \right) \tag{2-6a}$$

and nonlinear terms of the following form

$$\left(\sum_{\ell=0}^{\infty} A^{'(\ell)} \cos \ell\theta + \sum_{\ell=1}^{\infty} A^{''(\ell)} \sin \ell\theta \right) \left(\sum_{r=0}^{\infty} B^{'(r)} \cos r\theta + \sum_{r=1}^{\infty} B^{''(r)} \sin r\theta \right) =$$

$$\sum_{\ell=0}^{\infty} \sum_{r=0}^{\infty} A^{'(\ell)} B^{'(r)} \cos \ell\theta \cos r\theta + \sum_{\ell=0}^{\infty} \sum_{r=1}^{\infty} A^{'(\ell)} B^{''(r)} \cos \ell\theta \sin r\theta$$

$$+ \sum_{\ell=1}^{\infty} \sum_{r=0}^{\infty} A^{''(\ell)} B^{'(r)} \sin \ell\theta \cos r\theta + \sum_{\ell=1}^{\infty} \sum_{r=1}^{\infty} A^{''(\ell)} B^{''(r)} \sin \ell\theta \sin r\theta$$

$$\tag{2-6b}$$

where A and B denote the amplitudes of the Fourier series expansion. In order to eliminate the coordinate θ from the equations containing terms of the form given by (2.6b), the double series product terms must be converted to the form (2-6a). This may be accomplished by using trigonometric angle difference formulae

$$\sum_{\ell=0}^{\infty} \sum_{r=0}^{\infty} A^{'(\ell)} B^{'(r)} \cos \ell\theta \cos r\theta = \sum_{\ell=0}^{\infty} \sum_{r=0}^{\infty} A^{'(\ell)} B^{'(r)} [\cos(\ell-r)\theta + \cos(\ell+r)\theta]$$

$$= A^{'(0)} B^{'(0)} + \frac{1}{2} \sum_{k=1}^{\infty} A^{'(k)} B^{'(k)} + \sum_{n=1}^{\infty} \left\{ A^{'(0)} B^{'(n)} + A^{'(n)} B^{'(0)} \right.$$

51

$$+ \frac{1}{2} \sum_{k=1}^{\infty} \left(A'^{(k)} B'^{(n+k)} + A'^{(n+k)} B'^{(k)} \right) + \frac{1}{4} \sum_{k=1}^{n-1} \left(A'^{(k)} B'^{(n-k)} + A'^{(n-k)} B'^{(k)} \right) \Bigg\} \cos n\theta$$

$$(2-7a)$$

Similarly, the last term of the right hand side of Equation (2.6b) can be converted to a cosine series, whereas, the other terms of Equation (2.6b) can be converted to a sine series.

The nonlinear problem involving a homogeneous, orthotropic shell of revolution under unsymmetric loading can be described by substituting the complete Fourier series expansion (2-1, 2) into Equations (1-27) to (1-29). Then each of those could be reduced to the form

$$[\text{coefficient \#1}] \cos n\theta + [\text{coefficient \#2}] \sin n\theta = 0 \qquad (2-7b)$$

The requirement that the coefficients of the $\cos n\theta$ and $\sin n\theta$ terms vanish simultaneously, yields two sets of equations. The first set is:

$$\frac{T'^{(n)}_{\varphi\theta, \varphi}}{r_1} = -2 T'^{(n)}_{\varphi\theta} \frac{\cos\varphi}{r_o} + n \frac{N'^{(n)}_{\theta}}{r_o} - n \frac{M'^{(n)}_{\theta} \sin\varphi}{r_o^2} - M'^{(n)}_{\varphi\theta} \frac{\cos\varphi}{r_o} \left[\frac{1}{r_1} - \frac{\sin\varphi}{r_o} \right]$$

$$- f'^{(n)}_{\theta} - m^{(n)}_{\varphi} \frac{\sin\varphi}{r_o} - \frac{\sin\varphi}{r_o} \left[(N_{\theta} \Omega_{\varphi})^{(n)} - (N_{\varphi\theta} \Omega_{\theta})^{(n)} \right]$$

$$\frac{N'^{(n)}_{\varphi, \varphi}}{r_1} = -N'^{(n)}_{\varphi} \frac{\cos\varphi}{r_o} + N'^{(n)}_{\theta} \frac{\cos\varphi}{r_o} - n \frac{T'^{(n)}_{\varphi\theta}}{r_o} - nM'^{(n)}_{\varphi\theta} \left[\frac{\sin\varphi}{r_o^2} + \frac{1}{r_o r_1} \right] + \frac{J'^{*(n)}_{\varphi}}{r_1}$$

$$- f^{(n)}_{\varphi}$$

$$\frac{J'^{*(n)}_{\varphi, \varphi}}{r_1} = J'^{*(n)}_{\varphi} \frac{\cos\varphi}{r_o} - N'^{(n)}_{\theta} \frac{\sin\varphi}{r_o} - \frac{N''^{(n)}_{\varphi}}{r_1} + n^2 \frac{M''^{(n)}_{\theta}}{r_o^2} - 2n M'^{(n)}_{\varphi\theta} \frac{\cos\varphi}{r_o^2} - f''^{(n)}_{\zeta} + \frac{nm'^{(n)}_{\varphi}}{r_o}$$

$$+ \frac{1}{r_o} \left[n (N_{\varphi\theta} \Omega_{\theta})^{(n)} - n (N_{\theta} \Omega_{\varphi})^{(n)} \right] \qquad (2-8)$$

52

$$\frac{M'^{(n)}_{\varphi,\varphi}}{r_1} = M'^{(n)}_{\theta}\frac{\cos\varphi}{r_o} - M'^{(n)}_{\varphi}\frac{\cos\varphi}{r_o} - 2n\frac{M'^{(n)}_{\varphi\theta}}{r_o} + J'^{(n)}_{\varphi} + m'^{(n)}_{\theta}$$

$$\frac{U'^{(n)}_{,\varphi}}{r_1} = U'^{(n)}\frac{\cos\varphi}{r_o} + n\frac{V'^{(n)}}{r_o} + \frac{T'^{(n)}_{\varphi\theta}}{K_{33}} + \frac{M'^{(n)}_{\varphi\theta}}{r_o}\frac{\sin\varphi}{K_{33}} + (\Omega_\theta\Omega_\varphi)^{(n)}$$

$$\frac{V'^{(n)}_{,\varphi}}{r_1} = \frac{W'^{(n)}}{r_1} + (K_{22} - \nu_{\theta\varphi}^2 K_{11})^{-1}\left\{N'^{(n)}_{\varphi} - \nu_{\theta\varphi}N'^{(n)}_{\theta} + N'^{(n)}_{T\varphi} - \nu_{\theta\varphi}N'^{(n)}_{T\theta}\right\} - \tfrac{1}{2}(\Omega_\theta\Omega_\theta)^{(n)}$$

$$\frac{W'^{(n)}_{,\varphi}}{r_1} = \Omega'^{(n)}_{\theta} - \frac{V'^{(n)}}{r_1}$$

$$\frac{\Omega'^{(n)}_{\theta,\varphi}}{r_1} = (D_{22} - \nu_{\theta\varphi}^2 D_{11})^{-1}\left\{-M'^{(n)}_{\varphi} + \nu_{\theta\varphi}M'^{(n)}_{\theta} - M'^{(n)}_{T\varphi} + \nu_{\theta\varphi}M'^{(n)}_{T\theta}\right\}$$

$$N'^{(n)}_{\theta} = \nu_{\varphi\theta}N'^{(n)}_{\varphi} + (K_{11} - \nu_{\varphi\theta}^2 K_{22})\left[\frac{nU'^{(n)} + V'^{(n)}\cos\varphi - W'^{(n)}\sin\varphi}{r_o} + \tfrac{1}{2}(\Omega_\varphi\Omega_\varphi)^{(n)}\right]$$
$$- N'^{(n)}_{T\theta} + \nu_{\varphi\theta}N'^{(n)}_{T\varphi}$$

$$M'^{(n)}_{\theta} = \nu_{\varphi\theta}M'^{(n)}_{\varphi} - \frac{(D_{11} - \nu_{\varphi\theta}^2 D_{22})}{r_o}\left[\frac{nU'^{(n)}\sin\varphi - n^2 W'^{(n)}}{r_o} + \Omega'^{(n)}_{\theta}\cos\varphi\right] - M'^{(n)}_{T\theta} + \nu_{\varphi\theta}M'^{(n)}_{T\varphi}$$

$$M'^{(n)}_{\varphi\theta} = \left[\frac{-1}{\dfrac{r_o}{D_{33}} + \dfrac{\sin^2\varphi}{r_o K_{33}}}\right]\left\{-2n\Omega'^{(n)}_{\theta} + U'^{(n)}\left(\frac{\cos\varphi}{r_1} - \frac{\cos\varphi\sin\varphi}{r_o}\right) + nV'^{(n)}\left(\frac{\sin\varphi}{r_o} + \frac{1}{r_1}\right)\right.$$
$$\left. + 2nW'^{(n)}\frac{\cos\varphi}{r_o} + T'^{(n)}_{\varphi\theta}\frac{\sin\varphi}{K_{33}} + (\Omega_\theta\Omega_\varphi)^{(n)}\sin\varphi\right\}$$

$$N'^{(n)}_{\varphi\theta} = T'^{(n)}_{\varphi\theta} + \frac{M'^{(n)}_{\varphi\theta}}{r_o}\sin\varphi$$

$$J'^{(n)}_{\varphi} = J'^{*(n)}_{\varphi} + (N_{\varphi\theta}\Omega_\varphi)^{(n)} - (N_\varphi\Omega_\theta)^{(n)} \tag{2-8}$$

53

$$\Omega_{\varphi}^{'(n)} = \frac{nW^{'(n)}}{r_o} - \frac{U^{'(n)}\sin\varphi}{r_o} \tag{2-8}$$

A similar second set of equations can be obtained from the vanishing of the coefficients of the sin nθ terms in the aforementioned equations of the form (2-7b). This set of equations involves the ('') harmonics. It can also be obtained by setting n to -n in the set of Equations (2-8). Notice that the harmonic amplitudes in each set are coupled. Moreover as can be seen from Equations (2-9a, b) both sets of equations are coupled through the non-linear terms. Thus Equations (2-8) cannot be solved separately for each value of n, as in the linear case. The nonlinear terms of Equation (2-8) are:

$$(N_\theta \Omega_\varphi)^{(n)} = a \left\{ N_\theta^{'}{}^{(0)} \Omega_\varphi^{'}{}^{(n)} + \tfrac{1}{2} \sum_{k=1}^{\infty} \left(N_\theta^{'}{}^{(k)} \Omega_\varphi^{'}{}^{(n+k)} - N_\theta^{'}{}^{(n+k)} \Omega_\varphi^{'}{}^{(k)} \right) \right.$$

$$+ \tfrac{1}{4} \sum_{k=1}^{n-1} \left(N_\theta^{'}{}^{(k)} \Omega_\varphi^{'}{}^{(n-k)} + N_\theta^{'}{}^{(n-k)} \Omega_\varphi^{'}{}^{(k)} \right) + \Omega_\varphi^{''}{}^{(0)} N_\theta^{''}{}^{(n)} + \tfrac{1}{2} \sum_{k=1}^{\infty} \left(\Omega_\varphi^{''}{}^{(k)} N_\theta^{''}{}^{(n+k)} \right.$$

$$\left. - \Omega_\varphi^{''}{}^{(n+k)} N_\theta^{''}{}^{(k)} \right) + \tfrac{1}{4} \sum_{k=1}^{n-1} \left(\Omega_\varphi^{''}{}^{(k)} N_\theta^{''}{}^{(n-k)} + \Omega_\varphi^{''}{}^{(n-k)} N_\theta^{''}{}^{(k)} \right) \right\}$$

$$(N_{\varphi\theta}\Omega_\theta)^{(n)} = a \left\{ \Omega_\theta^{'}{}^{(0)} N_{\varphi\theta}^{'}{}^{(n)} + \tfrac{1}{2} \sum_{k=1}^{\infty} \left(\Omega_\theta^{'}{}^{(k)} N_{\varphi\theta}^{'}{}^{(n+k)} - \Omega_\theta^{'}{}^{(n+k)} N_{\varphi\theta}^{'}{}^{(k)} \right) \right.$$

$$+ \tfrac{1}{4} \sum_{k=1}^{n-1} \left(\Omega_\theta^{'}{}^{(k)} N_{\varphi\theta}^{'}{}^{(n-k)} + \Omega_\theta^{'}{}^{(n-k)} N_{\varphi\theta}^{'}{}^{(k)} \right) + N_{\varphi\theta}^{''}{}^{(0)} \Omega_\theta^{''}{}^{(n)}$$

$$+ \tfrac{1}{2} \sum_{k=1}^{\infty} \left(N_{\varphi\theta}^{''}{}^{(k)} \Omega_\theta^{''}{}^{(n+k)} - N_{\varphi\theta}^{''}{}^{(n+k)} \Omega_\theta^{''}{}^{(k)} \right)$$

$$\left. + \tfrac{1}{4} \sum_{k=1}^{n-1} \left(N_{\varphi\theta}^{''}{}^{(k)} \Omega_\theta^{''}{}^{(n-k)} + N_{\varphi\theta}^{''}{}^{(n-k)} \Omega_\theta^{''}{}^{(k)} \right) \right\} \tag{2-9a}$$

$$(\Omega_\theta \Omega_\varphi)^{(n)} = a \left\{ \Omega_\theta^{'}(0)\Omega_\varphi^{'}(n) + \frac{1}{2}\sum_{k=1}^{\infty}\left(\Omega_\theta^{'}(k)\Omega_\varphi^{'}(n+k) - \Omega_\theta^{'}(n+k)\Omega_\varphi^{'}(k)\right) \right.$$

$$+ \frac{1}{4}\sum_{k=1}^{n-1}\left(\Omega_\theta^{'}(k)\Omega_\varphi^{'}(n-k) + \Omega_\theta^{'}(n-k)\Omega_\varphi^{'}(k)\right) + \Omega_\varphi^{''}(0)\Omega_\theta^{''}(n)$$

$$+ \frac{1}{2}\sum_{k=1}^{\infty}\left(\Omega_\varphi^{''}(k)\Omega_\theta^{''}(n+k) - \Omega_\varphi^{''}(n+k)\Omega_\theta^{''}(k)\right)$$

$$\left. + \frac{1}{4}\sum_{k=1}^{n-1}\left(\Omega_\varphi^{''}(k)\Omega_\theta^{''}(n-k) + \Omega_\varphi^{''}(n-k)\Omega_\theta^{''}(k)\right) \right\}$$

$$(\Omega_\theta \Omega_\theta)^{(n)} = (1-a)\left\{ \Omega_\theta^{'}(0)\Omega_\theta^{'}(0) + \frac{1}{2}\sum_{k=1}^{\infty}\Omega_\theta^{'}(k)\Omega_\theta^{'}(k) \right\} + a\left\{ 2\Omega_\theta^{'}(0)\Omega_\theta^{'}(n) \right.$$

$$\left. + \sum_{k=1}^{\infty}\Omega_\theta^{'}(k)\Omega_\theta^{'}(n+k) + \frac{1}{2}\sum_{k=1}^{n-1}\Omega_\theta^{'}(k)\Omega_\theta^{'}(n-k) \right\}$$

$$+ (1-a)\left\{ \frac{1}{2}\sum_{k=1}^{\infty}\Omega_\theta^{''}(k)\Omega_\theta^{''}(k) \right\} + a\left\{ \sum_{k=1}^{\infty}\Omega_\theta^{''}(k)\Omega_\theta^{''}(n+k) \right.$$

$$\left. - \frac{1}{2}\sum_{k=1}^{n-1}\Omega_\theta^{''}(k)\Omega_\theta^{''}(n-k) \right\}$$

$$(\Omega_\varphi \Omega_\varphi)^{(n)} = (1-a)\left\{ \frac{1}{2}\sum_{k=1}^{\infty}\Omega_\varphi^{'}(k)\Omega_\varphi^{'}(k) \right\} + a\left\{ \sum_{k=1}^{\infty}\Omega_\varphi^{'}(k)\Omega_\varphi^{'}(n+k) - \frac{1}{2}\sum_{k=1}^{n-1}\Omega_\varphi^{'}(k)\Omega_\varphi^{'}(n-k) \right\}$$

$$+ (1-a)\left\{ \Omega_\varphi^{''}(0)\Omega_\varphi^{''}(0) + \frac{1}{2}\sum_{k=1}^{\infty}\Omega_\varphi^{''}(k)\Omega_\varphi^{''}(k) \right\} + a\left\{ 2\Omega_\varphi^{''}(0)\Omega_\varphi^{''}(n) + \sum_{k=1}^{\infty}\Omega_\varphi^{''}(k)\Omega_\varphi^{''}(n+k) \right.$$

$$\left. + \frac{1}{2}\sum_{k=1}^{n-1}\Omega_\varphi^{''}(k)\Omega_\varphi^{''}(n-k) \right\} \tag{2-9a}$$

$$(N_{\varphi_\theta}\Omega_\varphi)^{(n)} = (1-a)\left\{\frac{1}{2}\sum_{k=1}^{\infty} N_{\varphi_\theta}^{'}(k)\Omega_\varphi^{'}(k)\right\} + a\left\{\frac{1}{2}\sum_{k=1}^{\infty}\left(N_{\varphi_\theta}^{'}(k)\Omega_\varphi^{'}(n+k) + N_{\varphi_\theta}^{'}(n+k)\Omega_\varphi^{'}(k)\right)\right.$$

$$-\frac{1}{4}\sum_{k=1}^{n-1}\left(N_{\varphi_\theta}^{'}(k)\Omega_\varphi^{'}(n-k) + N_{\varphi_\theta}^{'}(n-k)\Omega_\varphi^{'}(k)\right)\right\} + (1-a)\left\{N_{\varphi_\theta}^{''}(0)\Omega_\varphi^{''}(0)\right.$$

$$+\frac{1}{2}\sum_{k=1}^{\infty} N_{\varphi_\theta}^{''}(k)\Omega_\varphi^{''}(k)\right\} + a\left\{N_{\varphi_\theta}^{''}(0)\Omega_\varphi^{''}(n) + \Omega_\varphi^{''}(0)N_{\varphi_\theta}^{''}(n)\right.$$

$$+\frac{1}{2}\sum_{k=1}^{\infty}\left(N_{\varphi_\theta}^{''}(k)\Omega_\varphi^{''}(n+k) + N_{\varphi_\theta}^{''}(n+k)\Omega_\varphi^{''}(k)\right) + \frac{1}{4}\sum_{k=1}^{n-1}\left(N_{\varphi_\theta}^{''}(k)\Omega_\varphi^{''}(n-k) + N_{\varphi_\theta}^{''}(n-k)\Omega_\varphi^{''}(k)\right)\right\}$$

$$(N_\varphi\Omega_\theta)^{(n)} = (1-a)\left\{N_\varphi^{'}(0)\Omega_\theta^{'}(0) + \frac{1}{2}\sum_{k=1}^{\infty} N_\varphi^{'}(k)\Omega_\theta^{'}(k)\right\} + a\left\{N_\varphi^{'}(0)\Omega_\theta^{'}(n) + N_\varphi^{'}(n)\Omega_\theta^{'}(0)\right.$$

$$+\frac{1}{2}\sum_{k=1}^{\infty}\left(N_\varphi^{'}(k)\Omega_\theta^{'}(n+k) + N_\varphi^{'}(n+k)\Omega_\theta^{'}(k)\right) + \frac{1}{4}\sum_{k=1}^{n-1}\left(N_\varphi^{'}(k)\Omega_\theta^{'}(n-k) + N_\varphi^{'}(n-k)\Omega_\theta^{'}(k)\right)$$

$$+(1-a)\left\{\frac{1}{2}\sum_{k=1}^{\infty} N_\varphi^{''}(k)\Omega_\theta^{''}(k)\right\} + a\left\{\frac{1}{2}\sum_{k=1}^{\infty}\left(N_\varphi^{''}(k)\Omega_\theta^{''}(n+k) + N_\varphi^{''}(n+k)\Omega_\theta^{''}(k)\right)\right.$$

$$-\frac{1}{4}\sum_{k=1}^{n-1}\left(N_\varphi^{''}(k)\Omega_\theta^{''}(n-k) + N_\varphi^{''}(n-k)\Omega_\theta^{''}(k)\right)\right\} \tag{2-9a}$$

$$f_\theta^{(n)} = F_\theta^{'}(n) + a\left\{F_\theta^{'}(n)\left(\epsilon_{\theta_o}^{'}(0) + \epsilon_{\varphi_o}^{'}(0)\right) + \frac{1}{2}\sum_{k=1}^{\infty}\left[F_\theta^{'}(n+k)\left(\epsilon_{\theta_o}^{'}(k) + \epsilon_{\varphi_o}^{'}(k)\right)\right.\right.$$

$$-F_\theta^{'}(k)\left(\epsilon_{\theta_o}^{'}(n+k) + \epsilon_{\varphi_o}^{'}(n+k)\right)\right] + \frac{1}{4}\sum_{k=1}^{n-1}\left[F_\theta^{'}(n-k)\left(\epsilon_{\theta_o}^{'}(k) + \epsilon_{\varphi_o}^{'}(k)\right) + F_\theta^{'}(k)\left(\epsilon_{\theta_o}^{'}(n-k)\right.\right.$$

$$\left.+\epsilon_{\varphi_o}^{'}(n-k)\right)\right] + F_\theta^{''}(0)\left(\epsilon_{\theta_o}^{''}(n) + \epsilon_{\varphi_o}^{''}(n)\right) + \frac{1}{2}\sum_{k=1}^{\infty}\left[F_\theta^{''}(k)\left(\epsilon_{\theta_o}^{''}(n+k)\right.\right.$$

$$+ \epsilon_{\varphi_o}''(n+k)) - F_\theta''(n+k)(\epsilon_{\theta_o}''(k) + \epsilon_{\varphi_o}''(k)) \Big] + \frac{1}{4}\sum_{k=1}^{n-1}{}' \Big[F_\theta''(k)(\epsilon_{\theta_o}''(n-k) + \epsilon_{\varphi_o}''(n-k))$$

$$+ F_\theta''(n-k)(\epsilon_{\theta_o}''(k) + \epsilon_{\varphi_o}''(k)) \Big] + F_\zeta'(0)\Omega_\varphi'(n) + \frac{1}{2}\sum_{k=1}^{\infty}(F_\zeta'(k)\Omega_\varphi'(n+k) - F_\zeta'(n+k)\Omega_\varphi'(k))$$

$$+ \frac{1}{4}\sum_{k=1}^{n-1}(F_\zeta'(k)\Omega_\varphi'(n-k) + F_\zeta'(n-k)\Omega_\varphi'(k)) + \Omega_\varphi''(0)F_\zeta''(n) + \frac{1}{2}\sum_{k=1}^{\infty}(\Omega_\varphi''(k) F_\zeta''(n+k)$$

$$-\Omega_\varphi''(n+k) F_\zeta''(k)) + \frac{1}{4}\sum_{k=1}^{n-1}(\Omega_\varphi''(k) F_\zeta''(n-k) + \Omega_\varphi''(n-k) F_\zeta''(k)) + F_\varphi'(0)\frac{U_{,\varphi}'(n)}{r_1}$$

$$+ \frac{1}{2}\sum_{k=1}^{\infty} \Big(F_\varphi'(k)\frac{U_{,\varphi}'(n+k)}{r_1} - F_\varphi'(n+k)\frac{U_{,\varphi}'(k)}{r_1} \Big)$$

$$\frac{1}{4}\sum_{k=1}^{n-1} \Big(F_\varphi'(k)\frac{U_{,\varphi}'(n-k)}{r_1} + F_\varphi'(n-k)\frac{U_{,\varphi}'(k)}{r_1} \Big) + F_\varphi''(n)\frac{U_{,\varphi}''(0)}{r_1}$$

$$+ \frac{1}{2}\sum_{k=1}^{\infty} \Big(\frac{U_{,\varphi}''(k)}{r_1} F_\varphi''(n+k) - \frac{U_{,\varphi}''(n+k)}{r_1} F_\varphi''(k) \Big)$$

$$+ \frac{1}{4}\sum_{k=1}^{n-1} \Big(\frac{U_{,\varphi}''(k)}{r_1} F_\varphi''(n-k) + \frac{U_{,\varphi}''(n-k)}{r_1} F_\varphi''(k) \Big) \Bigg\} \qquad (2\text{-}9a)$$

$$f_\varphi(n) = F_\varphi'(n) + (1-a)\Bigg\{ F_\varphi'(0)(\epsilon_{\theta_o}'(0) + \epsilon_{\varphi_o}'(0)) - F_\zeta'(0)\Omega_\theta'(0)$$

$$+ \frac{1}{2}\sum_{k=1}^{\infty} F_\varphi'(k)(\epsilon_{\theta_o}'(k) + \epsilon_{\varphi_o}'(k)) - \frac{1}{2}\sum_{k=1}^{\infty} F_\zeta'(k)\Omega_\theta'(k) \Bigg\}$$

$$+ a\Bigg\{ F_\varphi'(0)(\epsilon_{\theta_o}'(n) + \epsilon_{\varphi_o}'(n)) + F_\varphi'(n)(\epsilon_{\theta_o}'(0) + \epsilon_{\varphi_o}'(0))$$

$$+ \frac{1}{2}\sum_{k=1}^{\infty} \Big[F_\varphi'(k)(\epsilon_{\theta_o}'(n+k) + \epsilon_{\varphi_o}'(n+k)) + F_\varphi'(n+k)(\epsilon_{\theta_o}'(k) + \epsilon_{\varphi_o}'(k)) \Big]$$

$$+ \frac{1}{4}\sum_{k=1}^{n-1} \Big[F_\varphi'(k)(\epsilon_{\theta_o}'(n-k) + \epsilon_{\varphi_o}'(n-k)) + F_\varphi'(n-k)(\epsilon_{\theta_o}'(k) + \epsilon_{\varphi_o}'(k)) \Big]$$

$$-F'_\zeta(0)\,\Omega'_\theta(n) - F'_\zeta(n)\Omega'_\theta(0) - \tfrac{1}{2}\sum_{k=1}^{\infty}(F'_\zeta(k)\,\Omega'_\theta(n+k) + F'_\zeta(n+k)\,\Omega'_\theta(k))$$

$$-\tfrac{1}{4}\sum_{k=1}^{n-1}(F'_\zeta(k)\,\Omega'_\theta(n-k) + F'_\zeta(n-k)\,\Omega'_\theta(k)) + (1-a)\left\{\tfrac{1}{2}\sum_{k=1}^{\infty}F''_\varphi(k)\,(\epsilon''_{\theta_o}(k)\right.$$

$$+ \epsilon''_{\varphi_o}(k)) - \tfrac{1}{2}\sum_{k=1}^{\infty}F''_\zeta(k)\,\Omega''_\theta(k)\bigg\} + a\left\{\tfrac{1}{2}\sum_{k=1}^{\infty}\left[F''_\varphi(k)\,(\epsilon''_{\theta_o}(n+k) + \epsilon''_{\varphi_o}(n+k))\right.\right.$$

$$+ F''_\varphi(n+k)\,(\epsilon''_{\theta_o}(k) + \epsilon''_{\varphi_o}(k))\bigg] - \tfrac{1}{4}\sum_{k=1}^{n-1}\left[F''_\varphi(k)(\epsilon''_{\theta_o}(n-k) + \epsilon''_{\varphi_o}(n-k))\right.$$

$$+ F''_\varphi(n-k)\,(\epsilon''_{\theta_o}(k) + \epsilon''_{\varphi_o}(k))\bigg] - \tfrac{1}{2}\sum_{k=1}^{\infty}(F''_\zeta(k)\,\Omega''_\theta(n+k) + F''_\zeta(n+k)\,\Omega''_\theta(k))$$

$$+ \tfrac{1}{4}\sum_{k=1}^{n-1}(F''_\zeta(k)\,\Omega''_\theta(n-k) + F''_\zeta(n-k)\,\Omega''_\theta(k))\bigg\} - (1-a)\left\{\tfrac{1}{2}\sum_{k=1}^{\infty}n\,F'_\theta(k)\,\frac{V'}{r_o}(k)\right\}$$

$$- a\left\{\tfrac{1}{2}\sum_{k=1}^{\infty}n\,(F'_\theta(k)\,\frac{V'}{r_o}(n+k) + F'_\theta(n+k)\,\frac{V'}{r_o}(k)) - \tfrac{1}{4}\sum_{k=1}^{n-1}n(F'_\theta(k)\,\frac{V'}{r_o}(n-k)\right.$$

$$+ F'_\theta(n-k)\,\frac{V'}{r_o}(k))\bigg\} - (1-a)\left\{\tfrac{1}{2}\sum_{k=1}^{\infty}n\,F''_\theta(k)\,\frac{V''}{r_o}(k)\right\}$$

$$- a\left\{n\,F''_\theta(0)\,\frac{V''}{r_o}(n) + \tfrac{1}{2}\sum_{k=1}^{\infty}n\,(F''_\theta(k)\,\frac{V''}{r_o}(n+k) + F''_\theta(n+k)\,\frac{V''}{r_o}(k))\right.$$

$$+ \tfrac{1}{4}\sum_{k=1}^{n-1}n\,(F''_\theta(k)\,\frac{V''}{r_o}(n-k) + F''_\theta(n-k)\frac{V''}{r_o}(k))\bigg\} \qquad (2\text{-}9a)$$

$$f_\zeta(n) = F'_\zeta(n) + (1-a)\left\{F''_\zeta(0)\,(\epsilon''_{\theta_o}(0) + \epsilon''_{\varphi_o}(0)) + F'_\varphi(0)\,\Omega'_\theta(0)\right.$$

$$+ \tfrac{1}{2}\sum_{k=1}^{\infty}\left[F'_\zeta(k)\,(\epsilon'_{\theta_o}(k) + \epsilon'_{\varphi_o}(k)) + F'_\varphi(k)\,\Omega'_\theta(k)\right]\bigg\}$$

$$+ a\left\{F'_\zeta(0)\,(\epsilon'_{\theta_o}(n) + \epsilon'_{\varphi_o}(n)) + F'_\zeta(n)\,(\epsilon'_{\theta_o}(0) + \epsilon'_{\varphi_o}(0))\right.$$

$$+ \tfrac{1}{2}\sum_{k=1}^{\infty}\left[F'_\zeta(k)\,(\epsilon'_{\theta_o}(n+k) - \epsilon'_{\varphi_o}(n+k)) + F'_\zeta(n+k)\,(\epsilon'_{\theta_o}(k) + \epsilon'_{\varphi_o}(k))\right]$$

$$+ \frac{1}{4} \sum_{k=1}^{n-1} \left[F_\zeta^{'}(k) \; (\epsilon_{\theta_o}^{'}(n-k) + \epsilon_{\varphi_o}^{'}(n-k)) + F_\zeta^{'}(n-k) \; (\epsilon_{\theta_o}^{'}(k) + \epsilon_{\varphi_o}^{'}(k)) \right]$$

$$+ F_\varphi^{'}(0) \; \Omega_\theta^{'}(n) + F_\varphi^{'}(n) \; \Omega_\theta^{'}(0) + \frac{1}{2} \sum_{k=1}^{\infty} (F_\varphi^{'}(k) \; \Omega_\theta^{'}(n+k) + F_\varphi^{'}(n+k) \Omega_\theta^{'}(k))$$

$$+ \frac{1}{4} \sum_{k=1}^{n-1} (F_\varphi^{'}(k) \; \Omega_\theta^{'}(n-k) + F_\varphi^{'}(n-k) \; \Omega_\theta^{'}(k)) \Big\} + (1-a) \Big\{ \frac{1}{2} \sum_{k=1}^{\infty} F_\zeta^{''}(k) \; (\epsilon_{\theta_o}^{''}(k) + \epsilon_{\varphi_o}^{''}(k))$$

$$+ \frac{1}{2} \sum_{k=1}^{\infty} F_\varphi^{''}(k) \; \Omega_\theta^{''}(k) \Big\} + a \Big\{ \frac{1}{2} \sum_{k=1}^{\infty} \left[F_\zeta^{''}(k) \; (\epsilon_{\theta_o}^{''}(n+k) + \epsilon_{\varphi_o}^{''}(n+k)) \right.$$

$$+ F_\zeta^{''}(n+k) \; (\epsilon_{\theta_o}^{''}(k) + \epsilon_{\varphi_o}^{''}(k)) \Big] - \frac{1}{4} \sum_{k=1}^{n-1} \left[F_\zeta^{''}(k) \; (\epsilon_{\theta_o}^{''}(n-k) + \epsilon_{\varphi_o}^{''}(n-k)) \right.$$

$$+ F_\zeta^{''}(n-k) \; (\epsilon_{\theta_o}^{''}(k) + \epsilon_{\varphi_o}^{''}(k)) \Big] + \frac{1}{2} \sum_{k=1}^{\infty} (F_\varphi^{''}(k) \; \Omega_\theta^{''}(n+k) + F_\varphi^{''}(n+k) \; \Omega_\theta^{''}(k))$$

$$- \frac{1}{4} \sum_{k=1}^{n-1} (F_\varphi^{''}(k) \; \Omega_\theta^{''}(n-k) + F_\varphi^{''}(n-k) \Omega_\theta^{''}(k)) \Big\} - (1-a) \Big\{ \frac{1}{2} \sum_{k=1}^{\infty} F_\theta^{'}(k) \Omega_\varphi^{'}(k) \Big\}$$

$$- a \Big\{ \frac{1}{2} \sum_{k=1}^{\infty} (F_\theta^{'}(k) \Omega_\varphi^{'}(n+k) + F_\theta^{'}(n+k) \Omega_\varphi^{'}(k)) - \frac{1}{4} \sum_{k=1}^{\infty} (F_\theta^{'}(k) \; \Omega_\varphi^{'}(n-k) + F_\theta^{'}(n-k) \Omega_\varphi^{'}(k)) \Big\}$$

$$- (1-a) \Big\{ F_\theta^{''}(0) \; \Omega_\varphi^{''}(0) + \frac{1}{2} \sum_{k=1}^{\infty} F_\theta^{''}(k) \; \Omega_\varphi^{''}(k) \Big\} - a \Big\{ F_\theta^{''}(0) \; \Omega_\varphi^{''}(0) + F_\theta^{''}(n) \; \Omega_\varphi^{''}(0)$$

$$+ \frac{1}{2} \sum_{k=1}^{\infty} (F_\theta^{''}(k) \Omega_\varphi^{''}(n+k) + F_\theta^{''}(n+k) \Omega_\varphi^{''}(k)) + \frac{1}{4} \sum_{k=1}^{n-1} (F_\theta^{''}(k) \; \Omega_\varphi^{''}(n-k) + F_\theta^{''}(n-k) \Omega_\varphi^{''}(k)) \Big\} \tag{2-9a}$$

where $a = 0$ for $n = 0$, and $a = 1$ for $n \geq 1$. The nonlinear terms for the

second set of equations (obtained by a setting $-n$ for n and the double primes

for primes in Equations (2-8)) are given by

$$(N_\theta \, \Omega_\varphi)^{(n)} = (1-a) \Big\{ N_\theta^{'}(0) \; \Omega_\varphi^{''}(0) + \frac{1}{2} \sum_{k=1}^{\infty} N_\theta^{'}(k) \; \Omega_\varphi^{''}(k) \Big\} + a \Big\{ N_\theta^{'}(0) \; \Omega_\varphi^{''}(n)$$

$$+ N_\theta^{'}(n) \; \Omega_\varphi^{''}(0) + \frac{1}{2} \sum_{k=1}^{\infty} (N_\theta^{'}(k) \; \Omega_\varphi^{''}(n+k) + N_\theta^{'}(n+k) \; \Omega_\varphi^{''}(k))$$

59

$$+ \frac{1}{4} \sum_{k=1}^{n-1} (N_{\theta}^{'}(k) \Omega_{\varphi}^{''}(n-k) + N_{\theta}^{'}(n-k) \Omega_{\varphi}^{''}(k)) \Big\} + (1-a) \Big\{ \frac{1}{2} \sum_{k=1}^{\infty} N_{\theta}^{''}(k) \Omega_{\varphi}^{'}(k) \Big\}$$

$$+ a \Big\{ \frac{1}{2} \sum_{k=1}^{\infty} (N_{\theta}^{''}(k) \Omega_{\varphi}^{'}(n+k) + N_{\theta}^{''}(n+k) \Omega_{\varphi}^{'}(k)) - \frac{1}{4} \sum_{k=1}^{n-1} (N_{\theta}^{''}(k) \Omega_{\varphi}^{'}(n-k)$$

$$+ N_{\theta}^{''}(n-k) \Omega_{\varphi}^{'}(k)) \Big\}$$

$$(N_{\varphi\theta} \Omega_{\theta})^{(n)} = (1-a) \Big\{ \Omega_{\theta}^{'}(0) N_{\varphi\theta}^{''}(0) + \frac{1}{2} \sum_{k=1}^{\infty} \Omega_{\theta}^{'}(k) N_{\varphi\theta}^{''}(k) \Big\} + a \Big\{ \Omega_{\theta}^{'}(0) N_{\varphi\theta}^{''}(n)$$

$$+ \Omega_{\theta}^{'}(n) N_{\varphi\theta}^{''}(0) + \frac{1}{2} \sum_{k=1}^{\infty} (\Omega_{\theta}^{'}(k) N_{\varphi\theta}^{''}(n+k) + \Omega_{\theta}^{'}(n+k) N_{\varphi\theta}^{''}(k))$$

$$+ \frac{1}{4} \sum_{k=1}^{n-1} (\Omega_{\theta}^{'}(k) N_{\varphi\theta}^{''}(n-k) + \Omega_{\theta}^{'}(n-k) N_{\varphi\theta}^{''}(k)) \Big\} + (1-a) \Big\{ \frac{1}{2} \sum_{k=1}^{\infty} \Omega_{\theta}^{''}(k) N_{\varphi\theta}^{'}(k) \Big\}$$

$$+ a \Big\{ \frac{1}{2} \sum_{k=1}^{\infty} \Omega_{\theta}^{''}(k) N_{\varphi\theta}^{'}(n+k) + \Omega_{\theta}^{''}(n+k) N_{\varphi\theta}^{'}(k)) - \frac{1}{4} \sum_{k-1}^{n-1} (\Omega_{\theta}^{''}(k) N_{\varphi\theta}^{'}(n-k)$$

$$+ \Omega_{\theta}^{''}(n-k) N_{\varphi\theta}^{'}(k)) \Big\}$$

$$(\Omega_{\theta} \Omega_{\varphi})^{(n)} = (1-a) \Big\{ \Omega_{\theta}^{'}(0) \Omega_{\varphi}^{''}(0) + \frac{1}{2} \sum_{k=1}^{\infty} \Omega_{\theta}^{'}(k) \Omega_{\varphi}^{''}(k) \Big\} + a \Big\{ \Omega_{\theta}^{'}(0) \Omega_{\varphi}^{''}(n)$$

$$+ \Omega_{\theta}^{'}(n) \Omega_{\varphi}^{''}(0) + \frac{1}{2} \sum_{k=1}^{\infty} (\Omega_{\theta}^{'}(k) \Omega_{\varphi}^{''}(n+k) + \Omega_{\theta}^{'}(n+k) \Omega_{\varphi}^{''}(k)) + \frac{1}{4} \sum_{k=1}^{n-1} (\Omega_{\theta}^{'}(k) \Omega_{\varphi}^{''}(n-k)$$

$$+ \Omega_{\theta}^{'}(n-k) \Omega_{\varphi}^{''}(k)) \Big\} + (1-a) \Big\{ \frac{1}{2} \sum_{k=1}^{\infty} \Omega_{\theta}^{''}(k) \Omega_{\varphi}^{'}(k) \Big\} + a \Big\{ \frac{1}{2} \sum_{k=1}^{\infty} \Omega_{\theta}^{''}(k) \Omega_{\varphi}^{'}(n+k)$$

$$+ \Omega_{\theta}^{''}(n+k) \Omega_{\varphi}^{'}(k)) - \frac{1}{4} \sum_{k=1}^{n-1} (\Omega_{\theta}^{''}(k) \Omega_{\varphi}^{'}(n-k) + \Omega_{\theta}^{''}(n-k) \Omega_{\varphi}^{'}(k)) \Big\}$$

$$(\Omega_{\theta} \Omega_{\theta})^{(n)} = 2a \Big\{ \Omega_{\theta}^{'}(0) \Omega_{\theta}^{''}(n) + \frac{1}{2} \sum_{k=1}^{\infty} (\Omega_{\theta}^{'}(k) \Omega_{\theta}^{''}(n+k) - \Omega_{\theta}^{'}(n+k) \Omega_{\theta}^{''}(k))$$

$$+ \frac{1}{4} \sum_{k=1}^{n-1} (\Omega_{\theta}^{'}(k) \Omega_{\theta}^{''}(n-k) + \Omega_{\theta}^{'}(n-k) \Omega_{\theta}^{''}(k)) \Big\} \tag{2-9b}$$

$$(\Omega_\varphi \Omega_\varphi)^{(n)} = 2a \left\{ \frac{1}{2} \sum_{k=1}^{\infty} (\Omega_\varphi^{'(k)} \Omega_\varphi^{''(n+k)} - \Omega_\varphi^{'(n+k)} \Omega_\varphi^{''(k)}) \right.$$

$$\left. + \frac{1}{4} \sum_{k=1}^{n-1} (\Omega_\varphi^{'(k)} \Omega_\varphi^{''(n-k)} + \Omega_\varphi^{'(n-k)} \Omega_\varphi^{''(k)}) \right\}$$

$$(N_{\varphi\theta} \Omega_\varphi)^{(n)} = a \left\{ \Omega_\varphi^{''(0)} N_{\varphi\theta}^{'(n)} + \frac{1}{2} \sum_{k=1}^{\infty} (\Omega_\varphi^{''(k)} N_{\varphi\theta}^{'(n+k)} - \Omega_\varphi^{''(n+k)} N_{\varphi\theta}^{'(k)}) \right.$$

$$+ \frac{1}{4} \sum_{k=1}^{n-1} (\Omega_\varphi^{''(k)} N_{\varphi\theta}^{'(n-k)} + \Omega_\varphi^{''(n-k)} N_{\varphi\theta}^{'(k)}) + N_{\varphi\theta}^{''(\theta)} \Omega_\varphi^{''(n)}$$

$$\left. + \frac{1}{2} \sum_{k=1}^{\infty} (N_{\varphi\theta}^{''(k)} \Omega_\varphi^{'(n+k)} - N_{\varphi\theta}^{''(n+k)} \Omega_\varphi^{'(k)} + \frac{1}{4} \sum_{k=1}^{n-1} (N_{\varphi\theta}^{''(k)} \Omega_\varphi^{'(n-k)} \right.$$

$$\left. + N_{\varphi\theta}^{''(n-k)} \Omega_\varphi^{'(k)}) \right\}$$

$$(N_\varphi \Omega_\theta)^{(n)} = a \left\{ N_\varphi^{'(0)} \Omega_\theta^{''(n)} + \frac{1}{2} \sum_{k=1}^{\infty} (N_\varphi^{'(k)} \Omega_\theta^{''(n+k)} - N_\varphi^{'(n+k)} \Omega_\theta^{''(k)}) \right.$$

$$+ \frac{1}{4} \sum_{k=1}^{n-1} (N_\varphi^{'(k)} \Omega_\theta^{''(n-k)} + N_\varphi^{'(n-k)} \Omega_\theta^{''(k)}) + \Omega_\theta^{'(0)} N_\varphi^{''(n)}$$

$$+ \frac{1}{2} \sum_{k=1}^{\infty} (\Omega_\theta^{'(k)} N_\varphi^{''(n+k)} - \Omega_\theta^{'(n+k)} N_\varphi^{''(k)})$$

$$\left. + \frac{1}{4} \sum_{k=1}^{n-1} (\Omega_\theta^{'(k)} N_\varphi^{''(n-k)} + \Omega_\theta^{'(n-k)} N_\varphi^{''(k)}) \right\} \tag{2-9b}$$

$$f_\theta^{(n)} = F_\theta^{''(n)} + (1-a) \left\{ F_\theta^{''(0)} (\epsilon_{\theta_o}^{'(0)} + \epsilon_{\varphi_o}^{'(0)}) + \frac{1}{2} \sum_{k=1}^{\infty} F_\theta^{''(k)} (\epsilon_{\theta_o}^{'(k)} + \epsilon_{\varphi_o}^{'(k)}) \right\}$$

$$+ a \left\{ F_\theta^{''(0)} (\epsilon_{\theta_o}^{'(n)} + \epsilon_{\varphi_o}^{'(n)}) + F_\theta^{''(n)} (\epsilon_{\theta_o}^{'(0)} + \epsilon_{\varphi_o}^{'(0)}) \right.$$

$$+ \frac{1}{2} \sum_{k=1}^{\infty} \left[F_\theta^{''}(k) \left(\epsilon_{\theta_o}^{'}(n+k) + \epsilon_{\varphi_o}^{'}(n+k) \right) + F_\theta^{''}(n+k) \left(\epsilon_{\theta_o}^{'}(k) + \epsilon_{\varphi_o}^{'}(k) \right) \right]$$

$$+ \frac{1}{4} \sum_{k=1}^{n-1} \left[F_\theta^{''}(k) \left(\epsilon_{\theta_o}^{'}(n-k) + \epsilon_{\varphi_o}^{'}(n-k) \right) + F_\theta^{''}(n-k) \left(\epsilon_{\theta_o}^{'}(k) + \epsilon_{\varphi_o}^{'}(k) \right) \right] \Bigg\}$$

$$+ (1-a) \left\{ \frac{1}{2} \sum_{k=1}^{\infty} \left[F_\theta^{'}(k) \left(\epsilon_{\theta_o}^{''}(k) + \epsilon_{\varphi_o}^{''}(k) \right) \right] \right\} + a \left\{ \frac{1}{2} \sum_{k=1}^{\infty} \left[F_\theta^{'}(k) \left(\epsilon_{\theta_o}^{''}(n+k) + \epsilon_{\varphi_o}^{''}(n+k) \right) \right. \right.$$

$$\left. + F_\theta^{'}(n+k) \left(\epsilon_{\theta_o}^{''}(k) + \epsilon_{\varphi_o}^{''}(k) \right) \right] - \frac{1}{4} \sum_{k=1}^{n-1} \left[F_\theta^{'}(k) \left(\epsilon_{\theta_o}^{''}(n-k) + \epsilon_{\varphi_o}^{''}(n-k) \right) \right.$$

$$\left. \left. + F_\theta^{'}(n-k) \left(\epsilon_{\theta_o}^{''}(k) + \epsilon_{\varphi_o}^{''}(k) \right) \right] \right\} + (1-a) \left\{ F_\zeta^{'}(0) \, \Omega_\varphi^{''}(0) + \right.$$

$$+ \frac{1}{2} \sum_{k=1}^{\infty} F_\zeta^{'}(k) \Omega_\varphi^{''}(k) \Bigg\} + a \left\{ F_\zeta^{'}(0) \Omega_\varphi^{''}(n) + F_\zeta^{'}(n) \Omega_\varphi^{''}(0) + \frac{1}{2} \sum_{k=1}^{\infty} \left(F_\zeta^{'}(n+k) \Omega_\varphi^{''}(k) + F_\zeta^{'}(k) \Omega_\varphi^{''}(n+k) \right) \right.$$

$$+ \frac{1}{4} \sum_{k=1}^{n-1} \left(F_\zeta^{'}(n-k) \, \Omega_\varphi^{''}(k) + F_\zeta^{'}(k) \, \Omega_\varphi^{''}(n-k) \right) \Bigg\} + (1-a) \left(\frac{1}{2} \sum_{k=1}^{\infty} F_\zeta^{''}(k) \Omega_\varphi^{'}(k) \right)$$

$$+ a \left\{ \frac{1}{2} \sum_{k=1}^{\infty} \left(F_\zeta^{''}(n+k) \, \Omega_\varphi^{'}(k) + F_\zeta^{''}(k) \Omega_\varphi^{'}(n+k) \right) - \frac{1}{4} \sum_{k=1}^{n-1} \left(F_\zeta^{''}(n-k) \Omega_\varphi^{'}(k) \right. \right.$$

$$\left. \left. + F_\zeta^{''}(k) \Omega_\varphi^{'}(n-k) \right) \right\} + (1-a) \left\{ F_\varphi^{'}(0) \frac{U_{,\varphi}^{''}(k)}{r_1} + \frac{1}{2} \sum_{k=1}^{\infty} F_\varphi^{'}(k) \frac{U_{,\varphi}^{''}(k)}{r_1} \right\}$$

$$+ a \left\{ F_\varphi^{'}(n) \frac{U_{,\varphi}^{''}(0)}{r_1} + F_\varphi^{'}(0) \frac{U_{,\varphi}^{''}(n)}{r_1} + \frac{1}{2} \sum_{k=1}^{\infty} \left(F_\varphi^{'}(n+k) \frac{U_{,\varphi}^{''}(k)}{r_1} + F_\varphi^{'}(k) \frac{U_{,\varphi}^{''}(n+k)}{r_1} \right) \right.$$

$$\left. + \frac{1}{4} \sum_{k=1}^{n-1} \left(F_\varphi^{'}(n-k) \frac{U_{,\varphi}^{''}(k)}{r_1} + F_\varphi^{'}(k) \frac{U_{,\varphi}^{''}(n-k)}{r_1} \right) \right\} + (1-a) \Bigg\{$$

$$\frac{1}{2} \sum_{k=1}^{\infty} F_\varphi^{''}(k) \frac{U_{,\varphi}^{'}(k)}{r_1} \Bigg\} + a \left\{ \frac{1}{2} \sum_{k=1}^{\infty} \left(F_\varphi^{''}(n+k) \frac{U_{,\varphi}^{'}(k)}{r_1} + F_\varphi^{''}(k) \frac{U_{,\varphi}^{'}(n+k)}{r_1} \right) \right.$$

$$\left. - \frac{1}{4} \sum_{k=1}^{n-1} \left(F_\varphi^{''}(n-k) \frac{U_{,\varphi}^{'}(k)}{r_1} + F_\varphi^{''}(k) \frac{U_{,\varphi}^{'}(n-k)}{r_1} \right) \right\} \tag{2-9b}$$

$$f_\varphi^{(n)} = F_\varphi^{''}(n) + a \left\{ F_\varphi^{''}(n) \left(\epsilon_{\theta_o}^{'}(0) + \epsilon_{\varphi_o}^{'}(0) \right) + \frac{1}{2} \sum_{k=1}^{\infty} \left[F_\varphi^{''}(n+k) \left(\epsilon_{\theta_o}^{'}(k) + \epsilon_{\varphi_o}^{'}(k) \right) \right. \right.$$

$$\left. - F_\varphi^{''}(k) \left(\epsilon_{\theta_o}^{'}(n+k) + \epsilon_{\varphi_o}^{'}(n+k) \right) \right] + \frac{1}{4} \sum_{k=1}^{n-1} \left[F_\varphi^{''}(n+k) \left(\epsilon_{\theta_o}^{'}(k) + \epsilon_{\varphi_o}^{'}(k) \right) \right.$$

$$\left. + F_\varphi^{''}(k) \left(\epsilon_{\theta_o}^{'}(n-k) + \epsilon_{\varphi_o}^{'}(n-k) \right) \right] + F_\varphi^{'}(0) \left(\epsilon_{\theta_o}^{''}(n) + \epsilon_{\varphi_o}^{''}(n) \right)$$

$$+ \frac{1}{2} \sum_{k=1}^{\infty} \left[F_\varphi^{'}(k) \left(\epsilon_{\theta_o}^{''}(n+k) + \epsilon_{\varphi_o}^{''}(n+k) \right) - F_\varphi^{'}(n+k) \left(\epsilon_{\theta_o}^{''}(k) + \epsilon_{\varphi_o}^{''}(k) \right) \right]$$

$$+ \frac{1}{4} \sum_{k=1}^{n-1} \left[F_\varphi^{'}(k) \left(\epsilon_{\theta_o}^{''}(n-k) + \epsilon_{\varphi_o}^{''}(n-k) \right) + F_\varphi^{'}(n-k) \left(\epsilon_{\theta_o}^{''}(k) + \epsilon_{\varphi_o}^{''}(k) \right) \right]$$

$$+ F_\zeta^{''}(n) \Omega_\theta^{'}(0) - \frac{1}{2} \sum_{k=1}^{\infty} \left(F_\zeta^{''}(n+k) \Omega_\theta^{'}(k) - F_\zeta^{''}(k) \Omega_\theta^{'}(n+k) \right)$$

$$- \frac{1}{4} \sum_{k=1}^{n-1} \left(F_\zeta^{''}(n-k) \Omega_\theta^{'}(k) + F_\zeta^{''}(k) \Omega_\theta^{'}(n-k) \right) - F_\zeta^{'}(0) \Omega_\theta^{''}(n)$$

$$- \frac{1}{2} \sum_{k=1}^{\infty} \left(F_\zeta^{'}(k) \Omega_\theta^{''}(n+k) - F_\zeta^{'}(n+k) \Omega_\theta^{''}(k) \right) - \frac{1}{4} \sum_{k=1}^{n-1} \left(F_\zeta^{'}(k) \Omega_\theta^{''}(n-k) \right.$$

$$\left. + F_\zeta^{'}(n-k) \Omega_\theta^{''}(k) \right) + n \left[\frac{1}{2} \sum_{k=1}^{\infty} \left(F_\theta^{'}(n+k) \frac{V^{''}(k)}{r_o} - F_\theta^{'}(k) \frac{V^{''}(n+k)}{r_o} \right) \right.$$

$$+ \frac{1}{4} \sum_{k=1}^{n-1} \left(F_\theta^{'}(n-k) \frac{V^{''}(k)}{r_o} + F_\theta^{'}(k) \frac{V^{''}(n-k)}{r_o} \right) + F_\theta^{''}(0) \frac{V^{'}(n)}{r_o}$$

$$+ \frac{1}{2} \sum_{k=1}^{\infty} \left(F_\theta^{''}(k) \frac{V^{'}(n+k)}{r_o} - F_\theta^{''}(n+k) \frac{V^{'}(k)}{r_o} \right) + \frac{1}{4} \sum_{k=1}^{n-1} \left(F_\theta^{''}(k) \frac{V^{'}(n-k)}{r_o} \right.$$

$$\left. \left. + F_\theta^{''}(n-k) \frac{V^{'}(k)}{r_o} \right) \right] \right\} \tag{2-9b}$$

$$f_\zeta^{(n)} = F_\zeta^{''}(n) + a \left\{ F_\zeta^{''}(n) \left(\epsilon_{\theta_o}^{'}(0) + \epsilon_{\varphi_o}^{'}(0) \right) + \frac{1}{2} \sum_{k=1}^{\infty} \left[F_\zeta^{''}(n+k) \left(\epsilon_{\theta_o}^{'}(k) + \epsilon_{\varphi_o}^{'}(k) \right) \right. \right.$$

$$-F_\zeta''(k)\left(\epsilon_{\theta_o}'^{(n+k)}+\epsilon_{\varphi_o}'^{(n+k)}\right)\Bigg]+\frac{1}{4}\sum_{k=1}^{n-1}\Bigg[F_\zeta''^{(n-k)}\left(\epsilon_{\theta_o}'^{(k)}+\epsilon_{\varphi_o}'^{(k)}\right)$$

$$+F_\zeta''^{(k)}\left(\epsilon_{\theta_o}'^{(n-k)}+\epsilon_{\varphi_o}'^{(n-k)}\right)\Bigg]+F_\zeta'^{(0)}\left(\epsilon_{\theta_o}''^{(n)}+\epsilon_{\varphi_o}''^{(n)}\right)$$

$$+\frac{1}{2}\sum_{k=1}^{\infty}\Bigg[F_\zeta'^{(k)}\left(\epsilon_{\theta_o}''^{(n+k)}+\epsilon_{\varphi_o}''^{(n+k)}\right)-F_\zeta'^{(n+k)}\left(\epsilon_{\theta_o}''^{(k)}+\epsilon_{\varphi_o}''^{(k)}\right)\Bigg]$$

$$+\frac{1}{4}\sum_{k=1}^{n-1}\Bigg[F_\zeta'^{(k)}\left(\epsilon_{\theta_o}''^{(n-k)}+\epsilon_{\varphi_o}''^{(n-k)}\right)+F_\zeta'^{(n-k)}\left(\epsilon_{\theta_o}''^{(k)}+\epsilon_{\varphi_o}''^{(k)}\right)\Bigg]$$

$$+F_\varphi''^{(n)}\Omega_\theta'^{(0)}+\frac{1}{2}\sum_{k=1}^{\infty}\left(F_\varphi''^{(n+k)}\Omega_\theta'^{(k)}-F_\varphi''^{(k)}\Omega_\theta'^{(n+k)}\right)$$

$$+\frac{1}{4}\sum_{k=1}^{n-1}\left(F_\varphi''^{(n-k)}\Omega_\theta'^{(k)}+F_\varphi''^{(k)}\Omega_\theta'^{(n-k)}\right)$$

$$+F_\varphi'^{(0)}\Omega_\theta''^{(n)}+\frac{1}{2}\sum_{k=1}^{\infty}\left(F_\varphi'^{(k)}\Omega_\theta''^{(n+k)}-F_\varphi'^{(n+k)}\Omega_\theta''^{(k)}\right)$$

$$+\frac{1}{4}\sum_{k=1}^{n-1}\left(F_\varphi'^{(k)}\Omega_\theta''^{(n-k)}+F_\varphi'^{(n-k)}\Omega_\theta''^{(k)}\right)-F_\theta''^{(0)}\Omega_\varphi'^{(n)}$$

$$-\frac{1}{2}\sum_{k=1}^{\infty}\left(F_\theta''^{(k)}\Omega_\varphi'^{(n+k)}-F_\theta''^{(n+k)}\Omega_\varphi'^{(k)}\right)-\frac{1}{4}\sum_{k=1}^{n-1}\left(\Omega_\varphi'^{(n-k)}F_\theta''^{(k)}\right.$$

$$+\Omega_\varphi'^{(k)}F_\theta''^{(n-k)}\right)-\Omega_\varphi''^{(0)}F_\theta'^{(n)}-\frac{1}{2}\sum_{k=1}^{\infty}\left(\Omega_\varphi''^{(k)}F_\theta'^{(n+k)}-\Omega_\varphi''^{(n+k)}F_\theta'^{(k)}\right)$$

$$-\frac{1}{4}\sum_{k=1}^{n-1}\left(\Omega_\varphi''^{(k)}F_\theta'^{(n-k)}+\Omega_\varphi''^{(n-k)}F_\theta'^{(k)}\right)\Bigg\}\tag{2-9b}$$

where $a=0$ for $n=0$, and $a=1$ for $n\geq 1$. It is evident, that by assuming that a line of symmetry exists in the loading (as done in earlier references), only the symmetric or the antisymmetric half of the Fourier series expansion (2-1, 2) can be used, and consequently only one of the two aforementioned sets of equations is required. If we choose to use Equations (2-8) and (2-9a), for example, the latter are simplified further since all the double primed terms

become zero. As noted previously, revised equations can be formulated for the reinforced or laminated cases.

As will be discussed in Chapter 3, Equations (2-3) or (2-4) and (2-8) will be employed to establish the stiffness matrices and the load matrices of the various segments of the shell. The numerical solution of the equations for the linear analysis (2-3) may be attained by a technique described in Chapter 3. To apply this technique to the non-linear equations they must first be linearized by the use of a suitable method. For instance in Reference 20, the harmonic amplitudes of the shell functions are established throughout the shell by first solving the unsymmetric linear problem. The results may be employed in Equations (2-9a, b) to establish a numerical value for the nonlinear terms. In general, the linear analysis may yield a number of zero harmonic amplitudes. For instance, the linear analysis will yield nonzero harmonic amplitudes only for the values of n corresponding to a non-zero load in Equations (2-1). Thus, if for example, the load is described by the $n = 1, 2$ harmonics, the linear analysis will yield only the $\Omega_\theta^{(1)}$ and $\Omega_\theta^{(2)}$ harmonics of ω_θ. However, to establish the values of the non-linear terms in Equations (2-9a, b) additional harmonics of ω_θ are required, as for instance $\Omega_\theta^{(0)}$ and $\Omega_\theta^{(n)}$; where $n = 2, 3 \ldots P$, P being the harmonic at which the infinite series is truncated. To obtain the values of the non-linear terms, all the harmonics of the functions which are not established by the preceding cycle of the analysis, are set to zero. The numerical values of the non-zero non-linear terms are computed, and subsequently employed in Equations (2-4) or (2-8) resulting in an uncoupled system of equations which may be solved to yield another set of values for the harmonic amplitudes. It should be noted, that some of the equations for the harmonic amplitudes (2-4) or (2-8) may not contain actual load terms, but rather the numerically represented non-linear

65

terms. Subsequently, the values of the harmonic amplitudes are used to compute a new set of non-linear terms, and the process continues until the harmonic amplitudes are established to the desired accuracy. Moreover, it should be noted, that depending upon the number of non-zero nonlinear coupling terms established in each cycle of the analysis, the number of equations to be solved may vary per cycle. Although the aforementioned technique is the most straightforward, it may not converge, however, for certain cases [22, 131].

In another method [9, 14, 15, 99] the harmonic amplitudes are also established from the solution of the linear part of Equations (2-4) or (2-8). Instead of utilizing the numerical value of both terms in the non-linear products of Equations (2-9a, b) only one term is substituted numerically. Substitution of the linearized Equations (2-9a, b) into Equations (2-4) or (2-8), yields sets of coupled linear equations, which may be solved by any method that does not result in extremely large matrices; as for example, by a numerical integration method analogous to that presented in Reference 107. The foregoing methods are adequate only for problems in which the effect of non-linear terms is small [14, 131], although in Reference 20, it is indicated that these methods may be employed in the solution of problems involving relatively large deflections.

In the solution of non-linear problems the load should be applied in increments. When the solution converges for one load level, the load is increased by another increment and the process continues until the components of stress and displacement of the shell are established for any value of the load desired. If the load is continually increased, it will reach a value for which the solution diverges. This indicates that for this value of the load, the corresponding deformation pattern of the shell has reached a level of instability.

For ideally "perfect" shells having identical prebuckling and buckling deformation patterns, the classical buckling load is the value of the load prior to that for which the solution diverges. However, ideally "perfect" shells, whose buckling deformation pattern differs from their prebuckling deformation pattern may atain one or more states of instability for smaller values of the loading, which will not be obtained by the analysis outlined above. Other methods for establishing all the states of instability are presented in Chapter 4.

It should be indicated, that the aforementioned solution of the nonlinear equations may not converge for values of the load less than the maximum value for which the prebuckling deformation pattern of the shell is stable [22, 41, 131]. Thus, the aforementioned solution may yield conservative values of the load for which the prebuckling deformation pattern becomes unstable.

A method of proven convergence for the solution of nonlinear equations is Newton's method [17, 18], wherein each harmonic amplitude is expressed as the sum of two parts, an assumed solution, and a correction to the assumed solution:

$$Y_{m+1} = Y_m + \Delta Y \qquad\qquad (2-10)$$

Equation (2-10) may be substituted into either Equations (2-4, 5) or Equations (2-8, 9a). The resulting equations will contain terms of the type $(Y_m)(\Delta Y)$ as well as $(\Delta Y)^2$. In these equations the Y_ms are numerically known, from a previous iteration. In a buckling analysis the nonlinear $(\Delta Y)^2$ terms may be neglected. For a postbuckling analysis, however, these terms should be retained [129, 130]. Restricting ourselves to a nonlinear analysis for the prebuckling state, the linear ΔY correction equations will be uncoupled or

coupled depending upon whether axisymmetric (Equations (2-4) and (2-5)), or unsymmetric (Equations 2-8) and (2-9)) loading is considered. The procedure is as follows: First, the problem is solved for a small value of the load, where the linear theory is accurate. This may be accomplished by using the aforementioned ΔY equations, but setting all the Y_m terms to zero. The solutions for ΔY, and $Y_m = 0$, are substituted into Equation (2-10). The values of Y_{m+1} thus obtained are substituted for the Y_m (which in the previous step were set to zero) in the aforementioned ΔY equations, producing a set of linear, coupled (if the load is unsymmetric) equations. These equations are now solved for new ΔYs, and these, with the current Y_ms, are substituted in Equations (2-10) to produce a new set of Y_{m+1}s. This procedure continues until the harmonic amplitudes are established to the desired accuracy. The load on the shell is now increased by an increment and the whole procedure is repeated. The solution obtained for the previous value of the load, or a set of harmonic amplitudes obtained by extrapolation can be used as a starting point. Non convergence of the solution indicates that the last load increment has increased the value of the total load above the limit point (the point of zero slope of the load-displacement curve). The solution may be repeated using a smaller load increment, and values of the total load as close to the limit point as desired may be obtained. The last value of the load for which the solution converges is taken as the maximum value of the load for which the prebuckling deformation pattern of the shell is stable.

Reference 22 essentially utilizes the foregoing technique with one important simplification. The nonlinear terms which induce coupling of the harmonics are disregarded. This is necessary inasmuch as the finite difference technique employed in Reference 22 results in large matrix equations. Consequently, their solution becomes extremely time-consuming if the harmonics

68

are coupled. The penalty for this simplification is a slower convergence, and for more complex problems, possible divergence at loads less than the maximum value of the load for which the prebuckling deformation pattern of the shell is stable. In a numerical integration procedure of the type presented in Reference 107, the resulting matrices can be maintained at a reasonable size, and consequently it is not essential to make simplifications.

Thus, by employing any of the aforementioned methods, the nonlinear problem simplifies to that of successively solving linear equations, which in the most complex case (unsymmetric loads) involves harmonic coupling. The procedure for the solution of these types of equations is presented in Chapter 3.

For a postbuckling analysis, as noted earlier, the nonlinear terms in ΔY must be retained in order to cross bifurcation points [129, 130]. In addition, a method of proven convergence, such as the Newton iteration method must be used in the solution. Some difficulties do exist, however, in utilizing the equations for postbuckling investigations. The most important difficulty is exemplified by the case of a shell under axisymmetric loading only, wherein a postbuckled configuration may exist which is described by harmonic amplitudes other than the zeroth. In this case, a small "disturbance load" involving several harmonic amplitudes must be added to allow the shell to deform into the proper configuration in the postbuckling range. This disturbance load must be small in magnitude, as compared to the primary axisymmetric load, but it must also be described by a sufficient number of harmonics so that an adequate description of the postbuckled configuration may be obtained.

CHAPTER 3

SOLUTION FOR STATIC RESPONSE

Shell structures found in spacecraft, aircraft engines, or submersibles, are usually comprised of several, interconnected, singly and doubly curved shells. For a given shell geometry, the accuracy of the results obtained on the basis of the numerical integration method is dependent upon the length of the shell along the meridian. If the shell is long, the effect of the stress resultants and displacements at the one edge will have a negligible effect upon the stress resultants and displacements on the other edge. This could result in a number of terms in the stiffness matrices which are inaccurate, inasmuch as they constitute small differences of large numbers. This difficulty may be circumvented by subdividing the shell into segments by introducing fictitious boundaries. Such an approach is amenable to the use of local coordinate systems, and includes the unique self-checking features discussed in the Introduction. Equations for establishing the appropriate lengths of segments for shells of various geometries are presented in Reference 108, for linear and nonlinear analyses.

In this chapter, we shall first obtain all the matrices pertaining to single shell segments. Then we shall proceed to couple these matrices together and apply the boundary conditions, in order to obtain an overall matrix equation describing the equilibrum of the total structure. The solution of this equation yields the stress resultants and displacements, at the joints. These stress resultants and displacements are used in

establishing the distribution of the stress resultants and displacements throughout all the shell segments.

Coordinate Transformation Matrices: A typical shell segment is presented in Figure 8. Various possible geometries of shell segments are given in Figures 9 through 13. Since the various shell segments may be described by different coordinate systems and different geometric variables, the stress resultants and displacements referred to the coordinates of a segment must be transformed to the reference global coordinates. The edge forces on the typical shell segment in this global Z, R, θ system are shown in Figure 14. The components of stress resultants and moments referred to a local coordinate system are denoted by Greek subscripts $(T_{\varphi\theta}, N_\varphi, J_\varphi^*, M_\varphi)$, whereas the components of stress rsultants referred to the global coordinate system are denoted by Latin subscripts (F_T, F_Z, F_R). The global moment is denoted by M. The appropriate coordinate transformation matrices then are:

$$\{F(i)\} = [\text{IFT}]\,\{f(i)\} \qquad \begin{Bmatrix} F_T \\ F_Z \\ F_R \\ M \end{Bmatrix}(i) = \begin{bmatrix} -1 & 0 & 0 & 0 \\ 0 & \sin\varphi_i & \cos\varphi_i & 0 \\ 0 & -\cos\varphi_i & \sin\varphi_i & 0 \\ 0 & 0 & 0 & +1 \end{bmatrix} \begin{Bmatrix} T_{\varphi\theta} \\ N_\varphi \\ J_\varphi^* \\ M_\varphi \end{Bmatrix}(i) \qquad (3\text{-}1)$$

Figure 8 Typical Shell Segment

72

+Z

a

Ellipsoid

Specify a, $\beta = \dfrac{b}{a}$

b

i

out

in

j

ϕ_j

ϕ_i

i

out

in

j

Sphere

Specify a, $\beta = 1$

ϕ_j

a

ϕ_i
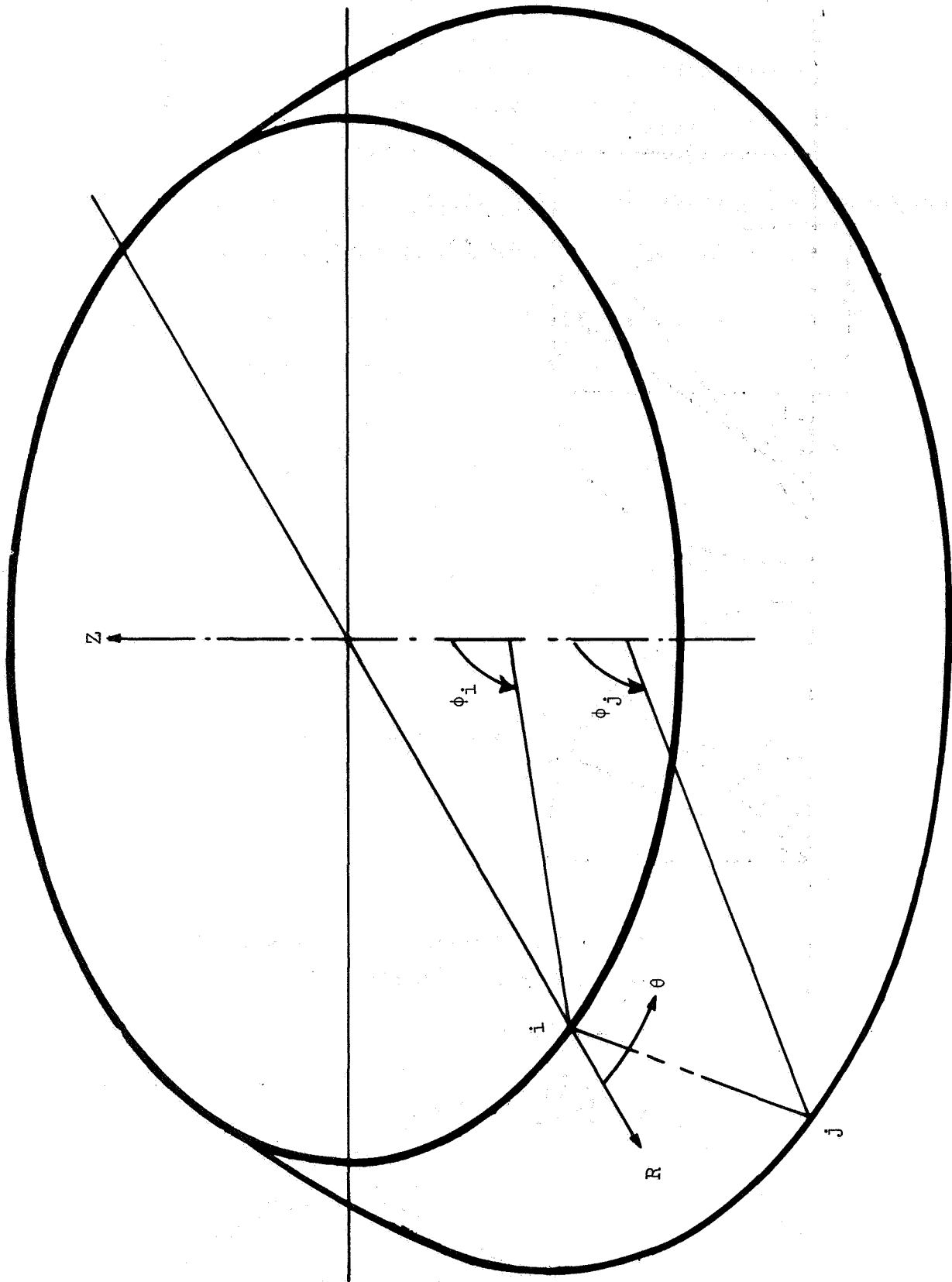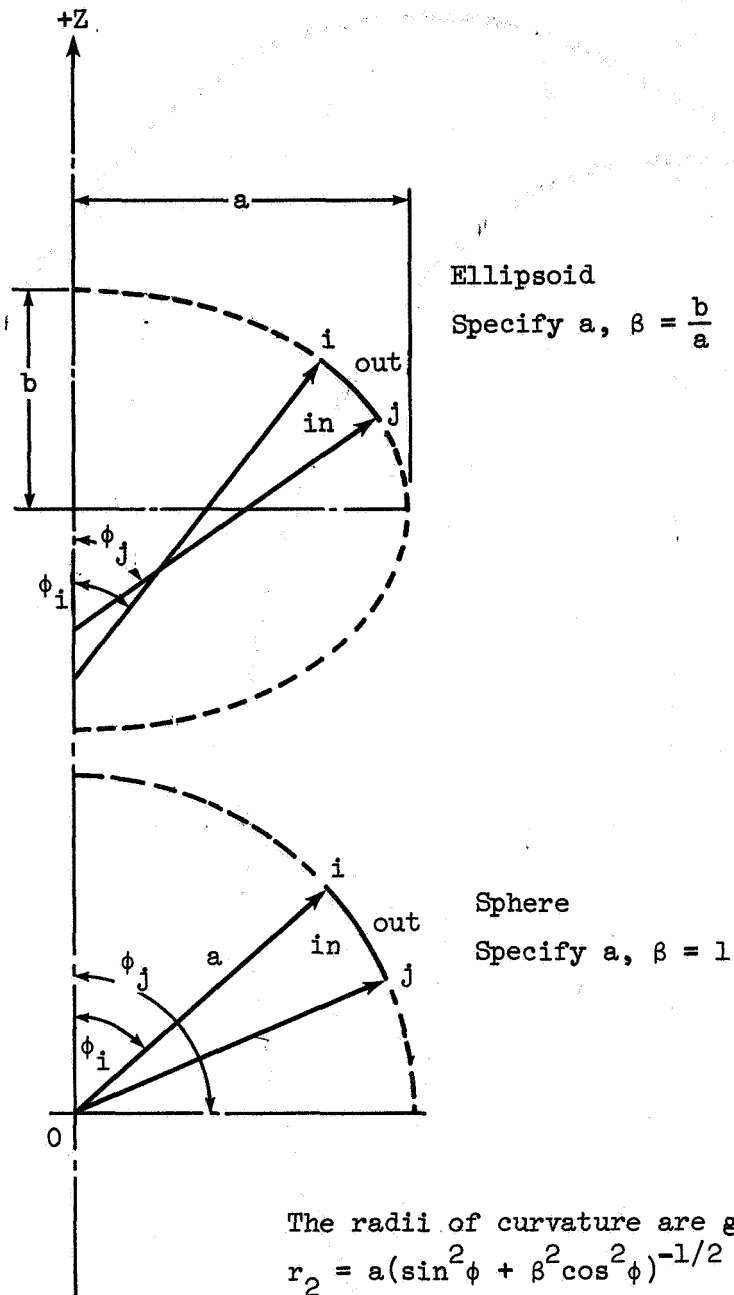
0

The radii of curvature are given as:

$$r_2 = a(\sin^2\phi + \beta^2\cos^2\phi)^{-1/2}$$

$$r_o = r_2 \sin\phi$$

$$r_1 = \left(\frac{\beta^2}{a^2}\right)r_2^2$$

Figure 9a Ellipsoid-Sphere

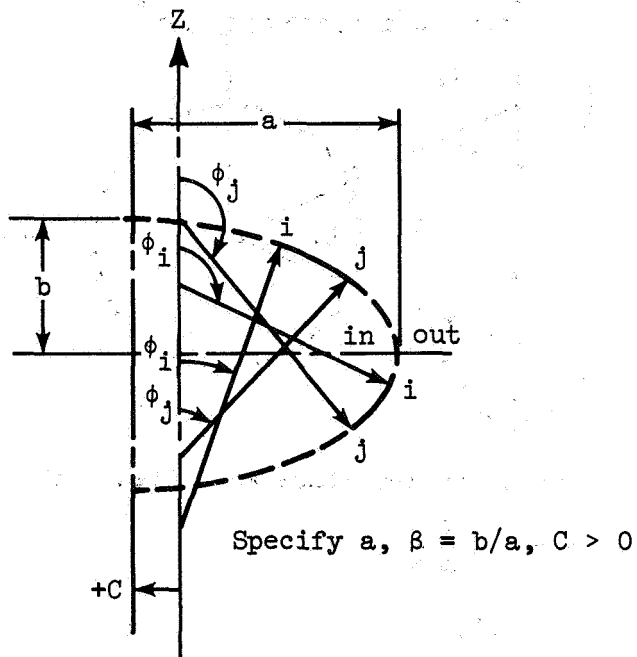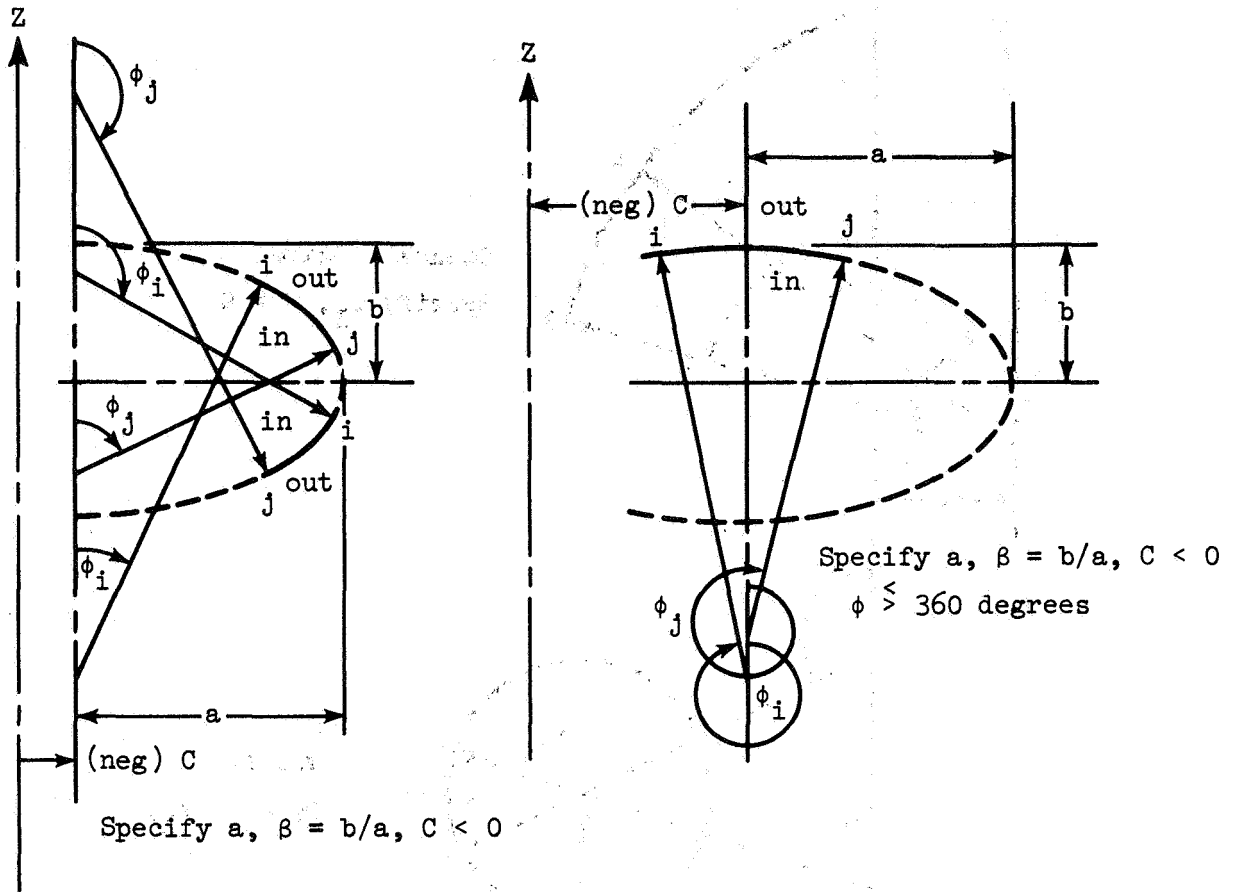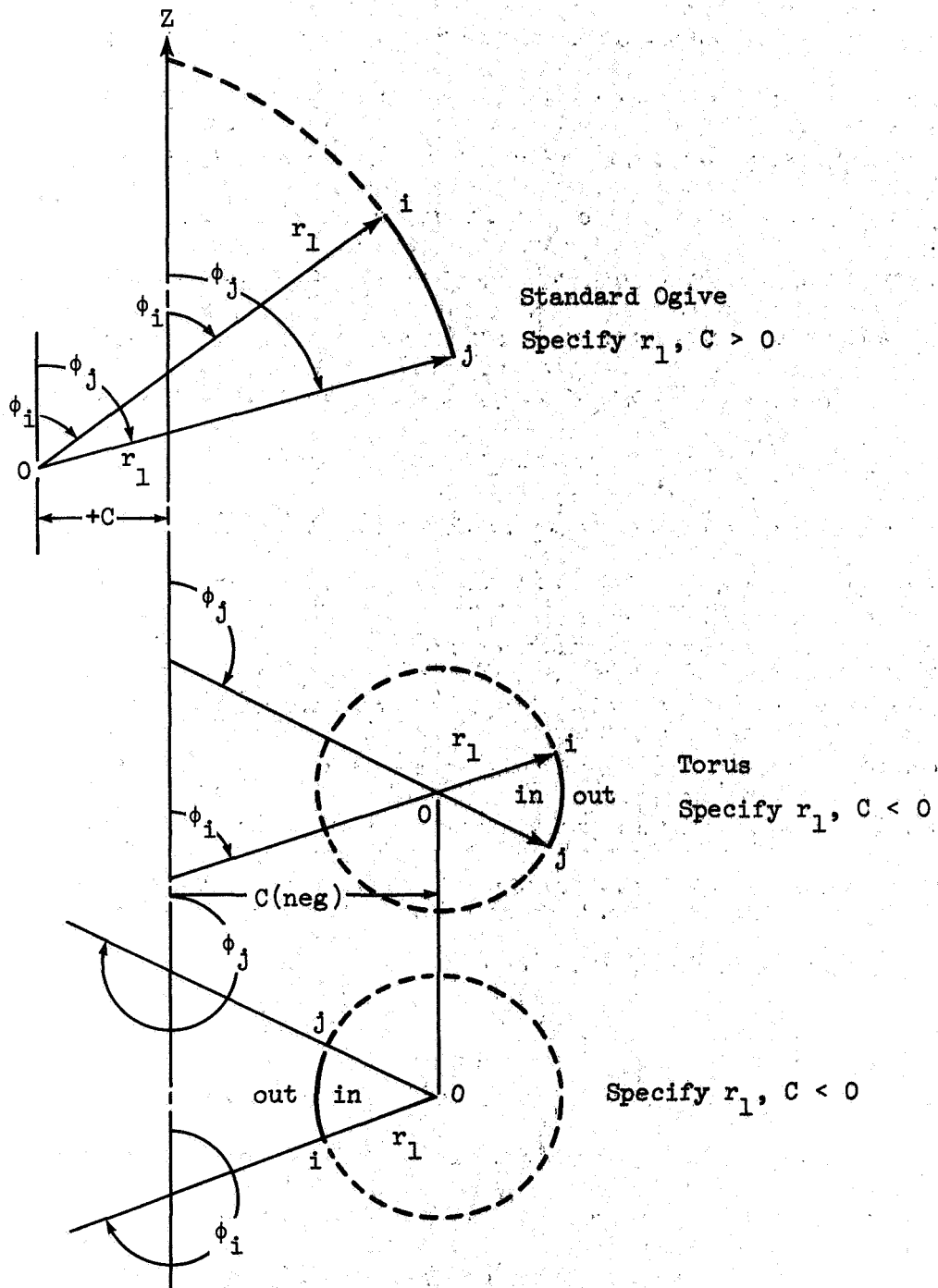Figure 9b Translated Ellipsoid

74

The radii of curvature are given as:

$$r_2 = r_1 - \frac{C}{\sin\phi}$$

$$r_o = r_2 \sin\phi$$

Figure 10 Torus-Ogive

75
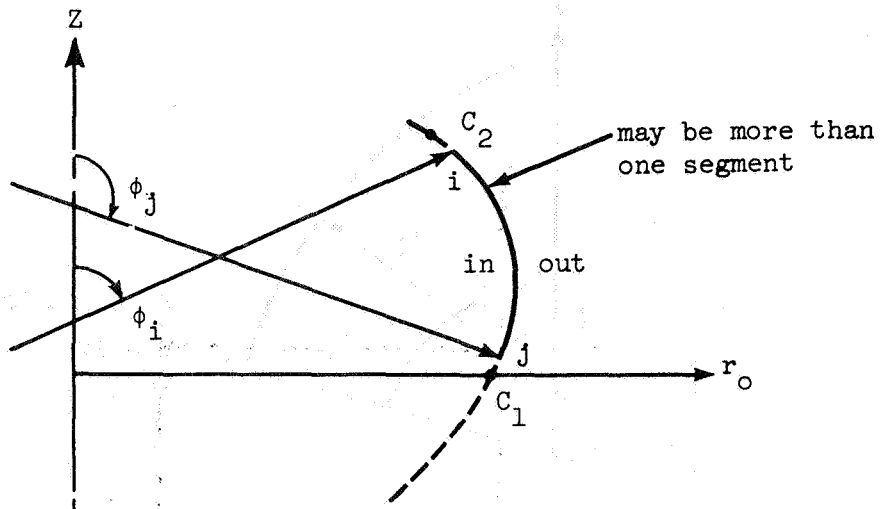
In the ranges of ϕ
$0° \leqslant \phi < 10°$
$170° < \phi < 190°$
$350° < \phi \leqslant 360°$
spherical, toroidal or elliptical segments can be used with sufficient accuracy.

"B" shape $10° \leqslant \phi \leqslant 170°$

Specify: Z versus r_o starting with
           $Z = 0$ at C_1, and going to C_2.

Note: Z vs r_o input table should overlap
        total range of ϕ input for all segments.
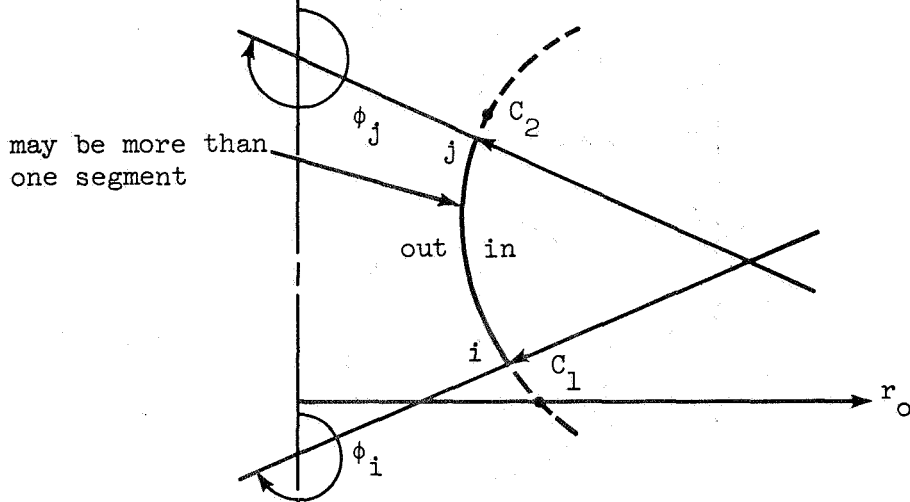
"A" shape $190° \leqslant \phi \leqslant 350°$

Specify: Z versus r_o starting with
           $Z = 0$ at C_1, and going to C_2.

Note: Z vs r_o input table should overlap
        total range of ϕ input for all segments.

Figure 11   General Geometry

76

+Z

r_o

i

s

in | out

j

Specify r_o

Figure 12 Cylinder

77

+Z

r_o →

s

i

out

in

j

Standard Cone

Specify $\phi > 0$

φ →

s

out

i

in

j

Plate

Specify $\phi = 0$

−φ

out

i

in

j

Inverted Cone

Specify $\phi < 0$

r_o →

s

The radius of curvature is given as:

$$r_o = s \cos\phi$$

Figure 13   Cone

78

Figure 14   Forces on Typical Shell Segment

$$\{F(j)\} = [\,JFT\,]\,\{f(j)\}$$

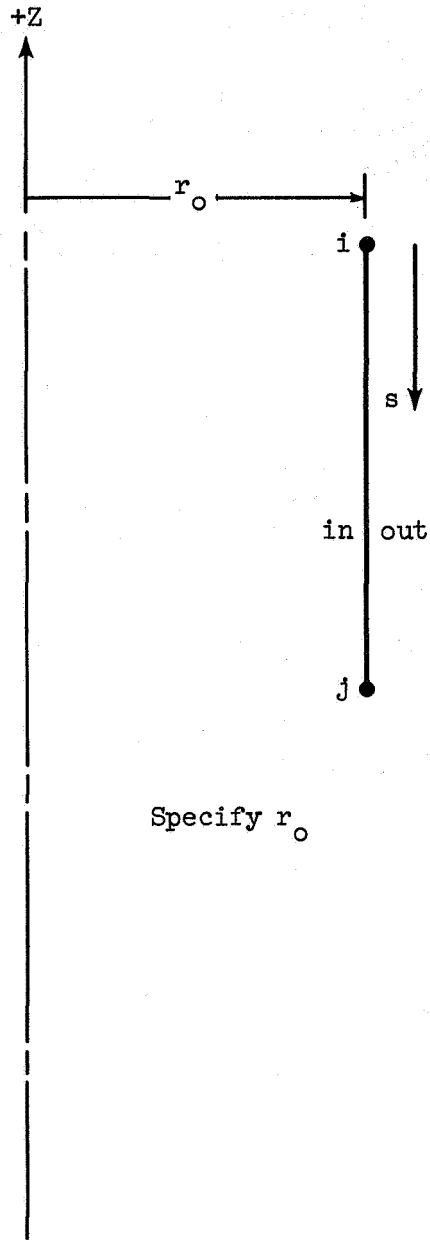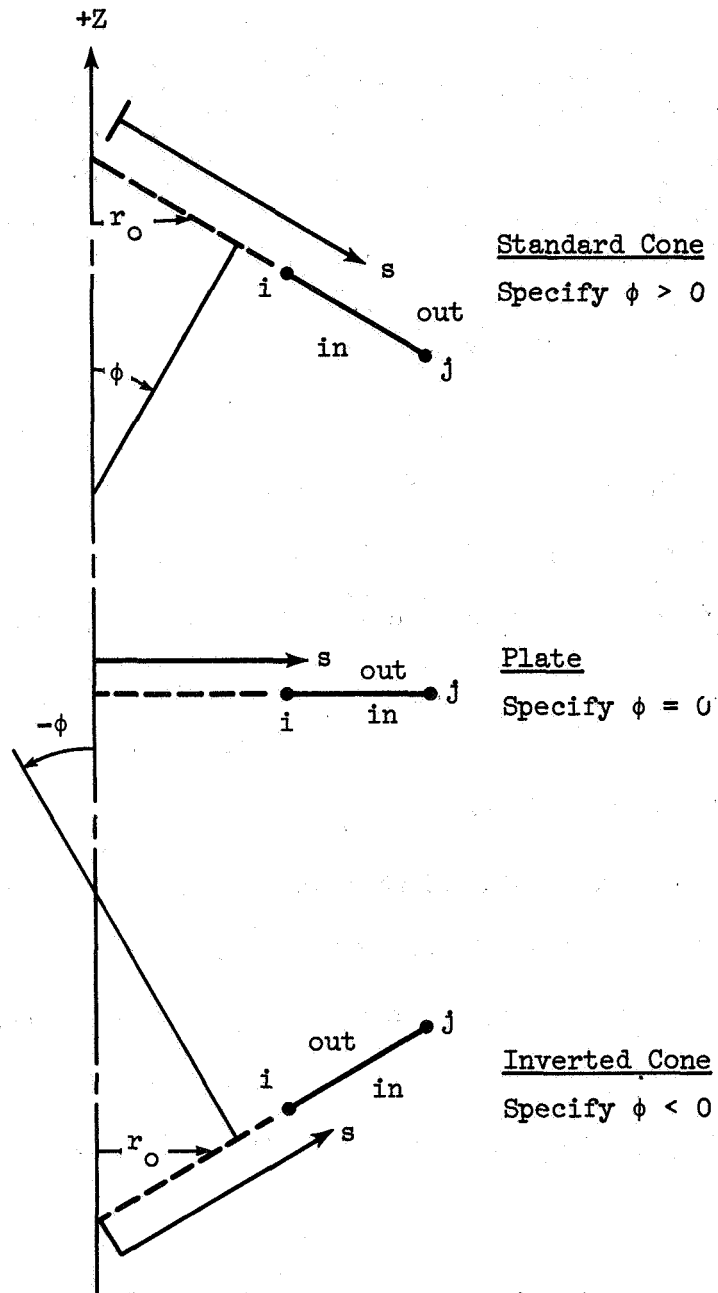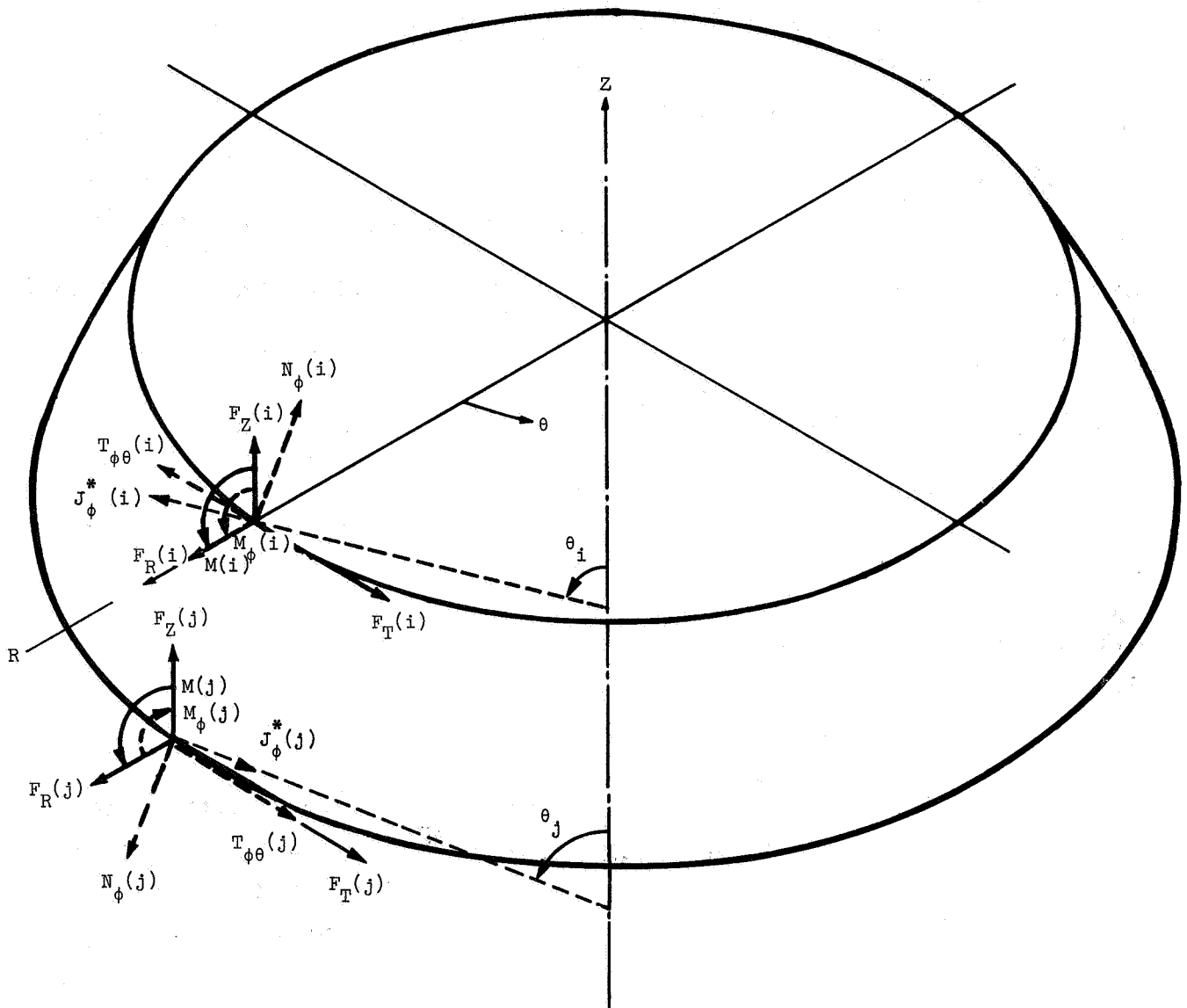$$\begin{Bmatrix} F_T \\ F_Z \\ F_R \\ M \end{Bmatrix}(j) = \begin{bmatrix} +1 & 0 & 0 & 0 \\ 0 & -\sin\varphi_j & -\cos\varphi_j & 0 \\ 0 & \cos\varphi_j & -\sin\varphi_j & 0 \\ 0 & 0 & 0 & -1 \end{bmatrix} \begin{Bmatrix} T_{\varphi\theta} \\ N_{\varphi} \\ J_{\varphi}^* \\ M_{\varphi} \end{Bmatrix}(j) \qquad (3\text{-}2)$$

and

$$\{\Delta(i)\} = [\,IDT\,]\,\{\delta(i)\}$$

$$\begin{Bmatrix} \Delta_T \\ \Delta_Z \\ \Delta_R \\ \Omega_{\theta} \end{Bmatrix}(i) = \begin{bmatrix} +1 & 0 & 0 & 0 \\ 0 & -\sin\varphi_i & -\cos\varphi_i & 0 \\ 0 & \cos\varphi_i & -\sin\varphi_i & 0 \\ 0 & 0 & 0 & -1 \end{bmatrix} \begin{Bmatrix} u \\ v \\ w \\ \omega_{\theta} \end{Bmatrix}(i) \qquad (3\text{-}3)$$

$$\{\Delta(j)\} = [\,JDT\,]\,\{\delta(j)\}$$

$$\begin{Bmatrix} \Delta_T \\ \Delta_Z \\ \Delta_R \\ \Omega_{\theta} \end{Bmatrix}(j) = \begin{bmatrix} +1 & 0 & 0 & 0 \\ 0 & -\sin\varphi_j & -\cos\varphi_j & 0 \\ 0 & \cos\varphi_j & -\sin\varphi_j & 0 \\ 0 & 0 & 0 & +1 \end{bmatrix} \begin{Bmatrix} u \\ v \\ w \\ \omega_{\vartheta} \end{Bmatrix}(j) \qquad (3\text{-}4)$$

where [IFT], [JFT], [IDT], [JDT] denote the I Force Transformation,
the J Force Transformation, the I Displacement Transformation, and
the J Displacement Transformation matrices, respectively. The subscripts
i and j refer to the meridional coordinates of the beginning and end of the

segment, respectively. These transformation relations are valid for the functions $F(\theta, \varphi_k)$ and $\Delta(\theta, \varphi_k)$ as well as, for the amplitudes of harmonics, $F^{(n)}(\varphi_k)$ and $\Delta^{(n)}(\varphi_k)$, $(k = i, j)$.

In the sequel, the pertinent matrix equations will be written for one harmonic at a time; this will not result in any loss of generality of the solution to be discussed. However, the harmonics are coupled for non-linear problems having an unsymmetric load. Thus, it would not be possible to write the matrix equations for only one harmonic. Consequently, the size of the matrices would be multiplied by N, the number of harmonics to be retained when the Fourier series expansions are truncated. Hence, for a nonlinear problem with unsymmetric load, if N harmonics are retained in the Fourier expansions, a typical transformation matrix may be denoted by [IFTN], and assumes the form

$$
[\text{IFTN}]_{4N \times 4N} =
\begin{bmatrix}
[\text{IFT}] & 0 & \text{--}0\text{--------} & 0 \\
0 & & & | \\
| & & & | \\
0 & & [\text{IFT}] & 0 \\
| & & & | \\
| & & & 0 \\
0 & \text{-- --} & 0 & \text{-- }0\,[\text{IFT}]
\end{bmatrix}
\tag{3-5}
$$

where "N" of the 4x4 [IFT] matrices are located on the diagonal. Notice, that for nonlinear problems involving unsymmetric loads, the other matrices such as the stiffness matrix, may not be block diagonal matrices. Such special matrices will be developed separately as the need arises.

Segment Stiffness Matrices: The suitable differential equations for each specific shell segment are solved for different sets of initial conditions by the Runge-Kutta forward integration method. Any satisfactory Runge-Kutta

81

formula may be used [125] - [127]. The one employed in this investigation is [128]:

$$Y_1 = Y_m + \frac{\Delta t}{2} \dot{Y}_m$$

$$Y_2 = Y_m + \frac{\Delta t}{2} \dot{Y}_1$$

(3-6)

$$Y_3 = Y_m + \Delta t \, \dot{Y}_2$$

$$Y_{m+1} = Y_m + \frac{\Delta t}{6} (\dot{Y}_m + 2 \dot{Y}_1 + 2 \dot{Y}_2 + \dot{Y}_3)$$

These relations may be employed to establish the value Y_{m+1} of a function at point (m+1) if the value Y_m of the function and its derivative $\dot{Y}_m$ with respect to the integration variable, are known at point m. The symbols used in the above relations are defined as:

$\Delta t =$ the integration interval from m to (m+1).

$Y_m =$ the value of the function at point m obtained by numerical integration.

$Y_{m+1} =$ the value of the function at point (m+1) obtained by numerical integration.

Y_1, $Y_2 =$ the first and second estimate respectively, of the values of the function at the mid-point between points m and (m+1).

$Y_3 =$ the first estimate of the value of the function at point (m+1).

$(\dot{\ }) =$ derivative of the function with respect to the integration variable.

The Runge-Kutta integration method is employed in establishing the values of the functions at the jth edge of a segment from the assumed values of the functions at the ith edge of the segment. A number of points are automatically chosen along the meridian of the shell segment, i, $i+1$, $i+2$ ... m ... $j-2$, $j-1$, j. The spacing of the points is denoted by Δt, and may vary from point to point. The derivatives of the functions at the ith boundary are established initially by Equations (1-24) through (1-26). The values of the functions and their derivatives at the ith boundary are then employed in establishing the value of the functions at point $(i+1)$. The process is repeated until the values of the functions at the jth edge are established

The process for establishing the values of the functions at point $m+1$ from those at point m is as follows. The values of Y_m (stress resultants and displacements) are employed in Equations (1-24) through (1-26) to establish the derivatives $\dot{Y}_m$. The values of Y_m and $\dot{Y}_m$ are employed to compute Y_1. These are the values of the predicted stress resultants and displacements at the point midway between m and $m+1$. Subsequently, they are employed in Equations (1-24) through (1-26) to establish the derivatives $\dot{Y}_1$. The values of Y_2 are then computed from Equation (3-6b). The values of Y_2 represent a corrected estimate of values of the stress resultants and displacements at the point midway between m and $m+1$. These values are then used in Equations (1-24) through (1-26) to establish the derivatives $\dot{Y}_2$. Subsequently, the values of Y_3 are computed from Equation (3-6c) and employed in computing the values of $\dot{Y}_3$.

The values Y_3 represent the first estimate of the values of the predicted stress resultants and displacements at the point (m+1). A corrected estimate Y_{m+1} of these functions is then computed using Equation (3-6d). Subsequently, the values of Y_3 and Y_{m+1} are compared, and if they differ by less than a set tolerance, d_1, the process is continued to establish the values of the functions at a point (m+2), located at an interval $2\Delta t$ from point (m). If the values of Y_3 and Y_{m+1} differ by more than the set tolerance, d_1, the current Δt is halved, and the process is repeated until the values of the functions Y_3 and Y_{m+1} differ by less than the tolerance d_1. Using the same interval Δt, employed in the previous step, the process is continued to establish the values of the functions at point (m+2). Thus, the interval Δt may vary from point to point. This procedure is referred to as automatic step control, and provides fo uniform accuracy in the solution of the differential equations.

As indicated previously, we will start by assuming the values of the eight shell functions (stress resultants and displacements) at the ith boundary of each segment, and we shall compute the corresponding values of the eight shell functions at the jth boundary. To isolate the influence of each of the eight functions we will set one function to unity and the others to zero. The process is outlined schematically in Fig. 15. In columns 1 through 4, one of the displacements at the ith edge is successively set to unity, while the remaining displacements and the stress resultants are set to zero. The corresponding values of the harmonics $f^{(n)}(j)$ of the stress resultants at the jth edge are represented by the matrix X_1, whereas the values of the harmonics $\delta^{(n)}(j)$ of the displacements

84

		Unit Displacements Applied				Unit Forces Applied				Distributed Load Applied (10 possible loading cases)			
Column Number		1	2	3	4	5	6	7	8	9	10	••••••	18
Initial Conditions $\{f^{(n)}(i)\}$ $\begin{array}{l} T_{\phi\theta}^{(n)}(i) \\ N_{\phi}^{(n)}(i) \\ J_{\phi}^{*(n)}(i) \\ M_{\phi}^{(n)}(i) \end{array}$		$\mathbf{0}$				$\mathbf{I_4}$				$\begin{matrix} 0 & \cdots & 0 \\ 0 & \cdots & 0 \\ 0 & \cdots & 0 \\ 0 & \cdots & 0 \end{matrix}$			
$\{\delta^{(n)}(i)\}$ $\begin{array}{l} U^{(n)}(i) \\ V^{(n)}(i) \\ W^{(n)}(i) \\ \Omega_{\theta}^{(n)}(i) \end{array}$		$\mathbf{I_4}$				$\mathbf{0}$				$\begin{matrix} 0 & \cdots & 0 \\ 0 & \cdots & 0 \\ 0 & \cdots & 0 \\ 0 & \cdots & 0 \end{matrix}$			
Final Conditions $\{f^{(n)}(j)\}$ $\begin{array}{l} T_{\phi\theta}^{(n)}(j) \\ N_{\phi}^{(n)}(j) \\ J_{\phi}^{*(n)}(j) \\ M_{\phi}^{(n)}(j) \end{array}$		$\mathscr{X}_1$				$\mathscr{X}_2$				$\mathscr{X}_3$			
$\{\delta^{(n)}(j)\}$ $\begin{array}{l} U^{(n)}(j) \\ V^{(n)}(j) \\ W^{(n)}(j) \\ \Omega_{\theta}^{(n)}(j) \end{array}$		$\mathscr{Y}_1$				$\mathscr{Y}_2$				$\mathscr{Y}_3$			

Figure 15   Calculations for Influence Coefficient and Load Coefficient Matrices

are represented by the matrix $\mathcal{Y}_1$. In columns 5 through 8, one of the stress resultants at the ith edge is successively set to unity, while the remaining stress resultants and all the displacements are set to zero. The corresponding values of the harmonics $f^{(n)}(j)$ of the stress resultants at the jth edge are represented by the matrix $\mathcal{X}_2$, whereas the values of the harmonics $\delta^{(n)}(j)$ of the displacements are represented by the matrix $\mathcal{Y}_2$. In columns 9 to 18, the stress resultants and displacements at the ith edge are all set to zero. The values of the harmonics $f^{(n)}(j)$ of the stress resultants at the jth edge due to the external distributed loads acting along the segment of the shell are represented by the $\mathcal{X}_3$ matrix, whereas the values of the harmonics $\delta^{(n)}(j)$ of the displacements are represented by the matrix $\mathcal{Y}_3$. Notice, that as many loading conditions as desired can be considered. In Fig. 15, ten loading columns are shown. The matrices $\mathcal{X}_1$, $\mathcal{X}_2$, $\mathcal{X}_3$, $\mathcal{Y}_1$, $\mathcal{Y}_2$, $\mathcal{Y}_3$ are referred to as the influence coefficient matrices. Each of the eight different edge conditions, and the ten loading conditions produce a column in the appropriate influence coefficient matrices.

Fig. 15 is applicable to a single harmonic of a linear problem or to a nonlinear problem with an axisymmetric load [107]. The nonlinear problem associated with unsymmetric loading is more complex. Fig. 16 represents a schematic diagram for establishing the influence coefficient matrices for nonlinear problems entailing, for example, the coupling of harmonics n and n'. The initial matrices for the values of the functions at edge i (the initial conditions) and the influence coefficient matrices

86

	Unit (n) Displacements Applied at (i)				Unit (n) Forces Applied at (i)				Unit (n') Displacements Applied at (i)				Unit (n') Forces Applied at (i)				Dist. Loads Zero IC NL Prob.
Run Number	1	2	3	4	5	6	7	8	9	10	11	12	13	14	15	16	17

Initial Condition

$\{f^{(n)}(i)\}$: $T_{\phi\theta}^{(n)}(i)$, $N_{\phi}^{(n)}(i)$, $J_{\phi}^{*(n)}(i)$, $M_{\phi}^{(n)}(i)$

Runs 1–4	Runs 5–8	Runs 9–12	Runs 13–16	Run 17
0	I_4	0	0	0

$\{\delta^{(n)}(i)\}$: $U^{(n)}(i)$, $V^{(n)}(i)$, $W^{(n)}(i)$, $\Omega_{\theta}^{(n)}(i)$

Runs 1–4	Runs 5–8	Runs 9–12	Runs 13–16	Run 17
I_4	0	0	0	0

$\{f^{(n')}(i)\}$: $T_{\phi\theta}^{(n')}(i)$, $N_{\phi}^{(n')}(i)$, $J_{\phi}^{*(n')}(i)$, $M_{\phi}^{(n')}(i)$

Runs 1–4	Runs 5–8	Runs 9–12	Runs 13–16	Run 17
0	0	0	I_4	0

$\{\delta^{(n')}(i)\}$: $U^{(n')}(i)$, $V^{(n')}(i)$, $W^{(n')}(i)$, $\Omega_{\theta}^{(n')}(i)$

Runs 1–4	Runs 5–8	Runs 9–12	Runs 13–16	Run 17
0	0	I_4	0	0

Final Condition

$\{f^{(n)}(j)\}$: $T_{\phi\theta}^{(n)}(j)$, $N_{\phi}^{(n)}(j)$, $J_{\phi}^{*(n)}(j)$, $M_{\phi}^{(n)}(j)$

Runs 1–4	Runs 5–8	Runs 9–12	Runs 13–16	Run 17
$\mathscr{X}_1^{(n,n)}$	$\mathscr{X}_2^{(n,n)}$	$^*\mathscr{X}_1^{(n,n')}$	$^*\mathscr{X}_2^{(n,n')}$	$^*\mathscr{X}_3^{(n)}$

$\{\delta^{(n)}(j)\}$: $U^{(n)}(j)$, $V^{(n)}(j)$, $W^{(n)}(j)$, $\Omega_{\theta}^{(n)}(j)$

Runs 1–4	Runs 5–8	Runs 9–12	Runs 13–16	Run 17
$\mathscr{Y}_1^{(n,n)}$	$\mathscr{Y}_2^{(n,n)}$	$^*\mathscr{Y}_1^{(n,n')}$	$^*\mathscr{Y}_2^{(n,n')}$	$^*\mathscr{Y}_3^{(n)}$

$\{f^{(n')}(j)\}$: $T_{\phi\theta}^{(n')}(j)$, $N_{\phi}^{(n')}(j)$, $J_{\phi}^{*(n')}(j)$, $M_{\phi}^{(n')}(j)$

Runs 1–4	Runs 5–8	Runs 9–12	Runs 13–16	Run 17
$^*\mathscr{X}_1^{(n',n)}$	$^*\mathscr{X}_2^{(n',n)}$	$\mathscr{X}_1^{(n',n')}$	$\mathscr{X}_2^{(n',n')}$	$^*\mathscr{X}_3^{(n')}$

$\{\delta^{(n')}(j)\}$: $U^{(n')}(j)$, $V^{(n')}(j)$, $W^{(n')}(j)$, $\Omega_{\theta}^{(n')}(j)$

Runs 1–4	Runs 5–8	Runs 9–12	Runs 13–16	Run 17
$^*\mathscr{Y}_1^{(n',n)}$	$^*\mathscr{Y}_2^{(n',n)}$	$\mathscr{Y}_1^{(n',n')}$	$\mathscr{Y}_2^{(n',n')}$	$^*\mathscr{Y}_3^{(n')}$

Figure 16   Calculations with Interaction

are now 16 x 16 matrices. In Fig. 16, the star matrices denote the effects of harmonic coupling. If there were no coupling, these matrices would be null matric

The differential equations for the nonlinear problem may be linearized by the Newtonian method. (As discussed in Chapter 2, the equations in ΔY are linearized by dropping the nonlinear terms in ΔY, and by using the previous values of Y in the product terms $(Y)(\Delta Y)$). Thus, superposition is possible for both the linear and the nonlinear problem. Consequently, the influence coefficients may be employed to yield the stress resultants and the displacements at the jth edge in terms of the actual stress resultants and displacements at the ith edge. Using Equations (3-1), to (3-4), the stress resultants and displacements may be expressed directly in global coordinates as

$$\{F(j)\} = [JFT] \{f(j)\} = [JFT] \left[\mathcal{X}_1 : \mathcal{X}_2 : \mathcal{X}_3\right] \left\{\begin{matrix} \delta(i) \\ f(i) \\ \ell \end{matrix}\right\} \qquad (3\text{-}7)$$

$$\{\Delta(j)\} = [JDT] \{\delta(j)\} = [JDT] \left[\mathcal{Y}_1 : \mathcal{Y}_2 : \mathcal{Y}_3\right] \left\{\begin{matrix} \delta(i) \\ f(i) \\ \ell \end{matrix}\right\} \qquad (3\text{-}8)$$

where $\{\ell\}$ is a scaling factor for the load. If the loading cases employed in establishing $\mathcal{X}_3$ and $\mathcal{Y}_3$ are the actual loadings considered, then the loading vector $\{\ell\}$ is a unit vector. Solving Equation (3-8) for vector $\{f(i)\}$, and employing Equations (3-3) and (3-1) to convert $\{\delta(i)\}$ and $\{f(i)\}$ into global coordinates, we obtain

$$\{F(i)\} = [IFT] \left[\mathcal{Y}_2\right]^{-1} \left([JDT]^T \{\Delta(j)\} - \left[\mathcal{Y}_1\right][IDT]^T \{\Delta(i)\} - \left[\mathcal{Y}_3\right]\{\ell\} \right) \qquad (3\text{-}9)$$

Using Equations (3-1) and (3-3) to convert the vectors $\{\delta(i)\}$ and $\{f(j)\}$ in

Equation (3-7) into global coordinates, and substituting in the resulting

equation, the values of $\{F(i)\}$ from Equations (3-9), we get

$$\{F(j)\} = [JFT]\left[X_1\right][IDT]\{\Delta(i)\} + [JFT]\left[X_2\right]\left[y_2\right]^{-1}\left([JDT]^T\{\Delta(j)\} - \left[y_1\right][IDT]^T\{\Delta(i)\}\right.$$

$$\left. - \left[y_3\right]\{\ell\}\right) + [JFT]\left[X_3\right]\{\ell\} \tag{3-10}$$

Equations (3-9) and (3-10) may be combined in the form

$$\{F\} = [k]\ \{\Delta\} + \{L\}$$

where, referring to Equations (3-9) and (3-10), we may write the stiffness

and load matrices in a combined form:

$$[k \vdots L] \equiv \begin{bmatrix} k(ii) & \vdots & k(ij) & \vdots & L(i) \\ \cdots & \vdots & \cdots & \vdots & \cdots \\ k(ji) & \vdots & k(jj) & \vdots & L(j) \end{bmatrix} \equiv$$

$$\begin{bmatrix} IFT & \vdots & 0 \\ \cdots & \vdots & \cdots \\ 0 & \vdots & JFT \end{bmatrix} \begin{bmatrix} 0 & \vdots & I_4 & \vdots & 0 \\ \cdots & \vdots & \cdots & \vdots & \cdots \\ X_1 & \vdots & X_2 & \vdots & X_3 \end{bmatrix} \begin{bmatrix} I_4 & \vdots & 0 & \vdots & 0 \\ \cdots & \vdots & \cdots & \vdots & \cdots \\ 0 & \vdots & y_2^{-1} & \vdots & 0 \\ \cdots & \vdots & \cdots & \vdots & \cdots \\ 0 & \vdots & 0 & \vdots & I_p \end{bmatrix} \begin{bmatrix} I_4 & \vdots & 0 & \vdots & 0 \\ \cdots & \vdots & \cdots & \vdots & \cdots \\ -y_1 & \vdots & JDT^T & \vdots & -y_3 \\ \cdots & \vdots & \cdots & \vdots & \cdots \\ 0 & \vdots & 0 & \vdots & I_p \end{bmatrix} \begin{bmatrix} IDT^T & \vdots & 0 & \vdots & 0 \\ \cdots & \vdots & \cdots & \vdots & \cdots \\ 0 & \vdots & I_4 & \vdots & 0 \\ \cdots & \vdots & \cdots & \vdots & \cdots \\ 0 & \vdots & 0 & \vdots & I_p \end{bmatrix} \tag{3-11}$$

Equation (3-11) may be verified by carrying out the matrix multiplication

and comparing the resulting matrix with Equations (3-9) and (3-10). As

evident from Equation (3-11), in order to compute the stiffness matrix [k]

89

and the load matrix [L], it is necessary to invert only the $\mathcal{Y}_2$ matrix. ($\mathcal{Y}_2$ is a 4x4 matrix in uncoupled cases, 4N x 4N in the unsymmetrically loaded nonlinear case.)

In other numerical integration methods, [97, 98] the influence coefficient matrices $\mathcal{X}_1$ and $\mathcal{Y}_1$ are used directly instead of calculating the stiffness matrices of the shell segment. There are, however, many significant advantages in employing the direct stiffness technique.

The procedure, employed in this investigation for the solution of the boundary value problem, subsequent to the formulation of the stiffness matrices of the shell segments, is exactly that employed in the finite element techniques. Thus, all the matrix manipulation methods developed for finite element solutions may be utilized in the present method, as for example, those for large scale matrix inversion, using packing techniques, or taking advantage of banding, etc. Moreover, the direct stiffness method can be applied without modification to arbitrarily branched shells, as well as to shells with discontinuos changes in meridian slope. Finally, the other techniques [97, 98] are more efficiently utilized with the use of Gaussian elimination procedures, such as Potters' [4] procedure. These methods however, may be prone occasionally to error accumulation in the calculation sequence [132], whereas the Choleski method and the transfer matrix method utilized herein, tend to involve negligible error accumulatior Therefore, many finite difference schemes, utilizing some form of the Gaussian elimination technique require double precision arithmetic.

90

Properties of the Stiffness Matrix $[k]$: In the solution of shell problems, for self-checking of the arithmetic, it is convenient to utilize the fully symmetric matrix $[\hat{k}]$, defined by

$$[\hat{k}] \equiv \begin{bmatrix} 2\pi\, r_o(i) & \vdots & \\ \circ\circ\circ\circ\circ\circ\circ\circ & \ddots & \cdots\cdots\cdots \\ & \vdots & 2\pi\, r_o(j) \\ & \vdots & \diagdown \end{bmatrix} [k] \tag{3-12}$$

and therefore,

$$[\hat{L}] \equiv \begin{bmatrix} 2\pi\, r_o(i) & \vdots & \\ \cdots\cdots\cdots & \ddots & \cdots\cdots\cdots \\ & \vdots & 2\pi\, r_o(j) \\ & \vdots & \diagdown \end{bmatrix} [L] \tag{3-13}$$

so that

$$[\hat{F}] = [\hat{k}]\,[\Delta] + [\hat{L}] \tag{3-14}$$

where

$$[\hat{F}] \equiv \begin{bmatrix} F(i) \\ \cdots\cdots \\ F(j) \end{bmatrix} \equiv \begin{bmatrix} 2\pi\, r_o(i)\,F(i) \\ \cdots\cdots\cdots \\ 2\pi\, r_o(j)\,F(j) \end{bmatrix}$$

F is measured in units of force/unit length, and $\hat{F}$ is measured in units of force.

In the case of the stiffness matrix $[k]$, for either linear problems or nonlinear problems with axisymmetric loading, the matrix required to convert $[k]$ into the symmetric matrix $[\hat{k}]$ may be obtained by inspection. This is not the case, however, for a nonlinear problem with unsymmetric

91

loading. There is no apriori reason in this case to assume that the stiff-ness matrix of the coupled harmonics can be converted to symmetric form inasmuch as this matrix relates a combination of harmonics of forces and displacements. Thus, the existence of a symmetric matrix must be proven. Consider, for instance, the case wherein the zeroth harmonic is coupled to any other harmonic, for example the Nth harmonic. For this case, the force-displacement relations may be written symbolically as :

$$\left\{ \begin{array}{c} F^{(0)} \\ \cdots \\ F^{(N)} \end{array} \right\} = \left[\begin{array}{ccc} k^{(0,0)} & \vdots & k^{(0,N)} \\ \cdots & \cdots & \cdots \\ k^{(N,0)} & \vdots & k^{(N,N)} \end{array} \right] \left\{ \begin{array}{c} \Delta^{(0)} \\ \cdots \\ \Delta^{(N)} \end{array} \right\} \qquad (3\text{-}15)$$

For the shells under consideration, in the absence of body forces, the Betti-Rayleigh reciprocal relations [133] are (where the primed quantities belong to one system of forces and displacements, and the unprimed to another):

$$\int_0^{2\pi} F(\theta) \, \Delta'(\theta) \, d\theta = \int_0^{2\pi} F'(\theta) \, \Delta(\theta) \, d\theta \qquad (3\text{-}16)$$

Inasmuch as we assume that the zero harmonic is coupled only with the Nth harmonic, we may write

$$\Delta(\theta) = \Delta^{(0)} + \Delta^{(N)} \cos N\theta \qquad F(\theta) = F^{(0)} + F^{(N)} \cos N\theta$$

$$\Delta'(\theta) = \Delta'^{(0)} + \Delta'^{(N)} \cos N\theta \qquad F'(\theta) = F'^{(0)} + F'^{(N)} \cos N\theta$$

$$(3\text{-}17a)$$

Substituting Equations (3-17a) into Equations (3-16) we obtain

$$\int_0^{2\pi} (F^{(0)} + F^{(N)} \cos N\theta)(\Delta'^{(0)} + \Delta'^{(N)} \cos N\theta) \, d\theta =$$

$$\int_0^{2\pi} (F'^{(0)} + F'^{(N)} \cos N\theta)(\Delta^{(0)} + \Delta^{(N)} \cos N\theta) \, d\theta$$

Integrating we obtain

$$2\pi F^{(0)} \Delta'^{(0)} + \pi F^{(N)} \Delta'^{(N)} = 2\pi F'^{(0)} \Delta^{(0)} + \pi F'^{(N)} \Delta^{(N)} \qquad (3\text{-}17b)$$

The force-displacement relations for the two sets of harmonic amplitudes, on the basis of Equation (3-15) are given by

$$F^{(N)} = k^{(N,\,0)} \Delta^{(0)} + k^{(N,\,N)} \Delta^{(N)} \qquad\qquad F'^{(N)} = k^{(N,\,0)} \Delta'^{(0)} + k^{(N,\,N)} \Delta'^{(N)}$$

$$F^{(0)} = k^{(0,\,0)} \Delta^{(0)} + k^{(0,\,N)} \Delta^{(N)} \qquad\qquad F'^{(0)} = k^{(0,\,0)} \Delta'^{(0)} + k^{(0,\,N)} \Delta'^{(N)}$$

Substituting the above relations into Equation (3-17b) we get

$$2\pi \, k^{(0,\,0)} \Delta^{(0)} \Delta'^{(0)} + 2\pi \, k^{(0,\,N)} \Delta^{(N)} \Delta'^{(0)} + \pi \, k^{(N,\,0)} \Delta^{(0)} \Delta'^{(N)} + \pi \, k^{(N,\,N)} \Delta^{(N)} \Delta'^{(N)}$$

$$= 2\pi \, k^{(0,\,0)} \Delta'^{(0)} \Delta^{(0)} + 2\pi \, k^{(0,\,N)} \Delta'^{(N)} \Delta^{(0)} + \pi \, k^{(N,\,0)} \Delta'^{(0)} \Delta^{(N)} + \pi \, k^{(N,\,N)} \Delta'^{(N)} \Delta^{(N)}$$

This relation may be rewritten as

$$2 \, k^{(0,\,N)} [\Delta^{(N)} \Delta'^{(0)} - \Delta'^{(N)} \Delta^{(0)}] = k^{(N,\,0)} [\Delta^{(N)} \Delta'^{(0)} - \Delta'^{(N)} \Delta^{(0)}]$$

This relation is valid if

$$2 \, k^{(0,\,N)} = k^{(N,\,0)} \,. \qquad\qquad\qquad (3\text{-}18)$$

thus indicating that the stiffness matrix of Equation (3-15) is unsymmetric.

However, it is relatively simple to form a matrix which can transform the

93

stiffness matrix of the coupled harmonics into symmetric form.   Note, that

each individual diagonal block ($k^{(0,\,0)}$ or $k^{(N,\,N)}$) of the stiffness matrix

for the coupled harmonics is not a symmetric matrix, but may be converted

readily into a symmetric matrix ($\widehat{k}^{(0,\,0)}$ or $\widehat{k}^{(N,\,N)}$) by Equation (3-12). Thus

in this specific case, the appropriate symmetric matrix corresponding to Equation

(3-15) is given by

$$
\widehat{[k]} =
\begin{bmatrix}
2 & & \vdots & \\
 & 2 & \vdots & O \\
\cdots & & 2 & \cdots & \cdots \\
 & & \vdots & 1 & \\
 O & & \vdots & & 1
\end{bmatrix}
\begin{bmatrix}
\widehat{k^{(0,\,0)}} & \vdots & k^{(0,\,N)} \\
\cdots\cdots & \cdots & \cdots\cdots \\
k^{(N,\,0)} & \vdots & \widehat{k^{(N,\,N)}}
\end{bmatrix}
\qquad (3\text{-}19)
$$

The following notation is introduced in order to identify data in

subsequent discussions and calculations:

$$
_s\widehat{[\,F\,]}^{(n)} = {}_s\widehat{[\,k\,]}^{(n)}\,{}_s[\,\Delta\,]^{(n)} + {}_s\widehat{[\,L\,]}^{(n)}
\qquad (3\text{-}20)
$$

where:

   s   indicates the sth segment of the shell connecting joints i and j,

   n   indicates the Fourier harmonic. (For coupled harmonic problems,
        the matrix superscript would be (n, n', n'') where n, n,' n'' are the
        coupled harmonics.)

Structure Matrices and Stiffness Analysis: The direct stiffness method

[134] is employed in calculating the interaction of the segments comprising

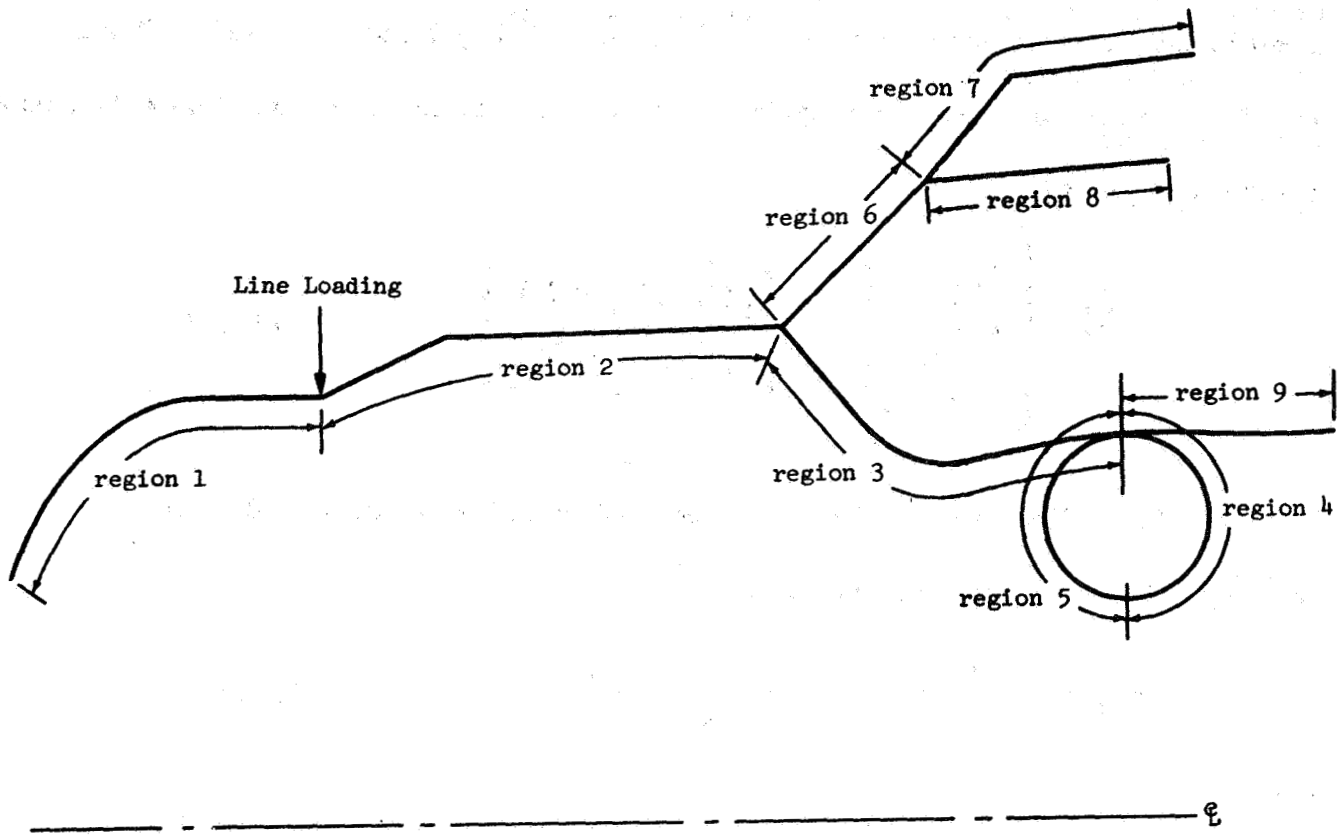the shell structure.   To increase the capacity of the program, the shell segments

Figure 17. Example of Region Topology

95

will first be coupled into regions using a Guyan [152] reduction procedure. These regions are defined as singly-connected shells with no internal concentrated line loadings (Figure 17). The next step is to construct the region stiffness matrix $[\hat{K}_R]$ and the matrix of fixed-end forces $[\hat{L}_R]$. This requires splitting each segments $[\hat{k}]$ matrix into its four 4x4 matrices (for coupled problems 4Nx4N), and inserting the portions into the region stiffness matrix in accordance with the topological arrangement. The $[\hat{L}]$ matrix is similarly split into two 4xP matrices, where P is the number of individual loadings considered separately. (For nonlinear cases, the stiffness matrix changes with the load, consequently, only one loading case can be considered at a time. Thus, the split load matrices are 4x1 for axisymmetric loading, and 4Nx1 for the unsymmetric coupled problem.) Thus, in addition to the geometric description of each segment, its position in the assembly must be specified. To this end, all segments begin (i) and end (j) at a joint. The sth segment is said to connect the ith and j^{th} joints. (Not the jth and i^{th} joints, since direction of increasing coordinate within the segment must be from i to j). To allow for the possibility of discontinuous centerlines within a region, kinematic links must be included. These links are rigid pieces which relate displacements across a discontinuity. Thus a kinematic link matrix $[SKL]$ must also be formed. Due to the topology and line-load requirements for regions, the equations of the coupled segments will be the following:

$$
\begin{bmatrix} F_{iR} \\ F_{jR} \\ \text{---} \\ (8xP) \\ 0 \end{bmatrix} = \begin{bmatrix} K_{11} & | & K_{12} \\ & | & \\ \text{---} & + & \text{---} \\ (8x8) & | & \\ K_{21} & | & K_{22} \end{bmatrix} \begin{bmatrix} \Delta_{iR} \\ \Delta_{jR} \\ \text{---} \\ (8xP) \\ \Delta \end{bmatrix} + \begin{bmatrix} L_{iR1} \\ L_{jR1} \\ \text{---} \\ (8xP) \\ L \end{bmatrix}
$$

(3-21)

96

where

$$\begin{bmatrix} \widehat{K_{11}} & K_{12} \\ \hline K_{21} & K_{22} \end{bmatrix} = \begin{bmatrix} & SKL & \end{bmatrix}^T \begin{bmatrix} \widehat{K'_{11}} & K'_{12} \\ \hline K'_{21} & K'_{22} \end{bmatrix} \begin{bmatrix} SKL_{11} & SKL_{12} \\ \hline SKL_{21} & SKL_{22} \end{bmatrix}$$

$$\begin{bmatrix} \widehat{L_{iR1}} \\ L_{jR1} \\ \hline L \end{bmatrix} = \begin{bmatrix} & SKL & \end{bmatrix}^T \begin{bmatrix} \widehat{L'_{iR}} \\ L'_{jR} \\ \hline L' \end{bmatrix}$$

and where iR, jR refer to the region initial and final points, and the $[\Delta]$, $[K']$, and $[L']$ are the deflection, stiffness, and load matrices of internal segments. If there are no internal kinematic links, $[SKL]$ will be an identity matrix. Partitioning Equation (3-21) will yield:

$$\begin{bmatrix} \widehat{F_R} \end{bmatrix} = \begin{bmatrix} \widehat{K_{11}} \end{bmatrix} \begin{bmatrix} \Delta_R \end{bmatrix} + \begin{bmatrix} \widehat{K_{12}} \end{bmatrix} \begin{bmatrix} \Delta \end{bmatrix} + \begin{bmatrix} \widehat{L_{R1}} \end{bmatrix} \tag{3-22a}$$

$$\begin{bmatrix} 0 \end{bmatrix} = \begin{bmatrix} \widehat{K_{21}} \end{bmatrix} \begin{bmatrix} \Delta_R \end{bmatrix} + \begin{bmatrix} \widehat{K_{22}} \end{bmatrix} \begin{bmatrix} \Delta \end{bmatrix} + \begin{bmatrix} \widehat{L} \end{bmatrix} \tag{3-22b}$$

Solving Equation (3-22b) for $[\Delta]$ and substituting into Equation (3-22a) yields:

$$\begin{bmatrix} \widehat{F_R} \end{bmatrix} = \begin{bmatrix} \widehat{K_R} \end{bmatrix} \begin{bmatrix} \Delta_R \end{bmatrix} + \begin{bmatrix} \widehat{L_R} \end{bmatrix}$$

$$\quad 8xP \qquad 8x8 \quad 8xP \qquad 8xP \tag{3-23}$$

where

$$\begin{bmatrix} \widehat{K_R} \end{bmatrix} = \begin{bmatrix} \widehat{K_{11}} \end{bmatrix} - \left(\begin{bmatrix} \widehat{K_{12}} \end{bmatrix} \begin{bmatrix} \widehat{K_{22}} \end{bmatrix}^{-1} \begin{bmatrix} \widehat{K_{21}} \end{bmatrix} \right)$$

$$\begin{bmatrix} \widehat{L_R} \end{bmatrix} = \begin{bmatrix} \widehat{L_{R1}} \end{bmatrix} - \left(\begin{bmatrix} \widehat{K_{12}} \end{bmatrix} \begin{bmatrix} \widehat{K_{22}} \end{bmatrix}^{-1} \begin{bmatrix} \widehat{L} \end{bmatrix} \right)$$

The next step is to construct the total structure stiffness matrix $\begin{bmatrix} \widehat{K_T} \end{bmatrix}$ and the total structure load matrix $\begin{bmatrix} \widehat{L_T} \end{bmatrix}$. This requires the splitting of the stiffness

97

matrix $\left[\widehat{K_R}\right]$ of each region into its four 4x4 component matrices (for coupled problems 4Nx4N), and inserting the portions into the total stiffness matrix, in accordance with the topological arrangement of the structure. The $\left[\widehat{L_R}\right]$ matrix is similarly split into two 4xP matrices, where P is the number of individual loadings considered separately. (For nonlinear cases, the stiffness matrix changes with the load, consequently, only one loading case can be considered at a time. Thus the split load matrices are 4x1 for axisymmetric loading, and 4Nx1 for the unsymmetric coupled problem). Therefore, in addition to the geometric description of each region, its position in the assembly must be specified. The initial point of all regions will be denoted by (i) whereas the end point will be denoted by (j). Inasmuch as there are four degrees of freedom at each joint, for a shell with M joints the total stiffness matrix is 4Mx4M (4MNx4MN for coupled problems). Hence using equilibrium relations for all the joints, we can form the following equation

$$[\widehat{F}]_T = [\widehat{K}]_T [\widehat{\Delta}]_T + [\widehat{L}]_T \qquad (3-24)$$

The subscript T denotes a matrix which includes terms for all the joints. Equation (3-24) characterizes the structure without taking into account any external boundary conditions. For axisymmetric and antisymmetric (n=0, 1) load cases, the matrix $[\widehat{K}]_T$ can be singular. This may be physically interpreted, as follows. The stiffness matrix permits calculation of the stress resultants from the displacements; thus, the inverse of the stiffness matrix would relate displacements to the stress resultants. The displacements, however, are not unique inasmuch as one valid solution may differ from another by rigid body motion. Hence, it can not be anticipated

98

that a relationship may be established relating all the valid displacement fields to the unique set of stress resultants; indicating that the total stiffness matrix is not invertible, that is, it is singular. However, the total stiffness matrix of a complete shell of revolution for harmonics other than n≠0, 1 need not be singular. For harmonics greater than unity, the stress resultant harmonics are self-equilibrating. Moreover, since the displacements are of the same harmonic order, rigid-body motion cannot exist.

Since the form of the $[\widehat{K}]_T$ matrix depends upon the topology of the regions , there is some leeway as to the distribution of the zero terms within this matrix. This may be accomplished by utilizing various numbering techniques for the regions of the structure. Several techniques may be employed to form the total structure stiffness matrix rendering it amenable to facile operation. One technique is to form a banded matrix. The numbering for topology of a typical common bulkhead tank, so as to produce a banded matrix, as shown in Figure 18. Operations with a banded matrix are more efficient, consume less time and less computer core storage. Another technique presented in Reference 135 does not employ banding but is also critically dependent upon judicious topology numbering. For cases where neither of the aforementioned techniques are feasible, the stiffness matrix may be compacted. This may be accomplished by eliminating the large amount of zeroes in the matrix from the computer storage. This technique in addition to minimizing computer core storage, may result in operational simplification.
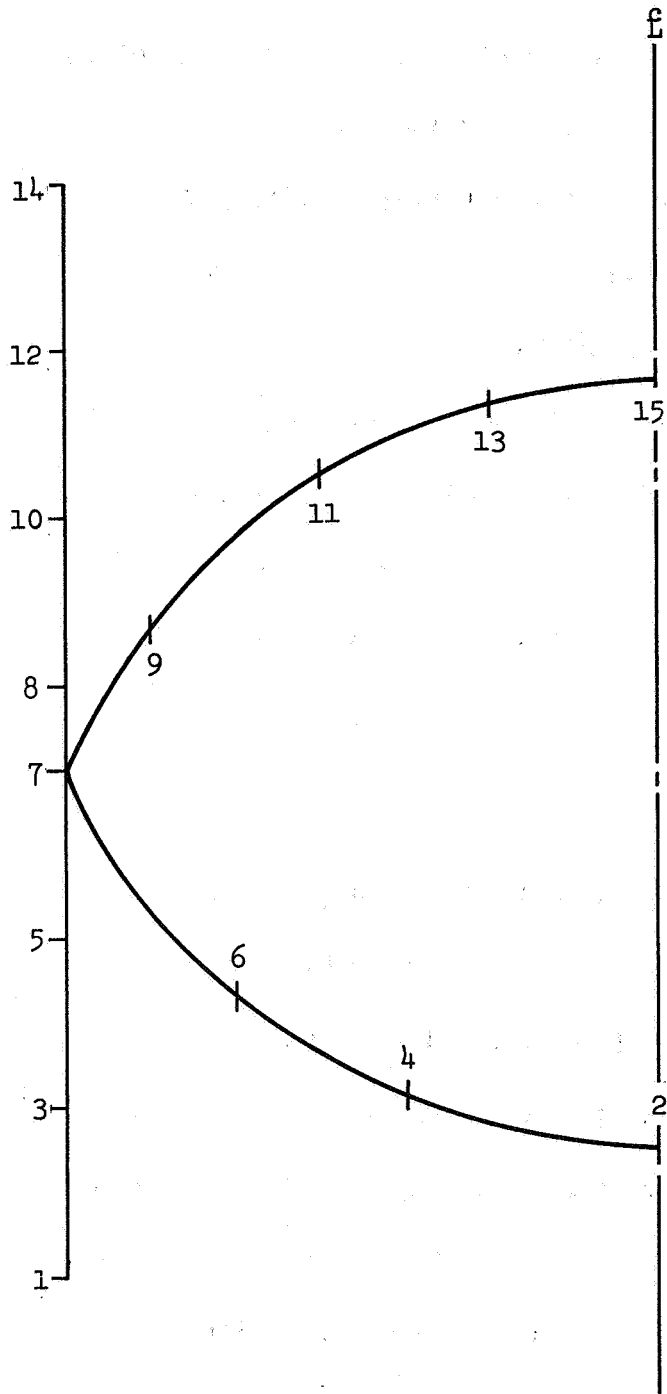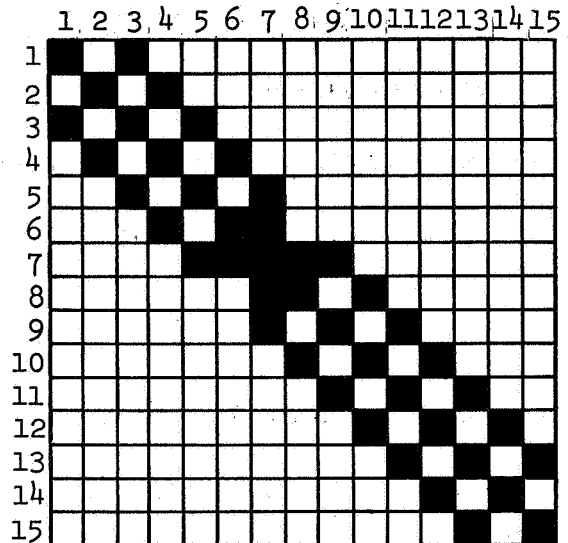
Figure 18 Sample Structural Numbering for Diagonalization of Stiffness Matrix

100

Reduced Stiffness: The stiffness matrix established previously must now be altered in order to take into account the existence of ring reinforcement, possible attachment of the shell to other structures, as well as to inhibit rigid body motion and satisfy specific support conditions.

In the case of ring-stiffened shells, the ring reinforcing matrices established in Appendix B, must be stacked in the stiffness matrix in accordance with the topology of the ring stiffeners.

If the shell of revolution under consideration is attached to other structures, the stiffness matrix should be modified to take into account the effect of these structures. For example, if the shell rests on an elastic support, such as a soil foundation or another structure, the stiffness matrix of that support can be written as

$$[F_m] = [K_m] [\Delta_m] \qquad (3-25)$$

where m denotes the joint of the shell at the elastic support. The stiffness $[K_m]$ should then be stacked into the total shell stiffness matrix $\widehat{[K]}_T$ at the location corresponding to joint m. The aforementioned technique may also be employed in solving problems associated with non-axisymmetric structures [111] being connected to the shell of revolution.

In the actual shell structure the displacements and rotations of the joints of the segments into which the shell must be subdivided, may assume specified values, or may be constrained externally. The number of displacements which are not specified will be referred to as the degrees of freedom of the shell structure. The total number of displacement components specified at the various joints in the structure, will be referred

to as the number of boundary conditions. In order to alter (reduce) the total the stiffness matrix to take into account the effect of the boundary conditions, a boundary condition matrix [BC] must be established. The formulation of the matrix may be illustrated by referring to the shell of revolution shown in Fig. 19.

For example, consider the shell of revolution shown in Figure 19a. The geometry of this shell suggests the subdivision of the shell into the 4 segments shown in Fig. 19b. Notice, that the segment between joints 2-3 may be considered as an equivalent ring stiffener, and its stiffness matrix may be computed, and stacked into the total stiffness matrix of the shell according to its topology, discussed previously. However, the length of the segment 2-3 may be taken as small as desired, whereas the lengths of the adjacent segments must increase appropriately to close the gap. In the limit, when the length becomes very small, the stiffness matrix of segment 2-3 will become a null matrix.

Such a segment will be referred to as a kinematic link. This link will affect only the boundary conditions of the adjacent segments. The use of a kinematic link where permissible, in lieu of an equivalent ring stiffener of chosen finite dimensions, will eliminate the need for computing the stiffness matrix of this ring. In the example structure, the [BC] matrix in this area will reflect only the kinematic relations between joints 2 and 3.

From Fig. 19b, it is evident that joint 1 is connected to a heavy boss. Thus, we may assume that this joint may move solely in the Z and θ (tangential) directions. As an alternative, it may be assumed the joint 1

102

Z

(18c) Detail of Joint
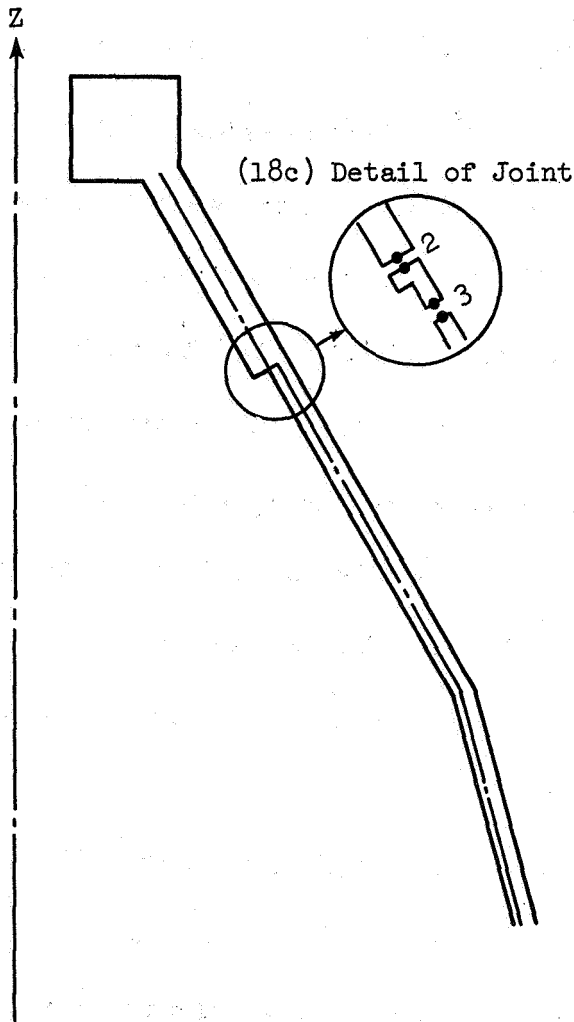
Figure 19a Shell Structure

Z

1

①

$r_o(3)$ 3

$r_o(2)$ 2

ΔZ

②

$\phi = \alpha$

4

$\phi = \beta$

③

5
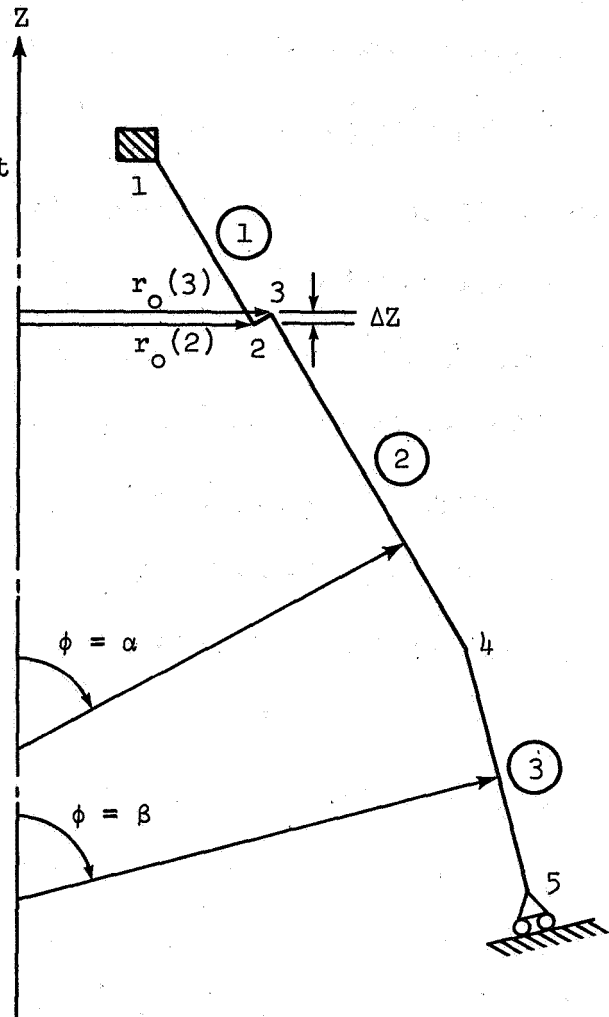
Figure 19b Idealization

Figure 19 Shell Structure and Idealization

is connected to an elastic support. In this case, the stiffness characteristics of the support may be appropriately inserted in the total shell stiffness matrix. Then, in the formulation of the boundary condition matrix, joint 1 should be considered totally unrestrained.

Referring to Fig. 19b, it is apparent that joint 4 is completely unrestrained. This joint is merely a point wherein the shell geometry changes. Therefore, the [BC] matrix will not impose any constraint on this joint.

Joint 5 (Fig. 19b) is provided with an external membrane support. Inasmuch as the stress resultants and displacements at the joints of the structure are specified in global coordinates, the [BC] matrix will contain a trigonometric coordinate transformation for joint 5.

Thus, the total displacement matrix may be expressed in terms of the matrix containing only the actually unspecified (unknown) displacements,

$$[\Delta]_T = [BC] [\Delta]_F \qquad\qquad (3\text{-}26)$$

For the example structure of Figure 19, Equation (3-26) is given by:

$$
\begin{bmatrix}
\Delta_T(1) \\
\Delta_Z(1) \\
\Delta_R(1) \\
\Omega_\theta(1) \\
\Delta_T(2) \\
\Delta_Z(2) \\
\Delta_R(2) \\
\Omega_\theta(2) \\
\Delta_T(3) \\
\Delta_Z(3) \\
\Delta_R(3) \\
\Omega_\theta(3) \\
\Delta_T(4) \\
\Delta_Z(4) \\
\Delta_R(4) \\
\Omega_\theta(4) \\
\Delta_T(5) \\
\Delta_Z(5) \\
\Delta_R(5) \\
\Omega_\theta(5)
\end{bmatrix}
=
[\,M\,]
\begin{bmatrix}
\Delta_T(1) \\
\Delta_Z(1) \\
\Delta_T(2) \\
\Delta_Z(2) \\
\Delta_R(2) \\
\Omega_\theta(2) \\
\Delta_T(4) \\
\Delta_Z(4) \\
\Delta_R(4) \\
\Omega_\theta(4) \\
\Delta_\zeta(5) \\
\Omega_\theta(5)
\end{bmatrix}
$$

where the matrix $[M]$ is:

row	C1	C2	C3	C4	C5	C6	C7	C8	C9	C10	C11	C12
$\Delta_T(1)$	1											
$\Delta_Z(1)$		1										
$\Delta_R(1)$												
$\Omega_\theta(1)$												
$\Delta_T(2)$			1									
$\Delta_Z(2)$				1								
$\Delta_R(2)$					1							
$\Omega_\theta(2)$						1						
$\Delta_T(3)$			$\dfrac{r_o(3)}{r_o(2)}$									
$\Delta_Z(3)$				1		$\begin{matrix}r_o(2)\\-r_o(3)\end{matrix}$						
$\Delta_R(3)$					1	$\begin{matrix}z_o(3)\\-z_o(2)\end{matrix}$						
$\Omega_\theta(3)$						1						
$\Delta_T(4)$							1					
$\Delta_Z(4)$								1				
$\Delta_R(4)$									1			
$\Omega_\theta(4)$										1		
$\Delta_T(5)$												
$\Delta_Z(5)$												
$\Delta_R(5)$											$-\cos\phi$	
$\Omega_\theta(5)$											$-\sin\phi$	
												1

(3-27)

The following items should be noted relative to Equation (3-27). There is a blank row in the $[BC]$ matrix for each displacement component or rotation specified as zero (fixed). There are no components for the dependent joint 3 in the matrix $[\Delta]_F$. The kinematic relations for this joint are given in the $[BC]$ matrix. The meridional component Δ_φ (5) does not appear since it is fixed, but the perpendicular component Δ_ζ (5) contributes to both Δ_Z (5) and Δ_R (5).

By using the definition of work, it may be shown that the stress resultants at the joints in the directions of the unconstrained displacement components may be expressed in terms of the total stress resultants at the joints. This relationship is

$$[\widehat{F}]_F = [BC]^T [\widehat{F}]_T \qquad (3\text{-}28)$$

Substituting Equations (3-24) and (3-26) into Equation (3-28), we obtain

$$[\widehat{F}]_F = [BC]^T [\widehat{K}]_T [BC][\Delta]_F + [BC]^T [\widehat{L}]_T \qquad (3\text{-}29)$$

Rewriting Equation (3-29) we have

$$[\widehat{F}]_F = [\widehat{K}]_F [\Delta]_F + [\widehat{L}]_F \qquad (3\text{-}30)$$

where

$$[\widehat{K}]_F = [BC]^T [\widehat{K}]_T [BC] \qquad (3\text{-}31a)$$

$$[\widehat{L}]_F = [BC]^T [\widehat{L}]_T \qquad (3\text{-}31b)$$

Inverting Equation (3-30), we get

$$[\Delta]_F = [\widehat{A}]_F ([\widehat{F}]_F - [\widehat{L}]_F) \qquad (3\text{-}32)$$

where

$$[\widehat{A}]_F \equiv [\widehat{K}]_F^{-1} \qquad (3\text{-}33)$$

Thus, the total displacement solution for the joints of the structure may be obtained by using Equations (3-32) and (3-26).

106

Thus for the region ends, combining Equations (3-26) and (3-32)

$$\{\Delta_R\} = [BC] [\hat{A}]_F \left(\{\hat{F}\}_F - \{\hat{L}\}_F \right) \tag{3-34}$$

and in the interior of each region, for each segment

$$\{\Delta\}_i = [SKL_{22}] \left\{ - [\hat{K}_{22}]^{-1} \left([\hat{K}_{21}] \{\Delta_R\} + [\hat{L}] \right) \right\} \tag{3-35}$$

<u>Final Stress Distribution:</u> As noted above, subsequent to obtaining the

end displacement at any segment, we convert to local coordinates, using

Equation (3-3)

$$[\delta(i)] = [IDT]^T [\Delta(i)] \tag{3-3'}$$

The stress resultants at every segment-edge are established in local

coordinates by combining Equations (3-1), (3-9), and (3-11)

$$[f(i)] = [IFT]^T \left(\begin{bmatrix} k_{ii} & \vdots & k_{ij} \end{bmatrix} \begin{bmatrix} \Delta(i) \\ \cdots \\ \Delta(j) \end{bmatrix} + [\ell(i)] \right) \tag{3-36}$$

The stress resultants in any elastic restraints may be established from

Equation (3-25).

Subsequent to obtaining the stress resultant and displacement

distribution at the edges of all the segments of the structure, the stress

resultant and the displacement distribution within each segment must be

established. This is necessary, inasmuch as in a shell structure having

a complex shell geometry, the maximum values of the stress resultants

and/or displacements may not occur at the edges of the segments. Finally,

it is essential to verify that the established solution satisfies the continuity

conditions at all the joints of the segments, thus insuring that the errors

induced during the integration process did not accumulate.

107

The establishment of the stress resultant and displacement distribution throughout each segment of the shell, and the checking of the established solutions, may be accomplished simultaneously by an integration throughout all the segments of the shell, as described previously in this chapter. This final integration, however, does not use the unit vectors described earlier as the initial conditions at joint i, but rather the stress resultant and displacement vectors obtained from Equations (3-3') and (3-36). From this integration the stress resultants and displacements of the jth end are obtained, as well as their distribution throughout the segments. The accuracy of the solution obtained by the numerical integration may be established by comparing the stress resultants and displacemnts at the jth end of every segment with their counterparts at the ith end (same structural point), of the corresponding adjacent segments.

It should be noted that for nonlinear problems the method of analysis presented in this chapter must be repeated several times for every load increment, as outlined in Chapter 2. After each trial solution the non-linear terms in the Newton-Raphson procedure are reevaluated using values obtained in the previous trial and a check for convergence at the current load level is made. Then the load can be incremented again and the procedure repeated (see Chapter 2).

While the current formulation is strictly valid only for shells of revolution, Reference 136 has shown how the concepts involved in this formulation might be extended to obtain approximate analyses of non-circular prismatic shells.

CHAPTER 4

CLASSICAL BUCKLING LOADS FOR SHELLS OF REVOLUTION
SUBJECTED TO STATIC LOADING

Various methods were presented in the preceding chapters for solving linear and nonlinear static problems for shells of revolution subjected to symmetric and unsymmetric loadings. In this chapter, methods for establishing the classical buckling load of shells of revolution will be presented. The classical buckling load is the load required to bring the idealized "perfect" shell to a bifurcation of its equilibrium (prebuckled) state. That is, we shall not be directly concerned either with the postbuckling behavior [159] or the effect of initial imperfections on the buckling loads and modes [160].

A method was presented in Chapter 2, for establishing the maximum value of the load wherein the prebuckling deformation of the shell corresponding to the applied load becomes unstable. Increments of the load were applied to the shell, and using Newton's method, the nonlinear response of the shell corresponding to each load increment was established. The maximum value of the load for which the prebuckling deformation of the shell becomes unstable was established as the point at which the solution ceased to converge. In addition to the lengthy computer time involved, this technique has other disadvantages. For example, in the case of axisymmetric loading, only the $n=0$ axisymmetric buckling load may be established with this technique without the use of "load perturbations". As will be discussed subsequently, in most cases of unsymmetric loading, the actual buckling mode may be established with the method discussed in Chapter 2. The principal difficulty in this case is the extensive computer time required for the analysis.

It should be noted, however, that the above method may be more useful in predicting shell imperfection sensitivity. In the case of axisymmetric imperfections for a spherical cap, this was demonstrated in Reference 158, wherein only the axisymmetric buckling mode was investigated. However, in combination with the "load perturbation" technique, this procedure can logically be extened to study unsymmetric modes. In order to study the effects of unsymmetric imperfections, a

109

coupled harmonic geometric and load formulation would be necessary. The beauty of the procedure is that no specialized imperfection analysis, other than the definition of the stress-free geometry for the most significant imperfection, is necessary. The procedure is also independent of imperfection magnitude. Given a general nonlinear equilibrium program, imperfection sensitivity may be investigated by merely adding another geometry to the program library.

Derivation of the Stability Equations: The stability equations for a shell of revolution can be obtained by the energy methods outlined in Reference 100. However, in this investigation, the procedure presented in Reference 137 will be employed. The typical variables in the general nonlinear Equations (1-27, 28, 29) presented in Chapter 1 for homogeneous orthotropic shells, will be denoted by Y, and will be decomposed into two components

$$Y = Y_P + Y_B \quad . \tag{4-1}$$

Y_P represents the value of the variable at the prebuckled equilibrium state. Y_B represents the change due to the buckling. The variables Y and Y_P must satisfy the general nonlinear Equations (1-27, 28, 29). Substituting Equation (4-1) into Equations (1-27, 28, 29) a set of nonlinear equations involving Y_P and Y_B are obtained. The set of prebuckling equations may be obtained from the above mentioned set by setting $Y_B = 0$. Subtracting the one set from the other, and neglecting terms nonlinear in Y_B, the following stability equations are obtained (For convenience of presentation the subscript B is omitted in all terms except for the "load" term.):

$$\frac{T_{\varphi\theta,\varphi}}{r_1} = -2T_{\varphi\theta}\frac{\cos\varphi}{r_o} - \frac{N_{\theta,\theta}}{r_o} + M_{\theta,\theta}\frac{\sin\varphi}{r_o^2} - M_{\varphi\theta}\frac{\cos\varphi}{r_o}\left[\frac{1}{r_1} - \frac{\sin\varphi}{r_o}\right] - \frac{\sin\varphi}{r_o}$$

$$\cdot\left\{N_{\theta P}\omega_\varphi + N_\theta\omega_{\varphi P} - N_{\varphi\theta P}\omega_\theta - N_{\varphi\theta}\omega_{\theta P}\right\} - f_{\theta B}$$

$$\frac{N_{\varphi,\varphi}}{r_1} = -N_\varphi\frac{\cos\varphi}{r_o} + N_\theta\frac{\cos\varphi}{r_o} - \frac{T_{\varphi\theta,\theta}}{r_o} - M_{\varphi\theta,\theta}\left[\frac{\sin\varphi}{r_o^2} + \frac{1}{r_o r_1}\right] + \frac{J_\varphi^*}{r_1} - f_{\varphi B} \tag{4-2}$$

$$\frac{J^*_{\varphi,\varphi}}{r_1} = -J^*_{\varphi}\frac{\cos\varphi}{r_o} - N_\theta\frac{\sin\varphi}{r_o} - \frac{N_\varphi}{r_1} - \frac{M_{\theta,\theta\theta}}{r_o^2} - 2M_{\varphi\theta,\theta}\frac{\cos\varphi}{r_o^2} - f_{\zeta B} - \frac{1}{r_o}$$

$$\cdot \left\{ N_{\varphi\theta P}\omega_\theta + N_{\varphi\theta}\omega_{\theta P} - N_{\theta P}\omega_\varphi - N_\theta\omega_{\varphi P} \right\}_{,\theta}$$

$$\frac{M_{\varphi,\varphi}}{r_1} = M_\theta\frac{\cos\varphi}{r_o} - M_\varphi\frac{\cos\varphi}{r_o} - \frac{2M_{\varphi\theta,\theta}}{r_o} + J_\varphi$$

$$\frac{u_{,\varphi}}{r_1} = u\frac{\cos\varphi}{r_o} - \frac{v_{,\theta}}{r_o} + \frac{T_{\varphi\theta}}{K_{33}} + \frac{M_{\varphi\theta}\sin\varphi}{r_o K_{33}} + \omega_{\theta P}\omega_\varphi + \omega_\theta\omega_{\varphi P}$$

$$\frac{v_{,\varphi}}{r_1} = \frac{w}{r_1} + (K_{22} - \nu^2_{\theta\varphi}K_{11})^{-1}\{N_\varphi - \nu_{\theta\varphi}N_\theta\} - \omega_{\theta P}\omega_\theta$$

$$\frac{w_{,\varphi}}{r_1} = \omega_\theta - \frac{v}{r_1}$$

$$\frac{\omega_{\theta,\varphi}}{r_1} = (D_{22} - \nu^2_{\theta\varphi}D_{11})^{-1}\{-M_\varphi + \nu_{\theta\varphi}M_\theta\}$$

$$N_\theta = \nu_{\varphi\theta}N_\varphi + (K_{11} - \nu^2_{\varphi\theta}K_{22})\left[\frac{u_{,\theta} + v\cos\varphi - w\sin\varphi}{r_o} + \omega_{\varphi P}\omega_\varphi\right]$$

$$M_\theta = \nu_{\varphi\theta}M_\varphi - \frac{(D_{11} - \nu^2_{\varphi\theta}D_{22})}{r_o}\left[\frac{w_{,\theta\theta} + u_{,\theta}\sin\varphi}{r_o} + \omega_\theta\cos\varphi\right]$$

$$M_{\varphi\theta} = \left[\frac{-1}{\frac{r_o}{D_{33}} + \frac{\sin^2\varphi}{r_o K_{33}}}\right]\left\{2\omega_{\theta,\theta} + u\left(\frac{\cos\varphi}{r_1} - \frac{\cos\varphi\sin\varphi}{r_o}\right) - v_{,\theta}\left(\frac{\sin\varphi}{r_o} + \frac{1}{r_1}\right)\right.$$

$$\left. - 2w_{,\theta}\frac{\cos\varphi}{r_o} + \frac{T_{\varphi\theta}}{K_{33}}\sin\varphi + \omega_{\theta P}\omega_\varphi\sin\varphi + \omega_\theta\omega_{\varphi P}\sin\varphi\right\} \qquad (4\text{-}2)$$

$$J_\varphi = J^*_\varphi + N_{\varphi\theta P}\omega_\varphi + N_{\varphi\theta}\omega_{\varphi P} - N_{\varphi P}\omega_\theta - N_\varphi\omega_{\theta P}$$

111

$$N_{\varphi\theta} = T_{\varphi\theta} + \frac{M_{\varphi\theta}}{r_o} \sin\varphi$$

$$\omega_\varphi = - \frac{w_{,\theta}}{r_o} - \frac{u \sin\varphi}{r_o} \qquad\qquad (4\text{-}2)$$

where

$$f_{\theta B} = F_\theta (\epsilon_{\theta_o} + \epsilon_{\varphi_o}) + F_\varphi \frac{u_{,\varphi}}{r_1} + F_\zeta \omega_\varphi$$

$$f_{\varphi B} = F_\varphi (\epsilon_{\theta_o} + \epsilon_{\varphi_o}) + F_\theta \frac{v_{,\theta}}{r_o} - F_\zeta \omega_\theta \qquad\qquad (4\text{-}3)$$

$$f_{\zeta B} = F_\zeta (\epsilon_{\theta_o} + \epsilon_{\varphi_o}) - F_\theta \omega_\varphi + F_\varphi \omega_\theta$$

Inasmuchas the variables Y and Y_P satisfy the given boundary conditions at the ends of the shell, the variables Y_B will satisfy homogeneous boundary conditions.

If reinforced or laminated shells are to be analyzed, Equation (4-1) must be substituted into Equations (1-31) or (1-32) instead of the corresponding equations in sets (1-28, 29). Thus, for ring-stringer reinforcement, the following equations must replace the corresponding equations in the set (4-2).

$$\frac{v_{,\varphi}}{r_1} = \frac{w}{r_1} - \omega_\theta P^\omega_\theta + \left(K_{22} + \frac{C_{22}^2}{D_{22}}\right)^{-1} \left\{ N_\varphi + \frac{C_{22}}{D_{22}}(M_\varphi) - \frac{K_{12}}{r_o}(u_{,\theta} + v\cos\varphi - w\sin\varphi) \right.$$

$$\left. - K_{12}\omega_\varphi P^\omega_\varphi - \frac{C_{22}D_{12}}{D_{22}} \left[\frac{w_{,\theta\theta} + u_{,\theta}\sin\varphi}{r_o^2} + \frac{\omega_\theta}{r_o}\cos\varphi \right] \right\}$$

$$\frac{\omega_{\theta,\varphi}}{r_1} = - \frac{C_{22}}{C_{22}^2 + K_{22}D_{22}} \left\{ N_\varphi - \frac{K_{12}}{r_o}(u_{,\theta} + v\cos\varphi - w\sin\varphi) - K_{12}\omega_\varphi P^\omega_\varphi \right\}$$

$$+ \frac{K_{22}}{C_{22}^2 + K_{22}D_{22}} \left\{ M_\varphi - D_{12} \left[\frac{w_{,\theta\theta} + u_{,\theta}\sin\varphi}{r_o^2} + \frac{\omega_\theta}{r_o}\cos\varphi \right] \right\}$$

$$N_\theta = K_{12}\left(K_{22} + \frac{C_{22}^2}{D_{22}}\right)^{-1} \left\{ N_\varphi + \frac{C_{22}}{D_{22}} M_\varphi \right\} + \left(\frac{K_{11}}{r_o} - \frac{K_{12}^2}{r_o}\left[K_{22} + \frac{C_{22}^2}{D_{22}} \right]^{-1} \right)$$

$$\cdot (u,_\theta + v\cos\varphi - w\sin\varphi + r_o {}^\omega \varphi_P {}^\omega \varphi) - \left(C_{11} + \frac{K_{12}C_{22}D_{12}}{D_{22}}\left[K_{22} + \frac{C_{22}^2}{D_{22}} \right]^{-1} \right)$$

$$\cdot \left(\frac{w,_{\theta\theta} + u,_\theta \sin\varphi}{r_o^2} + \frac{\omega_\theta}{r_o}\cos\varphi \right)$$

$$M_\theta = - \frac{D_{12}C_{22}}{C_{22}^2 + K_{22}D_{22}}\{N_\varphi\} + \frac{D_{12}K_{22}}{C_{22}^2 + K_{22}D_{22}}\{M_\varphi\}$$

$$+ \left(\frac{C_{11}}{r_o} + \frac{D_{12}K_{12}}{r_o}\left[\frac{C_{22}}{C_{22}^2 + K_{22}D_{22}} \right] \right)(u,_\theta + v\cos\varphi - w\sin\varphi + r_o {}^\omega \varphi_P {}^\omega \varphi)$$

$$+ \left(D_{11} - \frac{D_{12}^2 K_{22}}{C_{22}^2 + K_{22}D_{22}} \right)\left(\frac{w,_{\theta\theta} + u,_\theta \sin\varphi}{r_o^2} + \frac{\omega_\theta}{r_o}\cos\varphi \right) \tag{4-4}$$

For laminated shells the following equations must replace the corresponding equations in the set (4-2),

$$\frac{v,_\varphi}{r_1} = \frac{w}{r_1} - \omega_\theta P^\omega \theta + \left(K_{22} + \frac{C_{25}^2}{D_{22}} \right)^{-1} \left\{ N_\varphi + \frac{C_{25}}{D_{22}} M_\varphi - \left(K_{12} + \frac{C_{15}C_{25}}{D_{22}} \right) \right.$$

$$\cdot \left[\frac{1}{r_o}(u,_\theta + v\cos\varphi - w\sin\varphi) + \omega_\varphi P^\omega \varphi \right] - \left(\frac{C_{25}D_{12}}{D_{22}} - C_{15} \right)$$

$$\left. \cdot \left[\frac{w,_{\theta\theta} + u,_\theta \sin\varphi}{r_o^2} + \frac{\omega_\theta}{r_o}\cos\varphi \right] \right\}$$

$$\frac{\omega_{\theta,\varphi}}{r_1} = \left(C_{25} + \frac{K_{22}D_{22}}{C_{25}}\right)^{-1} \left\{ \frac{K_{22}}{C_{25}}M_\varphi - N_\varphi + \left(K_{12} - \frac{K_{22}C_{15}}{C_{25}}\right)\left[\frac{1}{r_o}(u_{,\theta} + v\cos\varphi - w\sin\varphi) \right.\right.$$

$$\left.\left. + \omega_\varphi P^{\omega_\varphi}\right] - \left(C_{15} + \frac{K_{22}D_{12}}{C_{25}}\right)\left[\frac{w_{,\theta\theta} + u_{,\theta}\sin\varphi}{r_o^2} + \frac{\omega_\theta}{r_o}\cos\varphi\right]\right\}$$

$$N_\theta = N_\varphi\left(\frac{K_{12}}{K_{22}} - \left[\frac{K_{12}C_{25}}{K_{22}} - C_{15}\right]\left[C_{25} - \frac{K_{22}D_{22}}{C_{25}}\right]^{-1}\right) + \left(\frac{K_{12}C_{25}}{K_{22}} - C_{15}\right)$$

$$\cdot\left(C_{25} + \frac{K_{22}D_{22}}{C_{25}}\right)^{-1}\left(\frac{K_{22}}{C_{25}}\right)M_\varphi + \left\{\left(K_{11} - \frac{K_{12}^2}{K_{22}}\right) + \left(\frac{K_{12}C_{25}}{K_{22}} - C_{15}\right)\right.$$

$$\left.\cdot\left(C_{25} + \frac{K_{22}D_{22}}{C_{25}}\right)^{-1}\left(K_{12} - \frac{K_{22}C_{15}}{C_{25}}\right)\right\}\left[\frac{1}{r_o}(u_{,\theta} + v\cos\varphi - w\sin\varphi) + \omega_\varphi P^{\omega_\varphi}\right]$$

$$+ \left\{\left(\frac{K_{12}C_{15}}{K_{22}} - C_{14}\right) - \left(\frac{K_{12}C_{25}}{K_{22}} - C_{15}\right)\left(C_{25} + \frac{K_{22}D_{22}}{C_{25}}\right)^{-1}\left(C_{15} + \frac{K_{22}D_{12}}{C_{25}}\right)\right\}$$

$$\cdot\left[\frac{w_{,\theta\theta}}{r_o^2} + \frac{u_{,\theta}\sin\varphi}{r_o^2} + \frac{\omega_\theta}{r_o}\cos\varphi\right] \tag{4-5}$$

$$M_\theta = M_\varphi\left[\frac{D_{12}}{D_{22}} + \left(C_{15} - \frac{D_{12}C_{25}}{D_{22}}\right)\left(K_{22} + \frac{C_{25}^2}{D_{22}}\right)^{-1}\frac{C_{25}}{D_{22}}\right] + N_\varphi\left(C_{15} - \frac{D_{12}C_{25}}{D_{22}}\right)$$

$$\cdot\left(K_{22} + \frac{C_{25}^2}{D_{22}}\right)^{-1} + \left\{\left(D_{11} - \frac{D_{12}^2}{D_{22}}\right) - \left(C_{15} - \frac{D_{12}C_{25}}{D_{22}}\right)\left(K_{22} + \frac{C_{25}^2}{D_{22}}\right)^{-1}\right.$$

$$\left.\cdot\left(\frac{C_{25}D_{12}}{D_{22}} - C_{15}\right)\right\}\left[\frac{w_{,\theta\theta} + u_{,\theta}\sin\varphi}{r_o^2} + \frac{\omega_\theta}{r_o}\cos\varphi\right] + \left\{\left(C_{14} - \frac{D_{12}C_{15}}{D_{22}}\right)\right.$$

$$\left. - \left(C_{15} - \frac{D_{12}C_{25}}{D_{22}}\right)\left(K_{22} + \frac{C_{25}^2}{D_{22}}\right)^{-1}\left(K_{12} + \frac{C_{15}C_{25}}{D_{22}}\right)\right\}\left[\frac{1}{r_o}(u_{,\theta} + v\cos\varphi - w\sin\varphi)\right.$$

$$\left. + \omega_\varphi P^{\omega_\varphi}\right]$$

114

Prior to presenting solutions to these equations, it must be decided how the prebuckled state will be established. In most earlier buckling analyses, this state was established on the basis of the linear membrane theory. This procedure yields accurate results for some shell geometries under certain boundary and loading conditions, and simplifies the analysis greatly. Recently, with the introduction of automated numerical analyses, the prebuckled state has been established on the basis of the linear bending theory, and even nonlinear bending theory. However, there is not sufficient evidence for a general conclusion as to when it is necessary to analyze the prebuckled state by a non-linear analysis. In the last few years, a number of shell problems have been solved where nonlinear buckling effects have been found to be significant, such as in the case of eccentrically meridionally stiffened **spherical** caps [29, 163-165]. Most of the general shell stability computer programs [28, 117, 138] have options for using nonlinear bending analysis for the prebuckling state.

Stability Under Axisymmetric Loading: As in the nonlinear static analysis, considered in Chapters 2 and 3, the stability analysis of shells of revolution will be different if the loading is axisymmetric or unsymmetric. In the case of axisymmetric loading, the terms in Equations (4-2) having a P subscript (prebuckling terms), and the load terms in Equations (4-3) are zeroth harmonic amplitudes (invariant with θ). However, the terms which do not have a P subscript (buckling terms), must be expressed in terms of the Fourier series (2-2). It should be noted, that in the case of buckling under axisymmetric loads, the primed and the double-primed harmonic amplitudes, generally will be coupled. However, each pair of harmonic amplitudes (the primed

and the double primed) will not be coupled with other pairs and, therefore, each pair may be considered separately.

$$\frac{T'_{\varphi\theta,\varphi}{}^{(n)}}{r_1} = -2T'_{\varphi\theta}{}^{(n)}\frac{\cos\varphi}{r_o} + n\frac{N'_\theta{}^{(n)}}{r_o} - nM'_\theta{}^{(n)}\frac{\sin\varphi}{r_o^2} - M'_{\varphi\theta}{}^{(n)}\frac{\cos\varphi}{r_o}$$

$$\cdot\left[\frac{1}{r_1} - \frac{\sin\varphi}{r_o}\right] - f_{\theta B}{}^{(n)} - \frac{\sin\varphi}{r_o}\left\{N_{\theta P}{}^{(0)}\Omega'_\varphi{}^{(n)} + N''_\theta{}^{(n)}\Omega_{\varphi P}{}^{(0)}\right.$$

$$\left. - N_{\varphi\theta P}{}^{(0)}\Omega''_\theta{}^{(n)} - N'_{\varphi\theta}{}^{(n)}\Omega_{\theta P}{}^{(0)}\right\}$$

$$\frac{N'_{\varphi,\varphi}{}^{(n)}}{r_1} = -N'_\varphi{}^{(n)}\frac{\cos\varphi}{r_o} + N'_\theta{}^{(n)}\frac{\cos\varphi}{r_o} - n\frac{T'_{\varphi\theta}{}^{(n)}}{r_o} - nM'_{\varphi\theta}{}^{(n)}\left[\frac{\sin\varphi}{r_o^2} + \frac{1}{r_o r_1}\right]$$

$$+ \frac{J'^{*(n)}_\varphi}{r_1} - f_{\varphi B}{}^{(n)}$$

$$\frac{J'^{*}_{\varphi,\varphi}{}^{(n)}}{r_1} = -J'^{*(n)}_\varphi\frac{\cos\varphi}{r_o} - N'_\theta{}^{(n)}\frac{\sin\varphi}{r_o} - \frac{N'_\varphi{}^{(n)}}{r_1} + n^2\frac{M'_\theta{}^{(n)}}{r_o^2} - 2nM'_{\varphi\theta}{}^{(n)}\frac{\cos\varphi}{r_o^2}$$

$$-f_{\zeta B}{}^{(n)} - \frac{1}{r_o}\left\{nN_{\varphi\theta P}{}^{(0)}\Omega''_\theta{}^{(n)} + nN'_{\varphi\theta}{}^{(n)}\Omega_{\theta P}{}^{(0)} - nN_{\theta P}{}^{(0)}\Omega'_\varphi{}^{(n)} - nN''_\theta{}^{(n)}\Omega_{\varphi P}{}^{(0)}\right\}$$

$$\frac{M'_{\varphi,\varphi}{}^{(n)}}{r_1} = M'_\theta{}^{(n)}\frac{\cos\varphi}{r_o} - M'_\varphi{}^{(n)}\frac{\cos\varphi}{r_o} - 2n\frac{M'_{\varphi\theta}{}^{(n)}}{r_o} + J'_\varphi{}^{(n)}$$

$$\frac{U'_{,\varphi}{}^{(n)}}{r_1} = U'^{(n)}\frac{\cos\varphi}{r_o} + n\frac{V'^{(n)}}{r_o} + \frac{T'_{\varphi\theta}{}^{(n)}}{K_{33}} + \frac{M'_{\varphi\theta}{}^{(n)}\sin\varphi}{r_o K_{33}} + \Omega_{\theta P}{}^{(0)}\Omega'_\varphi{}^{(n)} + \Omega''_\theta{}^{(n)}\Omega_{\varphi P}{}^{(n)}$$

$$\frac{V'_{,\varphi}{}^{(n)}}{r_1} = \frac{W'^{(n)}}{r_1} + (K_{22} - \nu_{\theta\varphi}{}^2 K_{11})^{-1}\{N'_\varphi{}^{(n)} - \nu_{\theta\varphi}N'_\theta{}^{(n)}\} - \Omega_{\theta P}{}^{(0)}\Omega'_\theta{}^{(n)}$$

116

$$\frac{W_{,\varphi}^{'(n)}}{r_1} = \Omega_\theta^{'(n)} - \frac{V^{'(n)}}{r_1}$$

$$\frac{\Omega_{\theta,\varphi}^{'(n)}}{r_1} = (D_{22} - \nu_{\theta\varphi}^2 D_{11})^{-1} \{-M_\varphi^{'(n)} + \nu_{\theta\varphi} M_\theta^{'(n)}\} \qquad (4\text{-}6)$$

$$N_\theta^{'(n)} = \nu_{\varphi\theta} N_\varphi^{'(n)} + (K_{11} - \nu_{\varphi\theta}^2 K_{22}) \left[\frac{nU^{'(n)} + V^{'(n)} \cos\varphi - W^{'(n)} \sin\varphi}{r_o} + \Omega_{\varphi P}^{(0)} \Omega_\varphi^{''(n)} \right]$$

$$M_\theta^{'(n)} = \nu_{\varphi\theta} M_\varphi^{'(n)} - \frac{(D_{11} - \nu_{\varphi\theta}^2 D_{22})}{r_o} \left[\frac{nU^{'(n)} \sin\varphi - n^2 W^{'(n)}}{r_o} + \Omega_\theta^{'(n)} \cos\varphi \right]$$

$$M_{\varphi\theta}^{'(n)} = \left[\frac{1}{\dfrac{r_o}{D_{33}} + \dfrac{\sin^2\varphi}{r_o K_{33}}} \right] \left\{ -2n\Omega_\theta^{'(n)} + U^{'(n)} \left(\frac{\cos\varphi}{r_1} - \frac{\cos\varphi \sin\varphi}{r_o} \right) + nV^{'(n)} \right.$$

$$\cdot \left(\frac{\sin\varphi}{r_o} + \frac{1}{r_1} \right) + 2nW^{'(n)} \frac{\cos\varphi}{r_o} + T_{\varphi\theta}^{'(n)} \frac{\sin\varphi}{K_{33}} + \Omega_{\theta P}^{(0)} \Omega_\varphi^{'(n)} \sin\varphi$$

$$\left. + \Omega_\theta^{''(n)} \Omega_{\varphi P}^{(0)} \sin\varphi \right\}$$

$$J_\varphi^{'(n)} = J_\varphi^{'*(n)} + N_{\varphi\theta P}^{(0)} \Omega_\varphi^{''(n)} + N_{\varphi\theta}^{''(n)} \Omega_{\varphi P}^{(0)} - N_{\varphi P}^{(0)} \Omega_\theta^{'(n)} - N_\varphi^{'(n)} \Omega_{\theta P}^{(0)}$$

$$N_{\varphi\theta}^{'(n)} = T_{\varphi\theta}^{'(n)} + \frac{M_{\varphi\theta}^{'(n)}}{r_o} \sin\varphi$$

$$\Omega_\varphi^{'(n)} = \frac{nW^{'(n)}}{r_o} - \frac{U^{'(n)} \sin\varphi}{r_o}$$

where

$$f_{\theta B}^{(n)} = F_\theta^{(0)} \left[\frac{1}{r_o} (nU^{''(n)} + V^{''(n)} \cos\varphi - W^{''(n)} \sin\varphi) + \frac{V_{,\varphi}^{''(n)}}{r_1} - \frac{W^{''(n)}}{r_1} \right.$$

$$\left. + \Omega_{\varphi P}^{(0)} \Omega_\varphi^{'(n)} + \Omega_{\theta P}^{(0)} \Omega_\theta^{''(n)} \right] + F_\varphi^{(0)} \frac{U_{,\varphi}^{'(n)}}{r_1} + F_\zeta^{(0)} \Omega_\varphi^{'(n)}$$

117

$$f_{\varphi B}^{(n)} = F_\varphi^{(0)} \left[\frac{1}{r_o} (nU'^{(n)} + V'^{(n)} \cos\varphi - W'^{(n)} \sin\varphi) + \frac{V'^{(n)}_{,\varphi}}{r_1} - \frac{W'^{(n)}}{r_1} \right.$$
$$\left. + \Omega_{\varphi P}^{(0)} \Omega_\varphi''^{(n)} + \Omega_{\theta P}^{(0)} \Omega_\theta'^{(n)} \right] + nF_\theta^{(0)} \frac{V''^{(n)}}{r_o} - F_\zeta^{(0)} \Omega_\theta'^{(n)} \qquad (4\text{-}7)$$

$$f_{\zeta B}^{(n)} = F_\zeta^{(0)} \left[\frac{1}{r_o} (nU'^{(n)} + V'^{(n)} \cos\varphi - W'^{(n)} \sin\varphi) + \frac{V'^{(n)}_{,\varphi}}{r_1} - \frac{W'^{(n)}}{r_1} \right.$$
$$\left. + \Omega_{\varphi P}^{(0)} \Omega_\varphi''^{(n)} + \Omega_{\theta P}^{(0)} \Omega_\theta'^{(n)} \right] - F_\theta^{(0)} \Omega_\varphi''^{(n)} + F_\varphi^{(0)} \Omega_\theta'^{(n)} .$$

As evident by the presence of the double primed terms in the above equations, the primed and double primed terms are coupled. A similar set of equations may be obtained involving primarily double primed harmonic amplitudes, with only a few single primed cross-coupling terms. From Equations (4-6, 7), it is apparent that for certain load conditions (axisymmetric non-torsional loads), the pairs of harmonic amplitudes (primed and double primed) may be uncoupled. Thus, for axisymmetric non-torsional loads, the buckling modes can be described by the half Fourier series expansions in Equations (2-2).

In establishing the buckling modes of shells subjected to torsional loads, in addition to other loads, the set of Equations (4-6, 7) must be solved simultaneously with the set of equations for the double-primed amplitudes, previously discussed. Equations (4-6, 7) are valid for orthotropic homogeneous shells. If reinforced or laminated shells are to be analyzed, Equations (4-4) or (4-5), respectively, must be employed instead of the corresponding equations in the sets (4-6, 7).

It is apparent from Equations (4-6, 7) that for shells subjected to axisymmetric loading, buckled shapes may correspond to any harmonic (n = 0, 1, 2···). Thus, the buckling loads corresponding to different harmonic buckled shapes must be established until the critical (minimum) load is determined.

<u>Stability Under Unsymmetric Loading</u>: The appropriate equations for the case of unsymmetric loading are analogous to the equations of the non-linear unsymmetric static problem presented in Chapter 2. Thus, they are more complex than Equations (4-6, 7), for the case of symmetric loading. For unsymmetric loading, when the loads and displacements are expanded in Fourier series (see Equations (2-1, 2)) the resulting equations involve product terms (see Equations (2-6a, b)). Thus, by referring to Chapter 2, the general equations for the stability of homogeneous orthotropic shells of revolution under unsymmetric load may be written as

$$\frac{T'_{\varphi\theta,\varphi}{}^{(n)}}{r_1} = -2T'_{\varphi\theta}{}^{(n)}\frac{\cos\varphi}{r_o} + n\frac{N'_{\theta}{}^{(n)}}{r_o} - n\frac{M'_{\theta}{}^{(n)}\sin\varphi}{r_o{}^2} - M'_{\varphi\theta}{}^{(n)}\frac{\cos\varphi}{r_o}$$

$$\cdot\left[\frac{1}{r_1} - \frac{\sin\varphi}{r_o}\right] - f_{\theta B}{}^{(n)} - \frac{\sin\varphi}{r_o}\{(N_{\theta P}\Omega_{\varphi})^{(n)} + (N_{\theta}\Omega_{\varphi P})^{(n)}$$

$$- (N_{\varphi\theta P}\Omega_{\theta})^{(n)} - (N_{\varphi\theta}\Omega_{\theta P})^{(n)}\}$$

$$\frac{N'_{\varphi,\varphi}{}^{(n)}}{r_1} = -N'_{\varphi}{}^{(n)}\frac{\cos\varphi}{r_o} + N'_{\theta}{}^{(n)}\frac{\cos\varphi}{r_o} - n\frac{T'_{\varphi\theta}{}^{(n)}}{r_o} - nM'_{\varphi\theta}{}^{(n)}\left[\frac{\sin\varphi}{r_o{}^2} + \frac{1}{r_o r_1}\right]$$

$$+ \frac{J'^{*(n)}_{\varphi}}{r_1} - f_{\varphi B}{}^{(n)}$$

$$\frac{J'^{*}_{\varphi,\varphi}{}^{(n)}}{r_1} = -J'^{*(n)}_{\varphi}\frac{\cos\varphi}{r_o} - N'_{\theta}{}^{(n)}\frac{\sin\varphi}{r_o} - \frac{N'_{\varphi}{}^{(n)}}{r_1} + n^2\frac{M'_{\theta}{}^{(n)}}{r_o{}^2} - 2nM'_{\varphi\theta}{}^{(n)}\frac{\cos\varphi}{r_o{}^2}$$

$$- f_{\zeta B}{}^{(n)} + \frac{1}{r_o}\{n(N_{\varphi\theta P}\Omega_{\theta})^{(n)} + \dot{n}(N_{\varphi\theta}\Omega_{\theta P})^{(n)} - n(N_{\theta P}\Omega_{\varphi})^{(n)} - n(N_{\theta}\Omega_{\varphi P})^{(n)}\}$$

$$\frac{M'_{\varphi,\varphi}{}^{(n)}}{r_1} = M'_{\theta}{}^{(n)}\frac{\cos\varphi}{r_o} - M'_{\varphi}{}^{(n)}\frac{\cos\varphi}{r_o} - 2n\frac{M'_{\varphi\theta}{}^{(n)}}{r_o} + J'_{\varphi}{}^{(n)} \qquad (4\text{-}8)$$

$$\frac{U'^{(n)}_{,\varphi}}{r_1} = U'^{(n)}\frac{\cos\varphi}{r_o} + \frac{nV'^{(n)}}{r_o} + \frac{T'^{(n)}_{\varphi\theta}}{K_{33}} + \frac{M'^{(n)}_{\varphi\theta}\sin\varphi}{r_o K_{33}} + (\Omega_\theta P \Omega_\varphi)^{(n)} + (\Omega_\theta \Omega_{\varphi P})^{(n)}$$

$$\frac{V'^{(n)}_{,\varphi}}{r_1} = \frac{W'^{(n)}}{r_1} + (K_{22} - \nu_{\theta\varphi}^2 K_{11})^{-1}\{N'^{(n)}_\varphi - \nu_{\theta\varphi}N'^{(n)}_\theta\} - (\Omega_\theta P \Omega_\theta)^{(n)}$$

$$\frac{W'^{(n)}_{,\varphi}}{r_1} = \Omega'^{(n)}_\theta - \frac{V'^{(n)}}{r_1}$$

$$\frac{\Omega'^{(n)}_{\theta,\varphi}}{r_1} = (D_{22} - \nu_{\theta\varphi}^2 D_{11})^{-1}\{-M'^{(n)}_\varphi + \nu_{\theta\varphi}M'^{(n)}_\theta\}$$

$$N'^{(n)}_\theta = \nu_{\varphi\theta}N'^{(n)}_\varphi + (K_{11} - \nu_{\varphi\theta}^2 K_{22})\left[\frac{nU'^{(n)} + V'^{(n)}\cos\varphi - W'^{(n)}\sin\varphi}{r_o} + (\Omega_{\varphi P}\Omega_\varphi)^{(n)}\right]$$

$$M'^{(n)}_\theta = \nu_{\varphi\theta}M'^{(n)}_\varphi - \frac{(D_{11} - \nu_{\varphi\theta}^2 D_{22})}{r_o}\left[\frac{nU'^{(n)}\sin\varphi - n^2 W'^{(n)}}{r_o} + \Omega'^{(n)}_\theta\cos\varphi\right]$$

$$M'^{(n)}_{\varphi\theta} = \left[\frac{-1}{\dfrac{r_o}{D_{33}} + \dfrac{\sin^2\varphi}{r_o K_{33}}}\right]\left\{-2n\Omega'^{(n)}_\theta + U'^{(n)}\left(\frac{\cos\varphi}{r_1} - \frac{\cos\varphi\sin\varphi}{r_o}\right) + nV'^{(n)}\left(\frac{\sin\varphi}{r_o} + \frac{1}{r_1}\right)\right.$$

$$\left. + 2nW'^{(n)}\frac{\cos\varphi}{r_o} + T'^{(n)}_{\varphi\theta}\frac{\sin\varphi}{K_{33}} + (\Omega_\theta P \Omega_\varphi)^{(n)}\sin\varphi + (\Omega_\theta \Omega_{\varphi P})^{(n)}\sin\varphi\right\}$$

$$J'^{(n)}_\varphi = J'^{*(n)}_\varphi + (N_{\varphi\theta P}\Omega_\varphi)^{(n)} + (N_{\varphi\theta}\Omega_{\varphi P})^{(n)} - (N_{\varphi P}\Omega_\theta)^{(n)} - (N_\varphi\Omega_{\theta P})^{(n)} \qquad (4\text{-}8)$$

$$N'^{(n)}_{\varphi\theta} = T'^{(n)}_{\varphi\theta} + \frac{M'^{(n)}_{\varphi\theta}}{r_o}\sin\varphi$$

$$\Omega'^{(n)}_\varphi = \frac{nW'^{(n)}}{r_o} - \frac{U'^{(n)}}{r_o}\sin\varphi$$

where, as in Equations (2-8), the above equations have been obtained by utilizing only the half of the series (2-1) with primed amplitudes. A similar set of equations may be obtained by using the half of the series (2-1) with the double

120

primed amplitudes. In Equations (4-8), the nonlinear terms involve coupling of the primed and double primed amplitudes, as well as the harmonics. The amplitudes of the harmonics in the nonlinear terms with a subscript P represent the effect of the prebuckled state. The nonlinear terms in Equations (4-8) may be obtained from Equations (2-9) with the appropriate addition of the P subscript. The buckling "load" terms $(f_{\theta B}^{(n)}, f_{\varphi B}^{(n)}, f_{\zeta B}^{(n)})$ are obtained from Equations (2-9) by omitting the first single term $(F_{\theta}^{(n)}, F_{\varphi}^{(n)}, F_{\zeta}^{(n)})$. If reinforced or laminated shells are to be analyzed, Equations (4-4) or (4-5) should be used in place of their counterparts in Equations (4-8).

Stability Considerations: In Chapter 2, it was noted that the resulting equations could be significantly simplified if a line of symmetry existed in the loading pattern. This was accomplished inasmuchas, in this case, the resulting deformation and stress pattern is symmetric with respect to this line of symmetry. In the case of buckling, if a line of symmetry exists in the loading pattern, and consequently in the prebuckling deformation and stress state, the loading pattern and the prebuckling deformation and stress state may be represented by only half of the Fourier series expansions. However, this does not denote that the buckling deformation shape may be represented by the same half-series expansions. Thus, the full series expansions must be used resulting in two different sets of equations corresponding to buckling modes "in-phase" and "out-of-phase" with the applied load. This was also the case for axisymmetric loading (no torsional loads). However, since in that case, each harmonic buckling shape could be investigated separately, the two sets of equations represent buckling shapes differing only by a rigid body motion. Thus, only one set of equations was sufficient for the analysis. If the shell was subjected to torsional loads, in addition to other axisymmetric

loads, the resulting sets of equations will be cross-coupled and must be solved simultaneously for each harmonic buckling mode. In the case of unsymmetric loading with a line of symmetry, the prebuckling harmonic amplitudes (e. g. primed) are coupled with the buckling harmonic amplitudes (primed <u>or</u> double-primed). Thus, the two sets of equations yield different buckling loads corresponding to in-phase or out-of-phase buckling shapes.

In Figure 20, the axisymmetric load versus the resulting deformation is plotted, whereas the unsymmetric load versus the resulting deformation is plotted in Figure 21. Under axisymmetric loading, the iteration technique described in Chapter 2 would proceed along line $0A'B'C'D'$ which corresponds to the axisymmetric nonlinear static analysis. Point D' is established as the buckling load referred to by Thompson [139] as the "snapping load". However, the actual (lowest) buckling load may correspond to a non-axisymmetric buckling configuration. (As shown in Fig. 20, point A', obtained on the basis of the stability analysis to be presented in this chapter, for the $n = n_1$ buckling configuration* may correspond to a buckling load lower than that corresponding to point D'.) Thus, for any assumed buckling configuration corresponding to an assumed value n, the solution to be presented in this chapter will yield a buckling load (points A' or B' or C'), whereas, the method presented in Chapter 2 will yield only point D' corresponding to $n = 0$. That is, the solution to be presented in this chapter permits a buckling configuration described by harmonics different from $n = 0$ (describing the applied loads), whereas, the solution presented in Chapter 2 yields an $n=0$ buckling configuration only, without resorting to "load perturbations". From experimental evidence, however the buckling configuration of shells of

---

*Notice, that in the case of axisymmetric loading, as discussed previously, the harmonics uncouple; consequently, the buckling configuration will correspond only to one harmonic.
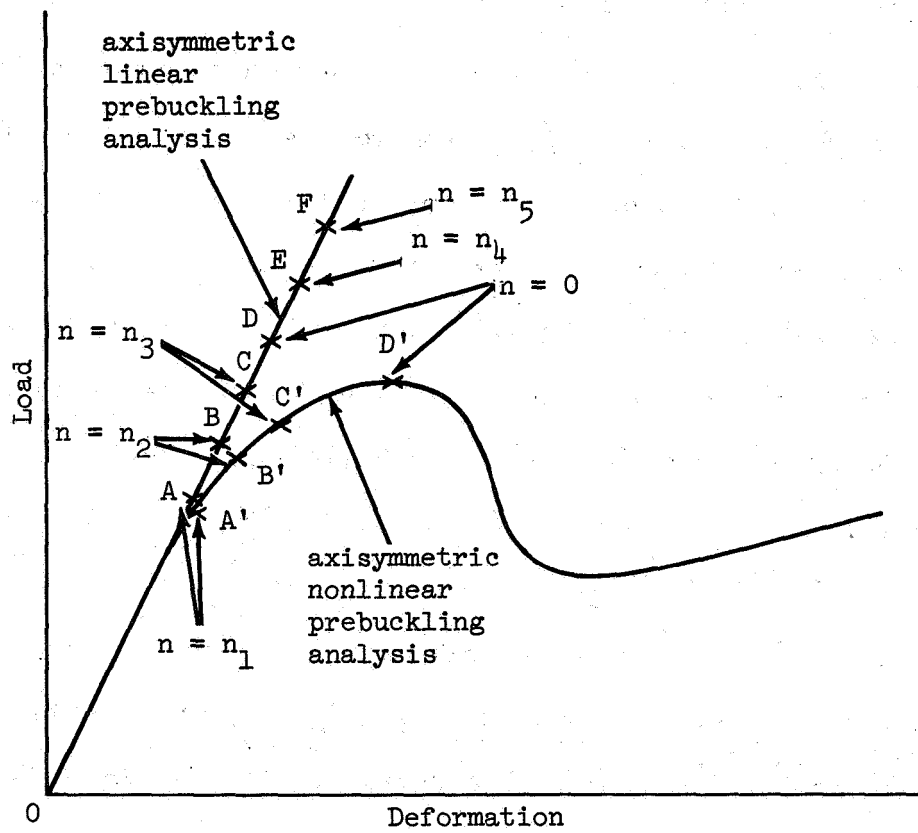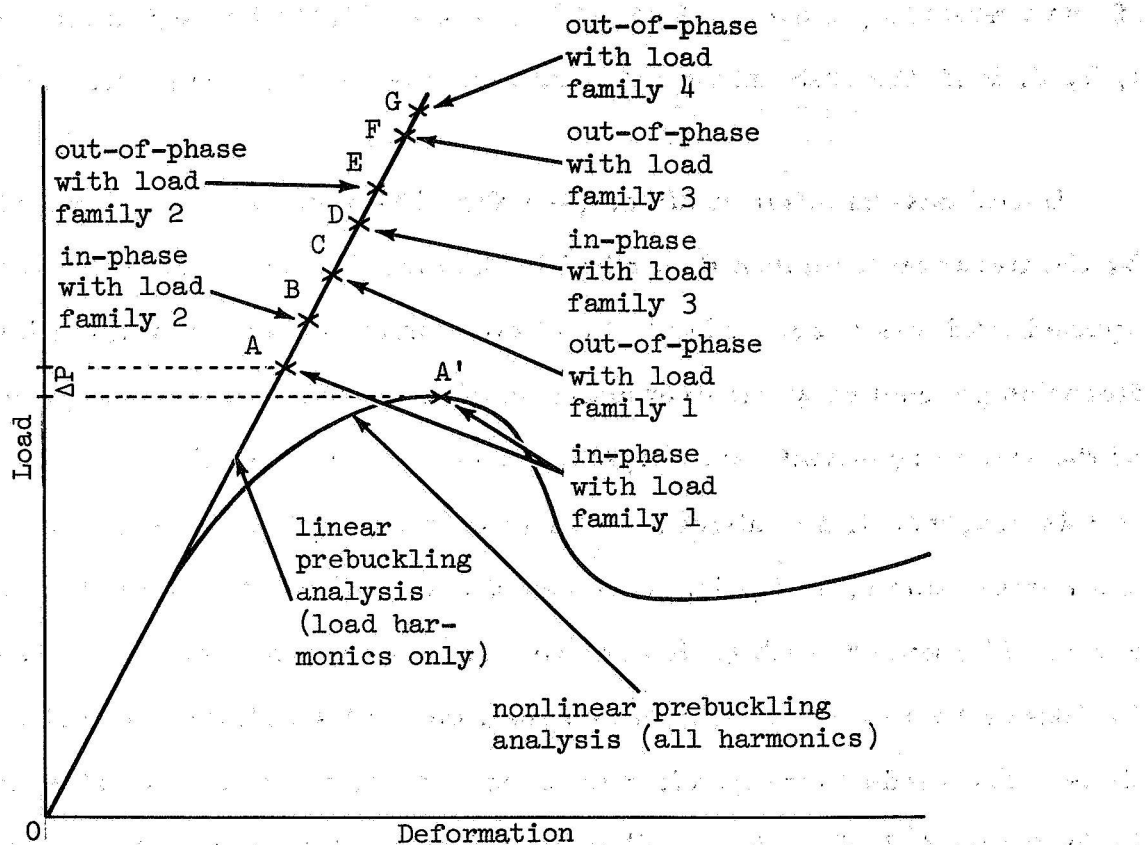
Figure 20   Shell Stability-Axisymmetric Load

out-of-phase
with load
family 4

out-of-phase
with load
family 3

in-phase
with load
family 3

out-of-phase
with load
family 1

in-phase
with load
family 1

out-of-phase
with load
family 2

in-phase
with load
family 2

linear
prebuckling
analysis
(load har-
monics only)

nonlinear prebuckling
analysis (all harmonics)

Load

Deformation

Figure 21 Shell Stability-Unsymmetric Load

124

revolution subjected to symmetric loads is not always described by the same harmonic as the applied loads. The two methods for buckling analysis to be discussed in this chapter may be employed to establish buckling loads for any buckling mode. That is, referring to Fig. 20, to establish points A', B', C', D' if the prebuckling state is described by the nonlinear bending theory, or points A, B, C, D if the prebuckling state is described by the linear bending theory.

Under unsymmetric loading, (see Fig. 21) point A' may be established by the iteration technique described in Chapter 2. Note, that even if the applied load was described only by a few Fourier harmonic amplitudes, the iteration procedure would eventually involve all the harmonic amplitudes of the stress resultants and displacements. In the methods to be described in this chapter, if a nonlinear prebuckling state is to be considered, all the harmonics couple, and point A' is established. If the prebuckled state is analyzed by linear bending theory, several buckling configurations described by different families of harmonics constitute mathematically acceptable solutions. The loads corresponding to these configurations are denoted in Fig. 21 by points A, B, C, D, E, F. These families of harmonics will be described subsequently. The buckled configuration corresponding to point A' is described by all the harmonic terms, whereas, the buckling configurations corresponding to points A, B, D are described by groups of harmonics each of which is contained in the terms describing the configuration corresponding to point A'. Thus, the loads corresponding to points A, B, D will be approximations of different order of accuracy to the critical buckling load defined by point A', rather than buckling loads corresponding to different buckling

configurations as in the case of a shell under axisymmetric loading.

The load corresponding to point A' may be obtained by incremental Newtonian iteration, using a **larger number of harmonic** terms for each successive load increment. Thus, the analysis is lengthy. Moreover, in the analysis, the Fourier series describing the buckling configuration must be truncated, consequently the load corresponding to point A' may be established approximately. Points A, B, D, however, may be obtained by one eigenvalue analysis (for each point). In this analysis, the Fourier series harmonic families describing the buckling configurations must be truncated. If a dominant harmonic group exists in the description of the actual buckling shape, and the same _number_ of Fourier terms is retained in the linear and non-linear analyses, the buckling load obtained on the basis of the linear analysis (point A) may actually be closer to the true buckling load than the load estimated on the basis of the non-linear analysis. Furthermore, the computer time required for obtaining the buckling load on the basis of the linear analysis is much smaller than that required for obtaining the buckling load on the basis of the non-linear analysis. It should be noted, that the smallest in-phase buckling load estimate (point A) will be larger than the actual in-phase buckling load. However, the smallest out-of-phase buckling load estimate (point C) may be smaller than the smallest in-phase buckling load estimate (point A) since they are estimates to different possible critical loads (in-phase and out-of-phase).

Solution by the Determinant Evaluation Method: The determinant evaluation method represents the classical approach to the stability problem. For any assumed value of the applied load, a static analysis is performed to establish the prebuckling stress and deformation components at every point chosen for Runge Kutta integration in every shell segment. This is accomplished by employing the methods described in Chapter 3 for either linear

or nonlinear theory. The results of this analysis are introduced as the terms with subscript P in Equations (4-6) and (4-7) if the load is axisymmetric, or Equations (4-8) if the loading is non-axisymmetric. These equations are then integrated using the the Runge-Kutta procedure in a fashion analogous to that of the static analysis of Chapter 3 and the prestressed stiffness matrices of the segments are formed. Note, that a load matrix associated with the stability analysis does not exist, inasmuch as the loads have been eliminated from the pertinent equations by taking into account that prior to buckling, the shell is in a state of equilibrium under the influence of the buckling loads. That is, the buckling state is a possible second state of equilibrium under the buckling loads. The prestressed stiffness matrices of each segment are 8 x 8 matrices for shells subjected to axisymmetric loading, or 8M x 8M matrices for shells subjected to unsymmetric loading, where M is the number of harmonic terms retained in the analysis.

The prestressed stiffness matrices of the segments are stacked to obtain the total matrix of the structure by a procedure identical to that discussed in detail in Chapter 3. This matrix is then reduced by employing the boundary conditions. Thus, we obtain an equation analogous to Equation (3-30) in the form

$$[\widehat{K}_P]_F [\Delta]_F = 0 \tag{4-9}$$

or

$$\det[\widehat{K}_P]_F = 0 \quad . \tag{4-10}$$

If the assumed load was the correct buckling load corresponding to the assumed harmonic buckling configuration, Equation (4-9) would be identically satisfied. Otherwise the determinant would not vanish.

127

Inasmuchas the prestressed stiffness matrix may be large, the evaluation of its determinant on a computer may involve overflow or underflow. To avoid this problem, the matrix $[\widehat{K_p}]_F$ is first converted into an upper triangular matrix by a technique such as Gaussian elimination [118]. The value of the determinant of such a matrix is the product of its diagonal terms. Since the determinant vanishes, these terms can be normalized by dividing each term by its absolute value. Thus, the value of the determinant is always ±1. A sign change of the determinant between two consecutive loads signifies that the value of the determinant vanishes between these two loads. This technique avoids the establishment of spurious sign changes [25].
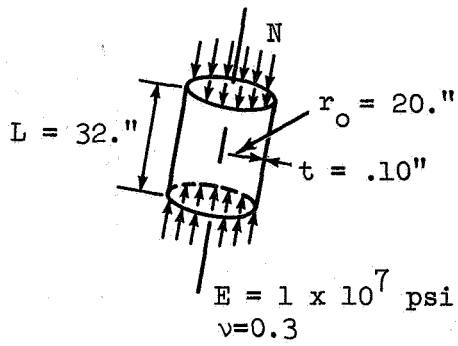
The assumed load is incremented until the determinant changes sign. The load increments may be either constant or varying. The latter may be established by extrapolation from the previous load increments.

When the prebuckled state is analyzed by the linear bending theory, only one static solution for one load is required. The prebuckling stress resultants and displacements corresponding to other values of the applied load may be established by superposition. When the prebuckled state is analyzed by the nonlinear theory, static solutions are necessary for each assumed value of the load. These solutions are established by the Newtonian method described in Chapter 2. Aside from the additional accuracy of a nonlinear prebuckling solution [29], other flexibility of analysis may be gained by including such an option. For example, while normal solution by a nonlinear prebuckling analysis does not include consideration of the local panel problem considered by Dickson and Brolliar [141], the similarity between the iterative natures of both solutions make a combination possible.

Thus, the consideration of the local panel stability problem prior to overall shell buckling, can be incorporated into the iterations needed for a nonlinear prebuckling analysis.

With the aforementioned procedure, all the possible buckling configuration may be checked. In the case of axisymmetric loading, each harmonic can be checked independently of the others. Since all harmonics $(n = 0 - \infty)$ cannot be investigated, the problem remains to insure that the lowest buckling load is associated with one of the harmonics checked. It should be indicated that an automated checking procedure may result in erroneous conclusions. Figure 22 presents the lowest buckling loads, obtained for different buckling configurations corresponding to the indicated harmonics for the classical problem of a circular cylinder subjected to end compression [142]. If an automatic procedure is programmed to establish a relative minimum within a given range of harmonics, the buckling loads corresponding to any of the harmonics $n = 2, 7, 9, 11$ could be obtained as a solution, whereas, the actual buckling load corresponds to $n = 2$. In this example, the values of the buckling loads obtained for $n = 2, 7, 9, 11$ do not differ appreciably, however, for each harmonic the buckled configurations differ considerably.

A basic difference in the stability analysis of shells subjected to axisymmetric and unsymmetric loading pertains to the type of buckling shapes that must be considered. If the nonlinear Equations (2-9) were converted to a form suitable for stability analysis, as previously discussed in this Chapter, and if only one load harmonic $(n \neq 0)$ is considered, several buckling configurations described by different families of harmonics are found as mathematically acceptable solutions. The prestressed stiffness matrices corresponding to these different buckling configurations assume the form of the

129
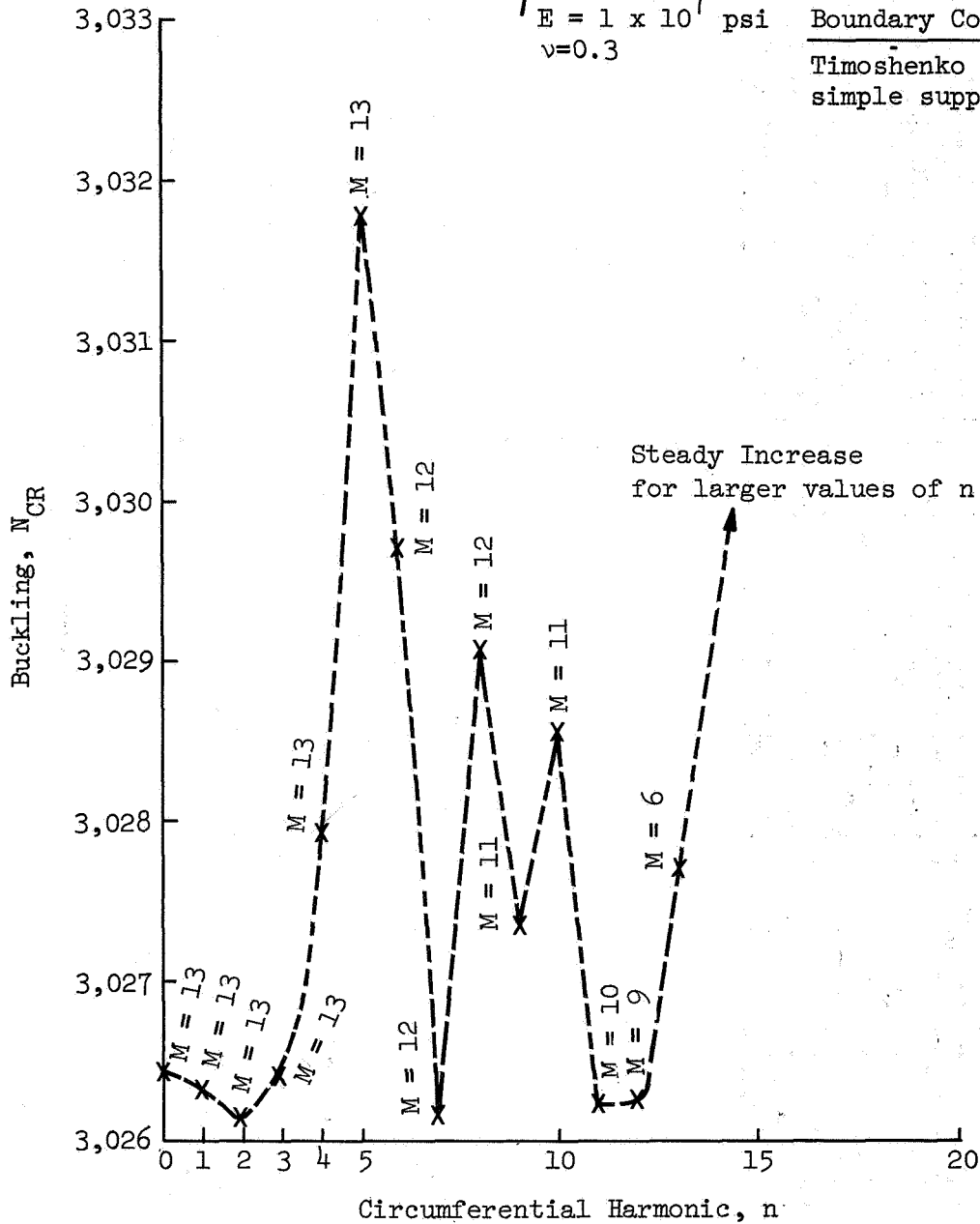
Figure 22   Sample Distribution of Harmonic Bulking Loads

130

Case I: Axisymmetric loading ($\ell = 0$) [all harmonics are uncoupled in the prestressed stiffness matrix]

Case II: Antisymmetric loading ($\ell = 0,1$) [all harmonics are coupled in the prestressed stiffness matrix]

Case III: Unsymmetric loading ($\ell = 0,2$) [Prestressed stiffness matrix reduces to two uncoupled families of harmonics]

Case IV: Unsymmetric loading ($\ell = 0,3$) [Prestressed stiffness matrix reduces to two uncoupled families of harmonics]

Case V: Unsymmetric loading ($\ell = 0,4$) [Prestressed stiffness matrix reduces to three uncoupled families of harmonics]

Figure 23a Forms of the Prestressed Stiffness Matrices Corresponding to Single Unsymmetric Harmonic Loads

131

Figure 23b Forms of the Prestressed Stiffness Matrix Corresponding to Three Harmonic (0,2,4) Loading.

132

trident matrices, shown in Fig. 23a, b. Figure 23 shows how these pre-stressed stiffness matrices corresponding to different harmonic loadings uncouple into families of harmonics. Each family of harmonics represents a different estimate of the buckling load (see Fig. 21, points A, B, C, D···), each associated with a different buckling configuration. If one of these configurations is a close approximation to the actual buckling configuration, then the buckling load corresponding to this configuration will be lower than all the other estimates (points B, C, D··· in Fig. 21) obtained on the basis of the linear prebuckling analysis. Furthermore, this estimate may be lower than the buckling load obtained on the basis of a nonlinear prebuckling analysis (point A', Fig. 21) retaining the same $\underline{number}$ of terms in the Fourier series.

In Reference 118 a stability analysis of a shell of revolution subjected to some types of unsymmetric loading is presented. However, in this reference several nonlinear terms usually included [20, 24, 28, 32, 117] in shell buckling analyses have been omitted. Also, only the family of harmonics which are multiples of the load is assumed to represent the configuration corresponding to the lowest buckling load. This assumption is based on the conclusion (invoking St. Venant's principle [118, p. 77]) that the effect of load harmonics with $\ell \geq 2$ disappear at a small distance (within a diameter of the latitude circle) away from the loaded edge. This conclusion, however, is not always valid. Transverse loads, such as $J_{\varphi}^{*(2)}$, have a short decay length; however, the decay lengths of the in-plane loads such as $N_{\varphi}^{(2)}$ or $T_{\varphi\theta}^{(2)}$ may be many times larger than the diameter of the latitude circle, even for shells with ring reinforcement [111, 143]. In certain cases, the assumptions of Reference 118 may lead to contradictory conclusions. For instance, consider a shell which buckles in the n = 10 harmonic configuration when subjected to axisymmetric load. If an $\ell = 3$

harmonic load is added to this shell, the assumptions of Reference 118 lead to two possible conclusions. If it is assumed that the additional load ($l = 3$ harmonic) represents only an edge effect, then the buckling configuration will be similar to that ($n = 10$) established when the shell was subjected to axisymmetric loading. Thus, the best estimate for the buckling load may correspond to a buckling configuration associated with the family of harmonics which contains $n = 10$ (see Figure 23a, b, Case IV). On the other hand, if the buckled configuration corresponding to the lowest load is obtained from the family of harmonics which are multiples of the loads, then the buckled configuration corresponding to the lowest buckling load in the aforementioned example should be obtained by $n = 0, 3, 6, 9, 12, 15. \ldots$.

The added complexity of the unsymmetric stability analysis, over the axisymmetric, can be seen from the above discussion. Even though only one load harmonic (l) is applied, and the prebuckling analysis is on the basis of linear bending theory, families of harmonics must be employed to establish the estimates for the buckled configurations. Thus, larger matrices are involved, and must be treated as discussed in Chapter 3 for the nonlinear unsymmetric static analysis. If the nonlinear theory is employed in the prebuckling analysis, all harmonics must be used to describe the buckled configuration.

The number of terms to be retained in the truncated Fourier series expansions of the shell functions requires further investigation in both cases of stability analysis of shells subjected to unsymmetric loading, and cases of

unsymmetric nonlinear stress analysis using the Newtonian iteration techniques [20, 22]. It may be possible to obtain accurate estimates of the buckling configuration by retaining only the $n = 0$ harmonic and a few more judiciously chosen harmonics from a family of harmonics, not necessarily in a consecutive order. If this were the case, it would be even more preferable to employ the eigenvalue approach rather than the Newtonian iteration procedure. In this case, a few terms from the dominant harmonic family would yield more satisfactory results than the same number of harmonic terms in the Newtonian iteration solution, since more significant terms would be contained in the eigenvalue solution. For instance, some shells such as relatively shallow ellipsoidal heads subjected to internal pressure, buckle in a relatively high harmonic pattern ($n \sim 50$). If the ellipsoid is subjected to an unsymmetric load, in addition to internal pressure, the question arises as to whether the buckled configuration can be approximated by some lower harmonics and some in the proximity of $n = 50$, omitting the intermediate members of the harmonic families, or all the harmonics up to $n = 50$ must be retained for a satisfactory approximation of the buckled configuration.

It should also be noted, that the high local wrinkling associated with high harmonics, may require the inclusion of shear deformation in the theory employed [113].

In conclusion, it may be stated that the determinant evaluation method, generally, has two basic disadvantages. Firstly, very extensive computer time is required for establishing the buckling load of shells of complex geometry. This is primarily due to the fact that if the magnitude of the buckling load cannot be estimated apriori, many load increments may have to be considered before the value of the load causing the determinant of the prestressed stiffness matrix to vanish is established. The second problem is even more complex, since it is possible that the low buckling loads are close together [145] even for buckling configurations described by a single harmonic. Thus, a load increment may skip two close roots without causing the sign of the determinant to change. To circumvent the foregoing disadvantages, other stability analysis techniques have been developed.

Eigenvalue Methods: When a problem involving the stability analysis of any structure is analyzed by finite element methods, it may be reduced to a linear eigenvalue problem of the form

$$([A] + \lambda[B])\{\Delta\} = 0 \tag{4-11}$$

where [A] is the stiffness matrix of the elements and [B] is the incremental stiffness matrix. Each of these matrices is formed separately by assuming a displacement function for the element. In finite difference or numerical integration techniques, however, a linear eigenvalue formulation is not readily deduced. The first eigenvalue-type analysis employing numerical integration techniques, was formulated by Cohen for natural vibrations of

shells [113], and subsequently for stability analysis of shells subjected to axisymmetric loads [117]. A similar method was later utilized in Reference 31 for finite differences. The method is iterative, based on the Stodola technique [114], and is essentially the inverse power method [115]. Basically, the homogeneous equations resulting from stability (vibrations) analysis are converted into a series of nonhomogeneous equations by assuming a buckled (vibration) shape and, thus, creating nonhomogeneous terms. The solution of this problem provides a more satisfactory estimate for the buckled configuration which, in turn, is employed to establish a new set of non-homogeneous terms. The procedure is repeated until the lowest eigenvalue (buckling load or frequency) is obtained for the harmonic configuration under consideration.

This method requires less computer time than the determinant evaluation method, and moreover, the possibility of skipping roots is eliminated. However, it has some disadvantages. In vibration problems, wherein it is necessary to compute higher frequencies, in order to establish the higher roots, all the lower roots must be swept out [114]. It has also been found, that the time required to establish two consecutive roots is a function of the ratio of the value of the lower root to the higher root. That is, the time is larger when this ratio approaches unity. Thus, in order to decrease the time required for establishing the second root, the origin should be shifted to the first root [116]. In stability problems, where only the lowest buckling load for a particular circumferential configuration is of interest, the aforementioned drawbacks of the inverse power method of solution do not exist. However, for a shell of complex geometry, convergence may be slow depending upon the initial choice of the eigenvectors (u, v, w) [114, 140].

In a recent investigation [138], the finite difference technique is applied to the shell energy integral, rather than the differential equations of equilibrium and separate stiffness and incremental stiffness matrices are formed. However, the inverse power method is still employed to solve the resulting linear eigenvalue problem.

To overcome the foregoing difficulties, a different formulation of the stability problem has been presented in Reference 157. The basic pre-stressed stiffness matrix, $[\widehat{K_p}]_F$ of the structure, is an unknown transcendental function of the prestress state variables. In vibration analysis, Przemieniecki[146] shows that the dynamic stiffness matrix is actually an infinite power series on the frequency. This finding may be extended to stability analysis. Thus, we obtain

$$[\widehat{K_p}]_F = [\widehat{K}]_F + \lambda[\widehat{K_I}]_F + \lambda^2[\widehat{K_{II}}]_F + \lambda^3[\widehat{K_{III}}]_F + \cdots \qquad (4\text{-}12)$$

where λ is the buckling load. In Reference 146, it is shown that the ratio of consecutive matrices $[\widehat{K_i}]_F / [\widehat{K_{i+1}}]_F$ is of the order of Young's Modulus of the structure. In formulating the stability problem by finite element methods (see Equation (4-11)), the matrix $[A]$ is an approximation to $[\widehat{K}]_F$, whereas the matrix $[B]$ is an approximation to $[\widehat{K_I}]_F$, to the order of accuracy of the assumed deflection functions for the element. In the numerical integration technique $[\widehat{K}]_F$ and $[\widehat{K_p}]_F$ can be formed exactly using the exact differential equations. However, it is impractical to form the other matrices. Inasmuchas the relative magnitudes of these matrices are known, the following solution technqiue has been proposed [157]. Using Equation (4-12), the stability Equation (4-9) can be cast into the following form:

$$\{[\widehat{K}]_F + \lambda[\widehat{K_I}]_F + \lambda^2[\widehat{K_{II}}]_F + \lambda^3[\widehat{K_{III}}]_F + \cdots\}[\Delta]_F = 0 \qquad (4\text{-}13a)$$

This equation may be rewritten in the following iterative form

$$\{[\widehat{K}]_F + \frac{\lambda_i}{\lambda_{i-1}} (\lambda_{i-1}[\widehat{K_I}]_F + \lambda_{i-1}^2[\widehat{K_{II}}]_F + \cdots)\} [\Delta]_F = 0 \qquad (4\text{-}13b)$$

or

$$\{[\widehat{K}]_F + \frac{\lambda_i}{\lambda_{i-1}} ([\widehat{K_p(\lambda_{i-1})}]_F - [\widehat{K}]_F)\} [\Delta]_F = 0 \qquad (4\text{-}14)$$

where λ_{i-1} is the buckling load estimated in the (i - 1)st trial.

The iteration Equation (4-14) is utilized as follows. As in the determinant evaluation method, the prebuckling analysis for the establishment of the prebuckling terms in Equations (4-6) or (4-8) is performed for a chosen value of the load on the basis of either linear or nonlinear bending theory. As in the determinant evaluation technique, the reduced prestressed stiffness matrix of the structure $[\widehat{K_p(\lambda_{i-1})}]_F$ is formed, where in this notation, λ_{i-1} signifies the chosen value of the load. The structure stiffness matrix, $[\widehat{K}]_F$ (without the prestress terms), is also formed, for the buckling configuration under consideration. The subtraction of these two matrices, as in Equation (4-14), isolates that part of the prestressed stiffness matrix which is dependent upon the buckling load. A linear eigenvalue (Equation (4-14)) problem is then formed, and solved for the new value of the load, λ_i. The iteration sequence converges when $\lambda_i = \lambda_{i-1}$ or λ_i/λ_{i-1} approaches unity to a desired degree of accuracy. Although this must be accomplished for each root desired, satisfactory approximations to higher roots are also available when λ_i/λ_{i-1} reaches unity for one root. This is due to the fact that the numerical integration technique does not lead to large matrix equations and, thus, there is computer storage available for an eigenvalue solution algorithm which provides all the roots of Equation (4-14). In this case, the convenient in-core algorithm used is the Householder [115]

method. Cohen [117] has shown that the numerical integration formulation of the stability problem produces real roots. This indicates that the matrices in the linear eigenvalue problem will both be symmetric, and one will be positive definite. Thus, the applicability of the Householder technique is assured [115].

The specialization required for the consideration of unsymmetric loading as opposed to axisymmetric loading, and nonlinear prebuckling analysis as opposed to linear prebuckling analysis, is applicable to this method as well as to the determinant evaluation procedure discussed previously. In this case, it should be noted that the stiffness matrix $[\widehat{K}]_F$ will not involve coupling of the harmonics, regardless if the load is symmetric or not. The $[\widehat{K}_p]_F$ matrix, however, will be coupled as described previously.

An iteration equation analogous to Equation (4-14) has been presented by Bushnell [138] for establishing the critical load at buckling of shells of revolution, using a nonlinear prebuckling state and finite differences. This Equation of Reference 138 may be obtained by rewriting equation (4-13b) as,

$$\{[\widehat{K_p(\lambda_{i-1})}]_F + \lambda_i([\widehat{K_p(\lambda_{i-1})}]_F - [\widehat{K}]_F)\}[\Delta]_F = 0 \qquad . \qquad (4\text{-}15)$$

In this case, for convergence $\lambda_i \to 0$. It should be noted, that in the formulation herein presented, iteration is necessary regardless of whether the prebuckling analysis is linear or nonlinear. This is due to the fact that the prestressed stiffness matrix is defined by Equation (4-12), whereas, in Reference 138 for the case of a linear prebuckling analysis, Equations (4-15) reduce to Equations (4-11), since the prestressed stiffness matrix is

approximated as being linear in the eigenvalue. Either of Equations (4-14)

or (4-15) can be employed to obtain a solution to the stability problem, after

few iteration cycles. Examples using Equations (4-14) will be presented in

Chapter 6.

Many stability problems have a double-loading system. For example,

if a tank with an insulating wall is manufactured at room temperature and

then partly filled with a cryogen, the tank is subjected to a state of stress.

If this tank is then accelerated, it is subjected to mechanical loads which

may cause buckling. The effect of the thermal prestress can easily be

considered in the analysis, by including it in the $[\widehat{K}]_F$ and $[\overline{K_p(\lambda_{i-1})}]_F$ ma-

trices of Equations (4-14). This will necessitate the solution of two static

prestress problems, one with the thermal loads and the other with com-

bined thermal and mechanical loading. Therefore, even for a linear pre-

buckling analysis, for shells subjected to unsymmetric load, the harmonics

will couple in the matrix $[\widehat{K}]_F$ as adjusted for the thermal effect.

CHAPTER 5

NATURAL VIBRATIONS

In this chapter, the free vibrations of shells of revolutions from a stress-free or a prestressed state are analyzed. The results of this analysis may be applied to establish the dynamic response of shells of revolution subjected to a harmonic exiting force or to any transient loading if the modal approach is to be employed.

<u>Dynamic Equilibrium:</u> The nonlinear equations of motion of shells of revolution may be obtained from the equilibrium Equations (1-20) by including the effects of meridional, circumferential, normal, and rotatory inertia. Thus, we obtain

$$r_1 N_{\theta,\theta} + \frac{1}{r_o}(N_{\varphi\theta}r_o^2)_{,\varphi} - Q_\theta r_1 \sin\varphi = -r_1 r_o(f_\theta^* + f_\theta) + r_1 r_o(a_0\ddot{u} - a_1\ddot{w}_\varphi)$$

$$(N_{\varphi}r_o)_{,\varphi} + r_1 N_{\varphi\theta,\theta} - N_\theta r_1 \cos\varphi - r_o Q_\varphi = -r_1 r_o(f_\varphi^* + f_\varphi) + r_1 r_o(a_0\ddot{v} + a_1\ddot{w}_\theta)$$

$$(Q_\varphi r_o)_{,\varphi} + r_1 Q_{\theta,\theta} + r_o N_\varphi + N_\theta r_1 \sin\varphi = -r_1 r_o(f_\zeta^* + f_\zeta) + r_1 r_o a_0\ddot{w} \qquad (5\text{-}1)$$

$$-r_1 M_{\varphi\theta,\theta} - (M_\varphi r_o)_{,\varphi} + M_\theta r_1 \cos\varphi + r_1 r_o Q_\varphi = -r_1 r_o m_\theta + r_1 r_o(a_1\ddot{v} + a_2\ddot{w}_\theta)$$

$$-(M_{\varphi\theta}r_o)_{,\varphi} - r_1 M_{\theta,\theta} - M_{\varphi\theta}r_1 \cos\varphi + r_1 r_o Q_\theta = -r_1 r_o m_\varphi + r_1 r_o(a_1\ddot{u} - a_2\ddot{w}_\varphi)$$

where the ($\dot{}$) signifies differentiation with respect to time; the load $f_i (i = \theta,\varphi, \zeta)$ and nonlinear terms $f_i^* (i = \theta,\varphi, \zeta)$ are defined in Equations (1-21) and (1-22) respectively, and

$$a_j = \int_h \rho \zeta^{(j)} d\zeta \qquad (5\text{-}2)$$

$\rho(\zeta)$ being the mass density. It is recognized, that generally, if the effect of rotatory inertia is significant, the effect of shear deformation is not

negligible. However, in this analysis, as in References 113 and 118, the effect of shear deformation will be neglected. In reinforced shells, the combined rotatory inertia of the skin and reinforcements may influence the results even when the effect of shear deformation is negligible. For monocoque or sandwich shells, $a_1 = 0$ since in these shells, ζ is measured from the centroid of their cross-sections. For reinforced or laminated shells, the a_j will all be different from zero.

Utilizing Equations (5-1) and following a procedure analogous to that presented in Chapter 1, a set of equations analogous to Equations (1-27) but including the inertia effects may be obtained. If a reinforced or a laminated shell is to be analyzed, Equations (1-31) or (1-32) may be employed without any modification. As in Chapter 4, in the case of stability of shells, the typical shell function denoted by Y will be considered as the sum of its values Y_P, in the prestressed equilibrium state and its change due to the vibrations, $Y_V e^{i\omega t}$. Thus, we have

$$Y = Y_P + Y_V e^{i\omega t} \tag{5-3}$$

where $i = \sqrt{-1}$ and ω is the circular frequency of vibration.

We shall postulate that the rotations due to the vibrations are small as compared to unity, and consequently, we shall disregard the terms involving products of these rotations with the stress resultant amplitudes due to the vibrations. Thus, following a procedure analogous to that described in Chapter 4, we obtain:

$$\frac{T_{\varphi\theta,\varphi}}{r_1} = -2T_{\varphi\theta}\frac{\cos\varphi}{r_o} - \frac{N_{\theta,\theta}}{r_o} + M_{\theta,\theta}\frac{\sin\varphi}{r_o^2} - M_{\varphi\theta}\frac{\cos\varphi}{r_o}\left[\frac{1}{r_1} - \frac{\sin\varphi}{r_o}\right] - \frac{\sin\varphi}{r_o}$$

$$\cdot \{N_{\theta P}\omega_\varphi + N_\theta\omega_{\varphi P} - N_{\varphi\theta P}\omega_\theta - N_{\varphi\theta}\omega_{\theta P}\} - \omega^2(a_0 u - a_1\omega_\varphi) - f_{\theta V} - \frac{\sin\varphi}{r_o}$$

$$\cdot \omega^2(a_1 u - a_2\omega_\varphi)$$

143

$$\frac{N_{\varphi,\varphi}}{r_1} = -N_\varphi \frac{\cos\varphi}{r_o} + N_\theta \frac{\cos\varphi}{r_o} - \frac{T_{\varphi\theta,\theta}}{r_o} - M_{\varphi\theta,\theta}\left[\frac{\sin\varphi}{r_o^2} + \frac{1}{r_o r_1}\right] + \frac{J_\varphi^*}{r_1} - \omega^2(a_0 v + a_1 \omega_\theta)$$

$$- f_\varphi v$$

$$\frac{J_{\varphi,\varphi}^*}{r_1} = -J_\varphi^* \frac{\cos\varphi}{r_o} - N_\theta \frac{\sin\varphi}{r_o} - \frac{N_\varphi}{r_1} - \frac{M_{\theta,\theta\theta}}{r_o^2} - 2M_{\varphi\theta,\theta}\frac{\cos\varphi}{r_o^2} - \frac{1}{r_o}\{N_{\varphi\theta}P\omega_\theta + N_{\varphi\theta}\omega_\theta P$$

$$- N_\theta P\omega_\varphi - N_\theta \omega_\varphi P\}_{,\theta} - \omega^2 a_0 w - f_\zeta v + \frac{\omega^2}{r_o}(a_1 u - a_2 \omega_\varphi)_{,\theta}$$

$$\frac{M_{\varphi,\varphi}}{r_1} = M_\theta \frac{\cos\varphi}{r_o} - M_\varphi \frac{\cos\varphi}{r_o} - 2\frac{M_{\varphi\theta,\theta}}{r_o} + J_\varphi + \omega^2(a_1 v + a_2 \omega_\theta)$$

$$\frac{u_{,\varphi}}{r_1} = u\frac{\cos\varphi}{r_o} - \frac{v_{,\theta}}{r_o} + \frac{T_{\varphi\theta}}{K_{33}} + \frac{M_{\varphi\theta}\sin\varphi}{r_o K_{33}} + \omega_\theta P\omega_\varphi + \omega_\theta \omega_\varphi P$$

$$\frac{v_{,\varphi}}{r_1} = \frac{w}{r_1} + (K_{22} - \nu_{\theta\varphi}^2 K_{11})^{-1}\{N_\varphi - \nu_{\theta\varphi}N_\theta\} - \omega_\theta P\omega_\theta \qquad (5\text{-}4)$$

$$\frac{w_{,\varphi}}{r_1} = \omega_\theta - \frac{v}{r_1}$$

$$\frac{\omega_{\theta,\varphi}}{r_1} = (D_{22} - \nu_{\theta\varphi}^2 D_{11})^{-1}\{-M_\varphi + \nu_{\theta\varphi}M_\theta\}$$

$$N_\theta = \nu_{\varphi\theta}N_\varphi + (K_{11} - \nu_{\varphi\theta}^2 K_{22})\left[\frac{u_{,\theta} + v\cos\varphi - w\sin\varphi}{r_o} + \omega_\varphi P\omega_\varphi\right]$$

$$M_\theta = \nu_{\varphi\theta}M_\varphi - \frac{(D_{11} - \nu_{\varphi\theta}^2 D_{22})}{r_o}\left[\frac{w_{,\theta\theta} + u_{,\theta}\sin\varphi}{r_o} + \omega_\theta \cos\varphi\right]$$

$$M_{\varphi\theta} = \left[\frac{-1}{\dfrac{r_o}{D_{33}} + \dfrac{\sin^2\varphi}{r_o K_{33}}}\right]\left\{2\omega_{\theta,\theta} + u\left(\frac{\cos\varphi}{r_1} - \frac{\cos\varphi\sin\varphi}{r_o}\right) - v_{,\theta}\left(\frac{\sin\varphi}{r_o} + \frac{1}{r_1}\right) - 2w_{,\theta}\frac{\cos\varphi}{r_o}\right.$$

$$\left. + \frac{T_{\varphi\theta}}{K_{33}}\sin\varphi + \omega_\theta P\omega_\varphi \sin\varphi + \omega_\theta \omega_\varphi P \sin\varphi\right\}$$

$$J_\varphi = J_\varphi^* + N_{\varphi\theta P}\omega_\varphi + N_{\varphi\theta}\omega_{\varphi P} - N_{\varphi P}\omega_\theta - N_\varphi\omega_{\theta P}$$

$$N_{\varphi\theta} = T_{\varphi\theta} + \frac{M_{\varphi\theta}}{r_o}\sin\varphi$$

$$\omega_\varphi = -\frac{w_{,\theta}}{r_o} - \frac{u\sin\varphi}{r_o}$$

where

$$f_{\theta V} = F_\theta(\epsilon_{\theta_o} + \epsilon_{\varphi_o}) + F_\varphi\frac{u_{,\varphi}}{r_1} + F_\zeta\omega_\theta$$

$$f_{\varphi V} = F_\varphi(\epsilon_{\theta_o} + \epsilon_{\varphi_o}) + F_\theta\frac{v_{,\theta}}{r_o} - F_\zeta\omega_\theta \qquad\qquad (5\text{-}5)$$

$$f_{\zeta V} = F_\zeta(\epsilon_{\theta_o} + \epsilon_{\varphi_o}) - F_\theta\omega_\varphi + F_\varphi\omega_\theta \qquad .$$

These equations can be integrated numerically to establish the frequencies and mode shapes of free vibration of shells of revolution subjected to axisymmetric or unsymmetric prestress. The numerical integration method has been employed only in establishing the frequencies of non-prestressed shells of revolution [112, 113]. A finite difference solution for axisymmetric states of prestress has been presented in Reference 24.

In the analysis of a reinforced or laminated shell, Equations (4-4) or (4-5) may be employed without any modification.

In the above equations, the term $e^{i\omega t}$ has been factored out. Thus, the solution of these equations will yield the amplitudes of stress resultants and displacements. It should be noted, that in Equations (5-4, 5) the terms involving products of rotations due to the prestress and stress resultant amplitudes due to vibration are retained. It is realized, however, that the rotations due to the prestress are small as compared to unity, and consequently their products with the stress resultant amplitudes due to vibration

may be negligible as compared to the stress resultants.

Vibration Under Prestress: For axisymmetric prestress, the pre-stress terms are of the zeroth harmonic, while the vibrations may involve any single harmonic of the Fourier components. For non-axisymmetric pre-stress, the prestress harmonics will couple with the vibration state harmonics in a fashion analogous to that discussed in Chapter 4 for buckling of shells subjected to non-axisymmetric loads. Inasmuch as the formulation of the problem of stability and the problem of vibration under prestress is similar, the analysis of the special cases of prestress presented in Chapter 4 is valid for the analysis of vibrations under prestress. Hence, Equations (4-6) may be employed for problems involving vibration under axisymmetric pre-stress, whereas, Equations (4-8) may be employed for problems associated with vibrations under non-axisymmetric prestress. These equations must be modified, firstly, by adding to the terms f_{iB} ($i = \theta, \varphi, \zeta$) the effects of in-ertia. Thus

$$f_{\theta V}^{(n)} = f_{\theta B}^{(n)} + \omega^2 (a_0 U^{(n)} - a_1 \Omega_\varphi^{(n)} + \frac{\sin\varphi}{r_0} [a_1 U^{(n)} - a_2 \Omega_\varphi^{(n)}])$$

$$f_{\varphi V}^{(n)} = f_{\varphi B}^{(n)} + \omega^2 (a_0 V^{(n)} + a_1 \Omega_\theta^{(n)}) \tag{5-6}$$

$$f_{\zeta V}^{(n)} = f_{\zeta B}^{(n)} + \omega^2 (a_0 W^{(n)} - \frac{1}{r_0} [na_1 U^{(n)} - na_2 \Omega_\varphi^{(n)}]) \quad .$$

Secondly, by adding the following term to Equation (4-6d) for vibrations under axisymmetric prestress and to Equation (4-8d) for vibrations under non-axisymmetric prestress

$$+\omega^2 (a_1 V^{(n)} + a_2 \Omega_\theta^{(n)}) \quad . \tag{5-7}$$

The variables with a subscript B are defined in Equations (4-7) for vibrations under axisymmetric prestress and are obtained from Equations (2-9) for vibrations under unsymmetric prestress.

If a reinforced or a laminated shell is to be analyzed, Equations (4-4) or (4-5) may still be utilized without any modification.

For free vibrations of non-prestressed shells all the terms with a subscript P, as well as the prestress loads F_i ($i = \theta, \varphi, \zeta$) vanish.

Numerical Solutions: The same two methods used for solving stability problems will be used in solving vibration problems. Thus in the sequel only a brief discussion of the application of these two methods will be presented.

Determinant Evaluation Method: In problems of vibration about a prestressed state, the necessary prestress terms must first be determined. This is done by means of the static analysis outlined in Chapter 3, using either linear or nonlinear theory. A value of the frequency is then assumed, and the vibration Equations (5-4,5) are utilized to form a stiffness matrix as in Chapter 4. In the case of vibrations this "dynamic stiffness matrix" [146] is a function of frequency. The natural frequencies are established as the frequencies which render the determinant of the dynamic stiffness matrix for the structure equal to zero. The techniques of finding these frequencies are the same as for finding the critical loads at buckling.

Linear Eigenvalue Methods: The two techniques discussed in Chapter 4 for stability are both applicable to the vibration problem. The equations, corresponding to Equations (4-14), suitable for analyzing vibrations under prestress can be formulated in the following manner. The prestress stiffness matrix, $[\widehat{K}_P]_F$, of the structure, is formed from the static solution for the shell subjected to the given prestress. The dynamic stiffness matrix, $[\widehat{K}_D]_F$,

of the structure, is formulated by assuming a value for the frequency and using the dynamic Equations (5-4, 5). Thus, following the stability formulation as discussed in Chapter 4, we may write

$$\{[\widehat{K_p}]_F + \frac{\omega_i^2}{\omega_{i-1}^2}([\widehat{K_D(\omega_{i-1}^2)}]_F - [\widehat{K_p}]_F)\}[\Delta]_F = 0 \qquad . \qquad (5\text{-}8)$$

These equations may be solved by the eigenvalue solution technique and the iteration procedure discussed in Chapter 4. It has been shown [113] that the numerical integration method for solving the vibration problems of shells of revolution yields real, positive frequencies. This indicates that in Equation (5-8) both matrices will be symmetric and positive definite. Thus, the applicability of the Householder technique is assured [115].

It should be noted that Equation (5-8) could be reformulated as follows,

$$\{[\widehat{K_D(\omega_{i-1}^2)}]_F + \omega_i^2([\widehat{K_D(\omega_{i-1}^2)}]_F - [\widehat{K_p}]_F)\}[\Delta]_F = 0 \quad . \qquad (5\text{-}9)$$

In this case, convergence is indicated as $\omega_i^2 \to 0$ while in Equation (5-8) convergence is indicated as $\omega_i^2/\omega_{i-1}^2 \to 1$.

The advantages of using the Householder technique and of using the formulations (5-8, 9) over the determinant method were noted in Chapter 4. Of specific importance in dynamics of shells is the ability to quickly estimate many frequencies while having completed an iteration solution for only one.

For problems of free vibrations of unprestressed shells of revolution the static stiffness matrix is used in place of the prestressed stiffness matrix of the structure. All other operations remain the same.

Critical Speeds of Rotating Shells: The matrix equations for shell

dynamics, referred to a coordinate system which rotates with the shell about

its axis of revolution with constant velocity, Ω, may be cast in the form

$$[\hat{M}]_F \{\ddot{\Delta}'\}_F + 2\Omega [\hat{D}]_F \{\dot{\Delta}'\}_F + ([\hat{K}_P]_F - \Omega^2 [\widehat{K_{PD}(\Omega^2)}]_F) \{\Delta'\}_F = \{0\} \quad (5\text{-}10)$$

where $\{\Delta'\}_F$ and $[\hat{K}_P]_F$ have been defined previously as the incremental displace-

ment vector, and the fixed preload stiffness matrix respectively, and where

$[\hat{K}_{PD}]_F$ is the variable load prestress stiffness matrix $\underline{including}$ the rotating

inertia terms of the incremental state. The additional matrices, $[\hat{M}]_F$ and

$[\hat{D}]_F$ contain the nonrotating inertia and the Coriolis dynamic effects,

respectively. The dynamic stability of a rotating shell may be investigated by

substituting

$$\{\Delta'\}_F = \{\Delta\}_F \; e^{i\omega t} \quad (5\text{-}11)$$

into Equation (5-10) to obtain

$$-\omega^2 [\hat{M}]_F \{\Delta\}_F + 2i\omega\,\Omega\,[\hat{D}]_F \{\Delta\}_F + ([\hat{K}_P]_F - \Omega^2 [\widehat{K_{PD}(\Omega^2)}]_F) \{\Delta\}_F = \{0\} \quad (5\text{-}12)$$

In the presently programmed version of the STARS vibrations program (STARS-2V),

Equation (5-12) is not solved in complete form but rather for special cases.

For the vibration case discussed previously in this chapter, $\Omega = 0$, and Equation

(5-12) will reduce to Equation (5-8). The code words FREV and VPRE will then

define the shell as being either stress-free or axisymmetrically prestressed.

For the case of critical speed analysis, $\omega = 0$, and Equation (5-12)

reduces to

$$([\hat{K}_P]_F - \Omega^2 [\widehat{K_{PD}(\Omega^2)}]_F) \{\Delta\}_F = \{0\} \quad (5\text{-}13)$$

In this case the matrix $[\hat{K}_{PD}]_F$ contains the effects of the centrifugal accelerations on both the prestressed and incremental deformation states of the shell. The code words CRSP and PCRS again are used to define the shell as being initially stress-free or axisymmetrically prestressed (static load).

At the request of NASA [166] a third option is also available wherein $\omega = f\Omega$. In this case the Coriolis effects are neglected and the Equation (5-12) reduces to

$$-f^2\Omega^2 [\hat{M}]_F \{\Delta\}_F + ([\hat{K}_P]_F - \Omega^2 [\hat{K}_{PD}(\Omega^2)]_F) \{\Delta\}_F = \{0\} \qquad (5\text{-}14)$$

The neglect of the Coriolis terms is not a serious violation and is consistent with the fact that torsional prestress in not allowed in the present programs. In addition, the effect of the Coriolis terms has been found to decrease for higher rotational speeds [167] such as those of interest for the present analysis. The above option may be utilized to approximate cases in the analysis of rotating shells wherein some additional dynamic load of unknown description is causing a "mass perturbation" upon the shell. This perturbation is described proportionally through the multiplier upon the critical speed, f, and is applied in whatever harmonic is being investigated for critical speeds. Again the code words CRSR and PCSR differentiate only between the non-existence or existence of static preload.

CHAPTER 6

NUMERICAL EXAMPLES

In this chapter, solutions using the programs herein documented will be compared to solutions utilizing other numerical methods. Comparisons of solutions for linear static problems involving axisymmetric and unsymmetric loading, as well as nonlinear, axisymmetric problems, are availabe in the literature [99, 102] and will not be presented herein.

The first set of problems to be investigated are static stability problems which will be analyzed by employing the solution technique presented in Chapter 4. This technique was first applied to problems involving cylinders. It was established that the technique produced accurate and rapid results using coarse structural idealizations [157]. Difficulty was not encountered in predicting load reversals, or obtaining higher eigenvectors, or eigenvectors which contained many waves within a segment. Thus, it is apparent that it is the number of integration points in a numerical integration method that is significant, rather than the number of segments. However, compared to finite element or finite difference methods, the segmentation utilized in the numerical integration method permits the use of much smaller matrices in the eigenvalue problem.

Numerical Examples - Problem 1: The first test problem involved the short cylinder shown in Figure 24, subjected to an axial compressive end-load. The problem was chosen using the sizing parameters of Reference 142 to insure a critical mode shape in which the cross section remains circular (n=0), and there is only one half-wave along the length of the cylinder (m=1). The

N_{cr}

20 in. R

t = 1.0 in.
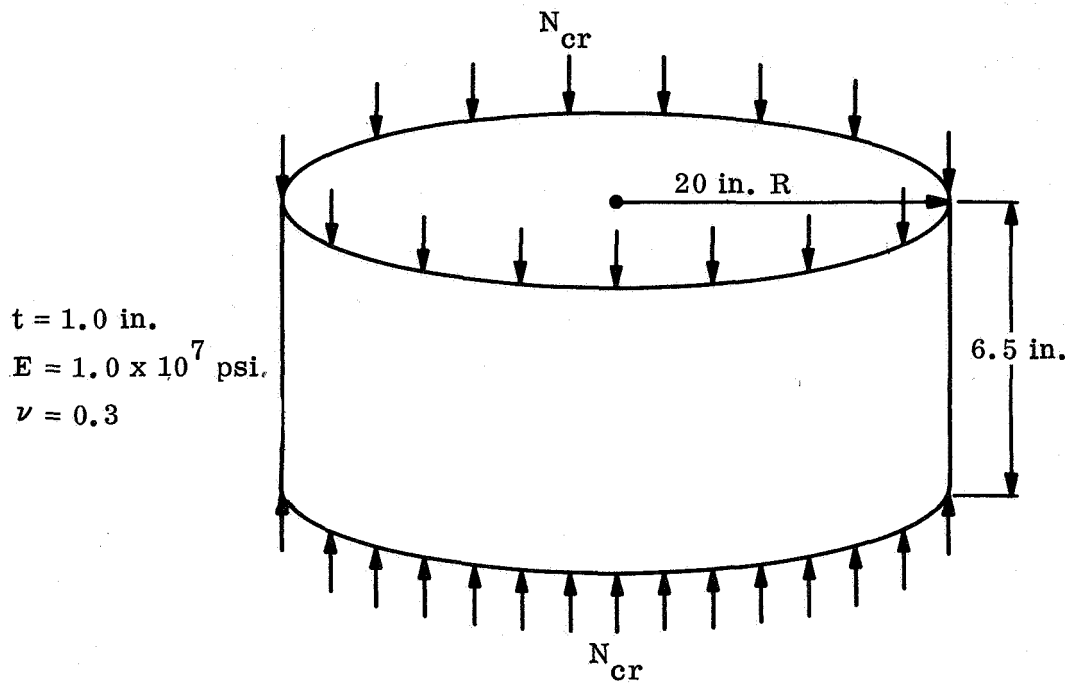E = 1.0 x 10^7 psi.
ν = 0.3

6.5 in.

N_{cr}

Figure 24   Short End-Loaded Cylinder

152

boundary conditions used were classical simple supports, i.e., radial deformation was unrestrained until the point of incipient buckling. Tables 1 through 3 show different aspects of the results.

The first table demonstrates the accuracy of the results and the speed of convergence. As can be seen, only two iterations are necessary for the prediction of the first root. The second table demonstrates the speed of convergence to higher eigenvalues due to the additional information obtained in the current method. For a first trial load value, approximations to higher eigenvalues are available as well as to the lowest. As can be seen from the table when the first eigenvalue is obtained, a good approximation is available for the second eigenvalue and it can be obtained with only one additional iteration. Although this capability may not be overly important in stability analysis, it is very useful in free vibration analysis. The third table demonstrates the various capabilities of the current method with a coarse grid. As can be seen, no difficulty was encountered in obtaining eigenvalues corresponding to eigenvectors with many waves within a segment. Only two iterations were used to obtain each value in Table 3, and therefore the values should not be considered as fully converged. The first entry in the table was used to test the sensitivity of the method to negative eigenvalues.

The last entry in Table 3 shows that an eigenvector with 15 half-waves in one segment was calculated correctly. The segment, of course, represents 8 degrees of freedom in the stiffness matrix. To calculate such an eigenvector correctly would require up to 4 nodes per half-wave in a finite element idealization. Thus the equivalent degree of freedom requirement would be of the order of 4x15x4+4 = 244 d.o.f. Even in numerical integration the number of integration points must be kept to a reasonable limit for time considerations.

Table 1: Buckling of Short Axially Loaded Cylinder

Timoshenko (Ref. 142)	Current Method (n=0)			
	2 Segments		4 Segments	
	Trial Load	Result	Trial Load	Result
	1×10^4	32.45×10^4	1×10^4	32.14×10^4
32.07×10^4	32×10^4	32.09×10^4	32×10^4	32.09×10^4

Table 2: Short Cylinder Buckling Load Convergence

Timoshenko (Ref.142)	Current Method (n=0) 4 Segments						Cumulative No. of Iterations
	1st Root		2nd Root		3rd Root		
	Trial	Result	Trial	Result	Trial	Result	
	$1x10^4$	$32.14x10^4$	$1x10^4$	$88.92x10^4$	$1x10^4$	$200.18x10^4$	1
$32.07x10^4$	$32x10^4$	$\underline{32.09x10^4}$	$32x10^4$	$88.68x10^4$	$32x10^4$	$199.22x10^4$	2
$88.12x10^4$			$88x10^4$	$\underline{88.2x10^4}$	$88x10^4$	$194.12x10^4$	3
$193.43x10^4$					$194x10^4$	$\underline{193.6x10^4}$	4

Table 3: Short Cylinder, High Buckling Loads

Timoshenko (Ref. 142)	Current Method (n=0) 2 Segments	
	Prediction	% Difference
$\lambda_1 = 32.07 \times 10^4$	32.09×10^4 *	.06
$\lambda_6 = 769.26 \times 10^4$	771.0×10^4	.23
$\lambda_7 = 1046.86 \times 10^4$	1050.1×10^4	.31
$\lambda_8 = 1367.21 \times 10^4$	1370.45×10^4	.24
$\lambda_9 = 1730.29 \times 10^4$	1750.8×10^4	1.2
$\lambda_{15} = 4806 \times 10^4$	5010×10^4	4.2
$\lambda_{18} = 6920 \times 10^4$	7321×10^4	5.8
$\lambda_{20} = 8544 \times 10^4$	8680×10^4	1.6
$\lambda_{25} = 13,350 \times 10^4$	$14,410 \times 10^4$	7.9
$\lambda_{28} = 16,746 \times 10^4$	$17,212 \times 10^4$	2.8
$\lambda_{30} = 19,224 \times 10^4$	$19,080 \times 10^4$	.75

* Starting trial value was set at 1×10^4 tension.

From the few test problems for this purpose it was noted that about 10 integration points is a conservatively sufficient number to accurately describe one half-wave in a prospective eigenvector.

Numerical Examples - Problem 2:   The second test problem involved a large, ring-stringer eccentrically reinforced cylinder (see Figure 25).   The loading was a fixed internal stabilizing pressure of 31 psi., in combination with a variable end load.   Classical simple support boundary conditions were again utilized to enable comparison with References 141 and 150.   The idealization used consisted of 20 segments for the whole structure, and 4 segments for the panel.   Comparisons with analytical results for the overall and panel buckling modes are presented in Tables 4, 5 and 6. 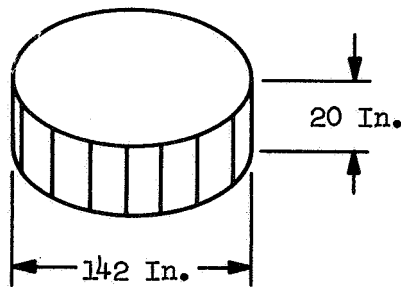 The overall critical mode was found to be n=0, m=13.   Table 4 shows the analytical results for the n=0 calculations, and it can be seen that for this problem also, the convergence characteristics are excellent.   By the fourth pass, the change from anticipated to corrected value of the critical load is only .00017%.   A comparison of the STARS-2B answers from the converged (fourth) pass, for estimates of some of the higher loads, shows an average difference of .57% (with a maximum of 2.0%) for the first 11 roots, and an average difference of 2.72% (with a maximum of 10%) for the first 18 roots, when compared to NASA TND 2960 (Ref. 150).   Thus, when the first root is converged, excellent estimates are available for a large number of the higher roots.   Similar results were obtained for the panel modes as shown in Table 5.   In this case convergence is obtained in two passes, although this is not verified until the third pass.   The answers from References 141 and 150 and the current work, should be close, but do not have to agree exactly, due to certain theoretical differences in the formulations.   Reference 150 uses Donrell shell theory, while the current effort utilizes a Love-Reissner-

156

0.11 In.　　　1.33 In.

0.087 In.　　2.65 In.

0.09 In.

External Rings

Rings and stringers are "smeared out".

7.44 In.

20 In.

160 In.

142 In.

0.1 In.

1 In.

External Stringers

a. Overall Shell

20 In.
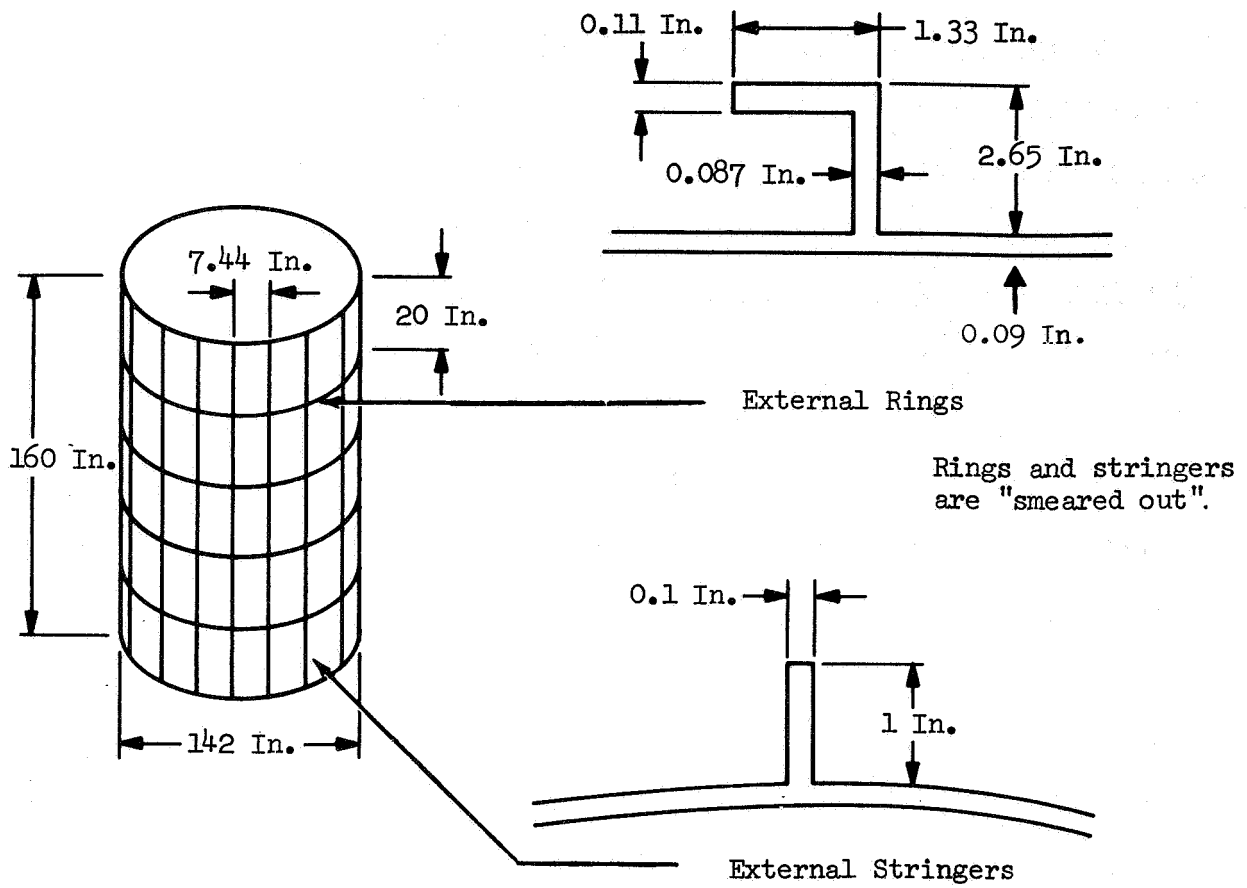
Ends are simply supported.
Stringers are "smeared out."

142 In.

b. Panel Shell

Notes:

Loading
    1) Compressive end load: N
    2) Internal stabilizing pressure: 31 psi
Boundary Conditions
    1) Ends are simply supported

Table 4: Overall Buckling of Reinforced Cylinder

Root No.	m	NASA TND 2960	NASA CR 1280	Current Method (20 segments)			
				$\text{Trial}_1(1\text{x}10^3)$	$\text{Trial}_2(6017.0)$	$\text{Trial}_3(5841.0)$	$\text{Trial}_4(5848.0)$
1=crit.	13	5848.15	5842.9	6017.77	5840.9	5848.3	5848.01
2	14	5877.97	5872.2	6073.60	5871.1	5879.6	5879.22
3	12	5974.05	5968.4	6126.76	5972.4	5978.8	5978.56
4	15	6032.72	6025.6	6264.54	6033.4	6043.1	6042.75
5	16	6290.95	6281.6	6445.00	6308.4	6315.4	6315.67
6	11	6301.05	6293.9	6569.61	6310.3	6319.6	6319.13
7	17	6637.3	6624.8	6971.53	6683.3	6695.9	6695.42
8	10	6898.31	6888.4	7040.98	6923.9	6928.9	6928.68
9	18	7060.56	7044.1	7448.06	7148.8	7162.6	7162.07
10	19	7552.39	7530.9	7940.50	7691.5	7704.7	7704.21
11	9	7875.44	7861.1	8023.79	7923.9	7928.1	7927.93
12	20	8106.50	8078.8	9574.56	8639.5	8683.2	8681.50
13	21	8718.03		9821.53	9180.8	9214.4	9213.05
14	22	9383.22		10196.41	9492.9	9496.4	9496.24
15	8	9414.65	9393.2	11002.30	10005.7	10039.9	10038.53
16	23	10099.1		12008.57	10949.3	10986.6	10985.08
17	24	10863.3		12010.31	11950.2	11952.7	11952.57
18	25	11674.00		13167.73	12009.9	12051.4	12049.73

n=0 = number of circumferential waves

m = number of longitudinal half-waves

Results are single precision IBM 360/75

Table 5: Panel Buckling of Reinforced Cylinder

Root No.	m	NASA TND 2960	NASA CR 1280	Current Method (4 segments)		
				Trial$_1$(1x10^3)	Trial$_2$(5480.0)	Trial$_3$(5471.0)
1=critical	1	5493.93	5449.6	5480.7	5470.3	5470.3
2	2	6204.83	6182.9	6325.5	6280.9	6281.0
3	3	10965.00	10881.3	11314.4	11168.0	11168.4
4	4	18626.90	18372.1	22557.5	21631.9	21633.7

n=10 = number of circumferential waves

m = number of longitudinal half-waves

Results are single precision IBM 360/75

Table 6: Buckling of Reinforced Cylinder, Reduction Scheme

Current Method (Guyan reduction 20 segments ⟶ 4 regions)				
Root No.	m	Trial$_4$(5848.0) no reduction	Trial$_4$(5848.0) reduction	% difference
1	13	5848.01	5848.01	0.0
2	14	5879.22	5957.65	1.3
3	12	5978.56	6280.32	5.0
4	15	6042.75	6546.69	8.3
5	16	6315.67	7065.60	11.9
6	11	6319.13	7302.11	15.5
7	17	6695.42	7925.64	18.4
8	10	6928.68	8130.09	17.3

Kempner accuracy shell theory. Reference 141 on the other hand, while utilizing basic Love-Reissner theory, does not simplify some Flügge accuracy terms such as $(1 \pm \zeta/R)$ when applying compatibility between rings or stringers, and the base shell. In addition, out-of-plane bending and twisting terms of the stiffeners are included therein.

It should be noted that this problem contains closely spaced eigenvalues (see Table 4). In the search of harmonics n = 1 and n = 2 the eigenvalues were even more closely spaced. The current method encountered no difficulties in any of these cases.

The overall shell buckling problem was also run using the matrix reduction scheme currently in the STARS -2B, -2V programs. The results are shown in Table 6. As can be seen, reducing the 20 segments to 4 regions does not affect the lowest root predictions, but does decrease the accuracy of the estimates for the higher roots. Thus, a consistent Guyan scheme can be used to analyze problems where idealizations demand a large number of segments. It is recognized that this scheme is basically for the reduction of static stiffness matrices, and other reduction schemes (for modal-eigenvalue problems) should be studied. However, the results of the current test problem serve to show the applicability of even the simpler reduction scheme within the accuracy of the STARS framework.

It is interesting to qualitatively compare the above convergence characteristics with those of BOSOR3 for a similar, stiffened cylinder problem (Ref. 138). In the STARS-2B stiffened cylinder problem, the analysis was started with an overall buckling load estimate of 17.1% of the converged critical load, and in four iterations the successive guesses were within .00017% of each other. In the STARS-2B panel problem, the corresponding numbers were

160

18.28%, and in three iterations, results were within .0128% of each other. In a similar stiffened cylinder problem solved with BOSOR3, using 91 finite difference stations, and starting with a buckling load estimate of 99.5% of the converged critical load, there is no convergence in single precision on the Univac 1108 computer. Use of double precision produced convergence, and after five iterations the successive guesses are within .00383% of each other. It must also be noted in the comparison that the STARS-2B technique also provided excellent estimates to a large number of higher roots, while BOSOR3 found only the single lowest critical value. The difference in accuracy and speed of convergence, as well as the results provided (single or many roots) by each of the methods, is due to two factors. The major difference in the quality of the results is the fact that the matrices generated by the current numerical integration procedure are more accurate than those obtained by either finite differences or the finite element method. The number of roots immediately available is simply the result of using different numerical eigenvalue solution schemes.

Numerical Examples - Problem 3: As shown in Figure 26, the third stability problem studied in the present investigation is the PS-9 prolate spheroid, tested experimentally at the David Taylor Model Basin [153] . For this shell, a variety of theoretical results are available, and are tabulated in Fig. 26. The solution of Mushtari and Galimov [154] is based on the assumption that many lobes develop in both the circumferential and meridional directions. As apparent from the experimental results (n = 3), this is evidently not the case for this shell. The error in the theoretical predictions of Reference 153 is probably due to the assumption that the buckling deformation is confined to a narrow equatorial band of the shell.
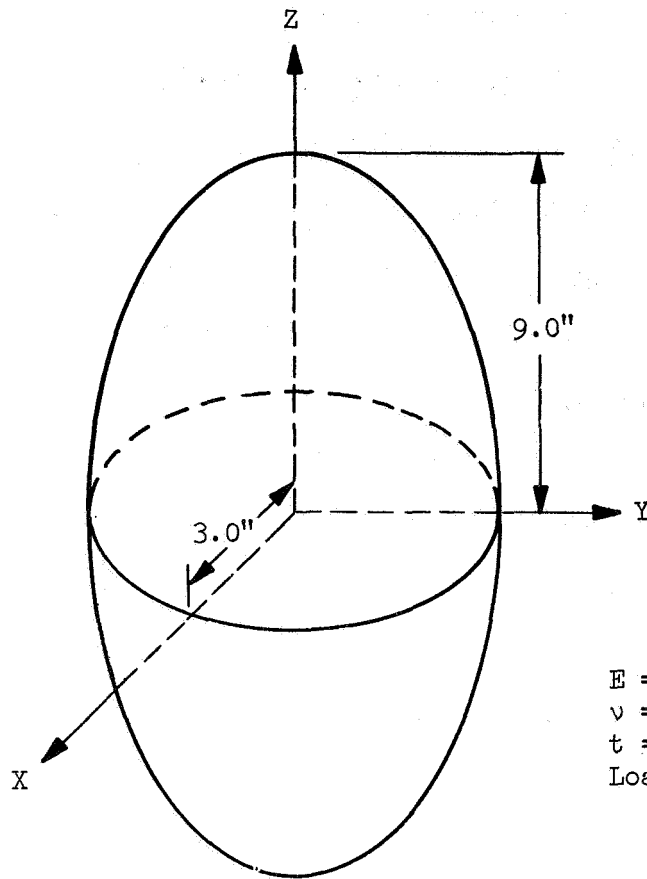
$$E = 3.25 \times 10^5 \text{ psi.}$$
$$\nu = .4$$
$$t = .189"$$
Load = uniform external pressure

	n = 2	n = 3	n = 4
Present Investigation	210.6	157.1*, 138.39†, 139.89‡, 139.1**, 135.1***	173.8
DTMB Experimental Results (Ref. 153)	—	137	—
DTMB Theory (Ref. 153)	> 197	197	197
Cohen [117]	208.8	(139.3) 138.7	174.0
Kalnins [118]	—	139.23	—
Mushtari & Galimov [154]		95.5 psi (no harmonic prediction)	

*   only membrane prestress terms included

†   membrane prestress and live pressure field terms included

‡   predeformation neglected

**   all consistent nonlinear terms retained

***   all consistent nonlinear terms retained (prestress matrices calculated with double precision arithmetic)

Figure 26   Hydrostatically Loaded Prolate Spheroid

162

In the present investigation, the effects upon the critical buckling load of various nonlinear terms in the Equations (4-6, 7) were studied. The first number in Fig. 26 (*) is the buckling load based on the assumption that only the membrane prestress terms ($N_{\theta P}$, $N_{\varphi P}$) are significant. The second value (+) is the buckling load based on the inclusion of the pressure rotation terms ($f_{\theta B}$, $f_{\varphi B}$, $f_{\zeta B}$ in Eq. (4-3)) but with the assumption that $\epsilon_{\theta_o}^{(n)} = \epsilon_{\varphi_o}^{(n)} = 0$. The third buckling load (‡) was calculated by retaining all nonlinear terms involving pressure or prestress, and neglecting only initial deformation. The final values of the buckling load, (**) and (***), are based on retaining all terms in Equations (4-6, 7), where the (***) result also includes the effect of double precision arithmetic in the calculation of the stiffness matrices. It may be observed that the greatest effect is obtained from the inclusion of the pressure rotation terms, and that the other effects are negligible by comparison. This is not surprising in the present problem since all the load is in the form of pressure, and predeformation (rotation) is expected to be minimal.

The buckling loads predicted in this investigation and those of Cohen [117] and Kalnins [118] are based on numerical integration. They are in excellent agreement with the experimental results. It is therefore apparent, inasmuchas the classical buckling load is obtained by experiment, that this prolate spheroid is not imperfection sensitive. It was expected that the predicted buckling loads will not be identical due to different assumptions in the theoretical formulations. Cohen uses Novozhilov [71] shell theory. Notice, that the number in parentheses given in Fig. 26, is obtained by the use of a nonlinear prebuckling state. In the present investigation and that of Kalnins [118] the Love-Reissner [16] shell theory is employed. However, Kalnins neglected some nonlinear terms, whereas in this investigation all consistent

163

terms [100, 137] are retained.

Numerical Examples - Problem 4: The last test problem involves the study of the effects of axisymmetric prestress upon the vibration characteristis of the spherical cap shown in Figure 27. The present analysis is compared to other available results in Figure 28. As can be seen, the present STARS-2V results agree well with the Ebner [169] calculations using the VALORS [28] program, except for the n = 0 harmonic where a substantial disagreement is found. Although Ebner claims qualitative agreement with Reference 170 wherein results are available for the free vibration of spherical caps with R/h = 100 and an 18° half opening angle, the following comparisons show otherwise:

	Ebner	STARS-2V	Ref. 170	Harmonic
$\omega/\Omega_0 =$	1.4984	1.2135	1.2649	0
$\omega/\Omega_0 =$	1.1730	1.15775	1.1907	1
$\omega/\Omega_0 =$	1.3425	1.3325	1.4398	2
$\omega/\Omega_0 =$	1.6522	1.6359	1.8166	3
$\omega/\Omega_0 =$	2.0629	2.0342	-	4

As can be seen above, Ebner's zeroth harmonic frequency is greater than that of Ref. 170, whereas the frequencies for all the other harmonics are smaller. Similarly Ebner's ω_0 is greater than ω_2. Neither of the above two items are consistent with the present analysis or Ref. 170. A further analysis with the Cohen program [166] has confirmed the STARS-2V results tabulated above.

The discrepancy in the Ebner calculations may possibly be explained by erroneous boundary conditions at the apex. Setting all displacements equal to zero as well as the meridional rotation is satisfactory only for n ≥ 2, at the apex. With this boundary condition utilized for n = 0, the STARS-2V program

yields a value of $(\omega/\Omega_o)^2 = 2.29136$. Thus for this problem the apex boundary condition has a substantial effect upon the frequency results. A similar error was found in the Kalnins [118] buckling analysis of problem 3. However, the effect for the buckling load in that problem proved negligible (see previous discussion and Fig. 26).
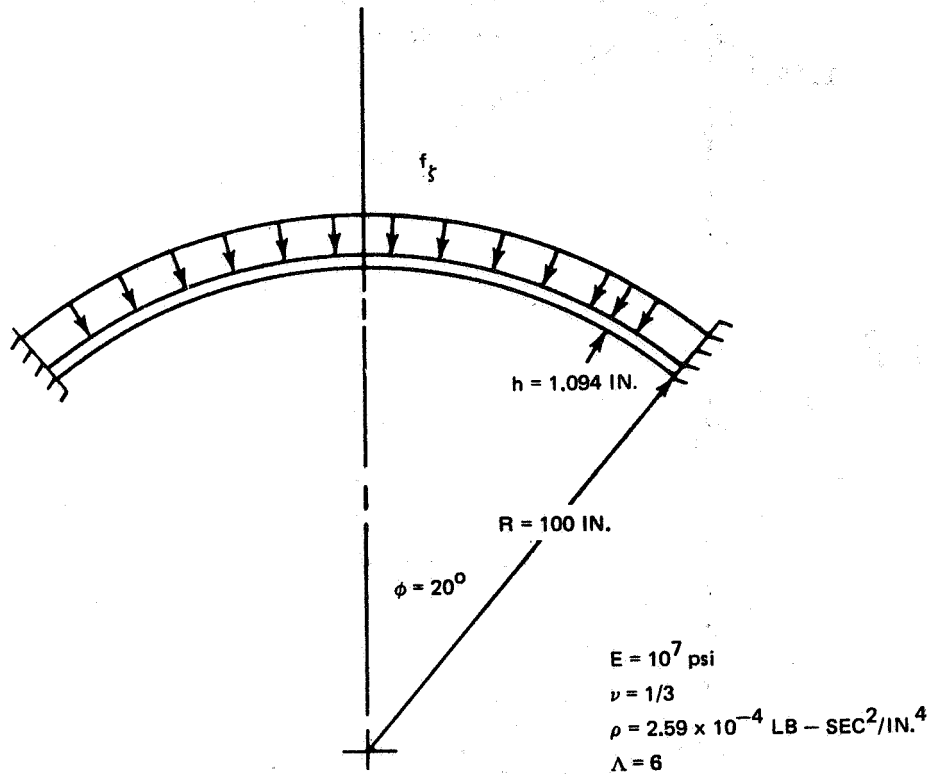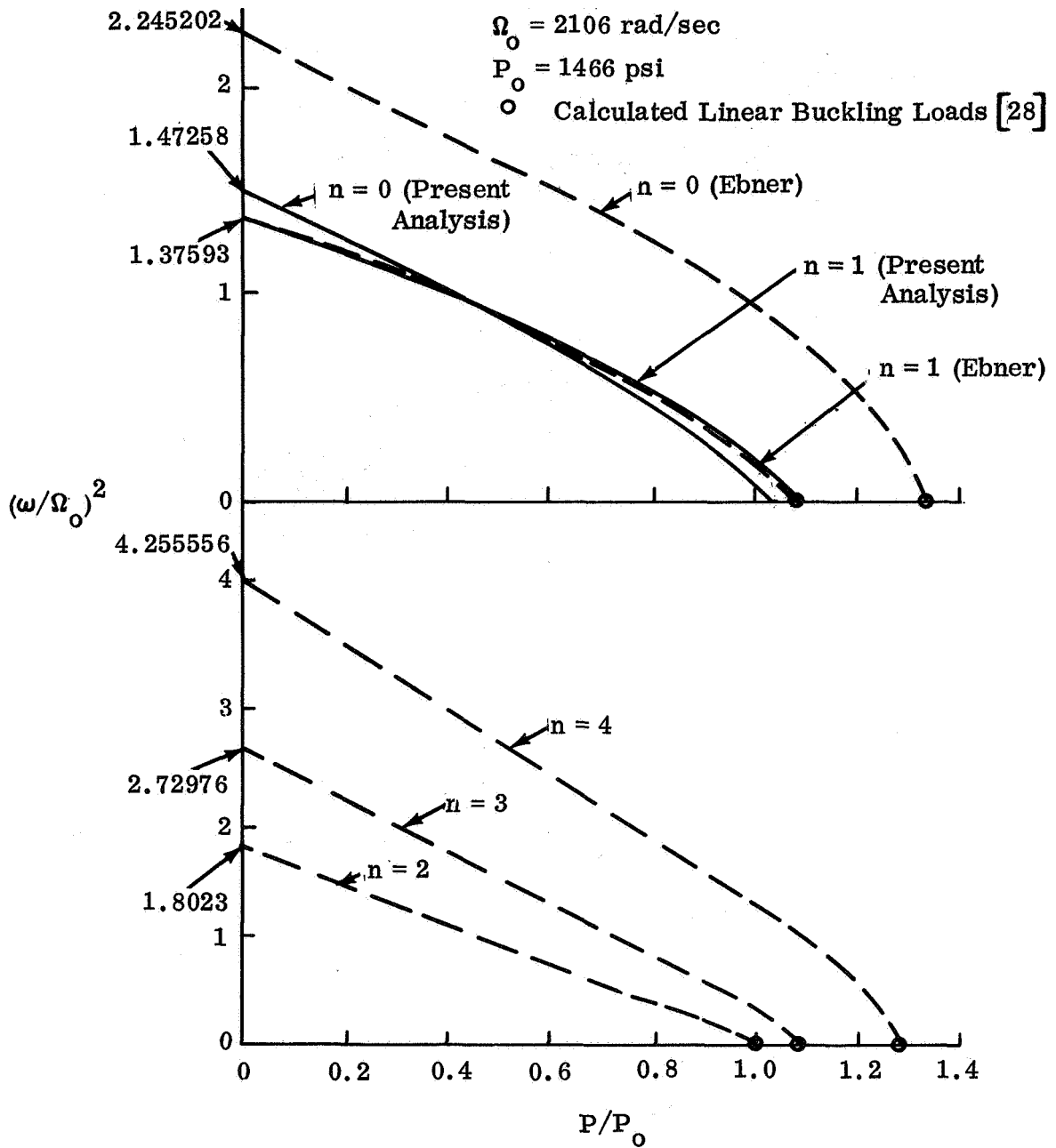
Fig. 27 Shallow Spherical Cap

Fig. 28 Variation of Natural Frequencies of Spherical Cap
with Nonlinear Prestress

REFERENCES

1. Radkowski, P., Davis, R., and Bolduc, M., "Numerical Analysis of Equations of Thin Shells of Revolution", American Rocket Society Journal, Vol. 32, 1962, pp. 36-41.

2. Radkowski, P., "Stress Analysis of Orthotropic Thin Multilayer Shells of Revolution", paper no. 2889-63, AIAA Launch and Space Vehicle Shell Structure Conference, April 1963.

3. Reissner, E., "On the Theory of Thin Elastic Shells", Reissner Anniversary Volume, J.W. Edwards Co., Ann Arbor, Mich., 1949, p. 232.

4. Potters, M., "A Matrix Method for the Solution of a Second Order Difference Equation in Two Variables", Mathematisch Centrum, Amsterdam, Holland, Report MR 19, 1955.

5. Sepetoski, W., Pearson, C., Dingwell, I., and Adkins, A., "A Digital Computer Program for the Generally Axially Symmetric Thin-Shell Problem", ASME Journal of Applied Mechanics, December, 1962, pp. 655-661.

6. Budiansky, B., and Radkowski, P., "Numerical Analysis of Unsymmetrical Bending of Shells of Revolution", AIAA Journal, Vol. 1, No. 8, August 1963, pp. 1833-1842.

7. Sanders, J.L., Jr., "An Improved First-Approximation Theory for Thin Shells", NASA Report 24, June 1959.

8. Greenbaum, G., "Comment on 'Numerical Analysis of Unsymmetrical Bending of Shells of Revolution' ", AIAA Journal, Vol. 2, No. 3, March 1964, pp. 590-592.

9. Cappelli, A., Nishimoto, T., and Radkowski, P., "The Analysis of Shells of Revolution Having Arbitrary Stiffness Distribution", Proceedings of the AIAA/ASME 8th Structures, Structural Dynamics and Materials Conference, March 1967, pp. 732-749.

10. Hubka, R., "A Generalized Finite-Difference Solution of Axisymmetric Elastic Stress States in Thin Shells of Revolution", Air Force Report AFBMD-TN-61-43, June 1961.

11. Giammo, T., "Generalized Finite Difference Shell Analysis-IBM 7090 Computer Program Vol. I", Space Technology Lab. Report 9852.31-6, January 1963.

12. Greenbaum, G., "Mark II Shell Program Instruction Report", Space Technology Lab. Report 4152-6016-KU000, August 1964.

13. Osborne, E., "Direct Solution of Linear Algebraic Equations Involving an Almost Band Matrix of Large Order," Space Technology Lab. Numerical Note NN-158, May 1961.

14. Wilson, P., and Spier, E., "Numerical Analysis of Small Finite Axisymmetric Deformation of Thin Shells of Revolution", General Dynamics/Astronautics Report ERR-AN-153, June 1962.

15. Wilson, P., and Spier, E., "Numerical Analysis of Large Axisymmetric Deformations of Thin Spherical Shells", AIAA Journal, Vol. 3, No. 9, December 1965, pp. 1716-1725.

16. Reissner, E., "On Axisymmetrical Deformations of Thin Shells of Revolution", Proceedings of the Symposium of Applied Math.,Vol. 3, 1949, pp. 27-52.

17. Thurston, G., "A Numerical Solution of the Non-Linear Equations for Axisymmetric Bending of Shallow Spherical Shells", ASME Journal of Applied Mechanics, Vol. 28, 1961, pp. 557-568.

18. Thurston, G., "Newton's Method Applied to Problems in Nonlinear Mechanics", ASME Journal of Applied Mechanics, June 1965, pp. 383-388.

19. Bushnell, D. "Nonlinear Analysis of Shells of Revolution", AIAA paper No. 66-529, AIAA 4th Aerospace Sciences Meeting, June 1966.

20. Ball, R., "A Geometrically Nonlinear Analysis of Arbitrarily Loaded Shells of Revolution", NASA CR-909, January 1968.

21. Schaeffer, H., and Ball, R., "Nonlinear Deflections of Asymmetrically Loaded Shells of Revolution", AIAA paper No. 68-292, AIAA/ASME 9th Structures, Structural Dynamics and Materials Conference, April 1968.

22. Greenbaum, G., and Conroy, D., "Post-Wrinkling Analysis of Highly Pressurized Cylindrical and Conical Shells of Revolution Subjected to Bending Loads-Vol. I-Theory and Computer Program Description", TRW Report 07823-6011-R000, October 1967.

23. Rosanoff, R., and Ginsburg, T., "Matrix Error Analysis for Engineers", Proceedings of the Matrix Methods in Structural Mechanics Conference, AFFDL-TR-66-80, November 1966, pp. 887-910.

24. Cooper, P., "Vibration and Buckling of Prestressed Shells of Revolution", NASA TN D-3831, March 1967.

25. Blum, R., and Fulton, R., "A Modification of Potters' Method for Solving Eigenvalue Problems Involving Tridiagonal Matrices", AIAA Journal, Vol. 4, No. 12, December 1966, pp. 2231-2232.

26. Rossettos, J., and Tene, Y., "Analysis of Prestressed Layered Shells with Applications to Buckling", AIAA Journal, Vol. 5, No. 9, September 1967, pp. 1720-1722.

27. Tene, Y., "Deformation of Asymmetrically Loaded, Symmetrically Prestressed Orthotropic Shells of Revolution", AIAA Journal, Vol. 6, No. 8, August 1968, pp. 1599-1602.

28. Heard, W., and Fulton, R., An Undocumented Series of Computer Codes known as SALOR, BALOR and VALOR developed at NASA, Langley Research Center, Virginia.

29. Bushnell, D., "Symmetric and Nonsymmetric Buckling of Finitely Deformed Eccentrically Stiffened Shells of Revolution", AIAA paper No. 67-110, AIAA 5th Aerospace Sciences Meeting, January 1967.

30. Bushnell, D., "Buckling of Spherical Shells Ring-Supported at the Edges," AIAA Journal, Vol. 5, No.11, November 1967, pp. 2041-2046.

31. Almroth, B., Bushnell, D., and Sobel, L., "Buckling of Shells of Revolution with Various Wall Constructions-Vol. 1 - Numerical Results", NASA CR-1049, May 1968.

32. Bushnell, D., Almroth, B., and Sobel, L., "Buckling of Shells of Revolution with Various Wall Constructions-Vol. 2 - Basic Equations and Method of Solution", NASA CR-1050, May 1968.

33. Bushnell, D., Almroth, B., and Sobel, L., "Buckling of Shells of Revolution with Various Wall Constructions-Vol. 3 - User's Manual for BOSOR", NASA CR-1051, May 1968.

34. Almroth, B., and Bushnell, D., "Computer Analysis of Various Shells of Revolution", AIAA Journal, Vol. 6, No. 10, October 1968, pp. 1848-1855.

35. Bushnell, D., "Buckling and Vibrations of Ring-Stiffened, Segmented Shells of Revolution, Part 2 - Numerical Results", presented at the First International Pressure Vessel Technology Conference, Delft, Holland, 1969.

36. Bushnell, D., "Computer Analysis of Complex Shell Structures", presented at the AIAA 8th Aerospace Sciences Meeting, January 1970.

37. Bushnell, D., "Analysis of Complex Shells of Revolution Under Combined Thermal and Mechanical Loading", presented at the 11th AIAA/ASME Structures, Structural Dynamics, and Materials Conference, April 1970.

38. Tsui, E., Brogan, F., and Stern, P., "Juncture Stress Fields in Multicellular Structures," Vol. 1, LMSC Report M-77-65-5, August 1965.

39. Bodewig, F., Matrix Calculus, North-Holland Publishing Co., Amsterdam, 1959.

40. Brogan, F., Forsberg, K., and Smith, S., "Experimental and Analytical Investigation of the Dynamic Behavior of a Cylinder with a Cutout", paper No. 68-318, AIAA/ASME 9th Structures, Structural Dynamics and Materials Conference, April 1968.

41. Brogan, F., and Almroth, B., "Buckling of Cylinders with Cutouts", AIAA paper No. 69-92, AIAA 7th Aerospace Sciences Meeting, January 1969.

42. Meyer, R., and Harmon, M., "Conical Segment Method for Analyzing Open Crown Shells of Revolution for Edge Loadings", AIAA Journal, Vol. 1, No. 4, April 1963, pp. 886-891.

43. Grafton, P., and Strome, D., "Analysis of Axisymmetric Shells by the Direct Stiffness Method", AIAA Journal, Vol. 1, No. 10, October 1963, pp. 2342-2347.

44. Friedrich, C., "Seal-Shell-2-A Computer Program for the Stress Analysis of a Thick Shell of Revolution with Axisymmetric Pressures, Temperatures, and Distributed Loads", AEC Research and Development Report WAPD-TM-398, December 1963.

45. Lu, Z., Penzien, J., and Popov, E., "Finite Element Solution for Thin Shells of Revolution", NASA CR-37, July 1964.

46. Percy, J., Pian, T., Klein, S., and Navaratna, D., "Application of Matrix Displacement Method to Linear Elastic Analysis of Shells of Revolution", AIAA Paper No. 65-142, AIAA 2nd Aerospace Sciences Meeting, January 1965.

47. Wilson, E., "Structural Analysis of Axisymmetric Solids", AIAA paper No. 65-143, AIAA 2nd Aerospace Sciences Meeting, January 1965.

48. Jones, R., and Strome, D., "A Survey of Analysis of Shells by the Displacement Method", AFFDL-TR-66-80, November 1966, pp. 205-229.

49. Jones, R., and Strome, D.", Direct Stiffness Method Analysis of Shells of Revolution Utilizing Curved Elements", AIAA Journal, Vol. 4, No. 9, Septermber 1966, pp. 1519-1525.

50. Stricklin, J., Navaratna, D., and Pian, T., "Improvements on the Analysis of Shells of Revolution by the Matrix Displacement Method", AIAA Journal, Vol. 4, No. 11, November 1966, pp. 2069-2071.

51. Khojasteh-Bakht, M., "Analysis of Elastic-Plastic Shells of Revolution Under Axisymmetric Loading by the Finite Element Method", University of California SESM Report 67-8, April 1967.

52. Brombolich, L., and Gould, P., "Finite Element Analysis of Shells of Revolution by Minimization of the Potential Energy Functional", Proceedings of the Symposium on Application of Finite Element Methods in Civil Engineering, November 1969, pp. 279-307.

53. Stricklin, J., Haisler, W., MacDougal, H., and Stebbins, F., "Nonlinear Analysis of Shells of Revolution by the Matrix Displacement Method", AIAA paper No. 68-177, AIAA 6th Aerospace Sciences Meeting, January 1968.

54. Stricklin, J., De Andrade, J., Stebbins, F., and Cwiertny, A., Jr., "Linear and Nonlinear Analysis of Shells of Revolution with Asymmetrical Stiffness Properties", AFFDL-TR-68-150, December 1969, pp. 1231-1251.

55. Haisler, W., and Stricklin, J., "Rigid-Body Displacements of Curved Elements in the Analysis of Shells by the Matrix-Displacement Mehthod", AIAA Journal, Vol. 5, No. 8, August 1967, pp. 1525-1527.

56. Irons, B., and Draper, K., "Inadequacy of Nodal Connections in a Stiffness Solution for Plate Bending," AIAA Journal, Vol. 3, 1965, p. 961.

57. Klein, S., and Sylvester, R., "The Linear Elastic Dynamic Analysis of Shells of Revolution by the Matrix Displacement Method", AFFDL-TR-66-80, November 1966, pp. 299-328.

58. Bacon, M., and Bert, C., "Unsymmetric Free Vibrations of Orthotropic Sandwich Shells of Revolution", AIAA Journal, Vol. 5, No. 3, March 1967, pp. 413-417.

59. Leimbach, K., Jones, C., and Whetstone, W., "Vibrational Characteristics of Orthotropic Shells of Revolution", Lockheed-Huntsville Report LMSC/HREC A791267, March 1968.

60. Adelman, H., Catherines, D., and Walton, W., Jr., "A Method for Computation of Vibration Modes and Frequencies of Orthotropic Thin Shells of Revolution having General Meridional Curvature", NASA TN D-4972, 1969.

61. Adelman, H., Catherines, D., and Walton, W., Jr., "A Geometrically Exact Finite Element for Thin Shells of Revolution", AIAA paper No. 69-56, AIAA 7th Aerospace Sciences Meeting, January 1969.

62. Abel, J., and Popov, E., "Static and Dynamic Finite Element Analysis of Sandwich Structures", AFFDL-TR-68-150, December 1969, pp. 185-212.

63. Stricklin, J., Martinez, J., Tillerson, J., Hong, J., and Haisler, W., "Nonlinear Dynamic Analysis of Shells of Revolution by Matrix Displacement Method", presented at the AIAA/ASME 11th Structures, Structural Dynamics, and Materials Conference, April 1970.

64. Navaratna, D., Pian, T., and Witmer, E., "Stability Analysis of Shells of Revolution by the Finite-Element Method", AIAA Journal, Vol. 6, No. 2, February 1968, pp. 355-361.

65. Melosh, R., "A Flat Triangular Shell Element Stiffness Matrix," AFFDL-TR-66-80, November 1966, pp. 503-514.

66. Zienkiewicz, O., Parekh, C., and King, I., "Arch Dams Analysed by a Linear, Finite Element, Shell Solution Program", University of Wales Report No. C/R/76/67, September 1967.

67. Clough, R., and Johnson, C., "A Finite Element Approximation for the Analysis of Thin Shells, "International Journal of Solids and Structures, Vol. 4, 1968, pp. 43-60.

68. Fulton, R., Eppink, R., and Walz, J., "The Accuracy of Finite Element Methods in Continuum Problems," presented at the 5th U.S. National Congress of Applied Mechanics, June 1966.

69. Walz, J., Fulton, R., and Cyrus, N., "Accuracy and Convergence of Finite Element Approximations", AFFDL-TR-68-150, December 1969, pp. 995-1029.

70. Gallagher, R., "The Development and Evaluation of Matrix Methods for Thin Shell Structural Analysis", Bell Aerosystems Report No. 8500-902011, June 1966.

71. Novozhilov, V., The Theory of Thin Shells, P. Noordhoff, Groningen, Netherlands, 1964.

72. Vlasov, V., "General Theory of Shells and its Application in Engineering", English translation by NASA, Office of Technical Services, 1964.

73. Szilard, R., and West, A., "Finite Curved Shell Elements and Consistent Mass Matrices for Static and Dynamic Analysis of Aerospace Structures", AFFDL-TR-66-194, December 1966.

74. Tsui, E., Massard, J., and Loden, W., "Element Stiffness Matrices of Thick-walled Orthotropic Shells with Applications", Proceedings of the Symposium on Applications of Finite Element Methods in Civil Engineering, November 1969, pp. 95-128.

75. Bogner, F., Fox, R., and Schmit, L., "A Cylindrical Shell Discrete Element", AIAA Journal, Vol. 5, No. 4, April 1967.

76. Schmit, L., Bogner, F., and Fox, R., "Finite Deflection Structural Analysis Using Plate and Shell Discrete Elements", AIAA Journal, Vol. 6, No. 5, May 1968.

77. Connor, J., and Brebbia, C., "Stiffness Matrix for Shallow Rectangular Shell Element", ASCE Journal of Engineering Mechanics, No. EM 2, April, 1968.

78. Brebbia, C., and Connor, J., "Geometrically Nonlinear Finite-Element Analysis", ASCE Journal of Engineering Mechanics, Vol. 95, April 1969, pp. 463-483.

79. Marguerre, K., "Zur Theorie der Gekrummenten Platte Grosser Formanderung," Proceedings of the 5th International Congress of Applied Mechanics, 1938.

80. Cantin, G., and Clough, R., "A Curved Cylindrical Shell Discrete Element ", AIAA Journal, Vol. 6, No. 5, May 1968.

81. Wempner, G., Oden, J., and Kross, D., "Finite-Element Analysis of Thin Shells, " ASCE Journal of Engineering Mechanics, No. EM 6, December 1968.

82. Ahmad, S., Irons, B., and Zienkiewicz, O., "Curved Thick Shell and Membrane Elements with Particular Reference to Axisymmetric Problems", AFFDL-TR-68-150, December 1969.

83. Key, S., and Beisinger, Z., "The Analysis of Thin Shells with Transverse Shear Strains by the Finite Element Method", AFFDL-TR-68-150, December 1969, pp. 667-710.

84. Olson, M., and Lindberg, G., "Vibration Analysis of Cantilevered Curved Plates Using a New Cylindrical Shell Finite Element", AFFDL-TR-68-150, December 1969, pp. 247-269.

173

85.   Greene, B., Jones, R., McLay, R., and Strome, D., "Dynamic Analysis of Shells Using Doubly-Curved Finite Elements", AFFDL-TR-68-150, December 1969, pp. 185-212.

86.   Gallagher, R., and Yang, T., "Elastic Instability Predictions for Doubly-Curved Shells", AFFDL-TR-68-150, December 1969, pp. 711-739.

87.   Utku, S., "Stiffness Matrices for thin Triangular Elements of Nonzero Gaussian Curvature", presented at the 4th Aerospace Sciences Meeting, June 1966.

88.   Utku, S., and Melosh, R., "Behavior of Triangular Shell Element Stiffness Matrices Associated with Polyhedral Deflection Distributions", AIAA paper No. 67-114, AIAA 5th Aerospace Sciences Meeting, January 1

89.   Prince, N., "A Curved Triangular Shell Element", Grumman Advanced Development Report No. ADR 02-11-67.2, August 1967.

90.   Svalbonas, V., "Arbitrarily Curved Triangular Shell Elements", Grumma: Advanced Development Report No. ADR 02-11-67.3, November 1967.

91.   Clough, R., and Tocher, J., "Finite Element Stiffness Matrices for Analysis of Plate Bending", AFFDL-TR-66-80, November 1966, pp. 515-5

92.   Argyris, J., and Scharpf, D., "The SHEBA Family of Shell Elements for the Matrix Displacement Method", Aeronautical Journal, October 1968, March 1969, May 1969.

93.   Dhatt, G., "Numerical Analysis of Thin Shells by Curved Triangular Elements Based on Discrete-Kirchhoff Hypothesis", Proceedings of the Symposium on Application of Finite Element Methods in Civil Engineering, November 1969.

94.   Strickland, G., and Loden, W., "A Doubly-Curved Triangular Shell Element", AFFDL-TR-68-150, December 1969, pp. 641-666.

95.   Bonnes, G., Dhatt, G., Giroux, Y., and Robichaud, L., "Curved Triangu Elements for the Analysis of Shells", AFFDL-TR-68-150, December 1969, pp. 617-639.

96.   Reissner, E., "On Some Problems in Shell Theory", Proceedings of the 1st Symposium on Naval Structural Mechanics, 1960.

97.   Cohen, G., "Computer Analysis of Asymmetrical Deformation of Orthotropic Shells of Revolution", AIAA Journal, Vol. 2, No. 5, May 1964 pp. 932-934.

98.   Kalnins, A., "Analysis of Shells of Revolution Subjected to Symmetrical and Nonsymmetrical Loads", paper No. 64-APM-33 presented at the ASME Summer Conference of the Applied Mechanics Div., June 1964.

99.   Mason, P., Rung, R., Rosenbaum, J., and Ebrus, R., "Nonlinear Numerical Analysis of Axisymmetrically Loaded Arbitrary Shells of Revolution", paper No. 64-439, presented at the AIAA Annual Meeting, June 1964.

100. Kempner, J., "Unified Thin Shell Theory," Polytechnic Institute of Brooklyn Report PIBAL No. 566, March 1960.

101. Rung, R., Mason, P., and Rosenbaum, J., "Unsymmetric Analysis of Shells of Revolution", Grumman Report No. ADR 02-11-65.3, December 1965.

102. Svalbonas, V., and Shulman, M., "User's Manual for "STARS"-Shell Theory Automated for Rotational Structures-IBM 360/75 Digital Computer Program", Grumman Report No. ADR 02-11-68.1, February 1968.

103. Svalbonas, V., "Unsymmetric Non-Linear Second Order Analysis of Orthotropic Shells of Revolution", Grumman Report No. ADR 02-11-66.1, April 1966.

104. Prince, N., Rung, R., and Svalbonas, V., "Unsymmetric Non-Linear First Order Analysis of Layered Orthotropic Shells of Revolution", Grumman Report No. ADR 02-11-66.2, May 1966.

105. Svalbonas, V., "Unsymmetric Non-Linear Analysis of Thick Orthotropic Sandwich Shells of Revolution", Grumman Report No. ADR 02-11-67.1, January 1967.

106. Kalnins, A., and Lestingi, J., "On Nonlinear Analysis of Elastic Shells of Revolution", ASME Journal of Applied Mechanics, March 1967, pp. 59-64.

107. Svalbonas, V., "Numerical Analysis of Shells, Vol. I: Unsymmetric Analysis of Orthotropic Reinforced Shells of Revolution", NASA CR 61299, September 1969.

108. Svalbonas, V., and Angrisano, N., "Numerical Analysis of Shells, Vol. II: User's Manual for STARS-II-Shell Theory Automated for Rotational Structures-II Digital Computer Program", NASA CR 61300, September 1969.

109. Angrisano, N., Hughes, F., and Svalbonas, V., "Numerical Analysis of Shells, Vol. III: Engineer's Program Manual for STARS-II-Shell Theory Automated for Rotational Structures-II, Digital Computer Program", NASA CR 61301, September 1969.

110. Angrisano, N., Hughes, F., and Svalbonas, V., (Revised by Cantrell, J., and Key, J.), "Numerical Analysis of Shells, Vol. IV: Engineer's Program Manual for STARS-II-Shell Theory Automated for Rotational Structures-II, UNIVAC 1108 Digital Computer Program", NASA MSFC Report-job 390700, May 1970.

111. Rung, R., Petricone, R., and Mahoney, J., "Submarine Structural Design System", Applied Technology Assoc. Report No. 132. R.1.70, March 1970.

112. Kalnins, A., "Free Vibration of Rotationally Symmetric Shells", Journal of the Acoustical Soc. of America, Vol. 36, No. 7, pp. 1355-1365, July 1964.

113. Cohen, G., "Computer Analysis of Asymmetric Free Vibrations of Ring-Stiffened Orthotropic Shells of Revolution", AIAA Journal, Vol. 3, No. 12, December 1965, pp. 2305-2312.

114. Hurty, W., and Rubinstein, M., Dynamics of Structures, Prentice-Hall, Inc., New Jersey, Second Printing, May 1965.

115. Wilkinson, J., The Algebraic Eigenvalue Problem, Clarendon Press, Oxford, 1965.

116. Kalnins, A., "Comments on the Analysis of Free Vibration of Rotationally Symmetric Shells", AIAA Journal, Vol. 4, No. 8, pp. 1497-1498, August 1966. Cohen, G., "Reply by Author to A. Kalnins", AIAA Journal, Vol. 4, No. 8, pp. 1498-1499, August 1966.

117. Cohen, G., "Computer Analysis of Asymmetric Buckling of Ring-Stiffened Orthotropic Shells of Revolution", AIAA paper No. 67-109, presented at the 5th Aerospace Sciences Meeting, January 1967.

118. Kalnins, A., "Static, Free Vibration, and Stability Analysis of Thin, Elastic Shells of Revolution", AFFDL-TR-68-144, March 1969.

119. Croll, J., and Scrivener, J., "Convergence of Hypar Finite-Difference Solutions", ASCE Journal of the Structural Div., Vol. 95, No. 5, pp. 809-830, May 1969.

120. Van der Neut, A., "General Instability of Orthogonally Stiffened Cylindrical Shells", NASA TN-D-1510, pp. 309-321, 1962.

121. Novozhilov, V., Foundations of the Nonlinear Theory of Elasticity, Graylock Press, New York, 1953.

122. Byrne, R., Jr., "Theory of Small Deformations of a Thin Elastic Shell", Seminar Reports in Mathematics, Univ. of Calif., Published in Math., N.S., Vol. 2, No. 1, pp. 103-152, 1944.

123. Flügge, W., Statik und Dynamik der Schalen, Edwards Brothers Inc., Ann Arbor, Mich., 1943.

124. Flügge, W., Stresses in Shells, Springer-Verlag, Berlin, second printing, 1962.

125. Luther, H., and Konen, H., "Some Fifth-Order Classical Runge-Kutta Formulas", SIAM Review, Vol. 7, No. 4, pp. 551-558, October 1965.

126. Luther, H., "Further Explicit Fifth-Order Runge-Kutta Formulas", SIAM Review, Vol. 8, No. 3, pp. 374-380, July 1966.

127. Rosser, J., "A Runge-Kutta for all Seasons", University of Wisconsin MRC Technical Summary Report No. 698, September 1966.

128. Ball, D., and Stoodley, G., "An IBM 704/7090 Program for the Numerical Solution of Ordinary Differential Equations," Grumman Report No. CR 61-2, October 1961.

129. Thurston, G., "Continuation of Newton's Method Through Bifurcation Points," ASME Journal of Applied Mechanics, pp. 425-430, September 1969.

130. Thurston, G., "A New Method for Computing Axisymmetric Buckling of Spherical Caps," paper presented at the 6th U.S. National Congress of Applied Mechanics, June 1970.

131. Haisler, W., Stricklin, J., and Stebbins, F., "Development and Evaluations of Solution Procedures for Geometrically Nonlinear Structural Analysis by the Direct Stiffness Method," AIAA paper No. 71-356, presented at the AIAA/ASME 12th Structures, Structural Dynamics and Materials Conference, April 1971.

132. Gatewood, B., and Ohanian, N., "Examples of Solution Accuracy in Certain Large Simultaneous Equation Systems," AFFDL-TR-66-80, pp. 911-924, November 1966.

133. Sokolnikoff, I., Mathematical Theory of Elasticity, McGraw-Hill Book Co., Inc., New York, Second Edition, 1956.

134. Turner, M., Clough, R., Martin, H., and Topp, L., "Stiffness and Deflection Analysis of Complex Structures," Journal of the Aeronautical Sciences, Vol. 23, No. 9, pp. 805-823, 854, September 1956.

135. Whetstone, W., "Computer Analysis of Large Linear Frames," ASCE Journal of the Structural Division, ST 11, pp. 2401-2417, November 1969.

136. Bushnell, D., "Stress, Buckling and Vibration of Prismatic Shells," paper presented at the AIAA 9th Aerospace Sciences Meeting January 1971.

137. Herrmann, G., and Armenakas, A., "Vibrations of Infinitely Long Cylindrical Shells Under Initial Stresses," AIAA Journal, January 1963, pp. 100-106.

138. Bushnell, D., "Analysis of Buckling and Vibration of Ring-Stiffened, Segmented Shells of Revolution," International Journal of Solids and Structures, Vol. 6, No. 1, pp. 157-181, January 1970.

139. Thompson, J., "Basic Principles in the General Theory of Elastic Stability," Journal of Mechanics and Physics of Solids, Vol. 11, pp. 13-20, 1963.

140. Pestel, E., and Leckie, F., Matrix Methods in Elastomechanics, McGraw-Hill Book Co., Inc., New York, 1963.

141. Dickson, J., and Brolliar, R., "The General Instability of Eccentrically Stiffened Cylindrical Shells under Axial Compression and Lateral Pressure," NASA CR-1280, January 1969.

142. Timoshenko, S., and Gere, J., _Theory of Elastic Stability_, McGraw-Hill Book Co., Inc., New York, Second Edition, 1961.

143. Svalbonas, V., and Reichel, G., "Effect of Reinforcement on the Attenuation and Diffusion Distances of Shell Edge Loads" Grumman memo STMECH 71.3, January 1971.

144. Kraus, H., _Thin Elastic Shells_, John Wiley & Sons, Inc., New York, 1967.

145. Svalbonas, V., and Reichel, G., "Density and Distribution of Buckling Loads and Modes for Cylindrical Shells," Grumman Memo STMECH 70.80, August 1970.

146. Przemieniecki, J., "Quadratic Matrix Equations for Determining Vibration Modes and Frequencies of Continuous Elastic Systems," AFFDL-TR-66-80, November 1966.

147. Kalnins, A., "Analysis of Thin Elastic Shells with Attached Systems," AIAA paper No. 67-45, presented at the 5th Aerospace Sciences Meeting, January 1967.

148. Ball, R., "A Program for the Nonlinear Static and Dynamic Analysis of Arbitrarily Loaded Shells of Revolution," presented at the Lockheed-Air Force Shell Conference, August 1970.

149. Liepins, A., "Asymmetric Nonlinear Dynamic Response and Buckling of Shallow Spherical Shells," NASA CR-1376, June 1969.

150. Block, D., Card, M., and Mikulas, M. Jr., "Buckling of Eccentrically Stiffened Orthotropic Cylinders," NASA TND-2960, August 1965.

151. Donnell, L., "Stability of Thin-Walled Tubes under Torsion," NACA TR 479, 1933.

152. Guyan, R., "Reduction of Stiffness and Mass Matrices," AIAA Journal, Vol. 3, No. 2, February 1965.

153. Hyman, B., and Healey, J., "Buckling of Prolate Spheroidal Shells under Hydrostatic Pressure," AIAA Journal, pp. 1469-1477, August 1967.

154. Mushtari, K., and Galimov, K., _Nonlinear Theory of Thin Elastic Shells_, Tatknigoizdat, Kazan 1957, Translated by the Israel Program for Scientific Translations, 1961.

155. Biezeno, C., and Grammel, R., _Engineering Dynamics_, Vol. II, Translated from German by M. Meyer, Blackie, London, 1954.

156. Shulman, M., and Svalbonas, V., "Analysis of Rings under Arbitrary Loads, Grumman Report No. ADR 02-11-67.4, December 1967.

157. Svalbonas, V., and Balderes, T., "A Procedure for Extending the STARS II Digital Computer Program to Shell Buckling Analysis," Grumman Report No. ADN 02-71.1, May 1971.

158. Kalnins, A., and Biricikoglu, V., "On the Stability Analysis of Imperfect Spherical Shells", Journal of Applied Mechanics, Transactions of the ASME, September 1970, pp. 629-634.

159. Hutchinson, J., and Koiter, W., "Post Buckling Theory", Applied Mechanics Reviews, December 1970, pp. 1353-1366.

160. Budiansky, B., and Hutchinson, J., "A Survey of Some Buckling Problems," AIAA Journal, Vol. 4, September 1966, pp. 1505-1510.

161. Kempner, J., and Chen, Y., "Post Buckling of an Axially Compressed Oval Cylindrical Shell," Proc. Twelfth Int. Congress Appl. Mech., Stanford Univ., 1968, Springer-Verlag 1969.

162. Hutchinson, J., and Amazigo, J., "Imperfection Sensitivity of Eccentrically Stiffened Cylindrical Shells," Harvard Univ. Rept. SM-10, April 1966.

163. Fitch, J., "The Buckling and Post Buckling Behavior of Spherical Caps Under Concentrated Load," Int. J. Solids Struct., Vol. 4, 1968, pp. 421-446.

164. Fitch, J., and Budiansky, B., "The Buckling and Post Buckling of Spherical Caps Under Axisymmetric Load," AIAA Journal, Vol. 8, 1970, pp. 686-692.

165. Cohen, G., "Effect of a Nonlinear Prebuckling State on the Post Buckling Behavior and Imperfection Sensitivity of Elastic Structures," AIAA Journal, Vol. 6, 1968, pp. 1616-1620.

166. Private communication.

167. Srinivasan, A., and Lauterback, G., "Traveling Waves in Rotating Cylindrical Shells", Journal of Engineering for Industry, November 1971, pp. 1229-1232.

168. Cheney, J., "Bending and Buckling of Thin-Walled Open-Section Rings", ASCE proceedings, EM5, October 1963, pp. 17-44.

169. Ebner, A., "Effects of Prestress on Vibration Behavior of Certain Shells of Revolution", AIAA Journal, Vol. 9, No. 4, April 1971, pp. 742-743.

170. Zarghamee, M., and Robinson, A., "A Numerical Method for Analysis of Free Vibration of Spherical Shells", AIAA Journal, Vol. 5, No. 7, July 1967, pp. 1256-1261.

179

RESULTANT STRESS-STRAIN RELATIONS FOR STIFFENED SHELLS

One method of obtaining the necessary relationships between stress resultants and strains for eccentrically reinforced shells is based upon an "equivalent energy" approach. The energy of the composite system in terms of stress resultants and strains is equated to the energy of an equivalent orthotropic shell.

The strain energy of a circumferential ring is given by [107]

$$U_R = \int_0^{2\pi r_o} \int_{A_R} \frac{E_R}{2} \epsilon_\theta^2 \, dA_R \, d\theta + \frac{G_R J_R}{2} \int_0^{2\pi r_o} k_{\theta\varphi}^2 \, d\theta \qquad (A-1)$$

where E_R and G_R are the modulus of elasticity and the shear modulus of the material from which the ring stiffeners are made, and J_R is the torsional constant of the ring stiffeners. We will now distribute the strain energy of each ring uniformly over one half the panel spacing on each side of the ring. If the rings are spaced a distance S_R apart, the total energy per panel length in the φ direction may be written in the form

$$U_R = \frac{1}{S_R} \int_0^{S_R} \left[\int_0^{2\pi r_o} \int_{A_R} \frac{E_R}{2} \epsilon_\theta^2 \, dA_R \, d\theta + \frac{G_R J_R}{2} \int_0^{2\pi r_o} k_{\theta\varphi}^2 \, d\theta \right] d\varphi$$

$$(A-2)$$

Assuming that the stiffeners are bonded to the shell and substituting Equation (1-13) for the total strain, ϵ_θ, we obtain

$$U_R = \frac{1}{S_R} \int_0^{S_R} \left[\int_0^{2\pi r_o} \int_{A_R} \frac{E_R}{2} \left(\epsilon_{\theta_o} - \zeta k_\theta \right)^2 \, dA_R \, d\theta + \frac{G_R J_R}{2} \int_0^{2\pi r_o} k_{\theta\varphi}^2 \, d\theta \right] d\varphi$$

180

This may be rewritten as

$$U_R = \frac{1}{S_R} \int_0^{S_R} \int_0^{2\pi r_o} \left(\frac{E_R A_R}{2} \epsilon_{\theta_o}^2 - E_R C_R A_R \epsilon_{\theta_o} k_\theta + \frac{E_R}{2} I_R k_\theta^2 + \frac{G_R J_R}{2} k_{\theta\varphi}^2 \right) d\theta \, d\varphi$$

(A-3)

where

$$\int_{A_R} dA_R = A_R \qquad \int_{A_R} \zeta \, dA_R = C_R A_R \qquad \int_{A_R} \zeta^2 dA_R = I_R$$

Similarly, the distributed strain energy per panel length in the θ direction of n meridional stiffeners spaced a distance S_S apart $(n S_S = 2\pi r_o)$ is given by

$$U_S = \frac{1}{S_S} \int_0^{S_R} \int_0^{2\pi r_o} \left(\frac{E_S A_S}{2} \epsilon_{\varphi_o}^2 - E_S C_S A_S \epsilon_{\varphi_o} k_\varphi + \frac{E_S}{2} I_S k_\varphi^2 + \frac{G_S J_S}{2} k_{\varphi\theta}^2 \right) d\theta \, d\varphi$$

(A-4)

The strain energy of the unstiffened shell along a panel length is

$$U = \frac{1}{2} \int_0^{2\pi r_o} \int_0^{S_R} \int_{\substack{\text{thickness} \\ \text{of shell}}} \left\{ \sigma_\theta (\epsilon_{\theta_o} - \zeta k_\theta) + \sigma_\varphi (\epsilon_{\varphi_o} - \zeta k_\varphi) \right.$$

$$\left. + \tau_{\varphi\theta} (\gamma_{\varphi\theta_o} - 2 \zeta k_{\varphi\theta}) \right\} d\theta \, d\varphi \, d\zeta$$

(A-5a)

This expression may be rewritten as

$$U = \frac{1}{2} \int_0^{2\pi r_o} \int_0^{S_R} \left(N_\theta \epsilon_{\theta_o} - M_\theta k_\theta + N_\varphi \epsilon_{\varphi_o} - M_\varphi k_\varphi + N_{\varphi\theta} \gamma_{\varphi\theta_o} - 2 M_{\varphi\theta} k_{\varphi\theta} \right) d\theta \, d\varphi$$

(A-5b)

Combining like terms of Equations (A-3), (A-4) and (A-5b) and using the two-dimensional stress-strain relations, we can obtain

$$N_\theta = \frac{E_\theta h}{1-\nu_{\varphi\theta}\nu_{\theta\varphi}}\left(\epsilon_{\theta_o} + \nu_{\theta\varphi}\epsilon_{\varphi_o}\right) + \frac{E_R A_R}{S_R}\epsilon_{\theta_o} - \frac{E_R C_R A_R}{S_R}k_\theta - N_{T\theta}$$

$$N_\varphi = \frac{E_\varphi h}{1-\nu_{\varphi\theta}\nu_{\theta\varphi}}\left(\epsilon_{\varphi_o} + \nu_{\varphi\theta}\epsilon_{\theta_o}\right) + \frac{E_S A_S}{S_S}\epsilon_{\varphi_o} - \frac{E_S C_S A_S}{S_S}k_\varphi - N_{T\varphi}$$

$$N_{\varphi\theta} = G_{\varphi\theta} h \gamma_{\varphi\theta_o}$$

$$M_\theta = \frac{-E_\theta h^3}{12(1-\nu_{\varphi\theta}\nu_{\theta\varphi})}\left(k_\theta + \nu_{\theta\varphi}k_\varphi\right) - \frac{E_R I_R}{S_R}k_\theta + \frac{E_R C_R A_R}{S_R}\epsilon_{\theta_o} - M_{T\theta}$$

$$M_\varphi = \frac{-E_\varphi h^3}{12(1-\nu_{\varphi\theta}\nu_{\theta\varphi})}\left(k_\varphi + \nu_{\varphi\theta}k_\theta\right) - \frac{E_S I_S}{S_S}k_\varphi + \frac{E_S C_S A_S}{S_S}\epsilon_{\varphi_o} - M_{T\varphi}$$

$$M_{\varphi\theta} = \frac{-G_{\varphi\theta} h^3}{6}k_{\varphi\theta} - \frac{G_S J_S}{2S_S}k_{\varphi\theta} - \frac{G_R J_R}{2S_R}k_{\varphi\theta} \qquad (A-6)$$

where (see Figure A-1) and subscripts θ and φ indicate coordinate directions, and

A_R, A_S = cross-sectional area of the rings and the meridional stiffeners, respectively;

C_R, C_S = eccentricity of the rings and the meridional stiffeners, respectively, measured from the reference surface of the shell (inwards positive);

I_R, I_S = moment of inertia of the rings and the meridional stiffeners, respectively, about the basic shell centroidal axis;
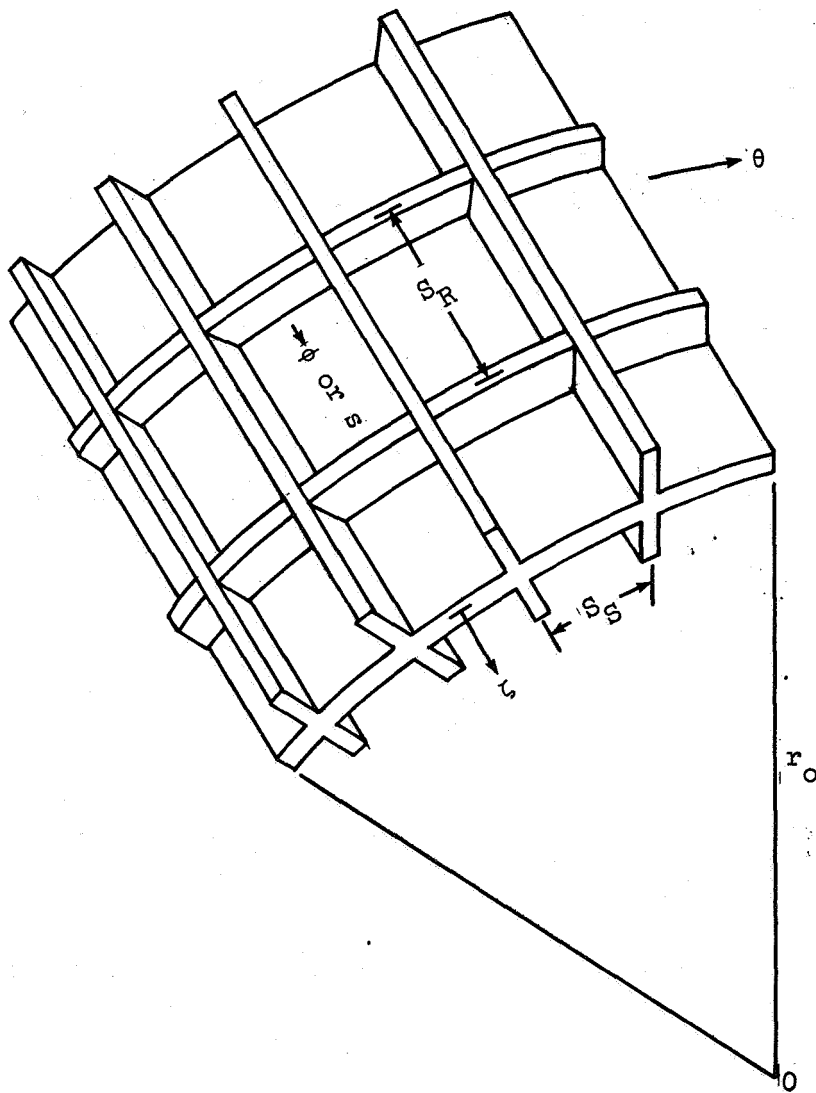
182

Figure A-1   Ring Stringer Reinforcement

J_R , J_S = torsional constant of the rings and the meriodional stiffeners, respectively;

S_R , S_S = spacing of the rings and the meridional stiffeners, respectively.

Equations (A-6) are the relations between the stress resultants and the components of strain and curvature for the ring and stringer reinforced shell. They may be employed in lieu of Equations (1-18) in cases where the spacing of the ring and stringer reinforcement is such that the smearing technique yields valid results. Equations (A-6) can be rewritten in the following abreivated form,

$$N_\theta = K_{11} \, \epsilon_{\theta_o} + K_{12} \, \epsilon_{\varphi_o} - C_{11} \, k_\theta - N_{T\theta}$$

$$N_\varphi = K_{22} \, \epsilon_{\varphi_o} + K_{12} \, \epsilon_{\theta_o} - C_{22} \, k_\varphi - N_{T\varphi}$$

$$N_{\varphi\theta} = K_{33} \, \gamma_{\varphi\theta_o}$$

$$M_\theta = D_{11} \, k_\theta + D_{12} \, k_\varphi + C_{11} \, \epsilon_{\theta_o} - M_{T\theta}$$

$$M_\varphi = D_{22} \, k_\varphi + D_{12} \, k_\theta + C_{22} \, \epsilon_{\varphi_o} - M_{T\varphi}$$

$$M_{\varphi\theta} = - 2 D_{33} \, k_{\varphi\theta} \tag{A-7}$$

where

$$K_{11} = \frac{E_\theta h}{1 - \nu_{\varphi\theta} \, \nu_{\theta\varphi}} + \frac{E_R \, A_R}{S_R} \qquad\qquad D_{11} = \frac{- E_\theta h^3}{12(1 - \nu_{\varphi\theta} \, \nu_{\theta\varphi})} - \frac{E_R \, I_R}{S_R}$$

$$K_{12} = \frac{\nu_{\theta\varphi} \, E_\theta h}{1 - \nu_{\varphi\theta} \, \nu_{\theta\varphi}} \qquad\qquad\qquad D_{12} = \frac{- \nu_{\theta\varphi} \, E_\theta h^3}{12(1 - \nu_{\varphi\theta} \, \nu_{\theta\varphi})}$$

184

$$K_{22} = \frac{E_\varphi h}{1 - v_{\varphi\theta} v_{\theta\varphi}} + \frac{E_S A_S}{S_S} \qquad D_{22} = \frac{-E_\varphi h^3}{12(1 - v_{\varphi\theta} v_{\theta\varphi})} - \frac{E_S I_S}{S_S}$$

$$K_{33} = G_{\varphi\theta} h \qquad D_{33} = \frac{G_{\varphi\theta} h^3}{12} + \frac{G_S J_S}{4 S_S} + \frac{G_R J_R}{4 S_R}$$

$$C_{11} = \frac{E_R C_R A_R}{S_R} \qquad C_{22} = \frac{E_S C_S A_S}{S_S} \qquad \text{(A-8)}$$

Notice that inasmuchas the assumption was made in the Love-Reissner-Kempner first order theory that $M_{\varphi\theta} = - M_{\theta\varphi}$, from the last of Equations (A-7) it is implied that $k_{\varphi\theta} = k_{\theta\varphi}$. From physical intuition, this relation may be approximate if the effects of the ring and meridional stiffeners are not identical, that is, the terms $G_R J_R / S_R$, and $G_S J_S / S_S$, in the torsional constant D_{33} are not equal.

Although Equations (A-6) and (A-7) were derived for a ring and stringer-stiffened shell, they could be extended to other cases by a suitable redefinition of the coefficients K_{ij}, C_{ij} and D_{ij} . For example, they may be extended to stiffened sandwich shells with equal or unequal face sheets, or to ring reinforced shells with corrugated skin in the meridional direction. Equations for the K_{ij}, C_{ij} and D_{ij} coefficients for the aforementioned cases are derived in References 32, 108.

A more general form of the Equations (A-7) for layered media may also be obtained:

$$N_\theta = K_{11} \epsilon_{\theta_o} + K_{12} \epsilon_{\varphi_o} - C_{14} k_\theta - C_{15} k_\varphi - N_{T\theta}$$

$$N_\varphi = K_{22} \epsilon_{\varphi_o} + K_{12} \epsilon_{\theta_o} - C_{15} k_\theta - C_{25} k_\varphi - N_{T\varphi}$$

$$N_{\varphi\theta} = K_{33} \gamma_{\varphi\theta_o}$$

$$M_\theta = D_{11} k_\theta + D_{12} k_\varphi + C_{14} \epsilon_{\theta_o} + C_{15} \epsilon_{\varphi_o} - M_{T\theta}$$

$$M_\varphi = D_{22} k_\varphi + D_{12} k_\theta + C_{15} \epsilon_{\theta_o} + C_{25} \epsilon_{\varphi_o} - M_{T\varphi}$$

$$M_{\varphi\theta} = - 2 D_{33} k_{\varphi\theta} \qquad\qquad\qquad\qquad\qquad \text{(A-9)}$$

These equations are derived in Reference 32. They are referred to a surface about which $N_{\varphi\theta}$ is independent of $k_{\varphi\theta}$, and $M_{\varphi\theta}$ is not dependent upon $\gamma_{\varphi\theta_o}$. These equations may be employed in cases involving shells with:

    a) homogeneous, sandwich, or multilayered skin reinforced by waffles at an arbitrary angle to the θ, φ coordinate system,

    b) semi-sandwich shells (skin + corrugations).

The appropriate expressions for the K_{ij}, C_{ij} and D_{ij} coefficients for each case may be found in Reference 32.

For a general isogrid reinforcement Equations (A-9c, f) must be revised as follows:

$$N_{\varphi\theta} = K_{33} \gamma_{\varphi\theta_o} - 2C_{16} k_{\varphi\theta}$$

$$\qquad\qquad\qquad\qquad\qquad\qquad\qquad\qquad\qquad \text{(A-10)}$$

$$M_{\varphi\theta} = -2D_{33} k_{\varphi\theta} + C_{16} \gamma_{\varphi\theta_o}$$

The necessary stiffness terms for the $\beta = 30°$ isogrid can then be defined as

$$K_{11} = \frac{E_\theta h}{1-\nu_{\varphi\theta}\nu_{\theta\varphi}} + \frac{E_R A}{S}\left(\frac{3\sqrt{3}}{4}\right) \qquad D_{11} = \frac{-E_\theta h^3}{12(1-\nu_{\varphi\theta}\nu_{\theta\varphi})} - \frac{E_R I}{S}\left(\frac{3\sqrt{3}}{4}\right)$$

$$K_{12} = \frac{\nu_{\theta\varphi}E_\theta h}{1-\nu_{\varphi\theta}\nu_{\theta\varphi}} + \frac{E_R A}{S}\left(\frac{\sqrt{3}}{4}\right) \qquad D_{12} = \frac{-\nu_{\theta\varphi}E_\theta h^3}{12(1-\nu_{\varphi\theta}\nu_{\theta\varphi})} - \frac{E_R I}{S}\left(\frac{\sqrt{3}}{4}\right)$$

$$K_{22} = \frac{E_\theta h}{1-\nu_{\varphi\theta}\nu_{\theta\varphi}} + \frac{E_R A}{S}\left(\frac{3\sqrt{3}}{4}\right) \qquad D_{22} = \frac{-E_\varphi h^3}{12(1-\nu_{\varphi\theta}\nu_{\theta\varphi})} - \frac{E_R I}{S}\left(\frac{3\sqrt{3}}{4}\right)$$

$$K_{33} = G_{\varphi\theta} h + \frac{E_R A}{S}\left(\frac{\sqrt{3}}{4}\right) \qquad D_{33} = \frac{G_{\varphi\theta} h^3}{12} + \frac{E_R I}{S}\left(\frac{\sqrt{3}}{4}\right)$$

$$C_{14} = C_{25} = \frac{E_R AC}{S}\left(\frac{3\sqrt{3}}{4}\right) \qquad C_{15} = C_{16} = \frac{E_R AC}{S}\left(\frac{\sqrt{3}}{4}\right) \qquad\qquad (A-11)$$

APPENDIX B

EQUATIONS FOR A DISCRETE RING

The most consistent method of analyzing shells reinforced with widely spaced rings is to consider the shell segments and the rings as discrete structural members subjected to the given external loads and to the required interface conditions. The theory utilized is an expansion of that due to Cheney [168] to include vibrations. The ring centroids and shear centers are allowed to be off-set, and the ring-shell connection can be eccentric. The necessary ring matrices for the programs are defined as:

[M]   Ring mass matrix (ring coordinates)

$\{L_M\}$ Ring centrifugal acceleration load matrix (global coordinates)

$[k_R]$ Ring prestressed stiffness matrix (ring coordinates)

$\{L_R\}$ Ring thermal load matrix (ring coordinates)

$[T_\Delta]$ Transformation matrix to attached shell joint and shell global coordinate system

The ring matrices are first converted to the shell joint and coordinate system,

$$\{\hat{F}_j\} = \lceil 2\pi r_{oj} \rfloor [T_\Delta]^T [k_R] [T_\Delta] \{\Delta_j\} + \lceil 2\pi r_{oj} \rfloor [T_\Delta]^T [L_R] \qquad (B-1)$$

and then stacked appropriately for segment and region joints. The thermal load matrix is computed on the basis of a linear (radial) thermal distribution for the ring.

The necessary matrices are presented in detail below:

188

$$M_{11} = -\rho\omega^2 \left(A + \frac{I_y}{r_c^2} n^2 \right)$$

$$M_{21} = \frac{-\rho\omega^2 I_{yx}}{r_c^2} n^2$$

$$M_{22} = -\rho\omega^2 \left(A + \frac{I_y}{r_c^2} n^2 \right)$$

$$M_{31} = -\rho\omega^2 \frac{I_y}{r_c^2} n$$

$$M_{32} = \frac{-\rho\omega^2 I_{yx}}{r_c^2} n$$

$$M_{33} = -\rho\omega^2 \left(A + \frac{I_y}{r_c^2} \right)$$

$$M_{41} = M_{42} = M_{43} = 0$$

$$M_{44} = -\rho\omega^2 \left(I_x + I_y \right) \tag{B-2}$$

$$L_{M_1} = L_{M_2} = 0$$

$$L_{M_3} = -\rho\omega^2 r_c A$$

$$L_{M_4} = -\bar{y} \left(\rho\omega^2 r_c A \right)$$

$$k_{R_{11}} = \frac{EA \, \epsilon_o \, r_c}{r_s^3} (n^2 - 1) + \frac{EA}{r_c r_s} \left(1 + \frac{x_c^2 n^4}{r_s^2} - \frac{2 \, x_c n^2}{r_s} \right) + \frac{EI_y}{r_c^3 r_s} \left(1 + n^4 - 2n^2 \right)$$

$$k_{R_{21}} = \frac{EA \, y_c}{r_c r_s^2} \left(\frac{x_c n^4}{r_s} - n^2 \right) + \frac{EI_y \, y_c}{r_c^3 r_s^2} \left(n^4 - n^2 \right) + \frac{EI_{xy}}{r_c^2 r_s^2} \left(n^4 - n^2 \right)$$

$$k_{R_{22}} = \frac{EA}{r_c r_s}\left(\epsilon_o n^2 + \frac{y_c^2 n^4}{r_s^2}\right) + EI_y\left(\frac{y_c^2}{r_c^3 r_s^3}\right)n^4 + \frac{EI_x n^4}{r_c r_s^3} + \frac{2\,EI_{xy} y_c n^4}{r_c^2 r_s^3} + \frac{GJn^4}{r_s^4}$$

$$k_{R_{31}} = \frac{EA}{r_s^2}\left(n - \frac{x_c n^3}{r_s}\right)$$

$$k_{R_{32}} = \frac{-EAy_c n^3}{r_s^3}$$

$$k_{R_{33}} = \frac{EAr_c}{r_s^3}n^2$$

$$k_{R_{41}} = \frac{EAy_c}{r_s^2}\left(\epsilon_o - \epsilon_o n^2 - \frac{r_s}{r_c} + \frac{x_c n^2}{r_c}\right) + \frac{EI_y y_c}{r_c^3 r_s}(n^2 - 1) + \frac{EI_{xy}}{r_c^2 r_s}(n^2 - 1)$$

$$k_{R_{42}} = \frac{EA}{r_c r_s}\left(\epsilon_o x_c n^2 + \frac{y_c^2 n^2}{r_s}\right) + \frac{EI_y y_c^2 n^2}{r_c^3 r_s^2} + \frac{EI_x n^2}{r_c r_s^2} + \frac{2\,EI_{xy} y_c n^2}{r_c^2 r_s^2} + \frac{GJn^2}{r_s^3}$$

$$k_{R_{43}} = -\frac{EAy_c n}{r_s^2}$$

$$k_{R_{44}} = \frac{EAy_c^2}{r_c r_s}(1 - \epsilon_o) + \frac{EI_x}{r_c r_s}(n^2 \epsilon_o - \epsilon_o + 1) + \frac{EI_y}{r_c r_s}\left(\epsilon_o n^2 + \frac{y_c}{r_c}\right) + \frac{2\,EI_{xy} y_c}{r_c^2 r_s} + \frac{GJn^2}{r_s^2}$$

$$L_{R_1} = \frac{E\alpha A(m_n x_c + b_n)}{r_s}$$

$$L_{R_2} = L_{R_3} = 0$$

$$L_{R_4} = \frac{-E\alpha A(m_n x_c + b_n)y_c}{r_s} - \frac{E\alpha I_{xy} m_n}{r_s} \tag{B-2}$$

$$m_n = \frac{T_I - T_O}{x_I - x_O} \qquad\qquad b_n = \frac{(T_O - T_F)x_I - (T_I - T_F)x_O}{x_I - x_O}$$

$$T_{\Delta_{11}} = T_{\Delta_{12}} = T_{\Delta_{21}} = T_{\Delta_{23}} = T_{\Delta_{34}} = T_{\Delta_{41}} = T_{\Delta_{42}} = T_{\Delta_{43}} = 0$$

$$T_{\Delta_{13}} = T_{\Delta_{22}} = T_{\Delta_{44}} = -1$$

$$T_{\Delta_{14}} = -\bar{y}$$

$$T_{\Delta_{24}} = \bar{x}$$

$$T_{\Delta_{31}} = -\frac{1}{(1-\frac{\bar{x}}{r_s})}$$

$$T_{\Delta_{32}} = -\frac{n\bar{y}}{r_s(1-\frac{\bar{x}}{r_s})}$$

$$T_{\Delta_{33}} = -\frac{n\bar{x}}{r_s(1-\frac{\bar{x}}{r_s})}$$
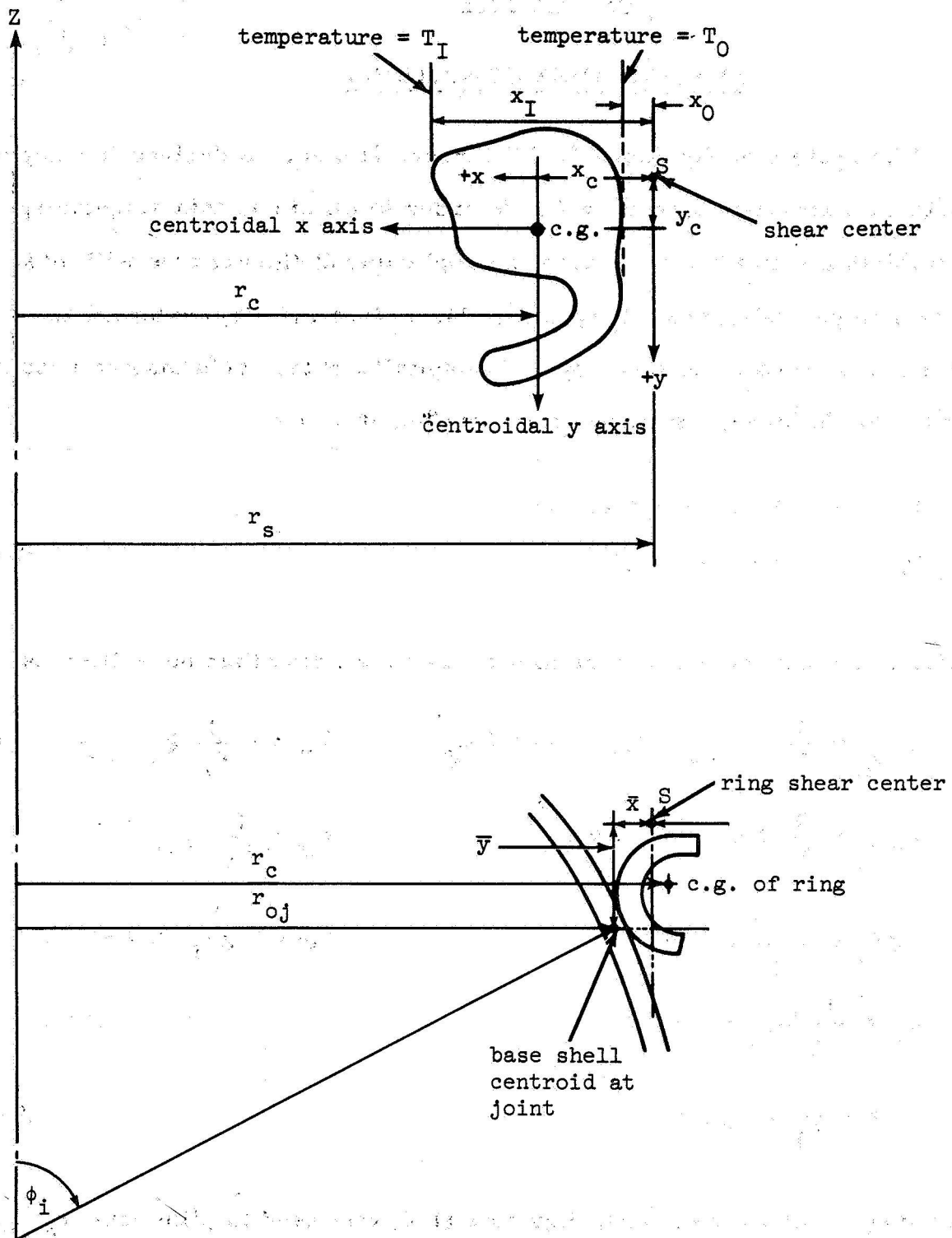
where the necessary notation is defined in Figure B-1

Figure **B-1**   Discrete Ring Geometry

APPENDIX C

SPECIAL APEX CONDITIONS

The system of Equations (1-27) through (1-29), as derived in Chapter 1, contains a singularity at $r_o = 0$. In order to eliminate this singularity, and establish a suitable set of equations applicable at the apex we will make the terms in parentheses in Equations (1-14c, d, f) and (1-12f) evaluated at $\varphi = 0$ equal to zero, and thus apply L'Hospital's rule. This may be accomplished if the following conditions are satisfied at $\varphi = 0$

$$u,_\theta + v = v,_\theta - u = w,_\theta = 0$$

$$\omega_{\varphi,\theta} - \omega_\theta = \omega_{\theta,\theta} + \omega_\varphi = 0 \tag{C-1}$$

The strain displacement relations at a smooth apex may then be written as

$$\epsilon_{\theta\theta_o} = \frac{1}{r_1}(u,_{\theta\varphi} + v,_\varphi - w) + \tfrac{1}{2}\omega_\varphi^2 \qquad k_\theta = -\frac{1}{r_1}(\omega_{\varphi,\theta\varphi} - \omega_{\theta,\varphi})$$

$$\epsilon_{\varphi\varphi_o} = \frac{1}{r_1}(v,_\varphi - w) + \tfrac{1}{2}\omega_\theta^2 \qquad k_\varphi = \frac{1}{r_1}\omega_{\theta,\varphi}$$

$$\epsilon_{\varphi\theta_o} = \frac{v,_{\theta\varphi}}{r_1} - \omega_\theta\omega_\varphi \qquad k_{\varphi\theta} = \frac{1}{2r_1}\omega_{\theta,\theta\varphi}$$

$$\omega_\theta = \frac{1}{r_1}(w,_\varphi + v)$$

$$\omega_\varphi = -\frac{1}{r_1}(w,_{\theta\varphi} + u) \tag{C-2}$$

In obtaining the above relations, Equation (1-8) was used to eliminate $r_{o,\varphi}$.

The equilibrium equations at the apex become:

$$N_{\theta,\theta} + 2N_{\varphi\theta} = 0$$

$$N_\varphi + N_{\varphi\theta,\theta} - N_\theta = 0$$

$$Q_\varphi + Q_{\theta,\theta} = - \left[N_{\varphi\theta}\, \omega_\theta - N_\theta\, \omega_\varphi \right]_{,\theta} - \left[N_\varphi\, \omega_\theta - N_{\varphi\theta}\, \omega_\varphi \right] \qquad (C\text{-}3)$$

$$- M_{\varphi\theta,\theta} - M_\varphi + M_\theta = 0$$

$$M_{\theta,\theta} + 2 M_{\varphi\theta} = 0$$

In a fashion similar to that of Reference 20, the variables of Equations (C-2, 3) may be expanded in a Fourier series in the θ direction, which involve only the part of the series (2-2) with the primed amplitudes. Thus from Equations (C-1) and (C-3) boundary conditions for the different harmonics are obtained, while from Equations (1-27) through (1-29), using L'Hospital's rule and the established boundary conditions, the appropriate differential equations are obtained [6, 8].

For the axisymmetric case (n= 0) the following conditions are obtained from Equations (C-1) through (C-3)

$$V^{(0)} = 0 \qquad\qquad N_{\varphi\theta}^{(0)} = 0$$

$$U^{(0)} = 0 \qquad\qquad M_{\varphi\theta}^{(0)} = 0$$

$$\Omega_\theta^{(0)} = 0 \qquad\qquad M_\theta^{(0)} = M_\varphi^{(0)}$$

$$\Omega_\varphi^{(0)} = 0 \qquad\qquad N_\theta^{(0)} = N_\varphi^{(0)}$$

$$J_\varphi^{*(0)} = 0 \qquad\qquad J_\varphi^{(0)} = Q_\varphi^{(0)} = - \left[\left(N_\varphi\, \Omega_\theta \right)^{(0)} - \left(N_{\varphi\theta}\, \Omega_\varphi \right)^{(\theta)} \right] = 0$$

$$N_{T\varphi}^{(0)} = N_{T\theta}^{(0)} \qquad\qquad M_{T\varphi}^{(0)} = M_{T\theta}^{(0)}$$

$$T_{\varphi\theta}^{(0)} = 0 \qquad\qquad\qquad\qquad\qquad\qquad\qquad (C\text{-}4)$$

Applying these relations and L'Hospital's rule to the Equation system (1-27) through (1-29), we obtain at the apex:

$$\frac{T^{(0)}_{\varphi\theta,\varphi}}{r_1} = 0 \qquad\qquad \frac{U^{(0)}_{,\varphi}}{r_1} = 0$$

$$\frac{N^{(0)}_{\varphi,\varphi}}{r_1} = 0 \qquad\qquad \frac{W^{(0)}_{,\varphi}}{r_1} = 0$$

$$\frac{J^{*(0)}_{\varphi,\varphi}}{r_1} = -\frac{N^{(0)}_{\varphi}}{r_1} - \frac{F_\zeta^{(0)}}{2}\left(1+2\epsilon^{(0)}_{\varphi_{\circlearrowleft}}\right) \qquad\qquad \frac{M^{(0)}_{\varphi,\varphi}}{r_1} = 0$$

$$\frac{V^{(0)}_{,\varphi}}{r_1} = \frac{W^{(0)}}{r_1} + (K_{22} - \nu_{\theta\varphi}^2 K_{11})^{-1}\left\{N^{(0)}_{\varphi}(1-\nu_{\theta\varphi}) + N^{(0)}_{T\varphi}(1-\nu_{\theta\varphi})\right\}$$

$$\frac{\Omega^{(0)}_{\theta,\varphi}}{r_1} = \left(D_{22} - \nu_{\theta\varphi}^2 D_{11}\right)^{-1}\left\{M^{(0)}_{\varphi}(\nu_{\theta\varphi}-1) + M^{(0)}_{T\varphi}(\nu_{\theta\varphi}-1)\right\}$$

$$N^{(0)}_\theta = N^{(0)}_\varphi \qquad\qquad M^{(0)}_{\varphi\theta} = 0$$

$$M^{(0)}_\theta = M^{(0)}_\varphi \qquad\qquad J^{*(0)}_\varphi = J^{(0)}_\varphi = 0 \qquad\qquad \text{(C-5)}$$

For the first antisymmetric harmonic (n=1) the following conditions are obtained from Equations (C-1) through (C-3) [20] .

$$U^{(1)} = -V^{(1)} \qquad\qquad M^{(1)}_\theta = 0$$

$$W^{(1)} = 0 \qquad\qquad M^{(1)}_\varphi = 0$$

$$\Omega^{(1)}_\theta = \Omega^{(1)}_\varphi \qquad\qquad N^{(1)}_\varphi = 0$$

$$M^{(1)}_{\varphi\theta} = 0 \qquad\qquad N^{(1)}_\theta = 0$$

$$T^{(1)}_{\varphi\theta} = 0 \qquad\qquad N^{(1)}_{\varphi\theta} = 0 \qquad\qquad \text{(C-6)}$$

Applying these relations, and L'Hopital's rule to the Equations (1-27) through (1-29) we obtain, at the apex:

$$\frac{T^{(1)}_{\varphi\theta,\varphi}}{r_1} = \frac{J^{(1)}_{\varphi}}{2r_1} \qquad\qquad \frac{U,^{(1)}_{\varphi}}{r_1} = 0$$

$$\frac{N^{(1)}_{\varphi,\varphi}}{r_1} = \frac{J^{(1)}_{\varphi}}{2r_1} \qquad\qquad \frac{V,^{(1)}_{\varphi}}{r_1} = 0$$

$$\frac{J^{*(1)}_{\varphi,\varphi}}{r_1} = 0 \qquad\qquad \frac{W,^{(1)}_{\varphi}}{r_1} = -\frac{V^{(1)}}{r_1}$$

$$\frac{M^{(1)}_{\varphi,\varphi}}{r_1} = J^{(1)}_{\varphi} \qquad\qquad \frac{\Omega^{(1)}_{\theta,\varphi}}{r_1} = 0$$

$$N^{(1)}_{\theta} = 0 \qquad\qquad M^{(1)}_{\varphi\theta} = 0$$

$$M^{(1)}_{\theta} = 0 \qquad\qquad J^{(1)}_{\varphi} = J^{*(1)}_{\varphi} \qquad\qquad \text{(C-7)}$$

For the second harmonic (n= 2), the following conditions are obtained from Equations (C-1) through (C-3) [20] .

$$U^{(2)} = 0 \qquad\qquad N^{(2)}_{\theta} = N^{(2)}_{\varphi}$$

$$V^{(2)} = 0 \qquad\qquad N^{(2)}_{\varphi\theta} = -N^{(2)}_{\varphi}$$

$$W^{(2)} = 0 \qquad\qquad M^{(2)}_{\theta} = M^{(2)}_{\varphi}$$

$$\Omega^{(2)}_{\theta} = 0 \qquad\qquad M^{(2)}_{\varphi\theta} = -M^{(2)}_{\varphi}$$

$$\Omega^{(2)}_{\varphi} = 0 \qquad\qquad\qquad\qquad\qquad \text{(C-8)}$$

Applying these relations, and L'Hopital's rule, to the Equations (1-27) through (1-29), we obtain, at the apex:

$$\frac{T^{(2)}_{\varphi\theta,\varphi}}{r_1} = 0$$

$$\frac{N^{(2)}_{\varphi,\varphi}}{r_1} = 0$$

$$\frac{J^{*(2)}_{\varphi,\varphi}}{r_1} = 0$$

$$\frac{M^{(2)}_{\varphi,\varphi}}{r_1} = 0$$

$$\frac{U^{(2)}_{,\varphi}}{r_1} = 3\left\{\left(K_{22} - \nu_{\theta\varphi}^2 K_{11}\right)^{-1}\left(N^{(2)}_{\varphi}[1-\nu_{\theta\varphi}] + N^{(2)}_{T\varphi}[1-\nu_{\theta\varphi}]\right)\right\} + \frac{T^{(2)}_{\varphi\theta}}{K_{33}} + \frac{M^{(2)}_{\varphi\theta}}{r_1 K_{33}}$$

$$\frac{V^{(2)}_{,\varphi}}{r_1} = \left(K_{22} - \nu_{\theta\varphi}^2 K_{11}\right)^{-1}\left\{N^{(2)}_{\varphi}[1-\nu_{\theta\varphi}] + N^{(2)}_{T\varphi}[1-\nu_{\theta\varphi}]\right\}$$

$$\frac{W^{(2)}_{,\varphi}}{r_1} = 0$$

$$\frac{\Omega^{(2)}_{\theta,\varphi}}{r_1} = \left(D_{22} - \nu_{\theta\varphi}^2 D_{11}\right)^{-1}\left\{M^{(2)}_{\varphi}\left(-1+\nu_{\theta\varphi}\right) + M^{(2)}_{T\varphi}\left(-1+\nu_{\theta\varphi}\right)\right\}$$

$$N^{(2)}_{\theta} = N^{(2)}_{\varphi} \qquad\qquad M^{(2)}_{\varphi\theta} = -M^{(2)}_{\varphi}$$

$$M^{(2)}_{\theta} = M^{(2)}_{\varphi} \qquad\qquad J^{(2)}_{\varphi} = J^{*(2)}_{\varphi} \qquad\qquad (C-9)$$

197

Finally for the other harmonics ($n \geq 3$) the following conditions are obtained from Equations (C-1) through (C-3) [20] .

$$U^{(n)} = 0 \qquad\qquad M_\varphi^{(n)} = 0$$

$$V^{(n)} = 0 \qquad\qquad N_\varphi^{(n)} = 0$$

$$W^{(n)} = 0 \qquad\qquad N_\theta^{(n)} = 0$$

$$\Omega_\theta^{(n)} = 0 \qquad\qquad M_\theta^{(n)} = 0$$

$$\Omega_\varphi^{(n)} = 0 \qquad\qquad M_{\varphi\theta}^{(n)} = 0$$

$$N_{\varphi\theta}^{(n)} = 0 \qquad\qquad\qquad\qquad\qquad\qquad\qquad (C-10)$$

Applying these relations, and L'Hopital's rule to the Equations (1-27) through (1-29) we obtain, at the apex:

$$\frac{T_{\varphi\theta,\varphi}^{(n)}}{r_1} = \frac{2 n J_\varphi^{(n)}}{(3+n^2)r_1} \qquad\qquad \frac{U,_\varphi^{(n)}}{r_1} = 0$$

$$\frac{N_{\varphi,\varphi}^{(n)}}{r_1} = \left(\frac{3 n^2 + 3}{3+n^2}\right) \frac{J_\varphi^{(n)}}{r_1} \qquad\qquad \frac{V,_\varphi^{(n)}}{r_1} = 0$$

$$\frac{J_{\varphi,\varphi}^{*(n)}}{r_1} = 0 \qquad\qquad \frac{W,_\varphi^{(n)}}{r_1} = 0$$

$$\frac{M_{\varphi,\varphi}^{(n)}}{r_1} = J_\varphi^{(n)} \qquad\qquad \frac{\Omega_{\theta,\varphi}^{(n)}}{r_1} = 0$$

$$N_\theta^{(n)} = 0 \qquad\qquad M_{\varphi\theta}^{(n)} = 0$$

$$M_\theta^{(n)} = 0 \qquad\qquad J_\varphi^{(n)} = J_\varphi^{*(n)} \qquad\qquad (C-11)$$

It should be noted that the nonlinear terms in these equations may be obtained from Equations (2.9a) and (2.9b). It must be emphasized that the above equations are valid only for a smooth apex (sin φ = 0, cos φ = 1). This method may be employed to obtain the appropriate equations for more complex apices. For a non-smooth apex ($\varphi = \varphi_o \neq 0$):

$$\sin \varphi = \sin \varphi_o \neq 0$$
$$\cos \varphi = \cos \varphi_o \neq 1$$

Equations (C-5) through (C-11) are utilized in the following manner in the numerical procedure discussed in Chapter 3. The apex boundary conditions from Equations (C-4, 6, 8, 10) are set in displacement form into the boundary condition matrix for the structure. The apex Equations (C-5, 7, 9, 11) are used only in the first step of the Runge-Kutta numerical integration procedure, when it is applied to the edge r_o = 0 of the segment adjacent to the apex. In subsequent steps the sets of Equations (1-27) through (1-29) are employed. This procedure, however, is rather cumbersome, and it will be used only when the applied loading varies rapidly near the apex. In other cases, the apex boundary conditions (C-4, 6, 8, 10) may be satisfied at a circle of a very small but finite value of r_o. The results obtained on the basis of this approximation will be satisfactory at points away from the apex [6, 8].

APPENDIX D

CONVERSION OF U.S. CUSTOMARY UNITS TO SI UNITS

The International System of Units (SI) was adopted by the
Eleventh General Conference on Weights and Measures in 1960. Conversion
factors for the units used in this report are given in the following
table:

Physical quantity	U.S. Customary Unit	Conversion factor (*)	SI Unit (**)
Length	in.	0.0254	meters (m)
Stress modulus	ksi	6.895×10^{6}	newtons/meter^2 (N/m^2)
Stress resultant	lbf/in.	175.1	newtons/meter (N/m)
Temperature change	°F	5/9	Kelvin (K)

* Multiply value given in U.S. Customary Unit by conversion factor to
   obtain equivalent value in SI Units.

** Prefixes to indicate multiple of units are as follows:

Prefix	Multiple
giga (G)	10^{9}
mega (M)	10^{6}
kilo (k)	10^{3}
deci (d)	10^{-1}
centi (c)	10^{-2}
milli (m)	10^{-3}

"The aeronautical and space activities of the United States shall be conducted so as to contribute . . . to the expansion of human knowledge of phenomena in the atmosphere and space. The Administration shall provide for the widest practicable and appropriate dissemination of information concerning its activities and the results thereof."
—NATIONAL AERONAUTICS AND SPACE ACT OF 1958

NASA SCIENTIFIC AND TECHNICAL PUBLICATIONS

TECHNICAL REPORTS: Scientific and technical information considered important, complete, and a lasting contribution to existing knowledge.

TECHNICAL NOTES: Information less broad in scope but nevertheless of importance as a contribution to existing knowledge.

TECHNICAL MEMORANDUMS: Information receiving limited distribution because of preliminary data, security classification, or other reasons. Also includes conference proceedings with either limited or unlimited distribution.

CONTRACTOR REPORTS: Scientific and technical information generated under a NASA contract or grant and considered an important contribution to existing knowledge.

TECHNICAL TRANSLATIONS: Information published in a foreign language considered to merit NASA distribution in English.

SPECIAL PUBLICATIONS: Information derived from or of value to NASA activities. Publications include final reports of major projects, monographs, data compilations, handbooks, sourcebooks, and special bibliographies.

TECHNOLOGY UTILIZATION PUBLICATIONS: Information on technology used by NASA that may be of particular interest in commercial and other non-aerospace applications. Publications include Tech Briefs, Technology Utilization Reports and Technology Surveys.

Details on the availability of these publications may be obtained from:

SCIENTIFIC AND TECHNICAL INFORMATION OFFICE

NATIONAL AERONAUTICS AND SPACE ADMINISTRATION
Washington, D.C. 20546